INCREASED SENSITIVITY OF ENZYME-BASED AMPEROMETRIC GLUCOSE BIOSENSORS AND THEIR APPLICATION AS TIME-TEMPERATURE INTEGRATORS

By

JOSÉ IGNACIO REYES DE CORCUERA

A dissertation submitted in partial fulfillment of
the requirements for the degree of

DOCTOR OF PHILOSOPHY IN ENGINEERING SCIENCE

WASHINGTON STATE UNIVERISTY
Department of Biological Systems Engineering

MAY 2004

To the Faculty of Washington State University:

The members of the Committee appointed to examine the dissertation of JOSÉ IGNACIO REYES DE CORCUERA find it satisfactory and recommend that it be accepted.

_____
Chair

_____

_____

_____

ACKNOWLEDGMENT

I would like to thank the constant support, patience and encouragement of my advisor, Dr. Ralph P. Cavalieri who opened to me the doors of independent research and trusted me often times more than myself and never let me get out of his office without a positive thought.

I would like to thank Dr. Joseph R. Powers, for the many hours of discussions and advice. For taking the time of listening to my ideas and helping me reject the wrong ones and pick some with potential. I am also grateful for helping me get the necessary money to keep going during the last two years of my research and for his concern beyond research.

My gratitude to Dr. Juming Tang for his contribution in reviewing my research and encouraging me in times when the dark tunnel seemed endless.

I would like to thank Dr. Herbert H. Hill for reviewing my work and helping me deliver the best work I could.

I would like to thank Dr. Dong-Hyun Kang for allowing me to collaborate in some of his projects, for the financial support I received from theses projects and especially for his friendship. Thanks also to Sun-Young Lee for her constant support in the catalase activity sensor project.

My deepest gratitude to all the professors who taught me at WSU. If I ever teach, I hope I can match the high standards that showed in your courses.

I will never be grateful enough to Alma my wife who beyond taking care of Carlos, Andrés and me she helped me in the laboratory for the last eight months carrying out the final experiments of this research.

I am forever grateful to my parents Inés and Carlos who gave me wings and taught me to fly, true instruments of God's love in my life.

I am very grateful to the faculty and friends of the Department of Biological Systems Engineering who taught and helped me. Especial thanks to Wayne DeWitt for all the pieces of equipment that he fabricated for me and without which any of my research projects would have been possible. Thanks to Vince Himsl who helped and taught me most of what I know about data acquisitions and some electrical circuits. Thanks to Frank Younce for his suggestions and helping me carry out some projects in the Pilot Plant. Thanks to John Anderson, Pat Huggins always kind and supportive in the complexities of the non-research phases of my Ph.D. and to all the staff of the department.

Thanks to the faculty and staff of the Department of Food Science and Human Nutrition. You hosted me so warmly especially the last two years of my Ph.D. even though I am just an engineer. Thanks to Carolee Armfiled for making sure that I had a paycheck on time, thanks to Rich Hoeft for making so many purchases for my projects. Thanks to Connie Barner and Jodi Anderson.

I am grateful to my fellow graduate students and friends most of whom I saw come and go. Thank you to many who set an example of high quality research in the laboratory, and especially high quality persons who encouraged me: Enrique, Eddie, Nori, Agnes, Jorge, Elba, José Luis, José María, Tong, Fernanda, Andy, José Angel, Federico, José Juan, Armen, Mara, David, Isela, Yi Fen, Dongsheng, Kunchalee, Miyuki,

Aldwin, and their beautiful families. Special thanks to Geoff Puzon whose most valuable and constant friendship kept me going and to his family who has embraced mine so many times with true charity.

I am grateful to the priests of St Thomas More and Sacred Heart Parishes, Fr. Tom, Fr. Edgar and Fr. Steve who through their ministries helped me keep priorities in what I believe is the right order.

Thanks to Fr. Ramiro Moreno M.Sp.S. for guiding my soul for so many years as a true spiritual father to me.

Thanks to Fr. François Marot who for the first time taught me the meaning of my mission.

I gratefully acknowledge the financial support from Fulbright/CONACyT (National Council for Science and Technology Mexico)

This research was funded in part by Washington State University International Marketing Program for Agricultural Commodities and Trade (IMPACT) Center and the Washington State University Agricultural Research Center.

INCREASED SENSITIVITY OF ENZYME-BASED AMPEROMETRIC GLUCOSE BIOSENSORS AND THEIR APPLICATION AS TIME-TEMPERATURE INTEGRATORS

Abstract

by José Ignacio Reyes De Corcuera, Ph.D.
Washington State University
May 2004

Chair: Ralph P. Cavalieri

This dissertation concerns the development of amperometric glucose oxidase-based biosensors using electrochemically-generated polymers as enzyme immobilization matrices. A potential novel application of amperometric enzyme biosensors as time-temperature integrators for food pasteurization is presented.

Chapter One gives an introduction to amperometric enzyme biosensors and time-temperature integrators and background to supplement the four manuscripts that form the main body of this dissertation.

Chapter Two reviews the different types of biosensors and their applications to the food and agricultural industries (Encyclopedia of Agricultural Food and Biological Engineering, Heldman, D. Editor. Marcel Dekker Inc. 2003 pp. 119-123).

Chapter Three describes a method for simultaneously determining film permeability to H_2O_2 and substrate surface area coverage of overoxidized polypyrrole films. The effects of polymer growth potential, electrolyte concentration, monomer concentration, glucose oxidase concentration and film thickness are discussed. (Synthetic Metals, **2004**, 142, (1-3) 71-79).

In Chapter Four, platinum platinization conditions were improved to produce a 60-fold increase in electrode sensitivity using glucose oxidase immobilized in poly-*o*-phenylenediamine. Glucose oxidase concentration was adjusted to obtain maximum current response. Potentiostatic platinization at –100 or –50 mV resulted in mechanically stable deposits unlike the commonly used –250 mV. Large concentrations of glucose oxidase did not inhibit the electropolymerization of o-phenylenediamine. (Submitted in revised form to the Journal of Electroanalytical Chemistry).

Chapter Five is a manuscript, that describes a novel exogenous time-temperature integrator (TTI) based on an amperometric glucose oxidase biosensor. The TTI consists of an enzyme entrapped within an electrochemically generated poly-o-phenylenediamine (PoPD) thin film deposited on the interior wall of a platinized stainless steel capsule. After thermal treatment, the TTI is mounted in a continuous flow system and connected to a potentiostat for amperometric detection of residual enzyme activity. A measurement is completed within five min of extracting the device from the heat treatment process. (Will be submitted for publication in the Journal of Agricultural and Food Chemistry).

Diagrams of instruments built for this research, LabVIEW computer programs and a collection of photographs of the pieces of equipment used for this research appear in six appendices.

TABLE OF CONTENTS

LIST OF FIGURES

LIST OF TABLES

Dedication

To Alma, Carlos and Andrés with all my love and gratitude.

Vanity of vanities! All things are vanity! What profit has man from all the labor, which he toils at under the sun? (Eccl. 1, 2-3)

DISSERTATION OUTLINE

The development and application of amperometric glucose oxidase biosensors and their application as time-temperature integrators for food pasteurization is presented in this dissertation. A general introduction and background, four manuscripts and recommendations for future research form the main body of the document. Four appendices supplement this dissertation with preliminary research on aspects not covered in the main body of the dissertation, technical information on equipment and laboratory procedures used during this research.

Chapter One is a general introduction in which instrumentation needs of the food industry and the potential role of biosensors and time temperature integrators in response to these needs are discussed. The context in which this research was carried out and a detailed background that supplements the contents of each of the articles that form this dissertation is also presented.

The first stage of this research dealt with learning what is a biosensor, what types of biosensors have been developed and to decide what line of research to develop. For that purpose a general literature review is presented in Chapter Two (Encyclopedia of Agricultural Food and Biological Engineering, Heldman, D. Editor. Marcel Dekker Inc pp. 119-123).

In Chapter Three, a method for simultaneous determination of film permeability to H_2O_2 and substrate surface area coverage of overoxidized polypyrrole is presented. The effects of polymer growth potential, electrolyte concentration, monomer

concentration, enzyme concentration and film thickness are discussed. (Synthetic Metals, **2004**, 142, (1-3), 71-79).

Platinum platinization conditions were improved to produce a 60-fold increase in electrode sensitivity using glucose oxidase immobilized in poly-*o*-phenylenediamine. Experimental results and a mathematical model are presented in Chapter Four (Submitted in revised form for publication to the Journal of Electroanalytical Chemistry).

Chapter Five describes a novel exogenous time-temperature integrator (TTI) based on an amperometric glucose oxidase biosensor. The TTI consists of the enzyme entrapped within an electrochemically generated poly-o-phenylenediamine (PoPD) thin film deposited on the interior wall of a platinized stainless steel capsule. (Will be submitted for publication to the Journal of Agricultural and Food Chemistry).

Electric diagrams of instruments and circuits built for this research and a list of their components are given in Appendix A. LabVIEW computer programs are presented in Appendices B through E. Appendix F is a collection of photographs of the equipment used for this research.

Ralph P. Cavalieri and Joseph R. Powers are the co-authors of the manuscripts. Dr. Cavalieri contributed to the editing of the four manuscripts. Dr. Powers contributed to the editing of the second, third and fourth manuscripts.

CHAPTER ONE

INTRODUCTION, OBJECTIVES AND BACKGROUND

CHAPTER ONE

INTRODUCTION, OBJECTIVES AND BACKGROUND

Introduction

Instrumentation for Food Quality

The need of healthier, safer, more convenient, competitively superior and seasonally invariant foods along with the need of more efficient processing plants with reduced waste production drive the development and improvement of food processes. However, scientific data on food quality changes during processing, packaging and distribution, is lacking mainly due to the lack of appropriate on-line instrumentation (Rizvi et al. 1993).

While level, flow, pressure and temperature sensors for on-line implementation are widespread; instruments for chemical analysis are scarce and often limited to pH and conductivity and pO_2 and pCO_2 for gases. On-line optical instruments such as refractometers, spectrophotometers, turbidity meters and color meters that may be used to assess food composition have been developed. However, their applicability is often limited by the presence of compounds that interfere with the measurement and that are present in variable amounts due to variability of raw materials. Unfortunately, often the quality of raw materials cannot be assessed and maintained.

Instrumentation for Food Safety

From a food safety perspective, it is necessary to ensure that pathogenic and spoilage microorganisms are destroyed during food processing. Usually, thermal treatments are used to eliminate microorganisms. Two main approaches can be used to ensure the safety of foods. First is the assessment of microbe survival by conventional plating methods that take up to 48 h. Some rapid methods including immunosensors are currently being researched. Alternatively, knowing the kinetics of thermal inactivation of a target microorganism, time and temperature are adjusted to ensure that the target microorganism has been destroyed to an 'acceptable' extent. This has led to the not uncommon practice of 'over-processing' foods to the detriment of other quality attributes such as texture, flavor and nutritional value. Also, this approach requires recording the time-temperature history at the coldest location (cold spot) of the product. In processes where traditional instrumentation, like thermocouples or resistance temperature detectors (RTDs) cannot be implemented because of mechanical or cost impediments, alternative means of measuring the time-temperature history are needed.

Biosensors in Food Analysis

Through thousands of years of evolution, living organisms have developed means of detecting and controlling the concentration of numerous compounds in complex mixtures in living organisms. Antibodies and enzymes are probably the best-known examples of natural sensing and controlling 'devices'. The ability to isolate and purify these proteins and other biological elements such as cells or organelles has allowed their integration with physicochemical transduction devices to produce biosensors. Biosensors

are defined as: ‘a self-contained analytical device that incorporates a biologically active material in intimate contact with an appropriate transduction element for the purpose of detecting (reversibly and selectively) the concentration or activity of chemical species in any type of sample’(Arnold and Meyerhoff, 1988). Figure 1 shows a general schematic representation of a biosensor.

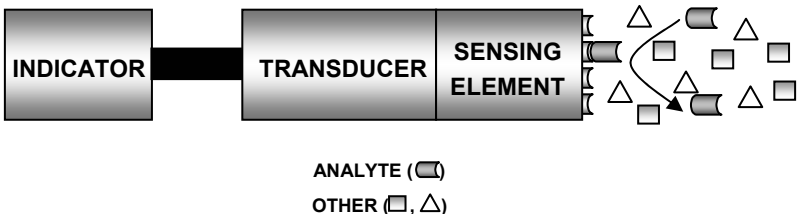

Figure 1. General schematic representation of a biosensor

The first biosensor, an enzyme-based glucose sensor, was developed by Clark and Lyons (Clark and Lyons, 1962). Since then, hundreds of biosensors have been developed in many research laboratories around the world. Figure 2 shows the number of

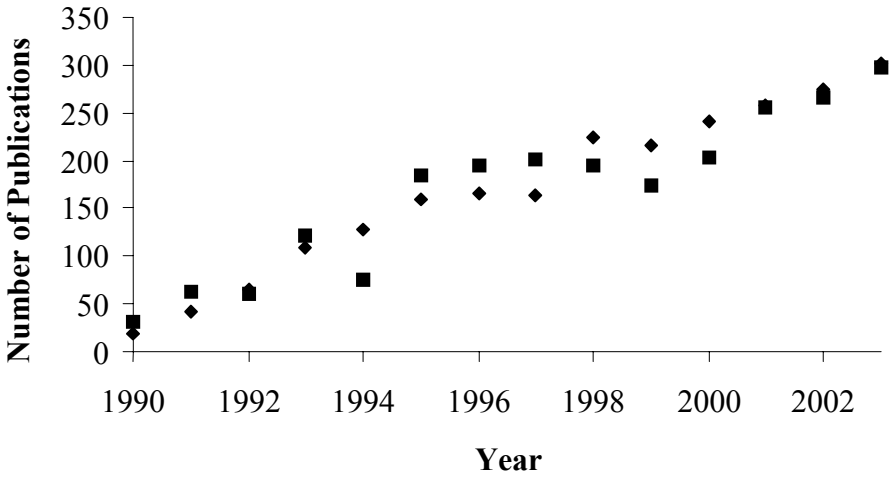

Figure 2. Number of publications with keyword ‘biosensor’ as reported by (6) OCLC Article First and (+) Elsevier Science Direct journal article databases.

publications provided by Online Computer Library Center Inc. (OCLC) Article First and Elsevier's Science Direct databases when the word 'biosensor' is entered as keyword. This figure shows a steady growth of the number of publications for the last thirteen years. It is surprising that very few biosensors have been commercialized in spite of the number of publications. This derives probably from the small number of analytes that have been extensively studied, that is, glucose, urea, lactate and alcohol. Many other analytes have been investigated to a limited extent, but apparently have not reached the commercial development. A major aspect in the commercialization of biosensors is of course the market. Medical diagnosis is the strongest driving force; hence, most of the efforts and funding are in this area. The enormous number of food components that determine their quality attributes and that are in complex mixtures make biosensors potential tools for monitoring such components during food processing and storage. However, relatively few biosensors for food applications are being developed. In a short review of the potential applications of biosensors to food quality control, Despande and Rocco (1994) pointed out that the potential applications of amperometric and potentiometric biosensors included the measurement of amino acids, amines, amides, heterocyclic compounds, carbohydrates, carboxylic acids, gases, cofactors, inorganic ions, alcohols and phenols. Typical analytes measured in the food industry are listed in Table 1 (modified from Scott (1998)). In that review no commercially available biosensor is mentioned. Table 2 lists the biosensors that have been researched for applications in the food industry. Figure 3 shows the number of publications provided by the OCLC Article First and Elsevier Science Direct databases when the keywords 'biosensor and food' and were used. On average, only 3.5% of the research carried out on

Table 1. Analytes that need to be detected in the food industry

Analyte	Foods	Typical Analytical Method
Acidity	Beverages, fruit, vegetables	Titration, pH meter
Alcohol	Beverages	
Antibiotics	Dairy, meat	HPLC, Microbial plate, Immunoassay
Color	Beverages, fish, fruit, meat, vegetables	Spectroscopy, Colorimetry
Fat type	Dairy, fish, meat, nuts	Extraction, Gravimetric techniques
Fatty Acids	Dairy, fish, meat, nuts, vegetables	GC, HPLC
Flavors	Beverages, cereal, dairy, fish, fruit, meat, vegetables	GC, HPLC
Hormones	Dairy, meat	HPLC, Immunoassay
Microbial Species Bacteria & fungi	Beverages, cereal, dairy, fish, fruit, meat, nuts, vegetables	Plate techniques Immunoassay
Minerals	Beverages, cereal, dairy, fish, fruit, meat, nuts, vegetables	Combustion, AAS, ICPMR, NAA, AES, X-ray fluorescence
Pesticides	Beverages, cereal, dairy, fish, fruit, meat, nuts, vegetables	GC, GC-MS, HPLC
Preservatives	Beverages, cereal, dairy, fish, fruit, meat, nuts, vegetables	Spectroscopy, HPLC
Protein	cereal, dairy, fish, fruit, meat, nuts, vegetables	Kjehldal digestion
Sugars and Sweeteners	Beverages, cereal, dairy, fruit, vegetables	Spectroscopy Refractometry HPLC, GC
Toxins - aflatoxins	Beverages, cereal, dairy, fish, fruit, meat, nuts, vegetables	HPLC Immunoassay
Vitamins - vitamin A - vitamin B - vitamin C - vitamin D - vitamin K	Beverages, cereal, dairy, fish, fruit, meat, nuts, vegetables	Spectroscopy HPLC Microbial plate Immunoassay
Water/ Moisture	Beverages, cereal, dairy, fish, fruit, meat, nuts, vegetables	Oven drying Karl Fisher titration Refractometry NMR NIR

Table 2. Enzyme biosensors that have been researched for food applications (modified from (Warsinke et al. 1998))

Analyte	Food	Enzyme	Linear Range (mM)
Glucose/ Sucrose	Beverages	IN/GOD	0.2-2.8 0.5-7.0
Glutamate	Seasonings	GLOD	0.001-1.0
Ethanol	Beer, wine	AOD ADH	0.001-0.8 1.0-100
Isocitrate	Fermentation broth	ICDH/POD	0.1-2.0
Lactose	Milk	β-GAL/POD	0.002-3.0
Putrescine	Fish	Putrescine oxidase	0.03-3.0 (μM)
Spermidine	Fish	Putrescine oxidase	
Cadaverine	Fish	Putrescine oxidase	
gluconolactone	Fermentation broth	GDH/GOD	0.02-1.0
Fatty acids	Oils	LOX	0.1-1.2
Acetic acid	Vinegar	AK/PK/LDH	10.80

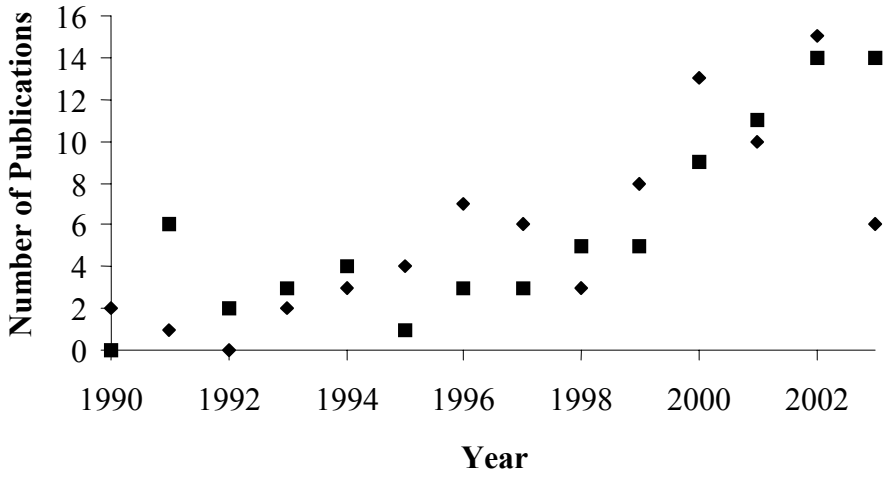

Figure 3. Number of publications with keywords 'biosensor' and 'food' as reported by (6) OCLC Article First and (+) Elsevier Science Direct journal article databases.

Still, the availability of commercial biosensors is well below the potential they seem to the food industry (Scott, 1998).

biosensors focused on foods. From an economic perspective, this can be explained by the relatively small market for these instruments in the food industry as compared to medical diagnosis market.

The difficulty of developing biosensors starts with the selection of the sensing element, which has to be sensitive, reversible and selective to the analyte. Once a sensing element is selected, the development of a biosensor requires increasing the stability of the biological sensing element taking into account its unique requirements. This occurs because the rate of degradation of enzymes and antibodies increases with temperature and in very high or very low pH environments. Also, while protein structure provides selectivity, reversibility and sensitivity, it also makes it difficult to develop a single technology for biosensor fabrication. That is, effective immobilization of the biological component while retaining activity depends on the biological component and on the environment to which it will be exposed. Furthermore, selection of the method of transduction depends on the type of physical or chemical change that the immobilized sensing element can produce. Other challenges in the commercial development of biosensors for on-line monitoring and control of food processes include the ability to sterilize, interferences by other food components, miniaturization and poor fabrication reproducibility caused by variability in biological elements as raw materials (Despande and Rocco, 1994). Because of the short operational life of the biological sensing element, two strategies have been adopted. The first deals with stabilization of the sensing element by chemical and physical means. The second is based on reducing the costs of fabrication to produce disposable sensors that are commercially viable. In biomedical applications the latter is being used while on-line processing industry requirements may not allow

frequent replacement. For industrial food applications the two main challenges are to produce ‘dipstick-type’ electrodes for batch measurements in the quality assurance laboratory and on-line sensors that allow direct sensing and rapid feedback for the control of processes.

Time-Temperature Integrators in Food Processing

In view of the need for assessing the quality of thermally processed foods in industry, there have been three main approaches: 1) The *in situ* method, which measures a quality attribute of the food before and/or after the process (e.g. enzyme activity to assess blanching of vegetables). 2) The physical-mathematical approach, which uses the temperature history of the product or its surroundings along with known kinetics of the change of a target quality attribute, to calculate the extent of that change. 3) Product history integrators defined as 'a small device that shows a time temperature dependent, easily, accurately and precisely measurable irreversible change that mimics the changes of a target quality parameter undergoing the same variable temperature exposure'. When considering only temperature changes with respect to time, product history integrators are called time-temperature integrators (TTI) (Hendrickx et al. 1994). Extrinsic and intrinsic TTIs from different origins (microbiological, enzymatic, chemical and physical) have been compared (Haentjens et al. 1998). Enzymatic TTIs offer the advantage of being relatively easy to assay, low cost and the thermal resistance of some enzymes to denaturation or loss of activity is similar to the thermal resistance of some pathogens. Furthermore, the thermal resistance of enzymes can be modified (though to a limited extent) and can be determined. α-amylase is probably the best known enzyme-based TTI.

(Van Loey et al. 1996). To effectively assess the temperature history at given point in any king of food extrinsic, isolated TTIs are the best option because they their thermal properties can be well characterized, they are isolated from chemical effects of food components, and can be placed at any desired location in the food. However, heat transfer between the food and the TTI must be maximized to minimize heating transient phase. Different types of encapsulation have been tried. Depending on the nature of the TTI, (liquid, powder or gel) two main problems may arise. First, temperature gradients inside the capsule may exist and be variable due to different degrees of 'packing'. Second, a part of the TTI may adhere to the surface of the capsule, making its recovery difficult for rapid assay.

Context and rationale of this research

In response to the food industry's needs, several research projects have been carried out through the collaboration of the Departments of Biological Systems Engineering and Food Science and Human Nutrition at Washington State University. These projects embrace mainly alternative technologies for industrial food processing such as microwave and radio frequency processes or non-thermal processes like high hydrostatic pressure or pulsed electric fields. Improvement of existing technologies and implementation of emerging technologies require adequate instrumentation for process control. This need led to several research projects that include, for example, the development of texture analyzers and enzyme activity sensors.

This project belongs to the area of instrumentation research. Being the first project in biosensors in the department, the first stage of this research dealt with learning

what is a biosensor, what types of biosensors have been developed and, after selecting an area of research, a very large amount of work was devoted to the development of infrastructure, that is, to equipping a laboratory and learning and developing experimental techniques from scratch. Therefore, the sequence and rationale for each of the manuscripts that constitute this dissertation derives not only from an initial set of objectives but also from the needs encountered and knowledge acquired as the project progressed. Figure 4 shows the decision tree that was followed and it is complemented by Table 3 that summarizes the general rationale for the decisions taken at the major steps of this project. I decided to work with amperometric enzyme biosensors because many enzymes produce or consume electroactive species that can be electrochemically detected and the sensitivity of such sensors can be increased by adjusting the potential. In addition I had some experience in enzyme activity sensors and electrochemistry.

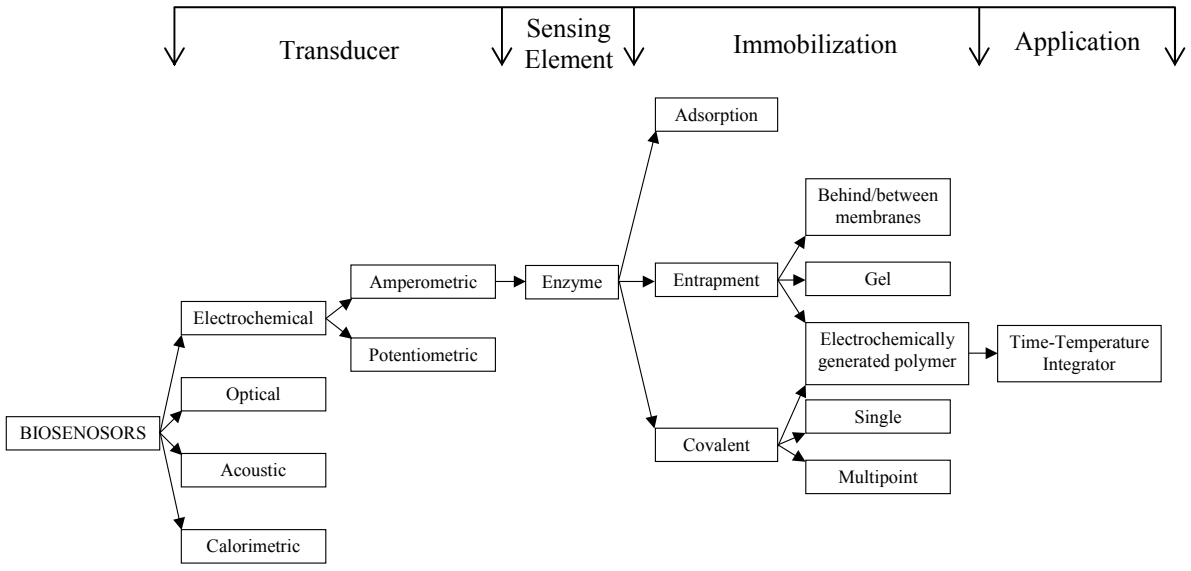

Figure 4. Decision tree for this research

From the literature review (Chapter Two), it appeared that fabrication of an enzyme biosensor using enzyme immobilization in electrochemically-generated polymers seemed the most promising technology because of the apparent simplicity of fabrication that involves a one step potentiostatic electropolymerization that results in films with controllable thickness with enzyme uniformly distributed and with permselective

Table 3. General rationale behind and output from the focus that was given to this research

	Topic	Transducer		Sensing element	Immobilization Matrix		Application
		Group	Type		Group	Type	
Focus/Decision	Biosensors	Electrochemical	Amperometric	Enzymes	Entrapment	Electrochemically generated polymers	Time-temperature integrator
Rationale	Industrial need	Experience in electrochemistry	Most compatible with enzymes	Experience with enzyme assays	Good enzyme retention	One step, uniform enzyme distribution	Industrial Need Original application for an enzyme biosensor
Output	Chapter two	Chapter four		Chapter three			Chapter five

properties that allow the rejection of interfering species. Polypyrrole and glucose oxidase were chosen for the first study (Chapter Three) because they are the most commonly used electropolymer-enzyme system. From this study we found that the use of polypyrrole has several drawbacks. Polypyrrole conductivity changes over time at potentials used for the detection of H_2O_2 produced by glucose oxidase. Therefore, it needs to be overoxidized to eliminate its electrical conductivity and work as an immobilization matrix only. Overoxidation requires time, and modifies the backbone and side chains of the polymer, which frequently results in detachment from the platinum electrode. In addition, nucleation is critical in the formation of polypyrrole films. Polypyrrole nucleation and growth is very irreproducible. Also, the presence of enzyme inhibits polypyrrole polymerization; therefore enzyme concentration cannot be large which results in

biosensors with low sensitivity. This directed the research to a different polymer and to focus on means of increasing the sensitivity of amperometric biosensors.

Poly-*o*-phenylenediamine (PoPD) was chosen because it is a non-conducting polymer that forms thin films upon electrochemical polymerization. Platinization has been used to increase the surface area of platinum electrodes, which results in an increase in sensor sensitivity to H_2O_2. However, the literature reports that increases in sensitivity are very small compared to the increase in electrode electrochemical surface area. Therefore, the next set of experiments dealt with improving platinization conditions and combining them with the use of PoPD as an immobilization matrix for GOD (Chapter Four).

Some enzymes have rates of thermal inactivation that are similar to those of microorganisms and have been used to make time-temperature integrators for assessment of the efficacy of thermal processing of foods. To the best of my knowledge, there is no commercial enzyme-based TTI. However, some TTIs have been developed using mainly α-amylases and peroxidase. While I was studying the thermal stability of GOD to look for means of stabilizing it and hence extending GOD biosensor operational life, I realized that its thermal stability was similar to that of peroxidase, which makes it a potential TTI candidate. In addition, assessing the activity of TTIs is either expensive or time consuming. Therefore, I hypothesized that biosensor technology could be applied to the development of rapid and inexpensive TTIs (Chapter Five).

This research remained focused on the hypothesis that the stability and sensitivity of enzymatic amperometric biosensors could be improved through use of electrically conducting polymers as an immobilization medium. As this research progressed,

anticipated and unanticipated technical and fundamental challenges were encountered. Through the objectives stated below, I pursued those challenges dealing with the increase of sensitivity that seemed necessary to gain as much understanding as possible of an already existing but not fully developed technology, to fill some scientific and engineering voids that I found in the literature and to advance biosensor research in the Department of Biological Systems Engineering.

Objectives

1. To review the biosensor literature and select an area of research.
2. To investigate the effect of fabrication conditions on electrode's response in terms of film permeability and electrode surface area coverage by studying the polypyrrole-glucose oxidase system
3. To increase the sensitivity of glucose oxidase amperometric biosensors through improved platinization conditions and the use of electrochemically generated poly-o-phenylenediamine as immobilization matrix.
4. To apply amperometric biosensor technology to the development of rapid and inexpensive time-temperature integrators

Background

Enzyme immobilization

The most common methods for enzyme immobilization are physical adsorption, covalent attachment, cross-linking and entrapment (see Figure 5).

Physical adsorption

Physical adsorption (Figure 5a) results from hydrophobic, hydrophilic or ionic interactions between the protein and a solid surface. It was the first immobilization method ever used in the fabrication of a biosensor (Clark and Lyons, 1962). The most commonly used supports for enzyme adsorption are silica, cellulose acetate membranes, PVC and polystyrene (Taylor, 1996). There is evidence that physical adsorption of enzymes may stabilize their activity (Zoungrana et al. 1997). However, this type of immobilization alone leads to enzyme leakage especially with changes of pH and temperature. Therefore, adsorption is frequently used in combination with other immobilization techniques. Adsorption often spontaneously occurs when an enzyme in solution is exposed to a solid phase that may be an insoluble monomer prior to polymerization, a polymer, colloidal metal particles etc.

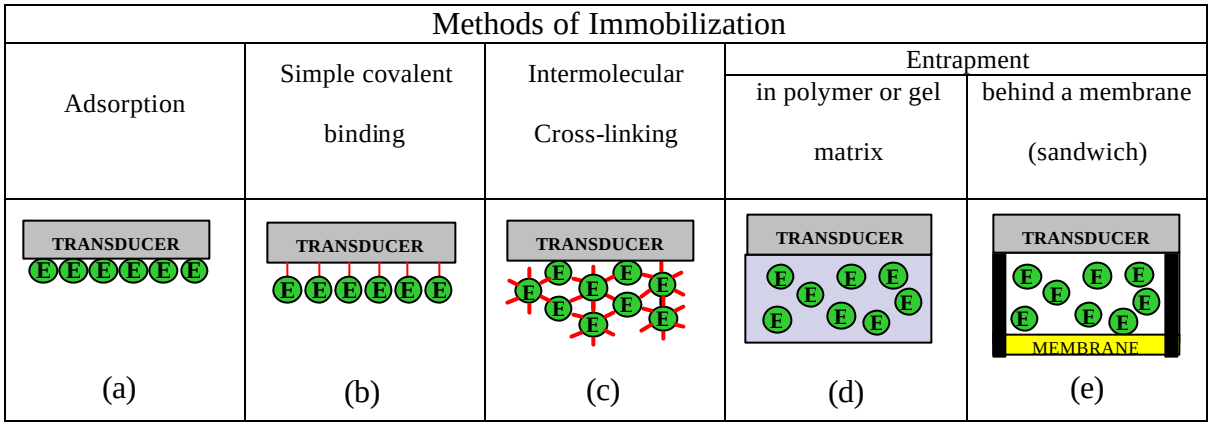

Figure 1. Schematic representation of different methods of enzyme immobilization

Covalent binding

Single covalent attachment

Covalent binding solves the problem of enzyme leakage but often results in loss of enzyme activity because covalent attachment often takes place under conditions that denature enzymes. However, covalently immobilized enzymes sometimes show greater resistance to pH and temperature variations (Taylor, 1996). Covalent binding has been widely used for immobilization of antibodies and to lesser extent for the immobilization of enzymes. In most instances covalent attachment of enzymes to solid supports (Figure 5 b) has been performed through activation of enzyme carboxylic side chains with a carbodiimide followed by condensation with a derivatized surface containing amino groups. In other cases activation of carboxylic derivatized surface with a carbodiimide followed by condensation with amino groups of the enzyme's side chains has been used (see Figure 6). (Schuhmann, 1991; Wolowacz et al. 1992; Divya et al. 1998).

Multiple covalent attachment

Intermolecular cross-linking

Intermolecular cross-linking (Figure 5c) has been widely used in the immobilization of enzyme for use in biosensors (Divya et al. 1998). Most of the time intermolecular crosslinking results in activity loss. Furthermore, due to its random mechanism and fast reaction rate it is difficult to obtain reproducible sensors. However indirect (through a dried gelatin layer), mild cross-linking with glutaraldehyde used in combination with other immobilization techniques has resulted in sensors with increased

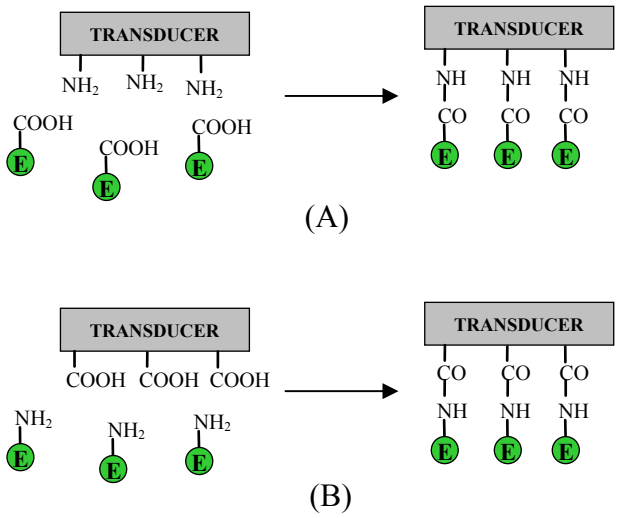

Figure 6. Covalent binding of an enzyme to a solid support through carbodiimide condensation.

stability (Khan and Wernet, 1997). The most commonly used crosslinking agent is glutaraldehyde whose aldehyde groups react with amine groups from protein's side chains as depicted in Figure 7.

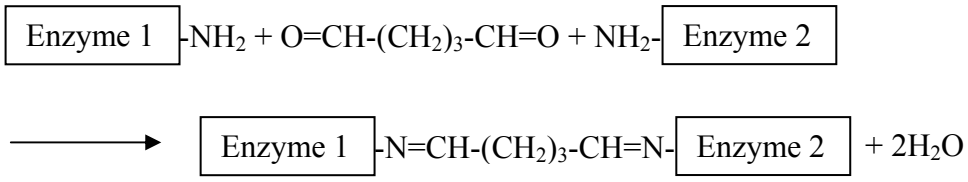

Figure 7. Intermolecular cross-linking with glutaraldehyde.

Intramolecular cross-linking

Intramolecular cross-linking for enzyme stabilization has been demonstrated using bifunctional reagents (Fernández-Lafuente et al. 1995) or a poly(glutaraldehyde-like) molecules (Fernández-Lafuente et al. 1993). Covalent bonds result from the reaction between aldehyde groups of the cross-linker and amine groups of the same

protein. Multipoint covalent attachment has been reported using soluble polysaccharides (Lenders and Crichton, 1984) or solid agarose gel supports (Guisán, 1988). Multiple covalent bonds result in reinforced quaternary and tertiary protein structure (Fernández-Lafuente et al. 1993) providing stabilization of up to 30,000-fold compared to enzyme in solution for a thermophilic esterase (Fernández-Lafuente et al. 1995). The main drawback of these techniques is that they cause loss of enzyme activity. These methods have not been tried with glucose oxidase or lactose oxidase. To the best of our knowledge intramolecular multipoint covalent attachment has not been reported for use in biosensors, nor has it been combined with electrochemical polymerization.

Entrapment

Between membranes

Enzymes have been entrapped by several methods. The first was between two semipermeable membranes (Figure 5e). This method of entrapment does not stabilize the enzyme. At best, it prevents enzyme leakage and decreases the flux of inhibitors or interfering compounds. Membranes are widely used for the latter purpose in most of the commercial electrochemical enzyme biosensors.

Self-assembled layers

Several enzymes and other proteins occur in natural bilipid membranes (BLMs) that are very thin and have been used for the fabrication of electrochemical biosensors. An advantage of BLMs is that ferrocene has been incorporated as a mediator. Other mediators may be incorporated too. Alcohol dehydrogenase was immobilized with stearic acid and the monolayer transferred onto a polypyrrole coated glass electrode (Pal et al.

1994). Glucose oxidase and monoamine oxidase both stabilized in amphiphilic polyelectrolytes have been immobilized using the Langmuir Blodgett technique (Eremenko et al. 1995). Another BLM sensor was used glucose oxidse immobilized in 3-mercaptopropionic acid using carbodiimide coupling, as demonstrated by Gooding et al. (1998). The electrochemistry of bilayer lipid membranes was reviewed by Tien et al. (1997). Self-assembled layers are reported to be more sensitive than electrodes made with other immobilization techniques. However, self-assembled layers are in general unstable and their use is limited to research with little if any possibility of resulting in stable biosensors (Taylor, 1996). Therefore, their application may be limited to disposable sensors or to well controlled measuring conditions.

Sol-gel technique

Sol-gel techniques have also been used to immobilize enzymes for biosensor applications. While these techniques provide an environment similar to that of the enzyme in solution and the resulting sols are ideal for optical transduction, this technique has two main limitations. First, the properties of the sol, namely volume and pore size, change as condensation reaction continues. Second, once the sol is dry and stable, the pore size is so small that the enzyme reaction is limited by diffusion (Bakul et al. 1994). To overcome these limitations, thin films have been tried (Wang et al. 1999); but these films easily crack. To prevent cracking and swelling of the hydrogel, organic-inorganic hybrid materials are being investigated (Guo and Dong, 1997, Wang et al. 1998, and Li et al. 1998). Most studies on enzyme entrapment and in particular entrapment in polymers deal mainly with increasing sensitivity and measuring range and decreasing response time and detection (Liu et al. 1998; Zhu et al. 2000). This has been approached by

increasing active enzyme concentration and retention in the immobilization matrix and reducing thickness. While electrostatic interactions between conducting polymers and enzymes may have stabilization effects, these have not been studied in depth nor have they been used as a strategy for enzyme stabilization. No extended operational life appears to derive from these techniques.

Polymerization

Entrapment can also be achieved by polymerization in a monomer-enzyme solution (Figure 5d). Depending on the type of polymer, polymerization can be driven chemically, electrically (electropolymerization) or by light (photopolymerization). The most frequently used polymerization technique in electrochemical biosensor fabrication is electropolymerization (Bartlett and Cooper, 1993; Trojanowicz et al. 1995; Cosnier, 1999). The most common monomers used for electrochemical polymerization are pyrrole, aniline and o-phenylenediamine (see Figure 8) but several other have been tried. Electropolymerization allows the accurate control of the polymer's growth and hence the thickness of the enzyme containing film that builds on the surface of the electrode. Electropolymerization also has the potential for use in co-immobilization of several

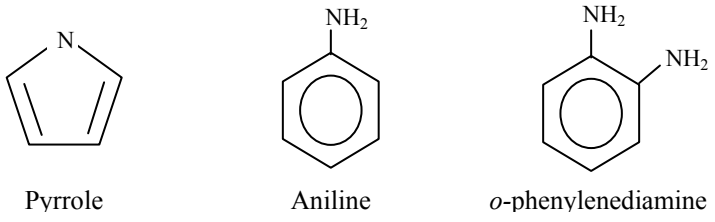

Figure 8. Most commonly used monomers for electrochemical polymerization

enzymes (Liu et al. 1998), in segregated layers with multiple enzymes

and in the fabrication of microsensors and arrays of microsensors (Bartlett and Cooper, 1993; Trojanowicz et al. 1995). There is evidence of direct electron transfer between the immobilized enzyme and conducting electropolymers (Cosnier, 1999). Polymer films may also work as a barrier against electrochemically interfering substances such as ascorbate (Palmisano et al. 1995; Coche-Guerente et al. 1995). Ultra-thin polypyrrole films grown from supporting electrolyte free solutions have been studied recently (Adeljou and Moline, 2001). Finally, redox mediators have been polymerized and have been shown to work as both enzyme hosts and charge mediators (Yang et al. 1998). Several studies have been published in the polymerization of pyrrole and its derivatives focusing in particular on solvent (Miras et al. 1991; Miras et al. 1991; Masuda and Kaeriyama, 1995; Saçak et al. 1997; Fusalba and Bélanger, 1999), metal support (Saçak et al. 1997; Su and Iroh, 1997), anions (Vork et al. 1990; Li, 1997), electrochemical parameters (Wang et al. 1989) and their electroanalytical (Holdcroft and Funt, 1988), optical, electrical (Aguilar-Hernández and Potje-Kamloth, 1999), conductance (Kankare and Kupila, 1992), thermoplastic, elastic (Wernet, 1991; Yamato et al. 1993) and morphological (Everson and Helms, 1991) properties. Incorporation of enzymes (mainly glucose oxidase) in such polymers has been addressed (Foulds and Lowe, 1986; Umana and Waller, 1986). The effects of enzyme concentration (Shin and Kim, 1995; Shin and Kim, 1996a), monomer type (Coche-Guerente et al. 1995) and concentration, ion nature and concentration (Mu and Jinquing, 1995) and buffer (Pei and Qian, 1992) on the electrochemical response to the analyte of interest (Bélanger et al. 1989) have been determined. However, the interaction of enzyme and monomer concentrations has not been investigated. Physical properties of the immobilization

matrix such as permeability (Hämmerle et al. 1992) and film thickness (Almeida et al. 1993; Shin and Kim, 1995) have been addressed but have not been correlated to the electropolymerization conditions. Most studies use electrode geometric surface area instead of the electrochemical surface area, which leads to errors in the interpretation of sensor reproducibility. Also, the decrease in effective surface area for electrochemical detection with polymer growth has not been addressed. Therefore, the confounded effects of diffusion and surface coverage cannot be separated, leading to inaccuracies in the interpretation of the electrochemical response of such electrodes. While some models exist that describe the steady state (Gough et al., 1982; Leypoldt and Gough, 1984; Bartlett and Whitaker, 1987a; Bartlett and Whitaker, 1987b; Lyons et al. 1991; Marchesiello and Genies, 1993; Gros and Bergel, 1995) or dynamic behavior (Bergel and Comtat Maurice, 1984; Tse and Gough, 1987; Lucisano and Gough, 1988; Bacha et al. 1993) of enzyme-based electrochemical biosensors, there is a lack of information to predict the parameters needed by such models. Also there are very few published studies on sensor optimization (Fortier et al. 1990; Adeloju et al. 1993; Shin and Kim, 1996b; Lin and Guthrie, 1998) most of which are not rigorous. Finally, multilayer electrodes have shown improved response and storage life (Trojanowicz et al. 1995) but no mathematical model incorporating multilayers has been published for optimization of such electrodes.

Combination of immobilization techniques has been used. An important increase of thermostability of enzymes covalently attached to monomers and followed by chemical copolymerization was demonstrated (Martinek et al. 1977). Adsorption has been combined with almost all other immobilization techniques. Electrodeposition has

been combined with cross-linking (Stonehuerner et al. 1992; Crumbliss et al. 1992) and covalent attachment has been combined with self-assembled monolayers (Gooding et al. 1998). However, only three studies have been published by one research group on multipoint covalent attachment combined with electrochemical polymerization (Wolowacz et al. 1992; Yon-Hin B.F.Y. et al. 1993; Yon Hin and Lowe, 1994) and increased enzyme stability was reported. Variations on this strategy offer the potential for large increase in enzyme stability. Furthermore, this strategy needs to be combined with others to obtain good reproducibility and higher sensitivity.

Electrode Platinization

Platinization

Electrochemical platinization of platinum is commonly done to increase the catalytic surface area of platinum electrodes. Platinum platinization dates from the late 19^{th} century. In early works platinization was carried out mostly from chloroplatinic acid and focused on bath composition. Lead acetate was identified as a grain growth inhibitor and it is still commonly used. In the early 1960s, with the development of operational amplifiers and potentiostats, quantitative electrochemical experiments became possible. One of the first reviews on platinum platinization (Feltham and Spiro, 1971) discusses these early works and effects of electrodeposition conditions on deposit appearance, deposit growth, surface area and reproducibility. The effects of substrate preparation and platinization conditions on adhesion are also discussed. Platinization from solutions containing 0.072 M (3.5%) chloroplatinic acid, 1.3×10^{-4} M (0.005%) lead acetate at current density of 30 $mA.cm^{-2}$ for up to 10 min was recommended for electrodes to be

used in conductance or electrocatalysis work. Potentiostatic deposition at 50 mV vs. normal hydrogen electrode (NHE) from 0.041 M (2%) chloroplatinic acid, 1 M HCl solution was recommended whenever platinized electrodes were to be used for analytical applications (Feltham and Spiro, 1971). Literature on platinization during the 1970s and early 1980s is rather scarce probably because several patents dealing with platinum bath composition were issued during the late 1960s. Two more recent short reviews discuss different platinization baths and deposition conditions (Baumgärtner and Raub, 1988; Hadian and Gabe, 2001). In general, platinization baths can be separated into those containing the divalent platinum and those containing the tetravalent form. Most platinization baths are acidic but some alkaline baths have also been developed (Le Penven et al. 1992; Basirun and Pletcher, 1998; Djokic, 2000). Table 4 shows some reported platinization baths and platinization conditions. There are few experimental studies comparing platinization baths (Pushpavanam and Natarajan, 1988; Hadian and Gabe, 2001). Comparing reports from different sources is difficult because substrates, substrate pretreatments, and analyses are different. Except for dinitrosulphatoplatinous acid that can be used at or near room temperature, temperatures above 70 ºC are recommended for all other baths to produce strong, adherent deposits. Gas evolution can cause non-uniformities in platinum deposits so bath formulation and deposition potential should be controlled to prevent it. Agitation and vertical orientation of the surface to plate can mitigate the effects of gas evolution.

Table 4. Summary of platinum baths and plating conditions

Platinum salt and concentration ($g \cdot L^{-1}$)	Other electrolyte	Other electrolyte concentration ($g \cdot L^{-1}$)	Temperature (ºC)	Current density ($A \cdot dm^{-2}$) or Potential (mV vs. Ag/AgCl)	Reference
$H_2(PtCl_6)$ 10-50	HCl	180-300	45-90	2.5-3.5	(Baumgärtner and Raub, 1988) and references there in
$(NH_4)PtCl_6$ 15	$Na_3C_6H_5O_7.2H_2O$ NH_4Cl	100 4-5	80-90	0.5-1.0	
$Pt(NH_3)_2(NO_2)_2$ 8-16.5 6-20	NH_4NO_3 $NaNO_2$ H_3PO_4 H_2SO_4	100 10 10-100 10-100	90-95 75-100	0.3-2.0 0.5-3.0	
$H_2Pt(NO_2)_2SO_4$ 10	H_2SO_4	pH 2.0	30-70	2.5	
$Na_2(Pt(OH)_6).2H_2O$ 20	NaOH	10	75	0.8	
$H_2(Pt(OH)_6)$ 20	KOH	15	75	0.75	
$K_2(Pt(OH)_6)$ 20	K_2SO_4	40	40	0.3-1.0	
$PtCl_4.5H_2O$ 7.5	NH4Cl $(NH_4)_2HPO_4$ Na_2HPO_4	20-25 20 100	70-90	0.3-1.0	
$H_2Pt(NO_2)_2SO_4$ 5	pH 1.8		Ambient (20-25)	0.5-1.0	(Pushpavanam and Natarajan, 1988)
$Pt(NH_3)_2(NO_2)_2$ 10	NH_4NO_3 $NaNO_2$ NH_3	100 10 to pH 7.5	65-70	1.5-2.0	
$K_2(Pt(OH)_6)$ 10	KOH $Na_2C_2O_4$ Na_2SO_4	10 5-6	70	1.0-1.5	
$Pt(NH_3)_4HPO_4$ 26 mM	Na_2HPO_4	28 mM (pH 10-11)	80-93	0.64	(Le Penven et al. 1992)
$Pt(NO_2)(H_2O)_3^+$ 6 (Pt basis)	KNO_2 CH_3SO_3H	42 mM 1.5 M	20-70	0.1-1.5	(Levason et al. 1998)
$Pt(NH_3)_4HPO_4$	Phosphate Buffer	30 mM pH 10.4	95	-700 mV	(Basirun and Pletcher, 1998)
$Pt(OH)_6^{2-}$ 6	KOH	20	60-70	<-600 mV	(Djokic, 2000)
$Pt(NH_3)_2(NO_2)_2$ 16.5	NH_4NO_3 $NaNO_2$ NH_4OH Na2HPO4 $(NH_4)_2HPO_4$	100 10 50 mL/L 85-213 40-158	84-8	025	(Hadian and Gabe, 2001)
$Na_2(Pt(OH)_6).2H_2O$ 20	NaOH $Na_2C_2O_4$ Na_2SO_4	5.6 5.6 33.7	80	0.75	

Platinization for amperometric biosensors

Most amperometric enzyme biosensors have been fabricated using polished platinum or graphite (glassy carbon) electrodes. However, to increase sensitivity, in particular for the fabrication of microelectrodes, platinum and other electrodes have been platinized (Zhang et al. 1996; Kim and Oh, 1996). In all cases chloroplatinic acid solutions at concentrations from 0.1% to 5% were used and in most cases platinization was carried out under potentiostatic conditions at typically -150 mV or more negative potentials. Temperature of platinization was not mentioned in these publications. The effect of potential on roughness of platinum deposits for fabrication of glucose biosensors has been reported (Kim and Oh, 1996) but enzyme was immobilized by crosslinking with BSA and glutaraldehyde. Galvanostatic platinization (Castner and Wingard, 1984; Kell and Davey, 1990) and platinization using potential cycling (Schuhmann, 1998) have also been reported. However studies on the effect of platinization conditions on biosensor response are scarce. To the best of our knowledge there has been no study on the effect of platinization potential on the response of amperometric biosensors based on enzyme immobilization in electrochemically-generated polymers. We carried out preliminary platinization experiments using 2 mM chloroplatinic acid 1 mM lead acetate and 0.1 M KCl at –250 mV vs. Ag/AgCl. Deposits were brittle and easily wiped off the platinum substrate.

Other recent applications of electrodeposition of platinum include surface-enhanced infrared absorption of CO (Bjerke et al. 1999), non-enzymatic detection of

glucose (Park et al. 2003) and fabrication of hydrogen peroxide sensors (Evans et al. 2002).

Stainless steel electroplating

The last objective of this dissertation deals with the application of biosensor technology to the fabrication of time-temperature integrators (TTIs). While further background on TTIs will be given in the next section, one of the preparation steps of the reported TTI (see Chapter Five) involves platinization of a stainless steel tube. Immobilization of glucose oxidase in PoPD electropolymerized directly on 316 stainless steel was attempted. However, o-phenylenediamine polymerizes at potentials greater than 400 mV vs. Ag/AgCl. Under these conditions, stainless steel oxidized and it was not possible to form an adherent polymer film. A recent study on the electrochemistry of some stainless steels provides information on the passivation and potentials at which stainless steel remains inert (Tomov and Tsoneva, 2000). Therefore, a platinization step was implemented in the procedure. There are few reports on stainless steel electroplating because in most cases plating is used to prevent corrosion and stainless steel is relatively inert. However, plating chromium on stainless steel is a very common practice in the manufacture of silverware. A standard practice for electroplating stainless steel gives general guidelines but needs to be adapted in function of the metal to plate (ASTM B 254, 1992). Another other study of platinization on different materials even discards stainless steel as a suitable substrate (Stoychev et al. 2001). Stainless steel activation is required to remove passive metal oxides that cause weak adhesion of deposits. Activation may consist of immersion in hot (50 ºC to 70 ºC) concentrated solutions of sulfuric and

hydrochloric acids. A nickel intermediate deposit (nickel strike) is also recommended to enhance adhesion (Wood, 1938; Dini, 1996). Platinic acid solutions in HCl are usually very acidic and therefore not recommended for non-noble substrates, therefore, alkaline platinization baths have been used for platinization of stainless steel (Djokic, 2000).

Time-temperature integrators

Assessment of the temperature history is necessary to ensure microbial inactivation during food processing or to ensure that the cold chain has not been broken during cold storage of fresh and minimally processed foods. It is not always possible or cost effective to instrument food processes with conventional temperature devices such as thermocouples or resistance temperature devices. Also, it is not possible to install temperature-recording devices in all packages of refrigerated foods. Therefore, alternative devices called time-temperature integrators (TTIs) have been developed. TTIs can be defined as small devices that show a time-temperature dependent, easily and precisely measurable irreversible change that accurately mimics the changes of a target quality attribute undergoing the same variable temperature exposure (Hendrickx et al. 1995).

TTIs for cold storage have been reviewed (Labuza et al. 1992). Some recent publications are available (Taoukis Petros et al. 1999; Giannakourou and Taoukis, 2003). Commercial devices have been developed but no further discussion on TTIs for refrigerated foods is given here because this research deals with TTIs for assessment of thermal processing.

Since the early 1920s, studies on the kinetics of thermal inactivation of microorganisms were carried out to establish endpoint of heat processes for food preservation, in particular canning. This approach, called physical-mathematical method, has been the subject of continuous research and has been recently reviewed (Stoforos et al. 1997). The physical-mathematical method has been commonly used in the food industry and has proved effective. However, variation in processing parameters and the existence of irreproducible temperature gradients (Smout et al. 2000) forces processors to over expose food to heat to the detriment of other quality attributes such as texture and flavor. Furthermore, over-processing does not obviate the need of microbial tests that are time consuming and hence do not allow rapid feedback for process control. To overcome the limitations of this approach TTIs have been developed and are the subject of current research. Some reviews on TTIs have been published (Hendrickx et al. 1995; Van Loey et al. 1996a; Van Loey et al. 1996b). TTIs have been classified according to their working principle: biological, chemical or physical; their origin: intrinsic (already present in the system) or extrinsic (added to the system); their form of application: dispersion, permeable or isolated. Depending on the number of components, TTIs can show single or multiple responses (Stoforos and Taoukis Petros, 1998). Depending on the way TTIs are applied, they can represent a single point of the process or an average. While in principle TTIs are meant to mimic 'any' quality attribute, most of research has focused on microbial inactivation because safety is the main concern for consumers and food processors. The majority of researched TTIs use a biological component. Non-pathogenic microorganisms have been used but assessing their survival requires tedious plate counting offering little advantage to the food processor. Conversely enzymes can be

assayed rapidly and some have thermal inactivation kinetics very close to pathogens of interest. Enzymes used as TTIs include β-galactosidase, lipase, nitrate reductase, peroxidase and α-amylase. In the last eight years (after the last published review on the topic), α-amylase has been the most commonly used enzyme for TTI fabrication (Van Loey et al. 1997; Haentjens et al. 1998; Tucker, 1999; Tucker, 2000; Tucker et al. 2002; Guiavarc'h et al. 2002a; Guiavarc'h et al. 2002b; Raviyan et al. 2003a; Raviyan et al. 2003b). Pectinmethylesterase (Guiavarc'h et al. 2003), triose phosphate isomerase (Hsu et al. 2000) and R-phycoerythrin (Smith et al. 2002) have also being studied. However, there is a tremendous amount of enzymes that needs to be explored.

Beyond conventional heating, recently TTIs have been developed for use with microwave and radio frequency heating (Raviyan et al. 2003a; Raviyan et al. 2003b) and the need for TTIs for non-thermal processing of food such as high hydrostatic pressure treatments has been identified (Claeys et al. 2003).

References

[1]. Adeljou, S.B. and Moline, A.N. (2001) Fabrication of ultra-thin polypyrrole-glucose oxidase film from supporting electrolyte-free monomer solution for potentiometric biosensing of glucose. *Biosens. Bioelectron.* **16**, 133-139.

[2]. Adeloju, S.B., Shaw, S.J. and Wallace, G.G. (1993) Polypyrrole-based potentiometric biosensor for urea. Part 2. Analytical optimization. *Anal. Chim. Acta* **281**, 621-627.

[3]. Aguilar-Hernández, J. and Potje-Kamloth, K. (1999) Opitcal and electrical characterization of a conducting polypyrrole composite prepared by *in situ* electropolymerization. *Physical Chemistry, Chemical Physics* **1**, 1735-1742.

[4]. Almeida, N.F., Beckman, E.J. and Ataai, M.M. (1993) Immobilization of glucose oxidase in thin polypyrrole films: Influence of polymerization conditions and film thickness on the activity and stability of the immobilized enzyme. *Biotechnol. Bioeng.* **42**, 1037-1045.

[5]. Arnold, M.A. and Meyerhoff, M.E. (1988) Recent advances in the development and analytical applications of biosensing probes. *Crit. Rev. Anal. Chem.* **20**, 149-196.

[6]. ASTM B 254 (1992) Standard practice for preparation of and electroplating stainless steel.

[7]. Bacha, S., Bergel, A. and Comtat, M. (1993) Modeling of amperometric biosensors by finite-volume method. *J. Electroanal. Chem.* **259**, 21-38.

[8]. Bartlett, P.N. and Cooper, J.M. (1993) A review of the immobilization of enzymes in electropolymerized films. *J. Electroanal. Chem.* **362**, 1-12.

[9]. Bartlett, P.N. and Whitaker, R.G. (1987a) Electrochemical immobilization of enzymes. Part I. Theory. *J. Electroanal. Chem.* **224**, 27-35.

[10]. Bartlett, P.N. and Whitaker, R.G. (1987b) Electrochemical immobilization of

enzymes. Part II. Glucose oxidase immobilised in poly-N-methylpyrrole. *J. Electroanal. Chem.* **224**, 37-48.

[11]. Basirun, W.J. and Pletcher, D. (1998) Studies of platinum electroplating baths. Part VI: Influence of some experimental parameters on deposit quality. *J. Appl. Electrochem.* **28**, 167-172.

[12]. Baumgärtner, M.E. and Raub, Ch.J. (1988) The electrodeposition of platinum and platinum alloys. *Plat. Met. Rev.* **32**, 188-197.

[13]. Bergel, A. and Comtat Maurice (1984) Theoretical evaluation of transient responses of an amperometric enzyme electrode. *Anal. Chem.* **56**, 2904-2909.

[14]. Bjerke, A.E., Griffiths, P.R. and Theiss, W. (1999) Surface-enhanced infrared absorption of CO on platinized platinum. *Anal. Chem.* **71**, 1967-1974.

[15]. Bélanger, D., Nadreau, J. and Fortier, G. (1989) Electrochemistry of the polypyrrole glucose oxidase electrode. *J. Electroanal. Chem.* **274**, 143-155.

[16]. Castner, J.F. and Wingard, L.B. (1984) Alterations in potentiometric response of glucose oxidase platinum electrodes resulting from electrochemical or thermal pretreatments of a metal surface. *Anal. Chem.* **56**, 2891-2896.

[17]. Claeys, W.L., Van Loey, I.A.M. and Hendrickx, M.E. (2003) Review: are intrinsic TTIs for thermally processed milk applicable for high-pressure

processing assessment? *Innov. Food Sci. Emerg. Technol.* **4**, 1-14.

[18]. Clark, L.C. and Lyons, C. (1962) Electrode systems for continuous monitoring of cardiovascular surgery. *Ann. N. Y. Acad. Sci.* **102**, 29-45.

[19]. Coche-Guerente, L., Cosnier, S., Innocent, C. and Mailley, P. (1995) Development of amperometric biosensors based on the immobilization of enzymes in polymer films electrogenerated from a series of amphiphilic pyrrole derivatives. *Anal. Chim. Acta* **311**, 23-30.

[20]. Cosnier, S. (1999) Biomolecule immobilization on electrode surfaces by entrapment or attachment to electrochemically polymerized films. A review. *Biosens. Bioelectron.* **14**, 443-456.

[21]. Crumbliss, A.L., Perine, S.C., Stonehuerner, J., Tubergen, K.R., Zhao, J. and O'Daly, J.P. (1992) Colloidal gold as biocompatible immobilization matrix suitable for the fabrication of enzyme electrodes by electrodeposition. *Biotechnol. Bioeng.* **40**, 483-490.

[22]. Despande, S.S. and Rocco, R.M. (1994) Biosensors and their potential use in food quality control. *Food Technol.* **48**, 146-150.

[23]. Dini, J.W. (1996) Plating on Invar, VascoMax C-200 and 440C stainless steel. *Surf. Coat. Technol.* **78**, 14-18.

[24]. Divya, P.S., Savitri, D. and Mitra, C.K. (1998) Covalent immobilization onto glassy carbon matrix-implications in biosensor design. *J. Biosci.* **23**,

131-136.

[25]. Djokic, S.S. (2000) Electrodeposition of platinum from an alkaline solution. *Plat. Surf. Finish.* **87**, 145-147.

[26]. Eremenko, A., Kurochkin, I., Chernov, S., Barmin, A., Yaroslavov, A. and Moskvitina, T. (1995) Monomolecular enzyme films stabilized by amphiphilic polyelectrolytes for biosensor devices. *Thin Solid Films* **260**, 212-216.

[27]. Evans, S.A.G., Elliott, J.M., Andrews, L.M., Bartlett, P.N., Doyle, P.J. and Denault, G. (2002) Detection of hydrogen peroxide at mesoporous platinum microelectrodes. *Anal. Chem.* **74**, 1322-1326.

[28]. Everson, M.P. and Helms, J.H. (1991) A scanning tunneling microscope study of the electrochemical polymerization of perchlorate-doped polypyrrole on highly oriented pyrolytic graphite. *Synth. Met.* **40**, 97-109.

[29]. Feltham, A.M. and Spiro, M. (1971) Platinized platinum electrodes. *Chem. Rev.* **71**, 177-193.

[30]. Fernández-Lafuente, R., Cowan, D.A. and Wood, N.P. (1995) Hyperstabilization of a thermophilic esterase by multipoint covalent attachment. *Enzyme Microb. Technol.* **17**, 366-372.

[31]. Fernández-Lafuente, R., Rodríguez, V., Bastida, A., Blanco, R.M. and Guisán, J.M. (1993) Stabilization of soluble proteins by intramolecular

crosslinking with polyfunctional macromolecules. Poly-(glutaraldehyde-like) structure. In: van den Tweel, W.J.J., Harder, A. and Buitelaar, R.M., (Eds.) *Stability and Stabilization of Enzymes*, Elsevier Science Publishers B.V.

[32]. Fernández-Lafuente, R., Rosell, C.M., Rodríguez, V., Guisán, J.M. and Guisán, J.M. (1995) Strategies for enzyme stabilization by intramolecular crosslinking with bifunctional reagents. *Enzyme Microb. Technol.* **17**, 517-523.

[33]. Fortier, G., Brassard, E. and Bélanger, D. (1990) Optimization of a polypyrrole glucose oxidase biosensor. *Biosens. Bioelectron.* **5**, 473-490.

[34]. Foulds, N.C. and Lowe, C.R. (1986) Enzyme entrapment in electrically conducting polymers. *J. Chem. Soc., Faraday Trans.* **82**, 1259-1264.

[35]. Fusalba, F. and Bélanger, D. (1999) Electropolymerization of polypyrrole and polyaniline-polypyrrole from organic acidic medium. *J. Phys. Chem. B* **103**, 9044-9054.

[36]. Giannakourou, M.C. and Taoukis, P.S. (2003) Application of a TTI-based distribution managment system for quality optimization of frozen vegetables at the consumer end. *J. Food Sci.* **68**, 201-209.

[37]. Gooding, J.J., Praig, V.G. and Hall, E.A.H. (1998) Platinum-catalyzed enzyme electrodes immobilized on gold using self assembled layers. *Anal. Chem.* **70**, 2396-2402.

[38]. Gough, D.A., Leypoldt, J.K. and Armour, J.C. (1982) Progress toward a potentially implantable enzyme-based glucose sensor. *Diabetes Care* **5**, 190-198.

[39]. Gros, P. and Bergel, A. (1995) Improved model of a polypyrrole glucose oxidase modified electrode. *J. Electroanal. Chem.* **386**, 65-73.

[40]. Guiavarc'h, Y., Deli, V., Van Loey, A.M. and Hendrickx, M.E. (2002a) Development of an ezymic time temperature integrator for sterilization processes based on Bacillus lichenformis α–amylase at reduced water content. *J. Food Sci.* **67**, 285-291.

[41]. Guiavarc'h, Y., Dintwa, E., Van Loey, A.M., Zuber, F. and Hendrickx, M.E. (2002b) Validation and use of an enzymic time-temperature integrator to monitor thermal impacts inside a solid/liquid model food. *Biotechnology Progress* **18**, 1087-1094.

[42]. Guiavarc'h, Y., Sila, D., Duvetter, T., Van Loey, A. and Hendrickx, M. (2003) Influence of sugars and polyols on the thermal stability of purified tomato and cucumber pectinmethylesterases: a basis for TTI development. *Enzyme Microb. Technol.* **33**, 544-555.

[43]. Guisán, J.M. (1988) Aldehyde-agarose gels as activated supports for immobilization-stabilization of enzymes. *Enzyme Microb. Technol.* **10**, 375-382.

[44]. Guo, Yizhu and Dong, Shaojun . (1997) Organic phase enzyme electrodes based

on organohydrogel. *Anal. Chem.* **69**, 1904-1908.

[45]. Hadian, S.E. and Gabe, D.R. (2001) Developments in platinum electroplating P & Q salt solution optimization. *Plat. Surf. Finish.* **88**, 93-98.

[46]. Haentjens, T.H., Van Loey, A.M., Hendrickx, M.E. and Tobback P.P. (1998) The use of α-amylase at reduced water content to develop time temperature integrators for sterilization processes. *Lebensm.-Wiss. Technol.* **31**, 467-472.

[47]. Hendrickx, M. E., Maesmans, G., De Cordt, S., Noronha, Joao, and Van Loey, A. M. (1995) Evaluation of the integrated time-temperature effect in thermal processing of foods. *CRC Crit. Rev. Food Sci. Nutr.* **35**, 231-262.

[48]. Hendrickx, M.E., Maesmans, G., De Cordt, S., Noronha, J. , Van Loey, A.M., Willocx and Tobback P.P. (1994) Advances in process modeling and assessment: the physical mathematical approach an product history integrators. In: Singh, R.P. and Oliveira, F.A.R., (Eds.) *Minimal processing of foods and process optimization*, pp. 315-336. Boca Raton: CRC Press

[49]. Holdcroft, S. and Funt, L. (1988) Preparation and electrocatalytic properties of conducting films of polypyrrole conatining platinum micorparticles. *J. Electroanal. Chem.* **240**, 89-103.

[50]. Hsu, Y.C., Sair, A.I., Booren, A.M. and Smith, D.M. (2000) Triose phosphate

isomerase, as an endogenous time-temperature integrator to verify adequacy of roast beef processing. *J. Food Sci.* **65**, 236-240.

[51]. Hämmerle, M., Schuhmann, W. and Schmidt, H.-L. (1992) Amperometric polypyrrole electrodes: effect of permeability and enzyme location. *Sens. Actuators, B* **6**, 106-112.

[52]. Kankare, J. and Kupila, E.-L. (1992) In-situ conductance measurement during electropolymerization. *J. Electroanal. Chem.* **322**, 167-181.

[53]. Kell, D.B. and Davey, C.L. (1990) Conductimetric and impedometric devices. Cass, A.E.G., (Ed.) 137 Oxford: IRL Press.

[54]. Khan, G.F. and Wernet, W. (1997) Design of enzyme electrodes for extended use and storage life. *Anal. Chem.* **69**, 2682-2687.

[55]. Kim, C.S. and Oh, S.M. (1996) Enzyme sensors prepared by electrodeposition on platinized platinum electrodes. *Electrochim. Acta* **41**, 2433-2439.

[56]. Labuza, T.P., Fu, B. and Taoukis, P.S. (1992) Prediction for shelf life and safety of minimally processed CAP/MAP chilled foods: A review. *J. Food Prot.* **55**, 741-750.

[57]. Le Penven, R., Levason, W. and Pletcher, D. (1992) Studies of platinum electroplating baths. Part I: the chemistry of a plating tetrammine bath. *J. Appl. Electrochem.* **22**, 415-420.

[58]. Lenders, J.P. and Crichton, R.R. (1984) Thermal stabilization of amylolytic

enzymes by covalent coupling to soluble polysaccharides. *Biotechnol. Bioeng.* **26**, 1343-1351.

[59]. Levason, W., Pletcher, D., Smith, A.M. and Berzins A.R. (1998) Studies of platinum electroplating baths. Part V: Solutions derived from $Pt(NO_2)_4^{2-}$ in aqueous acid. *J. Appl. Electrochem.* **28**, 18-26.

[60]. Leypoldt, J.K. and Gough, D.A. (1984) Model of a two-substrate enzyme electrode for glucose. *Anal. Chem.* **56**, 2896-2904.

[61]. Li, Y. (1997) Effect of anion concentration on the kinetics of electrochemical polymerization of pyrrole. *Electroanal. Chem.* **433**, 181-186.

[62]. Lin, L. and Guthrie, J.T. (1998) The application of computer-aided experiment design and of formulation optimization to biosensor assembly. In: Scott A.O., (Ed.) *Biosensors for Food Analysis*, pp. 61-70. Cambridge, UK: The Royal Society of Chemistry

[63]. Liu, H., Li, H., Ying, T., Sun, K., Qin, Y. and Qi, D. (1998) Amperometric biosensor sensitive to glucose and lactose based on co-immbilization of ferrocene, glucose oxidase, β-galactosidase and mutarotase in β-cyclodextrin polymer. *Anal. Chim. Acta* **358**, 137-144.

[64]. Lucisano, J.Y. and Gough, D.A. (1988) Transient response of the two-dimensional glucose sensor. *Anal. Chem.* **60**, 1272-1281.

[65]. Lyons, M.E.G., Bartlett, P.N., Lyons, C.H., Breen, W. and Cassidy John F.

(1991) Conducting polymer based electrochemical sensors: theoretical analysis of current response under steady state conditions. *J. Electroanal. Chem.* **304**, 1-6.

[66]. Marchesiello, M. and Genies, E. (1993) A theoretical model for an amperometric glucose sensor using polypyrrole as the immobilization matrix. *J. Electroanal. Chem.* **358**, 35-48.

[67]. Martinek, K., Klibanov, A.M., Goldmacher, V.S. and Berezlin, I.V. (1977) The principles of enzyme stabilization. I. Increase in thermostability of enzymes covalently bound to a complementary surface of a polymer support in a multipoint fasion. *Biochim. Biophys. Acta* **485**, 1-12.

[68]. Masuda, H. and Kaeriyama, K. (1995) Electrochemical polymerization of pyrrole with water-soluble polymeric electrolyte. *Synth. Met.* **69**, 513-514.

[69]. Miras, M.C., Barbero, C. and Haas, O. (1991) Preparation of polyaniline by electrochemical polymerization of aniline in acetonitrile solution. *Synth. Met.* **41-43**, 3081-3084.

[70]. Mu, S. and Jinquing, K. (1995) Bioelectrochemical activation and inhibition of polyaniline glucose oxidase electrode by cations. *Electrochim. Acta* **40**, 241-246.

[71]. Pal, P., Nandi, D. and Misra, T.N. (1994) Immobilization of alcohol dehydrogenase enzyme in a Langnuir-Blodgett film of stearc acid: its

application as an ethanol sensor. *Thin Solid Films* **239**, 138-143.

[72]. Palmisano, F., Guerrieri, A., Quinto, M. and Zambonin, P.G. (1995) Electrosynthesized bilayer polymeric membranes for effective elmination of electroactive interferents in amperometric biosensors. *Anal. Chem.* **67**, 1005-1009.

[73]. Park, S., Chung, T.D. and Kim, H.C. (2003) Nonenzymatic glucose detection using mesoporous platinum. *Anal. Chem.* **75**, 3046-3049.

[74]. Pei, Q. and Qian, R. (1992) Electrochemical polymerization of pyrrole in aqueous buffer solutions. *J. Electroanal. Chem.* **322**, 153-166.

[75]. Pushpavanam, M. and Natarajan, S.R. (1988) Platinum plating for decorative and functional applicatiosn. *Met. Finish.* **86**, 25-27.

[76]. Raviyan, P., Tang, J., Orellana, L. and Rasco, B. (2003a) Physicochemical properties of a time-temperature indicator based on immobilization of *Aspergillus oryzae* α–amylase in polyacrylamide gel as affected by degree of crosslinking agent and salt content. *J. Food Sci.* **68**, 2302-2308.

[77]. Raviyan, P., Tang, J. and Rasco B.A. (2003b) Thermal stability of α-amylase from Aspergillus oryzae entrapped in polyacrylamide gel. *J. Agric. Food Chem.* **51**, 5462-5466.

[78]. Rizvi, S.S.H., Singh, R.K., Hotchkiss, J.H., Heldmann, D.R. and Leung, H.K.

(1993) Research needs in food engineering, processing and packaging. *Food Technol.* **47**, 26S-35S.

[79]. Saçak, M., Karakişla, M. and Akbulut, U. (1997) A 316 steel electrode coated wiht polycarbonate for electropolymerization of aniline. *J. Appl. Polym. Sci.* **65**, 1103-1111.

[80]. Schuhmann, W. (1998) Enzyme biosensors based on conducting polymers. Mulchandani, A. and Rogers, K., (Eds.) 143-156. Totwa NJ: Humana Press.

[81]. Schuhmann, W. (1991) Amperometric substrate determination in flow-injection systems with polypyrrole-enzyme electrodes. *Sens. Actuators, B* **4**, 41-49.

[82]. Scott, A.O. (1998) Biosensors for food analysis: Perspectives. In: Scott, A.O., (Ed.) *Biosensors for Food Analysis*, pp. 181-195. Cambridge, UK: The Royal Society of Chemistry

[83]. Shin, M.C. and Kim, H.S. (1995) Effects of enzyme concentration and film thickness on the analytical performance of a polypyrrole/ glucose oxidase biosensor. *Anal. Lett.* **28**, 1017-1031.

[84]. Shin, M.C. and Kim, H.S. (1996a) Electrochemical characterization of polypyrrole/glucose oxidase biosensor: Part I. Influence of enzyme concentration on the growth and properties of the film. *Biosens. Bioelectron.* **11**, 161-169.

[85]. Shin, M.C. and Kim, H.S. (1996b) Electrochemical characterization of polypyrrole/glucose oxidase biosensor: Part II. Optimal preparation conditions for the biosensor. *Biosens. Bioelectron.* **11**, 171-178.

[86]. Smith, S.E., Orta-Ramirez, A., Ofolo, R.Y., Ryser, E.T. and Smith, D.M. (2002) R-phycoerithrin as a time-temperature integrator to verify the thermal processing adequacy of beef patties. *J. Food Prot.* **65**, 814-819.

[87]. Smout, C., Van Loey, A.M. and Hendrickx, M.E. (2000) Non-uniformity of lethality in retort processes based on heat distribution and heat penetration data. *J. Food Eng.* **45**, 103-110.

[88]. Stoforos, N.G., Noronha, J., Hendrickx, M.E. and Tobback P.P. (1997) A critical analysis of the mathematical procedures for the evaluation and design of in-container thermal processes for foods. *CRC Crit. Rev. Food Sci. Nutr.* **37**, 411-441.

[89]. Stoforos, N.G. and Taoukis Petros, S. (1998) A theoretical procedure for using multiple response time-temperature integrators for the design and evaluation of thermal processes. *Food Control* **9**, 279-287.

[90]. Stonehuerner, J.G., O'Daly, J.P., Zhao, J., Crumbliss, A.L. and Henkens, R.W. (1992) Comparizon of colloidal gold electrode fabrication methods: the preparation of a horseradish peroxidase enzyme electrode. *Biosensors and Biolelectronics* **7**, 421-428.

[91]. Stoychev, D., Papoutsis, A., Kelaidopoulou, A., Kokkinidis, G. and Milchev,

A. (2001) Electrodeposition of platinum on metallic and nonmetallic substrates. Selection of experimental conditions. *Mater. Chem. Phys.* **72**, 360-365.

[92]. Su, W. and Iroh, J.O. (1997) Formation of polypyrrole coatings onto low carbon steel by electrochemical process. *J. Appl. Polym. Sci.* **65**, 417-424.

[93]. Taoukis Petros, S., Koutsoumanis, K., and Nychas, G. J. E. (1999) Use of time-temperature integrators and predictive modelling for shelf life control of chilled fish under dynamic storage conditions. *Int. J. Food Microbiol.* **53**, 21-31.

[94]. Taylor, R.F. (1996) Immobilization methods. In: Taylor, R. and Schultz, J.S., (Eds.) *Handbook of Chemical and Biological Sensors*, pp. 203-219. Bristol: Institute of Physics Publishing

[95]. Tien, H.T. , Wurster, S.H. and Ottova, A.L. (1997) Electrochemistry of supported bilayer lipid membranes background and techniques for biosensor development. *Bioelectrochem. Bioenerg.* **42**, 77-94.

[96]. Tomov, T. and Tsoneva, I. (2000) Are stainless steel electrodes inert? *Bioelectrochemistry* **51**, 207-209.

[97]. Trojanowicz, M., Geschke, O. and Krawczynsky vel Krawczyk, T.C.K. (1995) Biosensors based on oxidases immobilized in various conducting Polymers. *Sens. Actuators, B* **28**, 191-199.

[98]. Tse, P.H.S. and Gough, D.A. (1987) Transient response of an enzyme electrode sensor for glucose. *Anal. Chem.* **59**, 2339-2341.

[99]. Tucker, G. (1999) A novel validation method: Application of time-temperature integrators to food pasteurization treatments. *Transactions of the Institution of Chemical Engineers Part C* **77**, 223-231.

[100]. Tucker, G. (2000) Estimation of pasteurization values using an enzymic time-temperature integrator. *Food Australia* **52**,131-136.

[101]. Tucker, G.S., Lambourne, T., Adams, J.B. and Lach, A. (2002) Application of a biochemical time-temperature integrator to estimate pasteurisation values in continuous food processes. *Inn. Food Sci. Emerg. Technol.* **3**, 165-174.

[102]. Umana, M. and Waller, J. (1986) Protein-modified electrodes. The glucose oxidase/polypyrrole system. *Anal. Chem.* **58**, 2979-2983.

[103]. Van Loey, A.M., Arthawan, A., Hendrickx, M.E., Haentjens, T.H. and Tobback P.P. (1997) The development and use of an α-amylase-based time-temperature integrator to evaluate in-pack pasteurization processes. *Lebensm.-Wiss. Technol.* **30**, 94-100.

[104]. Van Loey, A.M., Hendrickx, M.E., De Cordt, S., Haentjens, T.H. and Tobback P.P. (1996a) Quantitative evaluation of thermal processes using time-temperature integrators. *Trends Food Sci. Technol.* **7**, 16-26.

[105]. Van Loey, A.M., Hendrickx, M.E., Smout, C., Haentjens, T.H. and Tobback P.P. (1996b) Recent advances in process assessment and optimization. *Meat Sci.* **43**, S81-S98

[106]. Vork, F.T.A., Schuermans B.C.A.M. and Barendrecht, E. (1990) Influence of inserted anions on the properties of polypyrrole. *Electrochim. Acta* **35**, 567-575.

[107]. Wang, B., Li, B., Wang, Z., Xu, G., Wang, Q. and Dong, S. (1999) Sol-gel thin-film immobilized soybean peroxidase biosensor for the amperometric determination of hydrogen peroxide in acid medium. *Anal. Chem.* **71**, 1935-1939.

[108]. Wang, J., Chen, S.-P. and Lin, M.S. (1989) Use of different electropolymerization conditions for controlling the size-exclusion selectivity at polyaniline, polypyrrole and polyphenol films. *J. Electroanal. Chem.* **273**, 231-242.

[109]. Warsinke, A., Macholán, L., Stancik, L., Pfeiffer, D. and Scheller, F. (1998) A German approach. In: Scott, A.O., (Ed.) *Biosensors for Food Analysis*, pp. 101-104. Cambridge, UK: The Royal Society of Chemistry

[110]. Wernet, W. (1991) Thermoplastic and elastic conducting polypyrrole films. *Synth. Met.* **41-43**, 843-848.

[111]. Wolowacz, S.E., Yon Hin, B.F.Y. and Lowe, C.R. (1992) Covalent electropolymerization of glucose oxidase in polypyrrole. *Anal. Chem.*

64 , 1541-1545.

[112]. Wood, D. (1938) A simple method of plating nickel on stainless steel. *Metal Industry* **36**, 330-331.

[113]. Yamato, H., Wernet, W., Ohwa, M. and Rotzinger, B. (1993) Characterization of thermoplastic sulfated poly(β-hydroxyethers)/polypyrrole conducting composites. *Synth. Met.* **55-57**, 3550-3555.

[114]. Yang, R., Ruan, C. and Deng, J. (1998) A H_2O_2 biosensor based on immobilization of horseradish peroxidase in electropolymerized methylene green film on GCE. *J. Appl. Electrochem.* **28**, 1269-1275.

[115]. Yon-Hin B.F.Y., Smolander, M., Crompton, T. and Lowe, C.R. (1993) Covalent electropolymerization of glucose oxidase in polypyrrole. Evaluation of methods of pyrrole attachment to glucose oxidase on the performance of electropolymerized glucose sensors. *Anal. Chem.* **65**, 2067-2071.

[116]. Yon Hin, B.F.Y. and Lowe, C.R. (1994) An investigation of 3-functionalized pyrrole-modified glucose oxidase for covalent electropolymerization of enzyme films. *J. Electroanal. Chem.* **374**, 167-172.

[117]. Zhang, Z. , Liu, H. and Deng, J. (1996) A glucose biosensor based on immobilization of glucose oxidase in electropolymerized *o*-aminophenol film on platinized glassy carbon electrode. *Anal. Chem.* **68**, 1632-1638.

[118]. Zhu, M., Han, S. and Yuan, Z. (2000) β-Cyclodextrin polymer as the immobilization matrix for peroxidase and mediator in the fabrication of a sensor for hydrogen peroxide. *J. Electroanal. Chem.* **480** , 255-261.

[119]. Zoungrana, T., Findenegg, G.H. and Norde, W. (1997) Structure, stability and activity of adsorbed enzymes. *J. Colloid Interface Sci.* **190**, 437-448.

CHAPTER TWO

BIOSENSORS

(Encyclopedia of Agricultural, Food and Biological Engineering, Heldman, D. Editor. Marcel Dekker Inc, 2003 pp. 119-123).

CHAPTER TWO

BIOSENSORS

Introduction

Industrial instrumentation for analysis is scarce and often limited to pH and conductivity. There exist on-line optical instruments such as refractometers that may be used to assess composition. However, their applicability to biological material is often limited by the presence of interfering compounds in variable concentration that interfere with the measurement. In most cases, accurate analyses of biological materials are expensive and need to be performed in external laboratories equipped with more sophisticated instrumentation. Most of these analyses require previous purification that requires too much time relative to the processing time, making their on-line implementation impossible for control purposes. However, in living organisms, biological components like antibodies and enzymes work as natural sensing and controlling "devices." The ability of isolating and purifying these proteins and other biological elements such as cells or organelles has allowed their integration with physicochemical transduction devices to produce biosensors. The most widely accepted definition of a biosensors is: "a self-contained analytical device that incorporates a biologically active material in intimate contact with an appropriate transduction element for the purpose of detecting (reversibly and selectively) the concentration or activity of chemical species in any type of sample." (1) The first biosensor, an enzyme-based glucose sensor, was developed by Clark and Lyons. (2) Since then, hundreds of

biosensors have been developed in many research laboratories around the world. Over 200 research papers about biosensors have been published each year for the past three years.

The objective of this article is to review the principles of biosensor fabrication and operation, their existing and potential applications in the food and agricultural industries, and to briefly discuss recent research and future trends. For more comprehensive discussion on the topic, the reader is referred to several excellent books and reviews on which most of this article is based. (3–9)

Types Of Biosensors

Biosensors can be grouped according to their biological element or their transduction element. Biological elements include enzymes, antibodies, micro-organisms, biological tissue, and organelles. Antibody-based biosensors are also called immunosensors. When the binding of the sensing element and the analyte is the detected event, the instrument is described as an affinity sensor. When the interaction between the biological element and the analyte is accompanied or followed by a chemical change in which the concentration of one of the substrates or products is measured the instrument is described as a metabolism sensor. Finally, when the signal is produced after binding the analyte without chemically changing it but by converting an auxiliary substrate, the biosensor is called a catalytic sensor (10). The method of transduction depends on the type of physicochemical change resulting from the sensing event. Often, an important ancillary part of a biosensor is a membrane that covers the biological sensing element and has the main functions of selective permeation and diffusion control of analyte,

protection against mechanical stresses, and support for the biological element. The most commonly used sensing elements and transducers are described below.

Sensing Elements

Enzymes

Enzymes are proteins with high catalytic activity and selectivity towards substrates (see the article Enzyme Kinetics). They have been used for decades to assay the concentration of diverse analytes. (11) Their commercial availability at high purity levels makes them very attractive for mass production of enzyme sensors. Their main limitations are that pH, ionic strength, chemical inhibitors, and temperature affect their activity. Most enzymes lose their activity when exposed to temperatures above 60°C. Most of the enzymes used in biosensor fabrication are oxidases that consume dissolved oxygen and produce hydrogen peroxide [see Fig. 1]. Enzymes have been immobilized at the surface of the transducer by adsorption, covalent attachment, entrapment in a gel or an electrochemically generated polymer, in bilipid membranes or in solution behind a selective membrane. Several reviews of enzyme immobilization have been published. (12–19) Enzymes are commonly coupled to electrochemical and fiber optic transducers.

Antibodies

Antibodies are proteins that show outstanding selectivity. They are produced by - lymphocytes in response to antigenic structures, that is, substances foreign to the organism. Molecules larger than about 10 kDa can stimulate an immune response. Smaller molecules like vitamins or steroids can be antigenic (also called haptens) but

they do not cause an immune response unless they are conjugated to larger ones like bovine serum albumin. Many antibodies are commercially available and commonly used in immunoassays. Antibodies are usually immobilized on the surface of the transducer by covalent attachment by conjugation of amino, carboxyl, aldehyde, or sulfhydryl groups.

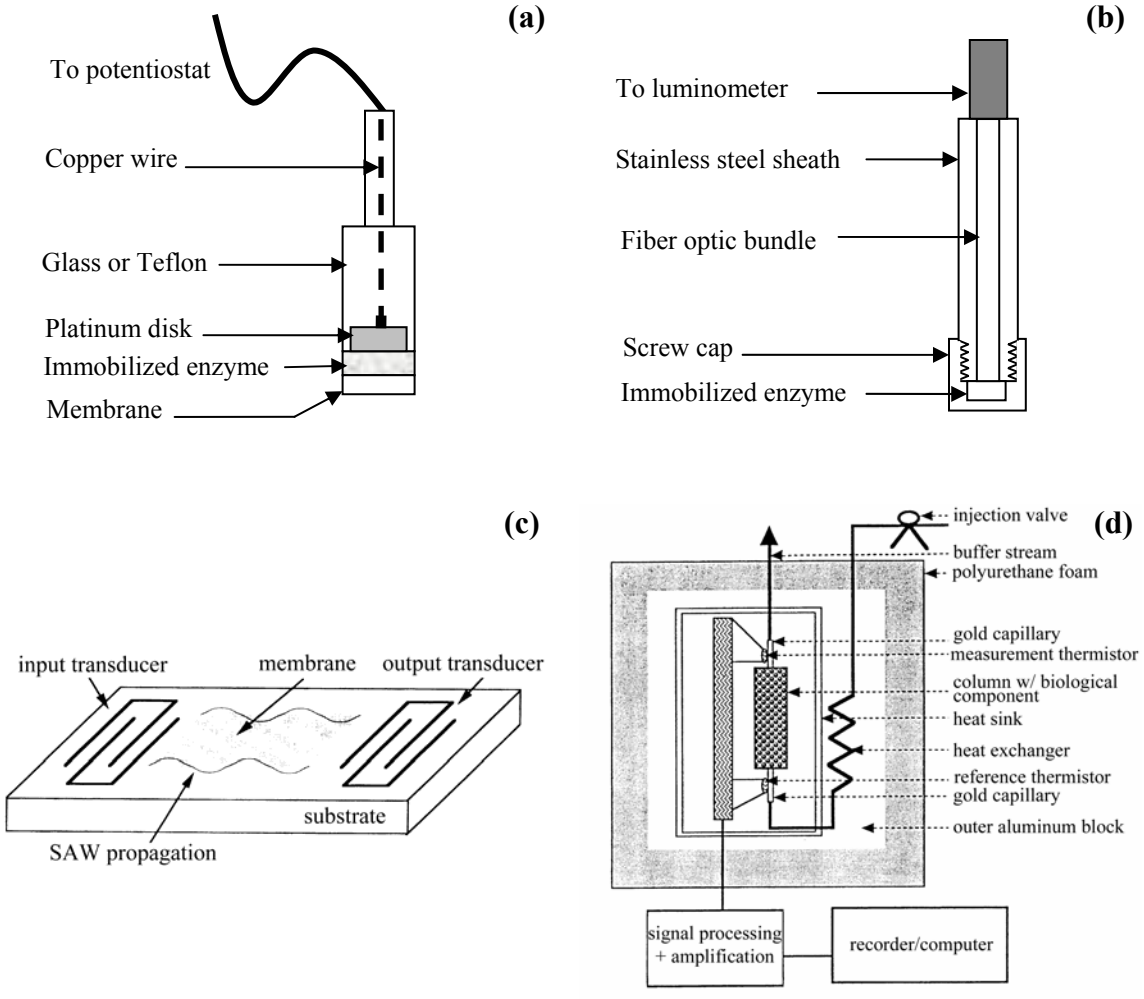

Figure 1. Schematic representation of (a) amperometric enzyme membrane electrode (7); (b) fiber optic enzyme sensor (7) ; (c) surface acoustic wave propagation sensor (3) ; and (d) enzyme thermistor. (3)

The surface of the transducer must be previously functionalized with an amino, carboxyl, hydroxyl, or other group. A review of conjugation techniques can be found elsewhere. (20) Antibodies share similar limitations with enzymes. Furthermore, binding may not be reversible and regeneration of the surface may require drastic changes in conditions like low pH, high ionic strength, detergents, etc. Therefore, efforts are being made to produce low cost, single use sensors. Probably the main potential advantage of immunosensors over traditional immunoassays is that they could allow faster and in-field measurements. Immunosensors usually employ optical or acoustic transducers.

Microbes

The use micro-organisms as biological elements in biosensors is based on the measurement of their metabolism, in many cases accompanied by the consumption of oxygen or carbon dioxide, and is, in most cases, measured electrochemically. (21) Microbial cells have the advantage of being cheaper than enzymes or antibodies, can be more stable, and can carry out several complex reactions involving enzymes and cofactors. Conversely, they are less selective than enzymes, they have longer response and recovery times, (22) and may require more frequent calibration. Micro-organisms have been immobilized, for example, in nylon nets, (21) cellulose nitrate membranes, (23) or acetyl cellulose. (24)

Other biological elements such as animal of vegetable tissue and membranes as well as organelles and nucleic acids have been researched but are out of the scope of this article. A summary of some biological elements and transducers used in the fabrication of biosensors is presented in Table 1.

Table 1. Biological elements and transducers commonly used in the fabrication of biosensors

Biological elements	**Transducers**
Enzymes	Electrochemical
Antibodies	Amperometric
RECEPTORS	Potentiometric
Cells	Ion selective
Membranes	Field effect transistors
Tissues	Conductimetric
Organisms	Optical
Organelles	Fiber optic (optrode)
Nucleic acids	Surface plasmon resonance (SPR)
Organic molecules	Fiber optic SPR
	Calorimetric
	Heat conduction
	Isothermal
	Isoperibol
	Acoustic
	Surface acoustic wave
	Piezocrystal microbalance

(Adapted from Refs. 4,5.)

Transducer Elements

Electrochemical

Amperometric and potentiometric transducers are the most commonly used electrochemical transducers. In amperometric transducers, the potential between the two electrodes is set and the current produced by the oxidation or reduction of electroactive species is measured and correlated to the concentration of the analyte of interest. Most electrodes are made of metals like platinum, gold, sliver, and stainless steel, or carbon-

based materials that are inert at the potentials at which the electrochemical reaction takes place. However, because some species react at potentials where other species are present, either a selective membrane is used or an electron mediator that reacts at lower potential is incorporated into the immobilization matrix or to the sample containing the analyte. Potentiometric transducers measure the potential of electrochemical cells with very low current. Field effect transistors (FET) are potentiometric devices based on the measurement of potential at an insulator–electrolyte interface. The metal gate of a FET can be substituted by an ion selective membrane to make a pH transducer (pH ISFET). Enzymes have been immobilized on the surface of such pH ISFET to produce enzyme-sensitized field effect transistors (ENFET). A complete description of such sensors can be found elsewhere. (25)

Optical

Fiber optic probes on the tip of which enzymes and dyes (often fluorescent) have been co-immobilized are used. These probes consist of at least two fibers. One is connected to a light source of a given wave length range that produces the excitation wave. The other, connected to a photodiode, detects the change in optical density at the appropriate wavelength [see Fig. 1]. Surface plasmon resonance (SPR) transducers, which measure minute changes in refractive index at and near the surface of the sensing element, have been proposed. SPR measurement is based on the detection of the attenuated total reflection of light in a prism with one side coated with a metal. When a p-polarized incident light passes through the prism and strikes the metal at an adequate angle, it induces a resonant charge wave at the metal/dielectric interface that propagates a

few microns. The total reflection is measured with a photodetector, as a function of the incident angle. For example, when an antigen binds to an antibody that is immobilized on the exposed surface of the metal the measured reflectivity increases. This increase in reflectivity can then be correlated to the concentration of antigen. The basic theory of SPR excitation and some examples of its application to biosensors are presented elsewhere. (26,27) A few SPR biosensors have been commercialized but no compact inexpensive portable device is available yet.

Acoustic

Electroacoustic devices used in biosensors are based on the detection of a change of mass density, elastic, viscoelastic, electric, or dielectric properties of a membrane made of chemically interactive materials in contact with a piezoelectric material. Bulk acoustic wave (BAW) and surface acoustic wave (SAW) propagation transducers are commonly used. In the first, a crystal resonator, usually quartz, is connected to an amplifier to form an oscillator whose resonant frequency is a function of the properties of two membranes attached to it. The latter is based on the propagation of SAWs along a layer of a substrate covered by the membrane whose properties affect the propagation loss and phase velocity of the wave. SAWs are produced and measured by metal interdigital transducers deposited on the piezoelectric substrate as shown in Fig. 1. (28)

Calorimetric

Calorimetric transducers measure the heat of a biochemical reaction at the sensing element. These devices can be classified according to the way heat is transferred.

Isothermal calorimeters maintain the reaction cell at constant temperature using Joule heating or Peltier cooling and the amount of energy required is measured. Heat conduction calorimeters measure the temperature difference between the reaction vessel and an isothermal heat sink surrounding it. Using highly conducting materials ensure quick heat transfer between the reaction cell and the heat sink. Finally, the most commonly used is the isoperibol calorimeter that also measures the temperature difference between the reaction cell and an isothermal jacket surrounding it. However, in this case the reaction cell is thermally insulated (adiabatic). This calorimeter has the advantage of being easily coupled to flow injection analysis systems (29) [see Fig. 1].

Applications

One of the major driving forces for the development of biosensors is biomedical diagnosis. The most popular example is glucose oxidase-based sensor used by individuals suffering from diabetes to monitor glucose levels in blood. Biosensors have found also potential applications in the agricultural and food industries. However, very few biosensors have been commercialized.

Agricultural Industry

Enzyme biosensors based on the inhibition of cholinesterases have been used to detect traces of organophosphates and carbamates from pesticides. Selective and sensitive microbial sensors for measurement of ammonia and methane have been studied. (30) However, the only commercially available biosensors for wastewater quality control are biological oxygen demand (BOD) analyzers based on micro-organisms like the bacteria

Rhodococcus erythropolis immobilized in collagen or polyacrylamide. Standard BOD5 measurements in which the effluent is pretreated and exposed to bacteria and protozoa require incubation at 20°C for 5 day. In contrast, BOD biosensors have throughputs of 2 to 20 samples per hour and can measure 0 mg L-1 to 500 mg L-1 BOD. When coupled with automatic sampling they can be implemented on-line. (30)

Food Industry

Biosensors for the measurement of carbohydrates, alcohols, and acids are commercially available. These instruments are mostly used in quality assurance laboratories or at best, on-line coupled to the processing line through a flow injection analysis system. Their implementation in-line is limited by the need of sterility, frequent calibration, analyte dilution, etc. Potential applications of enzyme based biosensors to food quality control include measurement of amino acids, amines, amides, heterocyclic compounds, carbohydrates, carboxylic acids, gases, cofactors, inorganic ions, alcohols, and phenols. (31) Biosensors can be used in industries such as wine beer, yogurt, soft drinks producers. Immunosensors have important potential in ensuring food safety by detecting pathogenic organisms in fresh meat, poultry, or fish.

Current Research And Trends

Because in many cases the transduction technology is well established, most of the research is focused on improving immobilization techniques of the biological element to increase sensitivity, selectivity, and stability. While critical, the latter has received relatively little attention probably in part because there is a tendency to design disposable

devices that are most useful in quality assurance laboratories but do not allow on-line implementation for process control. Another dynamic area of research is miniaturization of sensors and flow systems. Development of these technologies is mainly driven by the need for in vivo applications for medical diagnosis and may not find immediate use in the agricultural and food industries. After almost 40 yr of research in biosensors, a wide gap between research and application is evident. The lack of validation, standardization, and certification of biosensors has resulted in a very slow transfer of technology. With faster computers and automated systems this process should accelerate in the future.

References

1. Arnold M.A., Meyerhoff M.E., Recent Advances in the Development and Analytical Applications of Biosensing Probes, Crit. Rev. Anal. Chem., 20 (1988) 149–196.
2. Clark L.C., Lyons C., Electrode systems for continuous monitoring cardiovascular surgery., Ann. N. Y. Acad. Sci., 102 (1962) 29–45.
3. Kress-Rogers E. Handbook of Biosensors and Electronic Noses, CRC Press Inc., New York, 1997.
4. Kress-Rogers E. Instrumentation and Sensors for the Food Industry, Woodhead Publishing Lmtd., Cambridge, 1998.
5. Turner A.P.F., Karube I., Wilson G.S. Biosensors Fundamentals and Applications, Oxford Univeristy Press, Oxford, 1987.

6. Schmid R.D., Scheller F. Biosensors, Applications in Medicine, Environmental Protection and Process Control, VCH Publishers, New York, 1989.

7. Scott A.O. Biosensors for Food Analysis, The Royal Society of Chemistry, Cambridge, 1998.

8. Ramsay G. Commercial Biosensors, Winefordner J.D. John Wiley & Sons Inc., New York, 1998.

9. Wise D.L. Bioinstrumentation and Biosensors, Marcel Dekker, New York, 1991.

10. Schubert F., Wollenberger U., Scheller F.W., Müller H.G. Artificially Coupled Reactions with Immobilized Enzymes: Biological Analogs and Technical Consequences, Bioinstrumentation and Biosensors, Wise D.L. Marcel Dekker, Inc., New York, 1991, p. 19.

11. Guibault G.G. Analysis of Substrates, Handbook of Enzymatic Methods of Analysis, Schwartz M.K. Marcel Dekker, Inc., New York, 1976, pp. 189–344.

12. Cosnier S., Biomolecule Immobilization on Electrode Surfaces by Entrapment or Attachment to Electrochemically Polymerized Films. A Review, Biosens. Biolelectron., 14 (1999) 443–456.

13. Tien H.T., Wurster S.H., Ottova A.L., Electrochemistry of Supported Bilayer Lipid Membranes Background and Techniques for Biosensor Development, Bioelectrochem. Bioenerg., 42 (1997) 77–94.

14. Bartlett P.N., Cooper J.M., A Review of the Immobilization of Enzymes in Electropolymerized Films, J. Electroanal. Chem., 362 (1993) 1–12.

15. Scouten W.H., A Survey of Enzyme Coupling Techniques, Methods Enzymol., 135 (1987) 30–65.

16. Tien H.T., Wurster S.H., Ottova A.L., Electrochemistry of Supported Bilayer Lipid Membranes Background and Techniques for Biosensor Development, Bioelectrochem. Bioenerg., 42 (1997) 77–94.

17. Bartlett P.N., Whitaker R.G., Electrochemical Immobilization of Enzymes. Part I. Theory, J. Electroanal. Chem., 224 (1987) 27–35.

18. Bidan G., Electroconducting Polymers: New Sensitive Matrices to Build Up Chemical or Electrochemical Sensors. A Review, Sens. Actuators, B, 6 (1992) 45–56.

19. Guibault G.G. Immobilized Enzyme Electrode Probes, Solid Phase Biochemistry. Analytical and Synthetic Aspects, Elving P.J., Winefordner J.D., Kolthoff I.M., Scouten W.H. John Wiley & Sons, New York, 1983, pp. 479–505.

20. Hermanson G.T. Bioconjugute Techniques, Academic Press, San Diego, 1996.

21. Karube I. Micro-organism Based Biosensors, Biosensors Fundamentals and Applications, Turner A.P.F., Karube I., Wilson G.S. Oxford Science Publications, Oxford, 1987, pp. 13–29.

22. White S.F., Turner A.P.F. Mediated Amperometric Biosensors, Handbook of Biosensors and Electronic Noses. Medicine, Food and the Environment, Kress-Rogers E. CRC Press, New York, 1997, pp. 227–244.

23. Watanabe E., Tanaka M. Determination of Fish Freshness with a Biosensor System, Bioinstrumentation and Biosensors, Wise D.L. Marcel Dekker, Inc., New York, 1991, pp. 39–73.

24. Karube I., Sode K. Microbial Sensors for Process and Environmental Control, Bioinstrumentation and Biosensors, Wise D.L. Marcel Dekker, Inc., New York, 1991, pp. 1–18.

25. Kress-Rogers E. Chemosensors, Biosensors and Immunosensors, Instrumentation and Sensors for the Food Industry, Kress-Rogers E. Woodhead Publishing Lmtd., Cambridge, 1998, pp. 599–611. 636–639.

26. Lawrence Chris R., Geddes N.J. Surface Plasmon Resonance (SPR) for Biosensing, Handbook of Biosensors and Electronic Noses. Medicine, Food and the Environment, Kress-Rogers E. CRC Press, New York, 1997, pp. 149–168.

27. Tao N.J., Boussaad S., Huang W.L., Arechabaleta R.A., D'Agnese J., High Resolution Surface Plasmon Resonance Spectroscopy, Rev. Sci. Instrum., 70 (12) , (1999) 4656–4660.

28. D'Amico A., Di Natale C., Verona E. Acoustic Devices, Handbook of Biosensors and Electronic Noses. Medicine, Food and the Environment, Kress-Rogers E. CRC Press, New York, 1997, pp. 197–223.

29. Kröger S., Danielsson B. Calorimetric Biosensors, Handbook of Biosensors and Electronic Noses. Medicine, Food and the Environment, Kress-Rogers E. CRC Press Oxford Science Publications, New York, 1997, pp. 279–298.

30. Wittman C., Riedel K., Schmid R.D. Microbial and Enzyme Sensors for Environmental Monitoring, Handbook of Biosensors and Electronic Noses. Medicine, Food and the Environment, Kress-Rogers E. CRC Press, New York, 1997, pp. 305–306.

31. Despande S.S., Rocco R.M., Biosensors and Their Potential Use in Food Quality Control, Food Technol., 48 (6) , (1994) 146–150.

CHAPTER THREE

SIMULTANEOUS DETERMINATION OF FILM PERMEABILITY TO H_2O_2 AND SUBSTRATE SURFACE AREA COVERAGE OF OVEROXIDIZED POLYPYRROLE.

(Synthetic Metals, **2004**, 142, (1-3), 71-79)

CHAPTER THREE

SIMULTANEOUS DETERMINATION OF FILM PERMEABILITY TO H_2O_2 AND SUBSTRATE SURFACE AREA COVERAGE OF OVEROXIDIZED POLYPYRROLE.

Abstract

A method to simultaneously determine film permeability and surface area coverage of electrochemically generated and overoxidized polypyrrole films on platinum is presented. The method, similar to the Koutecky-Levich approach, is based on the rotating disk electrode but uses experimental data from bare and film-covered electrodes to compensate for deviations from ideality. We address the effects of polymer growth potential, electrolyte concentration, monomer concentration, enzyme concentration and film thickness in film permeability, substrate surface area coverage and film adhesion of polypyrrole films grown from aqueous solutions. Film thickness was measured using transmission electron microscopy of films deposited on thin platinum wires. Surface morphology is illustrated using scanning electron micrographs. Relevant effects of film permeability and thickness are related to the response of amperometric polypyrrole-enzyme biosensors found in the literature.

Keywords: permeability, surface area, overoxidized polypyrrole, rotating disk electrode, enzyme biosensor.

Introduction

The first polypyrrole-glucose oxidase (PPY-GOD) amperometric biosensors were fabricated in 1986 [1,2]. This electropolymer-enzyme combination is the most frequently reported in the literature. Electrochemically generated polymers are excellent matrices for enzyme entrapment because they can be grown from aqueous solutions at low potentials and produce films of controllable thickness [3] and size exclusion properties [4] with uniformly distributed enzymes. Despite these advantages, commercial development of this type of biosensor for industrial applications still requires optimization in terms of stability, sensitivity and response time. An important step in sensor design and optimization is the characterization of the diffusion and kinetic parameters of the immobilization matrix. For GOD and other oxidase-based amperometric biosensors, it is important to determine the permeability of the matrix to the analyte and to H_2O_2 produced by the enzymatic reaction because the transduction of most of these sensors is based on the oxidation of H_2O_2 at the transducer's surface. It is also critical that potentially interfering species like ascorbic acid be prevented from reaching the surface of the electrode. Many studies of PPY films have focused on the effects of the nature of the counter ion, the concentration of electrolyte [5] and the presence of surfactants [6] on film electrical conductivity, tensile strength, and elasticity [7]. However, while electrochemical determination of permeability of polymer films using electrodes covered by the film (but not deposited or adhered to it) has been studied using a rotating disk electrode [8-10], few studies exist for electrochemically generated polymers. In the first case, presumably the film does not block the metal surface area, therefore, only permeability needs to be determined which can simply be done using the method

proposed by Gough and Leypoldt [8]. Most assessments of permeability of hydrogen peroxide and ascorbic acid in polypyrrole and polypyrrole-enzyme films have been qualitative. Other studies indicate that enzyme presence inhibits polymer growth and that permeability and film roughness decrease as enzyme concentration increases [3]. Very few quantitative permeability studies have been published [11-14]. The main difficulty in determining the permeability of electrochemically-generated polymers is that the amperometric response of polymer-coated electrodes is affected not only by the permeability of the film but also by the partial surface area coverage of the electrode by the adhered polymer. Permeability and substrate surface area can be calculated from the Koutechy-Levich approach that uses double reciprocal plot of the diffusion current vs. the square root of the rotational speed. However, this method does not compensate for non-ideality of the hydrodynamics of the system and for data extrapolation. It has been used mainly for calculation of permeability alone [8,11,15,16] . In addition, if the polymer is electrically conductive, none of the available methods allow the determination of diffusion properties. In the case of PPY, exposing such electrodes to hydrogen peroxide solutions or applying oxidizing potentials above 700 mV vs. Ag/AgCl causes overoxidation of the polymer [17]. This phenomenon is accompanied by loss of electroactivity, changes of mechanical properties and even detachment of the film from the substrate metal [1,15,18] likely due to the breakage of the polymer backbone. However, polymer overoxidation is still commonly used in biosensor research [3,16,19-21]. Film permeability changes observed over time are probably due to polymer swelling. However this effect has not been fully characterized and may be one of the causes of the decrease in amperometric response of enzyme sensors based on electrochemically

generated polymers. Overoxidized polypyrrole has shown excellent permselectivity to some important interfering species [12,22]. Other non-conducting polymers like poly-*o*-phenylenediamine have also been studied in that respect [23].

To the best of our knowledge, no quantitative study of the permeability and substrate surface area coverage of PPY and PPY-GOD electrodes as a function of the polymer growth conditions has been conducted. Such studies are necessary to optimize the fabrication of enzyme-based biosensors.

In this paper we present a method to simultaneously determine film permeability and substrate surface area coverage of electrochemically generated polypyrrole film, using a rotating disk electrode. The proposed method is similar to Koutecky-Levich's but overcomes the issues of non-ideality and extrapolation. We address the effects of polymer growth potential, electrolyte concentration, monomer concentration, enzyme concentration and film thickness on film permeability to H_2O_2 and substrate surface area coverage of overoxidized polypyrrole films grown from aqueous solutions.

Theory

The method used to simultaneously determine permeability and substrate surface area coverage is a variant of the method for permeability determination proposed by Gough and Leypoldt (1979) [8] based on the Koutecky-Levich approach. In that method, the following equation is proposed:

$$i_d = i_L \left[\frac{1}{1 + \frac{P_S}{P_m}} \right] \tag{1}$$

Where i_d represents the measured diffusion current, i_L represents the Levich limiting current, and P_S and P_m represent the permeability of the solution and the membrane respectively.

The Levich current is calculated as:

$$i_L = 0.62nFAD^{2/3}\nu^{-1/6}C_B\omega^{1/2} \quad (2)$$

Where n is the number of electrons exchanged during the electrode reaction; F is the Faraday's number; A is the surface area of the electrode; D is the diffusion coefficient of the reacting species in solution; ν is the kinematic viscosity of the solution; C_B is the concentration of reacting species in the bulk of the solution; and ω is the rotation speed of the RDE.

The solution permeability is calculated as:

$$P_S = \frac{D}{\delta_d} \quad (3)$$

Where δ_d, the thickness of the diffusion layer on the liquid membrane interface is given by:

$$\delta_d = 1.6D^{1/3}\nu^{1/6}\omega^{-1/2} \quad (4)$$

The permeability of the membrane is calculated as:

$$P_m = \frac{\alpha D_m}{\delta_m} \quad (5)$$

Where α is the partition coefficient, D_m is the diffusion coefficient of the reacting species in the membrane (or film) and δ_m is the thickness of the membrane. Dividing the limiting current by the surface area we obtain:

$$j_L = \frac{i_L}{A} = 0.62nFD^{2/3}\nu^{-1/6}C_B\omega^{1/2} \tag{6}$$

and substituting equations 4, 5 and 6 into equation 1 we obtain:

$$j_d = \frac{i_d}{A} = 0.62nFD^{2/3}\nu^{-1/6}C_B\omega^{1/2}\left[\frac{1}{1+\frac{D/(1.6D^{1/3}\nu^{1/6}\omega^{-1/2})}{\alpha \cdot D_m/\delta_m}}\right] \tag{7}$$

Where j_d is the diffusion current density. Because upon deposition of PPY on the surface of the electrode, not all of its surface area may be available for reaction, a priori we cannot calculate j_d.

In the proposed method, i_d is measured at several rotational speeds. With a guessed value of A, j_d is calculated and with a guessed P_m, the estimated limiting current density j_{Lexp} is also obtained as a function of rotational speed from equation (6). j_L is linear with respect to the square root of the rotational speed and is independent of the film. However, since the surface area was guessed, j_{Lexp} calculated from experimental data will differ from the real current density j_{Lbare} measured at the bare electrode by a constant factor, provided that P_m is correct. Therefore, the experimental data points are fit to the curve by minimizing the standard deviation of the ratio j_{Lbare}/j_{Lexp} and changing the value of P_m. This was done using the Newton Method of Microsoft Excel solver. The surface area available is obtained by dividing the guessed surface area by the mean of the

ratio j_{Lbare}/j_{Lexp} obtained at each rotational speed. Alternatively, the intercept of a Koutecky-Levich plot of i_d^{-1} vs. ω^{-1} gives i_d^{-1} at infinite rotational speeds:

$$\frac{1}{i_d} = \frac{1}{nFAC_B P_m} + \frac{1}{0.62nFAD^{2/3}\nu^{-1/6}C_B}\frac{1}{\omega^{1/2}} \quad (7)$$

From the intercept, the product of A and P_m can be determined and A can be calculated from the slope. A limitation of this method is that it does not compensate for deviations from ideality and it requires extrapolation of the data.

Experimental

Materials

Potassium chloride, potassium ferricyanide, and glucose oxidase (prod. No. G9010) were purchased from Sigma Chemical Co. (St. Louis MI, USA). Pyrrole and ascorbic acid were from Aldrich Chemical Co. (Milwaukee WI, USA). Hydrogen peroxide was purchased from JT Baker (Phillipsbourg N.J. USA). Pyrrole was distilled under vacuum before use. All solutions were made with deionized ultra-filtered water ('milli Q').

Three rotating disk electrodes with geometric surface area of 0.19 cm^2 and electrode rotator model AFMSRX were purchased from Pine Instruments (Grove City PA, USA). Polymer growth and electrochemical measurements were carried out in an undivided 50-mL electrochemical cell using an EG&G 263A potentiostat from (Perkin Elmer Instruments Oak Ridge TN, USA), interfaced with a personal computer using a GPIB board or a DAQ-PCI-1200 analog to digital data acquisition board from National

Instruments (Austin TX, USA). Computer programs were written with LabVIEW 6.0. All potentials are referred to an Ag/AgCl, 3M KCl electrode. A platinum wire or foil was used as auxiliary electrode.

Experimental factors

PPY films were grown from de-aerated aqueous solutions on platinum electrodes. PPY films were overoxidized by applying 700 mV vs. Ag/AgCl in 0.1 M KCl for 2 h. Varied factors were: pyrrole concentration, KCl concentration, GOD concentration, integrated charge density (charge passed over time per unit surface area) and polymer growth potential. Levels for each of these factors are shown in Table 1. All experiments were carried out in duplicate. Surface area and diffusion coefficient determinations were carried out three consecutive times on each electrode (bare and polymer-covered).

Electrode Cleaning

Electrodes were immersed in concentrated sulfuric acid overnight, rinsed with deionized water, and any remaining adhering polymer was removed with paper tissue. Electrode potential was cycled 25 times between -0.20 and 1.45 mV in 0.1M H_2SO_4 at 500 $mV.s^{-1}$. In all cases characteristic current-potential patterns were obtained.

Determination of electrode surface area

Because the same electrodes were used for several treatments, and their effective surface areas may be affected by their history, the bare surface area was determined every time before polymer growth using linear sweep voltammetry between 0.4 and –0.4 V vs.

Ag/AgCl at 0.01 $V.s^{-1}$ in 0.004 M $K_3Fe(CN)_6$ plus 0.1M KCl solutions at different rotational speeds and solving equation (2) after linear regression of I_L *vs.* $\omega^{1/2}$. In this solution ferricyanide diffusion coefficient is 7.62 x 10^{-6} $cm^2.s^{-1}$ [24]. This procedure was repeated sequentially at least three times for each electrode and the mean of these determinations was taken as the surface area value for diffusion experiments in H_2O_2 and for comparison with the surface area available of the polymer-covered electrode.

Determination of H_2O_2 and ascorbic acid diffusion coefficients

Diffusion coefficient of 0.005M H_2O_2, 0.1 M KCl and 0.05M ascorbic acid were determined analogously to surface area determinations except that, knowing surface area, diffusion coefficients were solved from equation (2). Potential ranges were 0.3 to 1.2 V and 0.1 to 1.35 V and scan rates were 0.02 $V.s^{-1}$ and 0.004 $V.s^{-1}$ for H_2O_2 and ascorbic acid respectively.

Determination of Permeability and Surface Area Coverage

Film permeability to H_2O_2 and surface area coverage were determined according to the method described in the Theory section. Potential range, scan rate and H_2O_2 concentration were the same as for the determination of diffusion coefficient in solution.

Film morphology and thickness

Transmission electron microscopy (TEM) and scanning electron microscopy (SEM) studies were done on PPY-covered Pt wire to determine polymer film thickness and illustrate film morphology respectively. Pt wire with a diameter of 25.4 μm was

purchased from Omega Engineering Inc. Surface area of sections of bare and PPY-covered Pt wire and wire segment lengths were determined using Scion Image for Windows from Scion Corporation. The mean diameter of PPY-covered Pt wire was calculated as the ratio of the surface area of a section of wire (calculated by the computer program) and the length of the segment of the wire. Film thickness was calculated from the difference in diameter between film-covered and bare electrode.

Table 1. Studied factors and levels.

Adjusted factor	Levels of adjusted factor	Factors kept constant				
		E (mV)	δ ($mC.cm^{-2}$)	[Py] ($mol.L^{-1}$)	[KCl] ($mol.L^{-1}$)	[GOD] ($mol.L^{-1}$)
E (mV)	650, 700, 800		45	0.3	0.1	0
δ ($C.m^{-2}$)	900, 1800, 2700	650		0.3	0.1	0
[Py] ($mol.L^{-1}$)	0.3, 0.6, 0.9	650	90		0.1	0
[KCl] ($mol.L^{-1}$)	0.001, 0.01, 0.1	650	45	0.3		0
[GOD] ($U.mL^{-1}$)	0, 100, 200, 300	650	90	03	0.1	

Results and discussion

Determination of surface area and diffusion coefficients at bare electrodes

As anticipated, bare electrode surface areas varied after each cleaning procedure. Values varied between 0.16 and 0.20 cm^2. However, sequential determinations on the same electrode after cleaning gave standard deviations of the order 0.003 cm^2. Error in the preparation of ferricyanide solution and mounting the electrode on the rotator was also

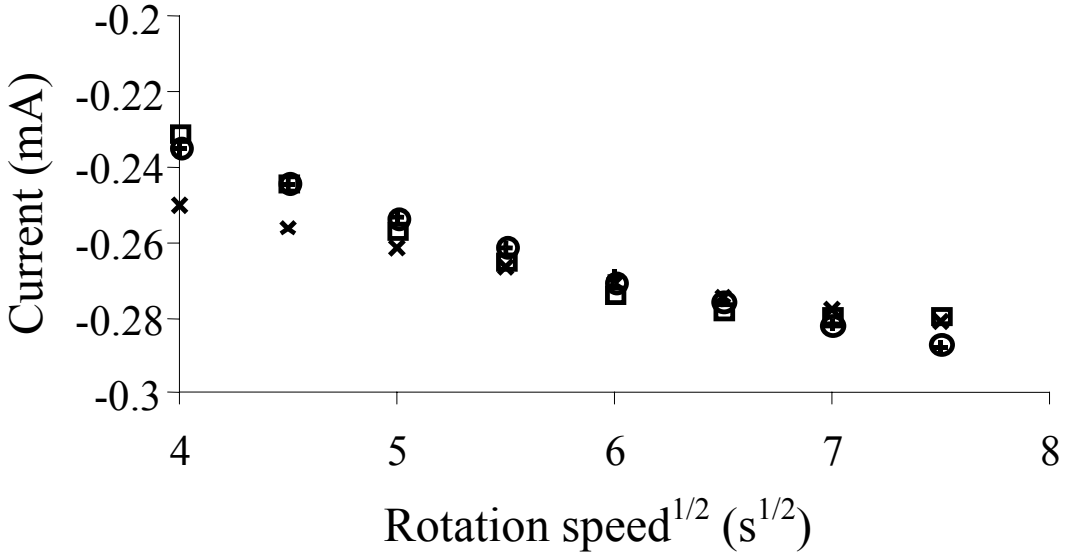

Figure 1. Diffusion current (i_d) at different rotation speeds for (○) experimental measurements of PPY-covered electrode; (□) values calculated by the proposed method using experimental measurements of i_L at the bare electrode to calculate the ratio j_{Lbare}/j_{Lexp}; (+); values calculated by the proposed method using a linear correlation of experimental measurements of i_L at the bare electrode to calculate the ratio j_{Lbare}/j_{Lexp} and (x) values calculated by minimizing the difference between experimental measurements of i_d and i_d calculated from linear correlation of i_L measurements at bare electrodes assuming A is the same for bare and PPY-covered electrodes. PPY film was grown from a solution containing 0.1 M KCl, 0.3 M Pyrrole at 650 mV vs. Ag/AgCl in 3M KCl. Film thickness was 1800 $C \cdot m^{-2}$.

addressed. The precision of the measurements using 5 solutions prepared independently and three electrodes was 0.01 cm^2. This value is the largest 95% confidence interval resulting from the three electrodes and is equivalent to a 6% deviation from the mean. Also no significant differences were found among the surface area of the three electrodes

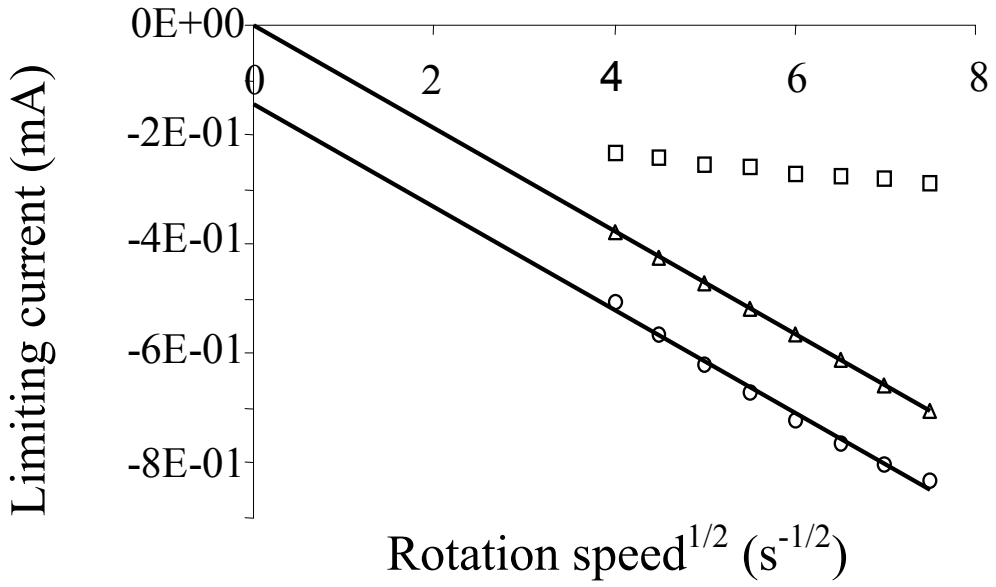

Figure 2. Limiting current vs. Rotation speed$^{0.5}$ of a Pt disk electrode (○) bare, experimental (□) bare, calculated (Δ) PPY-covered electrode. PPY film was grown from a solution containing 0.1 M KCl plus 0.3 M Pyrrole at 650 mV vs. Ag/AgCl in 3M KCl. Film Thickness was 1800 C·m^{-2}.

($p = 0.113$). From sensitivity analysis, using typical data, estimated errors in permeability and surface area coverage caused by an error of 0.01 cm^2 in the determination of surface area of bare electrodes were 6.3% and 5.9% respectively. Diffusion coefficients of H_2O_2 and ascorbic acid are presented in Table 2. Our results are of the same order of those published in the literature [11].

Table 2. Diffusion coefficients of H_2O_2 and ascorbic acid in 0.1 M KCl determined at rotated platinum disk electrodes.

Solute	*Diffusion Coefficient $(m^2 \cdot s^{-1}) \times 10^9$	Published Diffusion Coefficient $(m^2 \cdot s^{-1}) \times 10^9$	Standard Deviation $(m^2 \cdot s^{-1}) \times 10^9$	Number of Determinations
0.005 M H_2O_2 , 0.1 M KCl	4.61	2.0	0.40 (≈ 9%)	9
0.005 M Asc. Ac. 0.1 M KCl	1.83	----	0.06 (≈ 4%)	9

* Represents the mean of at least nine determinations using three electrodes. Determination of the surface area of the electrode impacts this determination.

Determination of Permeability and Surface Area Coverage

The first proposed method fits experimental results well as illustrated in Figure 1. However, the rotating disk electrode's behavior deviates from ideality as shown in Figure 2. Experimental limiting current is different from calculated. Because the apparent H_2O_2 diffusion coefficient in solution is calculated from the slope of i_L vs. $\omega^{1/2}$ (equation 2) from experiments using bare electrodes, calculated and experimental slopes are the same but the experimental intercept is not zero. This is mainly due to the geometry of the electrode as discussed by Riddiford [25]. Although the exposed part of the electrode is a disk, the body of the electrode is a cylinder. Also the solution volume is not infinite. Hence, flow patterns deviate from ideality. Because bare and film covered electrodes are exposed to the same dynamic conditions (rotational speeds, immersion depth, and container), the method uses experimental values of i_L at the bare electrode for determination of A and P_m. The main advantage of the proposed method as compared to the Koutecky-Levich method is that it compares experimental diffusion data of each film-

covered electrode to experimental diffusion data of the same bare electrode prior to electropolymerization and hence, compensates for non-idealities in flow dynamics and error in solution preparation or rotational speed. Thus, it results in better fits and better estimates of A and Pm. In addition, the Koutecky-Levich method has an intrinsic error from extrapolating data of the double reciprocal plot. The disadvantage of the proposed method is that it requires more experimental and computer work, the latter being insignificant with today's technology. Previous studies of diffusion at PPY-based electrodes have used Koutecky-Levich approach for the determination of permeability and apparent diffusion coefficient of PPY film[16] and have assumed that surface area of PPY- covered electrodes is equal to surface area of bare electrodes [11,15,16]. Under our experimental conditions we have evidence that this approach is incorrect as illustrated in Figure 1. Data fitted by minimizing the difference between experimental measurements of i_d and i_d calculated from linear correlation of i_L measurements at bare electrodes, assuming that A of PPY-covered electrodes is the same for bare electrodes, resulted in a poorer fit as compared to data fitted by adjusting the surface area using the proposed method. The best fit was obtained for values calculated by the proposed method using a linear correlation of experimental measurements of i_L at the bare electrode to calculate the ratio j_{Lbare}/j_{Lexp}. Using the linear correlation of experimental measurements of i_L at the bare electrode mitigates errors in the experimental procedure that would otherwise add to the error of the measurements at the PPY-covered electrode. Values of P_m and A resulting from each of the methods mentioned above along with those resulting from the Koutecky-Levich approach are presented in Table 3. Surface area of PPY covered electrode, $A_{PPY,}$ and P_m values were of the same order regardless of the method of

Table 3. Determination of permeability and surface area by different approaches for a PPY film grown from a solution containing 0.1 M KCl, 0.3 M pyrrole at 650 mV vs. Ag/AgCl in 3M KCl. Film thickness was 1800 $C.m^{-2}$.

Parameter	Using all i_{Lbare} data	Using correlated i_{Lbare} data	Assuming A_{PPY} equal to A_b	Koutecky-Levich approach
P_m ($m \cdot s^{-1}$) x 10^5	6.85	7.62	4.23	3.04
A (m^2) x 10^5	1.26	1.19	1.63	2.64
A x P_m ($m^3 \cdot s^{-1}$) x 10^{10}	8.61	9.10	6.92	8.00

determining them. However, A_{PPY} determined by the Koutecky-Levich method is larger than A_B at the bare electrode, which is impossible, unless some of the film had retained its electrical conductivity, which is unlikely after 2h of overoxidation. Therefore, all our discussion and data analysis is based on determination of P_m and A_{PPY} using the proposed method. Permeability to ascorbic acid was so low that it could not be recorded using this method under the experimental conditions. This observation is in agreement with previous reports on permselectivity of overoxidized PPY-GOD films [22].

Effect of Growth Potential

Permeability decreased with growth potential as shown in Figure 3a. The opposite trend was anticipated because a less uniform and porous film is created at higher growth potentials. However, because the films are less dense when grown at higher potentials, thickness increases causing an overall decrease in permeability. The effect of growth potential on film thickness grown to different integrated current densities is illustrated in Figure 4 where thickness was calculated using image analysis of transmission electron micrographs. Figure 4 also showed a linear relationship between thickness and integrated

current density as reported elsewhere [26,27]. Scanning electron micrographs presented on Figure 5 illustrate the surface morphology of films grown to 82 $mC \cdot cm^{-2}$ at different

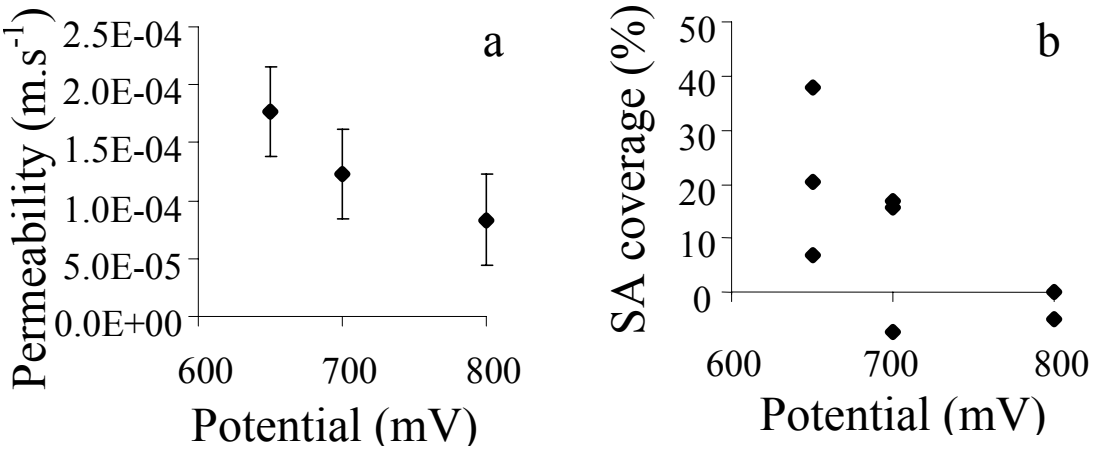

Figure 3. Effect of growth potential on a) film permeability and b) surface area coverage. Films were grown from aqueous solutions containing 0.3 M pyrrole, 0.1 M KCl. Film thickness was 450 $C \cdot m^{-2}$. Error bars represent 95% confidence intervals.

potentials. Linear regression of data from Figure 3a gave equation 8 with a correlation coefficient r^2 of 0.75.

$$P_m = -5.8 \times 10^{-7} E + 5.4 \times 10^{-4} \quad (8)$$

where E represents the polymer growth potential. This value is low due to the small change in permeability (i.e. low slope), and to the relatively large deviation of the experimental data that reflect the difficulty of growing repeatable films on large surface areas. This will be discussed later. Figure 3b shows that surface area coverage of the electrodes is extremely variable. As a matter of fact, because of the poor adhesion of deposited PPY films, after three to four sequential experiments, films detached from the metal surface.

Ellipsometric studies of PPY films grown from 0.025 M pyrrole aqueous solutions showed that as growth potential increases, the required charge to grow a given film thickness decreases which suggests that less dense films and hence more permeable films result from raising the growth potential, which is in agreement with our observations.

Effect of thickness

Permeability obviously decreased with film thickness since these parameters are inversely proportional as stated in equation 5. The mean apparent film diffusion coefficient αD_m calculated with the data from Figures 4 and 6a was 1.1 x 10^{-10} (± 4.3 x 10^{-11}) $m^2.s^{-1}$. Based on Holdcroft and Funt [28], most of the studies assume that 0.1 μm thick film corresponds to about 45 $mC.cm^{-2}$ (which was rounded after interpolating

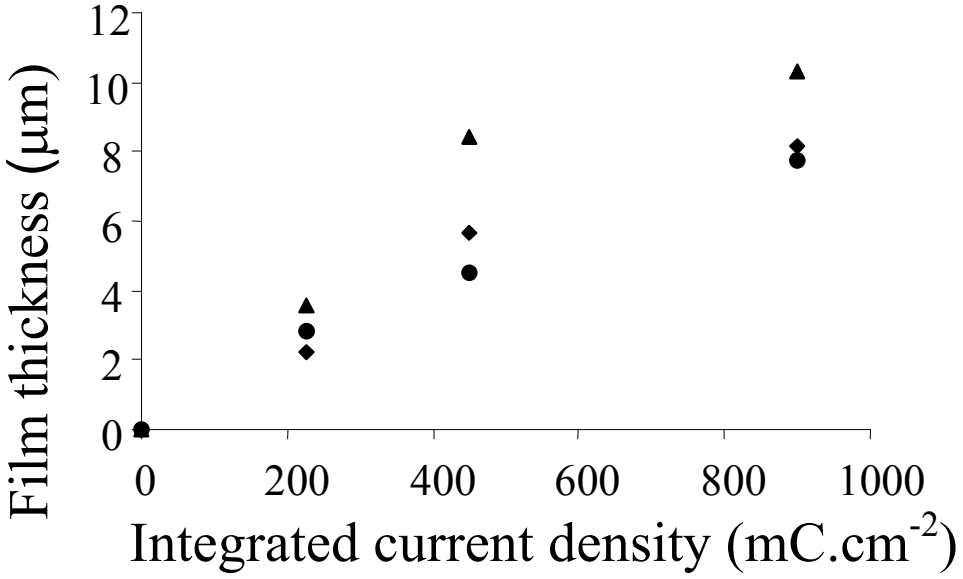

Figure 4. Film thickness vs. integrated current density for PPY films grown at (♦)600, (●)650 and (▲)700 mV from 0.3M Pyrrole, 0.1M KCl solutions.

Holdcroft and Funt's value of 41.07 mC·cm^{-2}). However, Holdcroft and Funt's estimate is based on the following relationship

$$\delta_m = \frac{(MWt)Q_{form}}{nF\rho A} \tag{9}$$

Where *MWt* is the molecular weight of a repeating pyrrole unit plus dopant, n is the number of electrons required for polymerization, ρ is the density of the polymer and Q_{form} is the charge of formation. Under their experimental conditions, Holdcroft and Funt assumed n to be 2 and ρ to be 1.5. Later studies showed that density of the film might vary depending on the growth conditions. Using ellipsometric, microgravimetric and electrochemical measurements, Rishpon and Gottesfeld [26] estimated that PPY and PPY-GOD films grown from aqueous solutions with 0.1 M phosphate buffer pH 7 plus

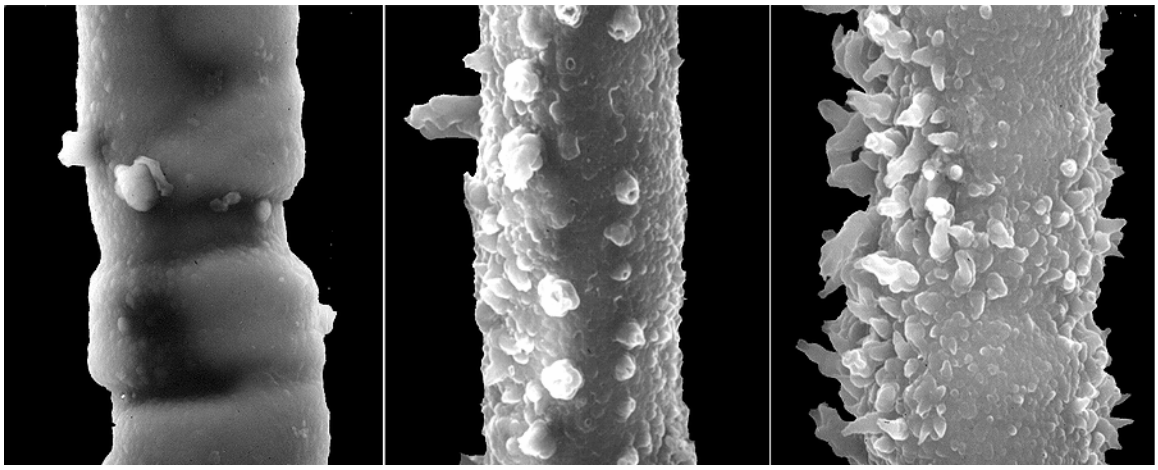

(A) (b) (c)

Figure 5. Scanning electron micrographs for 820 C·m^{-2} thick film: a) 600 mV, b) 650 mV and c) 700 mV

0.2 M pyrrole at 750 mV vs. SCE had densities of 0.6 g.cm^{-3} and 1.67 g.cm^{-3} respectively. Film thickness has been measured by ellipsometry [27,29] and an

equivalent expression of equation 9 was proposed

$$\delta_m = \frac{\bar{v}Q}{2.5F} \quad (10)$$

Where $\bar{v}$ is the molecular volume of the pyrrole monomer, Q is the total charge per unit of surface area. In this equation it is assumed that 2.5 electrons are required by each pyrrole molecule to polymerize with 100% efficiency without accounting for counterion and solvent. Also $\bar{v}$ is assumed to be 67 $cm^3.mol^{-1}$ as compared to 58 $cm^3.mol^{-1}$ in Holdcroft and Funt's study.

In this case a better correlation resulted on the following equation:

$Pm = -8.2 \times 10^{-7} Q + 2.4 \times 10^{-4}$

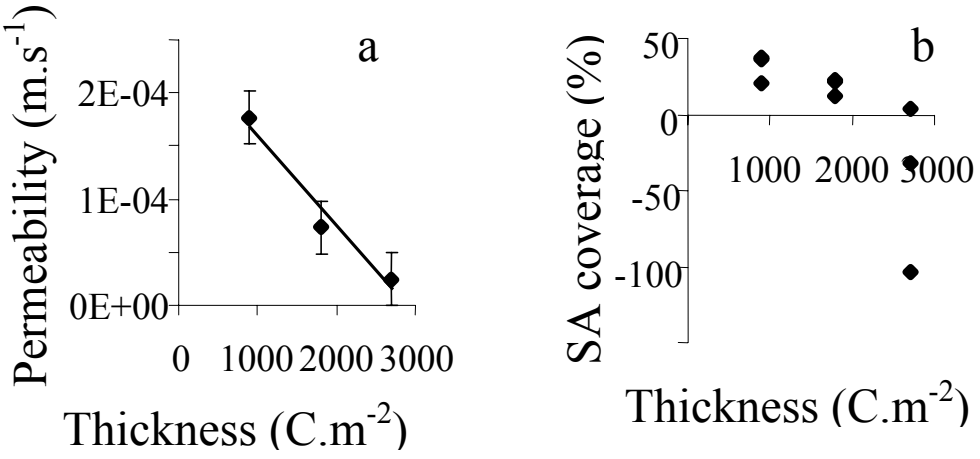

Figure 6. Effect of film thickness on a) film permeability and b) surface area coverage. Films were grown at 650 mV from aqueous solutions containing 0.3 M pyrrole, 0.1 M KCl. Error bars represent 95% confidence intervals.

with correlation coefficient of 0.91. Surface area coverage apparently decreased with film thickness too. However, at the highest thickness and hence the lowest permeability, very scattered data were obtained, the surface area was overestimated and the numerical

method had difficulty converging, which indicates that the application of the proposed method is probably limited to films with permeability greater that 5 x 10^{-5} m.s^{-1}. The

Table 4. Estimated PPY film thickness vs. total charge published.

Growth conditions	Charge required to grow a film 0.1 μm thick (mC·cm^{-2})	Method to determine thickness	Reference
0.3 M Pyrrole, 0.1 M KCl at 600 to 700 mV vs. Ag/AgCl	7.5 to 11	Image analysis of TEM	Our results
Acetonitrile, 1% water, 0.1 M tetrabutylammonium tetrafluoroborate and 0.06 M pyrrole. Galvanostatic growth at 316 μA.cm^{-2}	50.6		[34]
Acetonitrile and aqueous solutions under various pyrrole concentrations and potentials	14 to 66	Ellipsometry	[27]
0.025 M pyrrole, 0.5 M KNO_3	36	Ellipsometry	[29]
0.2 M 1-(2-carboxyethyl)pyrrole 0.1M $(C_4H_9)NBF_4$ in propylene carbonate	17.3	Surface roughness meter	[35]
0.5 M Pyrrole, 0.2 M Et_4NBF_4 in acetonitrile. Galvanostatically	24	Profilometry	[36]
0.1 M pyrrole, 0.1M KCl 71.2 mA.cm^2 Galvanostatically	41	Estimation	[26]
0.2 M $(C_4H_9)NBF_4$ 1M pyrrole	24	Profilometry	[37]

apparent decrease in surface area coverage (Figure 6b) might be due the effects of overoxidation causing polymer shrinkage. Thicker films might produce a stronger force on the polymer-platinum interface upon shrinking resulting in increased detachment.

Another possible explanation to the overestimation of the surface area is that thicker films may require longer overoxidation time. Therefore, part of the PPY film may still be electroactive and may contribute to H_2O_2 oxidation. Also, assuming that during the determination of film permeability the film gradually detaches from the substrate, this would result in a larger slope than if the film remained uniformly attached and would also result in an apparent larger surface area. Finally, Table 4 presents different estimates of PPY film thickness found in the literature.

Effect of pyrrole concentration

PPY film permeability and apparent surface area coverage increased and then decreased with pyrrole concentration as depicted in Figure 7a. The growth rate of films (grown in this case to 90 $mC.cm^{-2}$) increased with the increase in pyrrole concentrations as observed elsewhere [27] which was expected simply by the law of mass action. The higher the concentration, the faster the polymerization took place and the denser the resulting films. Ellipsometric studies [27], showed little effect of pyrrole concentration on the charge-thickness relationship for films grown from 0.1 M and 0.2 M pyrrole solutions in acetonitrile which would suggest that films have the same density and most probably same permeability for a given thickness. However, the range of concentrations studied here is wider and in fact the difference in permeability is small enough to be detected at smaller concentration ranges. The same bimodal behavior was reported for the effect of pyrrole concentration on the current response of glucose oxidase electrodes with optimum around 0.25 M [30] or 0.3 M [21]. Other authors [3] reported a continuous decrease in current response in the range of 0.05 to 0.4 M. However it is difficult to

compare the results because films were grown under different enzyme concentrations and different film thicknesses. For instance, in the last case, films were thinner and were deposited on gold while the two former were thicker and deposited on platinum. While we do not have any experimental evidence, it is reasonable to hypothesize that at relatively low monomer concentrations, as monomer concentration increases, the rate of polymerization increases by mass action. At this level, as the polymer grows the monomer is consumed faster than it diffuses from the bulk resulting in a more permeable structure. At relatively high monomer concentrations, while the polymer grows faster, monomer is abundant enough so that it is always available to react with growing polymer resulting on a more compact less permeable film.

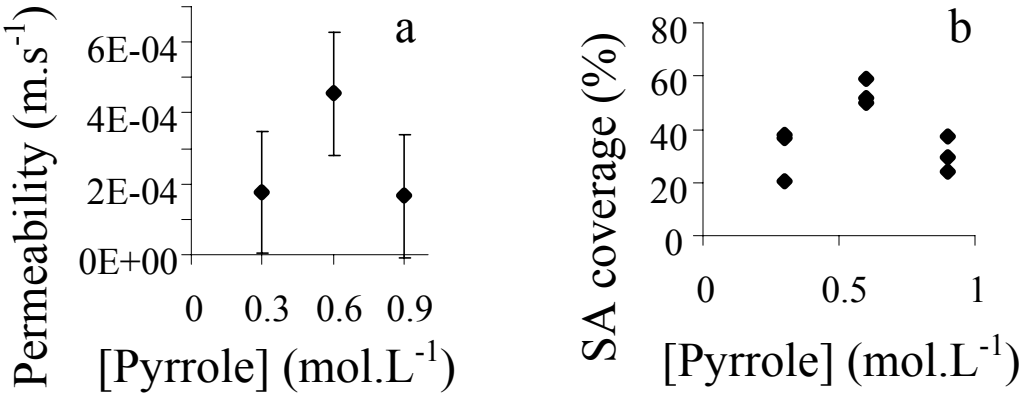

Figure 7. Effect of pyrrole concentration on a) film permeability and b) surface area coverage. Films were grown at 650 mV from aqueous solutions containing 0.1 M KCl. Film thickness was 900 $C \cdot m^{-2}$. Error bars represent 95% confidence intervals.

Effect of KCl concentration

Increasing the concentration of supporting electrolyte (KCl) increased the rate of polymerization and the permeability of the resulting films until a constant value is

reached as depicted in Figure 8a. Here again, a more permeable membrane is the result of a faster polymerization. However, since the only role of the supporting electrolyte is as charge carrier, once it reaches certain concentration, the rate of reaction becomes limited by the polymerization reaction. While we obtained very scattered surface area coverage data with low KCl concentrations, there is an apparent decrease of surface area coverage with the increase of KCl concentration (Figure 7b). This may be due to the increased polymerization time as KCl concentration decreased. In other words at low KCl concentration, polymerization takes place slowly, allowing more monomer molecules to diffuse through the thin film being formed to the platinum surface and to polymerize there, blocking more surface area.

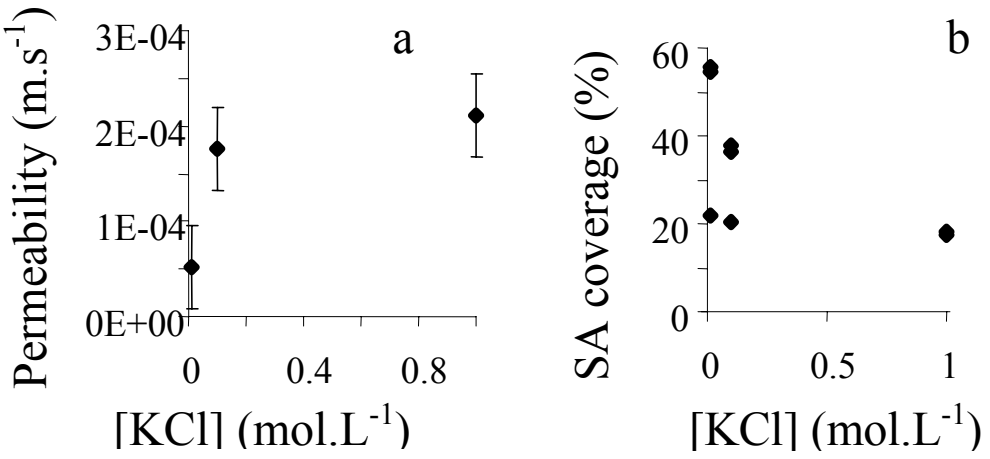

Figure 8. Effect of KCl concentration on a) film permeability and b) surface area coverage. Films were grown at 650 mV from aqueous solutions containing 0.3 M pyrrole. Film thickness was 450 $C \cdot m^{-2}$. Error bars represent 95% confidence intervals.

Effect of GOD concentration

Permeability decreased with the presence of GOD as well as the rate of polymerization as reported elsewhere [31-33] (Figure 9a). Analogously to the case of KCl, the decrease in the rate of polymerization would allow enough time for monomer

molecules to diffuse to the surface of the growing polymer, resulting in a more compact film. Increases in refractive index of GOD-containing PPY films were observed and suggests an increase in polymer density[26] which would be reflected in a decrease in permeability. Linear regression of permeability against glucose oxidase concentration is given by:

$Pm = 3.7 \times 10^{-7} [GOD] + 1.76 \times 10^{-4}$

with correlation coefficient of 0.91. No trend could be observed for surface area because data were very scattered as shown in Figure 9b.

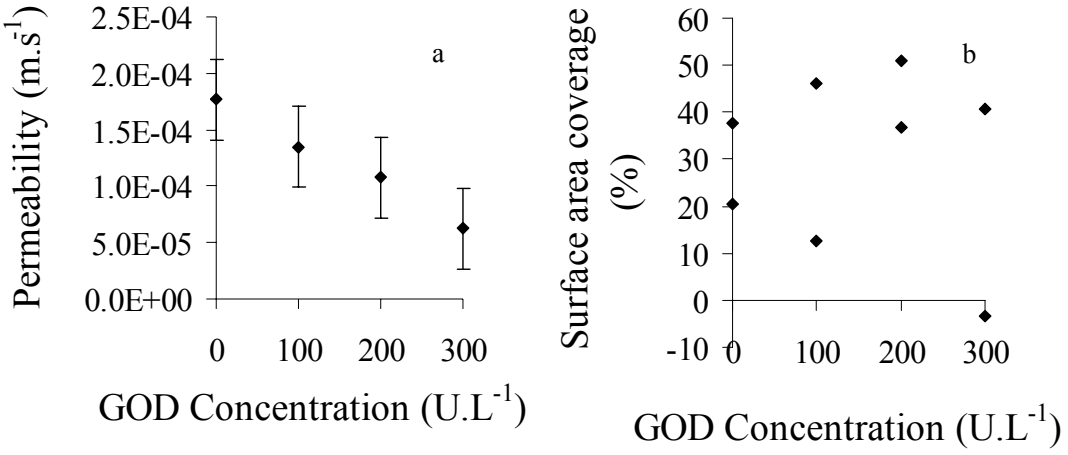

Figure 9. Effect of GOD concentration on a) film permeability and b) surface area coverage. Films were grown at 650 mV from aqueous solutions containing 0.3 M pyrrole, 0.1M KCl. Film thickness was 900 $C \cdot m^{-2}$. Error bars represent 95% confidence intervals.

Conclusions

The proposed method allows determining simultaneously permeability and substrate surface area coverage of overoxidized PPY films. This model fit the experimental data better than the Koutecky-Levich approach under the experimental conditions used in this study. Effects of polymer growth potential, film thickness,

monomer concentration, electrolyte concentration and enzyme concentration on permeability and surface area determinations agree with the literature. However, unlike previous work, we present quantitative values of permeability and surface area coverage. Results obtained using the proposed method indicate that the very large variability in the fabrication of overoxidized polypyrrole films on polished platinum disk electrodes is mainly due to the variability in surface area coverage. Quantification of surface area coverage gives a more accurate determination of permeability allowing correlation of permeability with growth potential, film thickness and enzyme concentration. Variability in the determination of permeability of films may be due mainly to non-uniform growth of polymer. This non-uniformity is due to the heterogeneous roughness of platinum disks that varies among electrodes. While seldom used in the fabrication of PPY-GOD sensors, electrodeposition of platinum black prior to polymerization favors the uniform nucleation of PPY. The presented method should provide a better means of estimating parameters used for the design and optimization of PPY-GOD biosensors. When the polymer film is conducting and the analyte of interest is being oxidized at its surface, none of the available methods included the proposed one allow the determination of film permeability or surface area.

From a brief literature review and our own measurements, we conclude that film thickness is strongly affected by electropolymerization conditions. Therefore, using the relationship between film thickness and total polymerization charge from the literature should be done only if the experimental conditions are identical. It is recommended to report the total polymerization charge as a measure of thickness.

Acknowledgement

The authors are grateful for the financial support of Mr. Reyes De Corcuera by CONACyT (National Council for Science and Technology Mexico), Fulbright and for the financial support of the WSU IMPACT center.

References

[1] M. Umana and J. Waller, Anal. Chem. 58, (1986) 2979.

[2] N.C. Foulds and C.R. Lowe, J. Chem. Soc., Faraday Trans. 82, (1986) 1259.

[3] M.-C. Shin, H.-S. Kim, Biosensors & Biolelectronics 11, (1996) 161

[4] J. Wang, S.-P. Chen, M.S. Lin, J. Electroanal. Chem 273, (1989) 231.

[5] Y. Li, Electroanal. Chem. 433, (1997) 181.

[6] Y. Li and J. Ouyang, Synth. Met. 113, (2000) 23.

[7] S.B. Adeloju, S.J. Shaw, G.G. Wallace, Anal. Chim. Acta 281, (1993) 611

[8] D.A. Gough and J.K. Leypoldt, Anal. Chem. 51, (1979) 439.

[9] D.A. Gough and J.K. Leypoldt, Anal. Chem. 52, (1980) 1126.

[10] D.A. Gough, J.K. Leypoldt, J.C. Armour, Diabetes Care 5, (1982) 190.

[11] P. Gros and A. Bergel, J. Electroanal. Chem 386, (1995) 65.

[12] F. Palmisano, C. Malitesta, D. Centonze, P.G. Zambonin, Anal. Chem. 67, (1995)

2207.

[13] A. Witkovski , M.S. Freund, A. Brajter-Toth, Anal. Chem. 63, (1991) 622.

[14] A. Witkovski and A. Brajter-Toth, Anal. Chem. 64, (1992) 635.

[15] C. Hsueh and A. Brjter-Toth, Anal. Chem. 66, (1994) 2458.

[16] D. Bélanger, J. Nadreau, G. Fortier, Electroanalysis 4, (1992) 933.

[17] D. Bélanger, J. Nadreau, G. Fortier, J. Electroanal. Chem 274, (1989) 143.

[18] Guiseppi-Elie, A.; Wallace, G. C.; Matsue, T. *Handbook of Conducting Polymers*, Skotheim. Jerje A.; Elsenbaumer, R. L.Reynolds, J. R., Eds.; 2nd ed.; Marcel Dekker Inc.: New York, 1998.

[19] M. Hämmerle, W. Schuhmann, H.-L. Schmidt, Sens. Actuators, B 6, (1992) 106.

[20] M.-C. Shin, H.-S. Kim, Biosensors & Biolelectronics 11, (1996) 171

[21] G. Fortier, E. Brassard, D. Bélanger, Biosensors & Biolelectronics 5, (1990) 473.

[22] F. Palmisano, D. Centonze, A. Guerrieri, P.G. Zambonin, Biosensors and Bioelectronics 8, (1993) 393.

[23] D. Centonze, C. Malitesta, F. Palmisano, P.G. Zambonin, Electroanalysis 6, (1994) 423.

[24] Sawyer, D. T.; Sobkowiak, A.; Roberts, J. L. *Electrochemistry for Chemists*, second ed.; John Wiley & Sons Inc.: New York, 1995.

[25] Riddiford, A. C. *Electrochemistry*, Delahay, P., Ed.; John Wiley and Sons: New York, 1966.

[26] J. Rishpon and S. Gottesfeld, Biosensors & Biolelectronics 6, (1991) 142.

[27] S.J. Higgins and A. Hamnett, Electrochim. Acta 36, (1991) 2123.

[28] S. Holdcroft and L. Funt, J. Electroanal. Chem 240, (1988) 89.

[29] A. Hamnet, S.J. Higgins, P.R. Fisk, W.J. Albery, J. Electroanal. Chem 270, (1989) 479.

[30] N.F. Almeida , E.J. Beckman, M.M. Ataai, Biotechnol. Bioeng. 42, (1993) 1037.

[31] P. Janda and J. Weber, J. Electroanal. Chem 300, (1991) 119.

[32] S. Yabuki, F. Mizutani, M. Asai, Biosens. Bioelectron. 6, (1991) 311.

[33] T. Tatsuma, T. Watanabe, T. Watanabe, J. Electroanal. Chem 356, (1993) 245.

[34] L.S. Curtin, G.C. Komplin, W.J. Pietro, J. Phys. Chem. 92, (1988) 12.

[35] K. Kojima, T. Yamauchi, M. Shimomura, S. Miyauchi, Polymer 39, (1998) 2079.

[36] R.M. Penner, L.S. Van Dyke, C.R. Martin, J. Phys. Chem. 92, (1988) 5274.

[37] R.A. Bull, F.-R.F. Fan, A.J. Bard, J. Electrochem. Soc. 129, (1982) 1009.

CHAPTER FOUR

IMPROVED PLATINIZATION CONDITIONS PRODUCE 60-FOLD INCREASE IN SENSITIVITY OF AMPEROMETRIC BIOSENSORS USING GLUCOSE OXIDASE IMMOBILIZED IN POLY-O-PHENYELENEDIAMINE

(Revised manuscript submitted to the Journal of Electroanalytical Chemistry)

CHAPTER FOUR

IMPROVED PLATINIZATION CONDITIONS PRODUCE 60-FOLD INCREASE IN SENSITIVITY OF AMPEROMETRIC BIOSENSORS USING GLUCOSE OXIDASE IMMOBILIZED IN POLY-O-PHENYELENEDIAMINE

Abstract

Platinization has been used to increase electrode surface area and, therefore, electrode sensitivity. However there are few studies about platinization conditions and their effect on the reaction diffusion of enzyme biosensors. We report the fabrication of sensitive (192 ± 48 $\mu A.cm^{-2}.mM^{-1}$) amperometric glucose sensors. Repeatability (precision) was 2.32% ± 1.22% of the measured value, the limit of detection was 0.94 mM and was linear up to at least 25 mM. Sensor-to-sensor variability was 24%. High sensitivity was achieved by improving the conditions of platinization and entrapment of glucose oxidase in poly-o-phenylenediamine. Potentiostatic platinization at –100 or –50 mV vs. Ag/AgCl resulted in mechanically stable deposits unlike the commonly used –250 mV. Large concentrations of glucose oxidase did not inhibit the electropolymerization of o-phenylenediamine. H_2O_2 diffusion experiments using polished and platinized, bare and polymer-covered rotating disk electrodes suggest that H_2O_2 diffuses from the bulk of the solution through the polymer film to be oxidized at the platinized surface and the diffusion is apparently one-dimensional with platinization compensating for the coverage of catalytic sites by the polymer. Conversely, when on a platinized electrode, glucose oxidase is immobilized in a thin poly-o-phenylenediamine film, substrate rapidly diffuses through the porous matrix and H_2O_2 is produced

throughout the enzyme-polymer film. Under these conditions, diffusion is apparently multidirectional and platinization results in an effectively large increase in surface area that results in high amperometric response. A mathematical model of the reaction-diffusion matrix of polished electrodes supports this interpretation of the increased response.

Keywords: Glucose biosensor, platinization, poly-o-phenylenediamine, sensitivity, electropolymerization.

Introduction

Since the first enzyme biosensor fabricated by entrapment of glucose oxidase (GOD) in electrochemically generated polypyrrole was realized (Umana and Waller, 1986, Foulds and Lowe, 1986), hundreds of publications have appeared dealing with this technique and its advantages, which include the accurate control of the polymer's growth and hence of the thickness of the enzyme-polymer film, the potential for co-immobilization of several enzymes (Liu et al., 1998), the use of segregated layers with multiple enzymes (Cosnier, 1999) or the fabrication of microsensors and arrays of microsensors (Trojanowicz et al., 1995, Bartlett and Cooper, 1993). Polymer films may also work as a barrier for electrochemically interfering substances such as ascorbate (Coche-Guerente et al., 1995, Palmisano et al., 1995). Ultra-thin polypyrrole films grown from supporting electrolyte-free solutions have been studied recently (Adeljou and Moline, 2001). Finally, redox mediators have been polymerized and hence have been shown to work as both enzyme hosts and charge mediators (Yang et al., 1998). The

effects of enzyme concentration (Shin and Kim, 1995, Shin and Kim, 1996), monomer type (Coche-Guerente et al., 1995) and concentration, ion nature and concentration (Mu and Jinquing, 1995) and buffer (Pei and Qian, 1992) on the electrochemical response to the analyte of interest (Bélanger et al., 1989) have been determined. Despite all the virtues mentioned above, enzyme biosensors based on electrochemically-generated polymers have two main deficiencies: their long-term stability has not been demonstrated and their sensitivity remains relatively low, typically less than 10 $\mu A.cm^{-2}.mM^{-1}$ for glucose oxidase-based biosensors (Trojanowicz et al., 1995, Fortier et al., 1990, Yon Hin and Lowe, 1994, Chen et al., 2002, Fortier et al., 1990, Yon Hin and Lowe, 1994). An exception is the work by Coche-Guerente et al. (1994) where sensitivities of up to 34 $\mu A.cm^{-2}.mM^{-1}$ were reported for GOD immobilized in poly(amphiphilic pyrrole). Other approaches such as adsorption in porous carbon or in carbon pastes have produced sensitivities of approximately 10 $\mu A.cm^{-2}.mM^{-1}$ (Kulys and Hansen, 1994). To the best of our knowledge, the most sensitive GOD electrode (68 $\mu A.cm^{-2}.mM^{-1}$) was made by Bharathi and Nogami (2001) who electrodeposited gold sol-GOD mixtures by potential cycling. The high sensitivity was presumably due to the high surface area produced by the electrodeposited gold clusters, the three-dimensional conductivity and the porosity of the matrix. Electrodes fabricated by immobilization of GOD in poly-o-phenylenediamine (PPD), a non-conducting polymer, have typical sensitivities of less than 12 $\mu A.cm^{-2}.mM^{-1}$ (Malitesta et al., 1990, Quinto et al., 2000, Guerrieri et al., 1998). Electrode platinization has been recommended as a strategy to increase the sensitivity of biosensors. Electrodes have been platinized from different platinization baths (Baumgärtner and Raub, 1988) under galvanostatic (Kell and Davey, 1990), potentiostatic (Kim and Oh, 1996) or

potential cycling (Schuhmann1998) conditions. However studies on the effect of platinization on biosensor response are scarce. Kim and Oh (1996) studied the effect of platinization potential on electrode roughness and on the amperometric response to glucose after immobilization of GOD by crosslinking with bovine serum albumin (BSA) and glutaraldehyde. However, while platinized electrodes had amperometric response 30 to 40 times that of polished electrodes, sensitivity was approximately 15 $\mu A.cm^{-2}\cdot mM^{-1}$. A similar approach was used earlier (Ikariyama et al., 1988) and GOD was also immobilized in a growing platinum deposit on platinum microelectrodes allowing high sensitivity and very low limit of detection (Ikariyama et al., 1989). However, while platinum surface conditioning minimized electrochemical response to saccharides, other electroactive species such as ascorbate interfered with amperometric detection. Among other strategies such as coating the electrode with permselective membranes and the use of mediators that allow amperometric measurements at lower potentials, several papers have been published detailing the permeability of PPD and its ability to exclude interfering species (Palmisano et al., 1995). PPD is a non-conducting polymer that has the advantage of producing adherent thin films that do not require overoxidation like PPY. Also, overoxidation of PPY has sometimes results in film detachment probably due to the breakage of the polymer's side chains and backbone (Hsueh and Brjter-Toth, 1994).

To the best of our knowledge, there has been no study on the effect of platinization potential on the response of amperometric biosensors based on enzyme immobilization in electrochemically-generated polymers. Also, we have not found any study on the effects of enzyme load, polymerization potential, or platinum surface area coverage by PPD on the resulting sensors.

In this paper we present a glucose sensor that exhibits greater sensitivity than others fabricated by entrapment in electrochemically-generated polymers. To obtain such result we addressed the effects of platinization potential, platinization charge, and enzyme load. A mathematical model of the reaction-diffusion matrix of polished electrodes is used to support the interpretation of our results.

Materials

Glucose oxidase (EC 1.1.3.4 type X-S from *Aspergillus niger*), o-phenylenediamine free base (PD), chloroplatinic acid hexahydrate, hydrogen peroxide, and potassium chloride were purchased from Sigma Chemical Co. (St Louis, MO, USA). Lead acetate trihydrate was purchased from Aldrich Chemical Co. (Milwaukee, WI, USA). Platinum wire (1 mm diameter) was purchased from Fisher Scientific (Fair Lawn, NJ, USA). All other reagents and solvents were purchased from Sigma-Aldrich or Baker Analyzed and were reagent grade. Deionized, ultrafiltered ($\Omega > 18$ MΩ.cm) water was used for all aqueous solutions.

Equipment

Electropolymerization and electrochemical measurements were performed with a potentiostat/galvanostat, EG&G 263A, (Perkin Elmer Instruments Oak Ridge, TN, USA), interfaced to a personal computer, through a GPIB or PCI analog to digital board, National Instruments (Austin, TX, USA). All potentials are reported with respect to Ag/AgCl, 3.0 M KCl reference electrode. The counter electrode, a 5 mm diameter platinum disk electrode model AFE1E050 from Pine Instruments Co. (Grove City PA,

USA), tightly inserted into a plastic tube that worked as reaction cell, was placed parallel to the working electrode. The distance between the working and the counter electrode was 3 mm for all the platinization and polymer growth experiments. A miniature Ag/AgCl reference electrode model EE008 from Cypress Systems Inc. (Lawrence, KS, USA) was used.

Software

Cyclic voltammetry was carried out with Power Suite software (Perkin Elmer, Oak Ridge, TN, USA). All other operations and data acquisition and processing were controlled with computer programs written using LabVIEW 6i (National Instruments, Austin, TX, USA). Numerical solution of the mathematical model was done using MATLAB (The Mathworks, Inc., Natick, MA, USA).

Methods

Platinum electrode fabrication and characterization

Platinum wire (1 mm in diameter 5 mm long) was sealed in soft glass. Electrodes were polished with 220 grit and 600 grit abrasive papers, then with 5 μm and 0.05 μm alumina slurries. Electrodes were then cleaned for 15 min in an ultrasonic bath, immersed in concentrated sulfuric acid overnight, and rinsed with deionized ultrafiltered water. Finally, electrode potential was cycled 80 times between -0.20 and 1.45 mV vs. Ag/AgCl in 0.1M H_2SO_4 at 500 $mV.s^{-1}$. In all cases the characteristic current-potential pattern for Pt was obtained. When reused, electrodes underwent the cleaning procedure described above, starting from the polishing step with 5 μm alumina.

Platinization of platinum electrodes

Potentiostatic platinization of the electrodes was carried out at from –50 to -250 mV vs. Ag/AgCl in 2 mM H_2PtCl_6, 1 mM $Pb(C_2H_3O_2)$ (as crystal growth promoter), 0.1 M KCl oxygen-free solution to a total charge density of 0.5 or 2.0 $mC.cm^{-2}$. Electrodes were rinsed with deionized ultrafiltered water. Surface area increase was determined by cyclic voltammetry in 0.5 M H_2SO_4.

Immobilization of glucose oxidase

Electropolymerization was carried out in 5 mM o-phenylenediamine (oPD), 2 M acetate buffer pH 5.2, and 1 to 50 $g.l^{-1}$ GOD oxygen-free solutions at 650 mV vs. Ag/AgCl for 35 min. Before polymerization potential was applied, electrodes were immersed for 5 min in the monomer-enzyme solution to allow monomer and enzyme to diffuse into the platinized matrix. Three electrodes were prepared for each level of GOD concentration.

Electrode testing

Electrode amperometric response at 700 mV vs. Ag/AgCl to glucose solutions was tested by immersion in 0.1 M phosphate buffer pH 7 glucose solutions. Steady state current response in stirred solutions was used.

To determine linearity, sensitivity and limit of detection, at least three electrodes were tested at glucose concentrations ranging from 0 to 25 mM. Sensor to sensor

reproducibility was calculated using four polished and four electrodes platinized to 0.5 $mC \cdot cm^{-2}$ and ten electrodes platinized to 2.0 $mC \cdot cm^{-2}$.

Mathematical modeling

A model mathematical model based on the one proposed by Leypoldt and Gough (1984), later modified and expanded to GOD immobilized in electrochemically generated polypyrrole by Gros and Bergel (1995) was used. In these two previous studies a shooting method was used. We used MATLAB and the bvp4c routine, which is a finite difference method with a 3-stage Lobatto IIIa collocation formula. In Gros and Bergel report, it was demonstrated that 90% of the response of the sensor was due to the immobilized enzyme within the electropolymerized film and that adsorbed enzyme at the polymer-metal and polymer-solution interfaces accounted for the remaining 10%. Furthermore, the assumption of uniform distribution of the enzyme in the electrochemically-generated polymer is supported by the good fit of the model to the experimental data at different film thickness. Our model only accounts for entrapped GOD. Convergence is highly dependent on the initial guess in a collocation routine. Therefore, for the first calculation, O_2 and H_2O_2 concentration profiles were assumed parabolic (but opposite in sign) as shown in Gros and Bergel (1995). Table 1 summarizes the model.

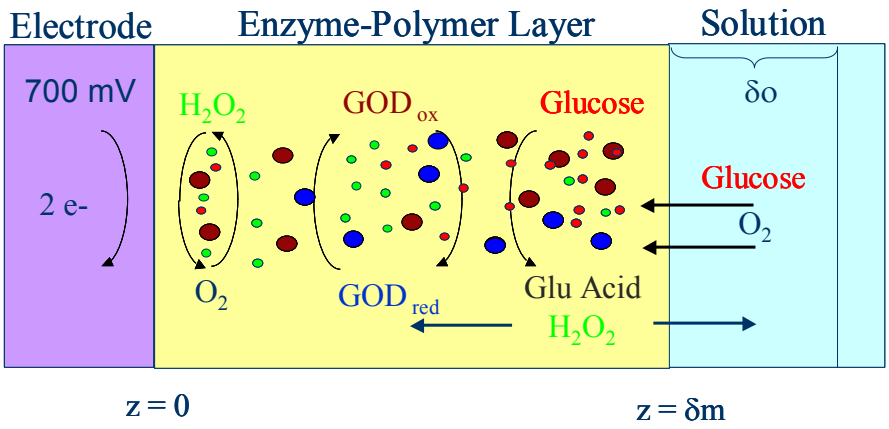

Figure 1. Schematic representation of the amperometric detection of glucose at the GOD-PPD electrode

Table 1. Mathematical model.

Equations	Boundary condition 1	Boundary condition 2
$D_G \frac{d^2C_G}{dz^2} - r(C_G, C_O) = 0$ $D_O \frac{d^2C_O}{dz^2} - r(C_G, C_O) = 0$ $D_H \frac{d^2C_H}{dz^2} + r(C_G, C_O) = 0$ $r(C_G, C_O) = \frac{v_{\max} C_G C_O}{C_G C_O + K_G C_O + K_O C_G}$	At z = 0 $\frac{dC_G}{dz} = 0$ $D_O \frac{dC_O}{dz} = -D_H \frac{dC_H}{dz}$ $C_H = 0$	$C_H = 0$ in the bulk. At z = δ_m^i $\frac{dC_G}{dz} = \frac{1}{\delta_m^o}\left(C_G^b - \frac{C_G}{\alpha_G}\right)$ $\frac{dC_O}{dz} = \frac{1}{\delta_m^o}\left(C_O^b - \frac{C_O}{\alpha_O}\right)$ $\frac{dC_H}{dz} = -\frac{C_H}{\delta_m^o \alpha_H}$
$\frac{d^2\overline{C}_G}{dx^2} - \phi^2 R(\overline{C}_G, \overline{C}_O) = 0$ $\frac{d^2\overline{C}_O}{dx^2} - \phi^2 R(\overline{C}_G, \overline{C}_O) = 0$ $\frac{d^2\overline{C}_H}{dx^2} + \phi^2 R(\overline{C}_G, \overline{C}_O) = 0$ $R(\overline{C}_G, \overline{C}_O) = \frac{(1 + \nu_G + (\nu_O / C_O^*))\overline{C}_G \overline{C}_O}{\overline{C}_G \overline{C}_O + \nu_G \overline{C}_O + \nu_O \overline{C}_G}$	At x = 0 $\frac{d\overline{C}_G}{dx} = 0$ $\frac{d\overline{C}_O}{dx} = -\frac{d\overline{C}_H}{dx}$ $\overline{C}_H = 0$	At x = 1 $\frac{d\overline{C}_G}{dx} = \frac{\delta_m^i}{\delta_m^o \alpha_G}\left(1 - \frac{\overline{C}_G}{\alpha_G}\right)$ $\frac{d\overline{C}_O}{dx} = \frac{\delta_m^i}{\delta_m^o \alpha_O}\left(\overline{C}_O^* - \frac{\overline{C}_O}{\alpha_O}\right)$ $\frac{d\overline{C}_H}{dx} = \frac{\delta_m^i \overline{C}_H}{\delta_m^o \alpha_H^2}$
$\nu_G = \frac{K_G}{\alpha_G C_G^b}$; $\nu_O = \frac{D_O K_O}{\alpha_G D_G C_G^b}$; $\phi^2 = \sigma_G^2 \frac{\nu_G}{1 + \nu_G + (\nu_O / \overline{C}_O^*)}$; $\sigma_G^2 = \frac{v_{\max} \delta_m^i}{D_G K_G}$ $\overline{C}_G = \frac{C_G}{\alpha_G C_G^b}$; $\overline{C}_O = \frac{D_O C_O}{\alpha_G D_G C_G^b}$; $\overline{C}_O^* = \frac{\alpha_O D_O C_O^b}{\alpha_G D_G C_G^b}$; $\overline{C}_H = \frac{D_H C_H}{\alpha_G D_G C_G^b}$; $x = \frac{z}{\delta_m^i}$ $i = nAFD_H\left(\frac{\partial C_H}{\partial x}\right)_{x=0}$		

Definition of variables

A electrode surface area

$\overline{C}_j$ dimensionless concentration of species j

$\overline{C}_j^*$ Effective substrate concentration ratio

C_j concentration of species j

D_j diffusion coefficient of species j

F Faraday's constant

i Current

K_j Michaelis-Menten constant relative to species j

n Number of electrons exchanged

v_{max} maximum enzymatic reaction rate (activity of glucose oxidase in the polymer)

x dimensionless distance from the surface of the electrode

z distance from the surface of the electrode

α_j partition coefficient of species j

δ_m thickness of polymer film

ϕ Thiele modulus

σ Relative catalytic activity

ν_G, ν_O Intermediate variables

Subscripts

G glucose

O oxygen

H hydrogen peroxide

Superscripts

i internal (enzyme-polymer film)

o external (polymer film)

Values of the parameters used in the model from Gros and Bergel (1995) and references therein.

$K_G = 33$ mol·m^{-3}

$K_O = 0.2$ mol·m^{-3}

$\alpha_G = 0.8$

$\alpha_O = 0.8$

$\alpha_H = 0.8$

$D_G = 4.0 \times 10^{-14}$ m^2·s^{-1}

$D_O = 5.0 \times 10^{-13}$ m^2·s^{-1}

$D_H = 5.0 \times 10^{-13}$ m^2·s^{-1}

$v_{max} = 60$ mol.m^{-3}·s^{-1}

Results and Discussion

Electrode platinization

Electrode platinization at potentials between –150 and –250 mV vs. Ag/AgCl resulted in a uniform black platinum deposit. However, such deposits were brittle and fell off the electrode easily upon gently wiping the tip with a paper tissue. Platinization at –50 mV resulted in an almost transparent yellowish film and deposits grown at –100 mV were brownish and opaque for films grown to 0.5 mC·cm^{-2} and black for films grown to 2

$mC \cdot cm^{-2}$. Platinum deposits grown at –50 and –100 mV did not fall off the electrode upon wiping them with a paper tissue. At the beginning of the platinization process, current decreased due to the formation of concentration gradients between the bulk of the solution and the surface of the electrode. After this initial phase, platinization current increased with time as a result of the formation of the platinum black deposit and the increase of the effective surface area of the electrode. The rate of platinization increased with the increase in negative potential, and the increase in platinization current with time was more pronounced for deposits grown at more negative potentials, suggesting that larger surface areas are produced at more negative potentials. Cyclic voltammograms in 0.5 M H_2SO_4 of electrodes platinized at -250 mV, to –50 mV vs. Ag/AgCl at a scan rate of 100 mV/s showed the typical profile for polycrystalline platinum. Electrochemical surface area was calculated by integrating the total charge under the hydrogen adsorption peaks of cyclic voltammograms in 0.5 M H_2SO_4 and assuming 2.1×10^{-4} $C \cdot cm^{-2}$ (Angerstein-Kozolowska H., 1984). The increase in electrochemical surface area for electrodes grown to 0·5 $mC.cm^{-2}$ was in the range of 21.6 to 30.7 times that of the polished electrodes while electrodes platinized at –100 mV vs. Ag/AgCl to 2.0 $mC \cdot cm^{-2}$ had surface area 120 times larger than polished electrodes. Roughness factors in Table 2 show that the surface area increases with increasing negative potentials. Kim and Oh (1996) reported roughness (ratio of the electrochemical surface area and the geometric surface area) in the range of 230 to 375 for the same range of platinization potentials for electrodes platinized to a charge density of 2 $C \cdot cm^{-2}$. We obtained larger roughness probably because our platinization bath was 10 times less concentrated than that of Kim and Oh (1996), which may have led to less compact

Table 2. Effect of platinization potential on electrodes' roughness

Platinization Potential (mV vs. Ag/AgCl)	Platinization Charge density ($mC \cdot cm^{-2}$)	Roughness*	Relative Standard Deviation (%)
Polished		14	35.7
-50	0.5	310	3.5
-100	0.5	321	1.2
-150	0.5	338	8.9
-200	0.5	406	3.2
-250	0.5	441	2.3
-100	2.0	1691	3.6

* Roughness was calculated as the ratio of the electrochemical surface area determined from the H_2 adsorption peaks and the geometric surface area.

deposits due to slower diffusion from the bulk to the surface of the growing deposit. Kim and Oh (1996) used electrodes platinized at –250 mV for enzyme immobilization because of the higher surface area of such electrodes. However, enzyme was immobilized by electrodeposition followed by crosslinking with BSA and glutaraldehyde. The crosslinking with BSA and glutaraldehyde acts as a glue to keep the brittle black platinum layer from breaking and falling off the electrode. The disadvantage of this procedure is that it resulted in lower sensitivity. Because immobilization of GOD in PPD deposited on electrodes platinized at potentials more negative than –100 mV resulted in excessively fragile sensors, we chose to platinize all the electrodes at –100 mV. While polished electrodes gave a certain amount of variability in their cyclic voltammograms, platinized electrodes resulted in almost invariable profiles. Figure 2 shows scanning electron micrographs (SEM's) of electrodes platinized to 2.0 $mC.cm^{-2}$. Platinum deposits at –50 (Figure 2a) and –100 mV (Figure 2b) have a crystallite appearance. Platinum deposits at –150 mV (Figure 2c) show a transition to dendrite-like structure and those

grown at –200 (Figure 2d) or –250 mV (Figure 2e) have a dendrite-like structure. These results are in agreement with an earlier report (Kim and Oh, 1996).

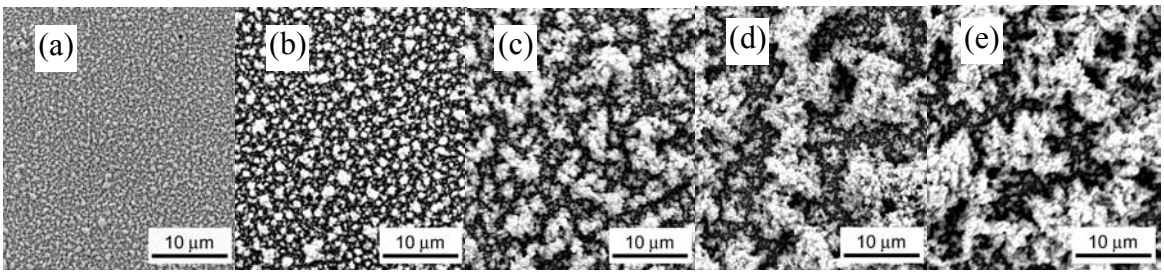

Figure 2. Scanning electron micrographs of platinum disk electrodes (1 mm diameter) platinized to 2.0 $mC \cdot cm^{-2}$ at (a) –50, (b) –100, (c) –150, (d) –200 and (e) –250 mV vs. Ag/AgCl.

SEM's show that pore size increases with increasing negative potential. The more compact structure of platinum deposits grown at lower potentials explains why these deposits are mechanically more stable than those grown at larger potentials.

Effect of roughness on polymerization charge

To assess the relative amount of immobilized enzyme among electrodes with different roughness resulting from platinization at different potentials, polymerization charge was recorded for films grown at 650 mV for 15 min from solutions containing 1 $g.l^{-1}$ GOD. Polymerization charge increased with electrode roughness as depicted in Figure 3. However, the increase levels off as roughness increases, suggesting that the polymer grew throughout all the electrochemical surface area for electrodes with small roughness (thinner platinum deposits) while for electrodes with higher roughness (thicker platinum deposits) monomer diffusion through the platinum deposit is slower and polymerization occurs at an outer layer of the porous matrix resulting in a lack of monomer in the inner part of the matrix.

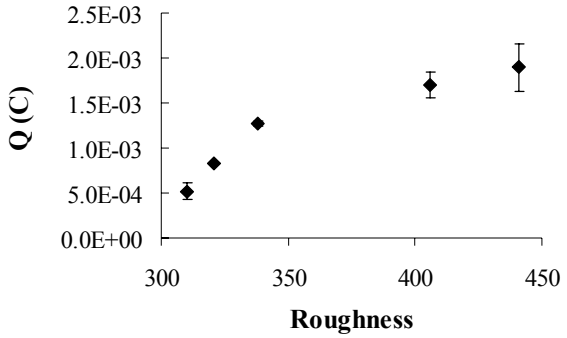

Figure 3. Effect of roughness on final polymerization charge for electrodes grown from 5 mM oPD, 0.1 M KCl, 1 $g{\cdot}l^{-1}$ GOD at 650 mV vs. Ag/AgCl for 15 min. Electrodes were platinized at from –50 to –250 mV vs. Ag/AgCl to 0.5 $mC{\cdot}cm^{-2}$. Error bars represent +/- one standard deviation of three measurements. Each measurement was taken from a different electrode.

Effect of enzyme load

The effect of GOD concentration was studied to increase the electrode's response. GOD concentration could be increased up to 50 $g.l^{-1}$ without decrease in polymerization rate of GOD-PD at 650 mV vs. Ag/AgCl. The ability to immobilize high concentrations of GOD is one of the two main factors that lead to highly sensitive electrodes as shown in Figure 4. In contrast, GOD inhibits pyrrole polymerization (Shin and Kim, 1996, Schuhmann, 1991) which result in electrodes with lower sensitivity. Current response increased with GOD concentration between 0.5 and 10 $g.l^{-1}$ however, electrodes grown with 50 $g.l^{-1}$ had a lower response. This is in agreement with previous reports (Shin and Kim, 1996, Fortier et al., 1990). This decrease in response is attributed to a transition between kinetically controlled and diffusion controlled regimes. As the concentration of enzyme increases, substrate is consumed in an outer layer of the immobilization matrix and larger amounts of H_2O_2, the product of the enzymatic reaction, diffuse back to the bulk of the solution instead of reaching the surface of the electrode.

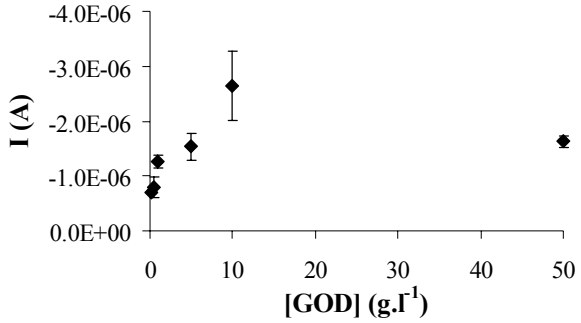

Figure 4. Effect of enzyme load in electrode's mean current response to 10 mM glucose. GOD-PPD films were grown at 650 mV vs. Ag/AgCl for 1800 s on electrodes platinized at –100 mV vs. Ag/AgCl to a charge density of 0.5 $mC \cdot cm^{-2}$. Electrodes were allowed to equilibrate with enzyme-monomer solution for 5 min before electropolymerization. Error bars represent +/- one standard deviation of three measurements. Each measurement was taken from different electrodes.

Effects of platinization on electrode response

There has been some discussion of the interpretation of the increase in sensitivity of platinized electrodes compared to polished electrodes (Kim and Oh, 1996). However, while the increase in surface area is about two orders of magnitude, the increase in sensitivity is much smaller. In experiments using rotating disk electrodes (RDE's) the response of a PPD covered polished electrode to 0.005 M H_2O_2, 0.1 M KCl was between 1.7 and 3.4 times lower than the response of a polished bare electrode. This is due to the diffusion barrier imposed by the membrane and to the partial coverage of the platinum catalytic sites by the polymer. While the polymer grows uniformly throughout the platinum surface, the apparent coverage of catalytic platinum sites available for oxidation of H_2O_2 was approximately 14% as estimated by a modified Kouteki-Levich method (Reyes-De-Corcuera et al., 2003). Platinized electrodes and PPD covered platinized and bare polished electrodes gave very similar response to 0.005 M H_2O_2, as illustrated in

Figure 5. Considering that diffusion of H_2O_2 through the film is longitudinal with respect to the axis of the electrode, oxidation of H_2O_2 at the platinum black layer will occur until a platinum site becomes available for adsorption. As long as the polymer blocks a catalytic site, hydrogen peroxide will continue diffusing through the platinum black layer until it finds a platinum site available. Hence, assuming that H_2O_2 oxidation is not the rate limiting step of the process, once the surface area with sites available for H_2O_2 oxidation equals the geometric surface area of the electrode, any additional platinum site available deeper in the platinum black layer will not be reached by the H_2O_2. This explains why the platinized PPD-covered electrode's response was similar to the polished bare electrode's.

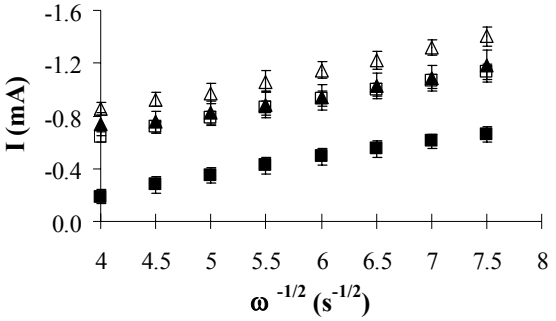

Figure 5. Mean current response at 700 mV vs. Ag/AgCl to 0.005 M H_2O_2, 1 M KCl for (□) polished Pt RDE, (■) polished PPD-covered Pt RDE, (△) platinized Pt RDE and (▲) platinized PPD-covered Pt RDE at different rotation speeds. Error bars represent +/- one standard deviation of three measurements performed with three different electrodes.

The effect of H_2O_2 concentration on the response of polished, platinized, polished and PPD-covered and platinized and PPD-covered 1 mm diameter disk electrodes in stirred solutions is depicted in Figure 6. At concentrations below 0.2 mM, electrodes' response was linear regardless of the treatment. PPD-covered electrodes gave smaller

responses than bare electrodes and platinized electrodes gave larger responses than polished electrodes. Platinized bare electrodes sensitivity was approximately three times larger than polished bare electrodes. This is much smaller than the increase of roughness determined by cyclic voltammetry in H_2SO_4; which confirms that the system is mainly

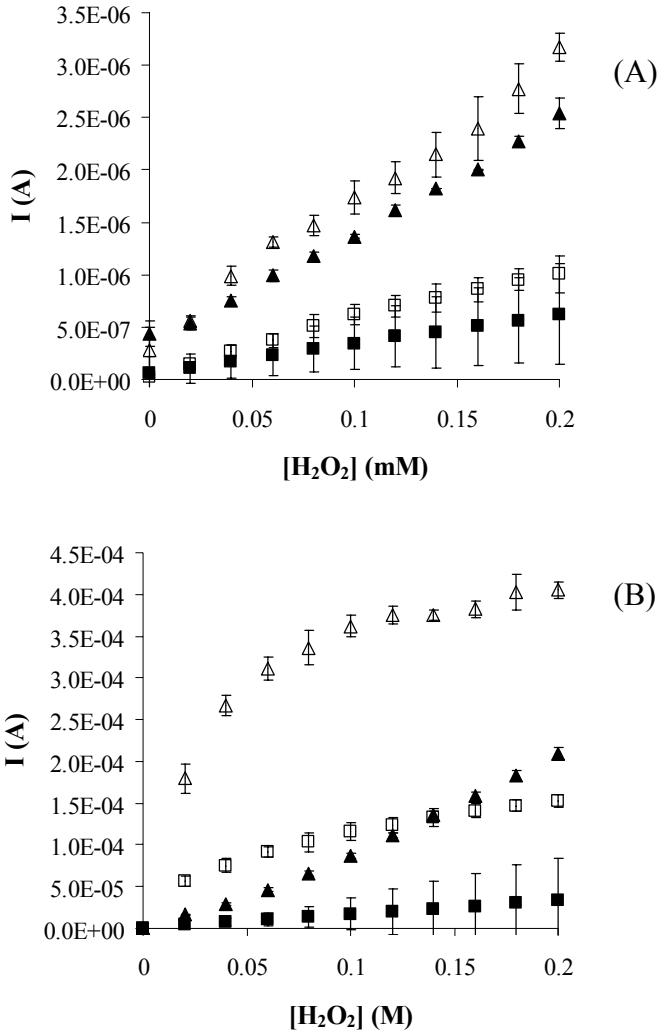

Figure 6. Amperometric response at 700 mV vs. Ag/AgCl to stirred solutions of (A) 0-0.2 mM H_2O_2 and (B) 0-0.2 M H_2O_2 for (□) polished Pt electrode, (■) polished PPD-covered Pt electrode, (△) platinized Pt electrode and (▲) platinized PPD-covered Pt electrode. Solutions were stirred using a magnetic stirrer at constant rate. Electrodes (1 mm diameter) were platinized at –100 mV vs. Ag/AgCl. Error bars represent +/- one standard deviation.

under film diffusion control. In other words, one would expect about a three-fold increase in sensor sensitivity due to platinization. At concentrations above approximately 20 mM H_2O_2 oxidation becomes limiting at bare electrodes and the electrode's response deviates from linearity as reported in a detailed study on the kinetics of hydrogen peroxide oxidation at polished platinum electrodes (Hall et al., 1998). Polished PPD-covered and platinized PPD-covered electrodes were linear up to at least 0.2 M H_2O_2 (r^2 of 1.000 and 0.990 respectively) as depicted in Figure 6B. The observed increase in liner range is due to the diffusion barrier created by the PPD. However, such regime would not be found in biosensors because the concentration of H_2O_2 inside the reaction-diffusion membrane is limited by the concentration of O_2, which is about 280 $\mu mol.l^{-1}$ in the bulk of the solution. These results would suggest that platinization, more than increasing the surface area with respect to the geometric surface area, compensates for the surface area coverage caused by polymer deposition. However, the glucose sensitivity of platinized electrodes with 10 $g.l^{-1}$ GOD immobilized was up to 64 times the response of polished electrodes with the same concentration of immobilized enzyme (see Table 3). In the GOD-free PPD-covered electrode, or in the case of thick enzyme-polymer films where most of the enzymatic reaction occurs in an outer layer of the film, H_2O_2 diffusion becomes one-dimensional and platinization compensates for the blockage of platinum reaction sites by the polymer or adsorbed enzyme. In the case of thin films, where the film is thinner than the pore size of the platinum deposit, platinization not only compensates for surface area coverage, it also works as part of the immobilization matrix, allowing for entrapment of larger amounts of enzyme than on polished electrodes. This is reflected by the increase in total

polymerization charge discussed earlier. Also because the polymer film is very thin, the substrate diffuses rapidly into the porous matrix and then through the enzyme immobilization matrix where H_2O_2 is and quickly oxidized at the black platinum surface and diffusion becomes multidirectional. Figure 7 depicts the typical response of polished and platinized electrodes.

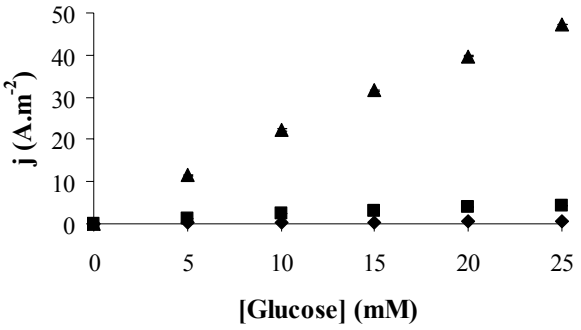

Figure 7. Typical calibration curve for electrodes (♦) polished, (■) platinized to 0·5 mC·cm^{-2} and (▲) platinized to 2.0 mC·cm^{-2}. Glucose solutions were prepared in 0.1 M phosphate buffer pH 7.0. Electrochemical polymerization was carried out from 5 mM o-phenylenediamine, 10 g·l^{-1} GOD in 0.2 M acetate buffer pH 5.2 at 650 mV vs. Ag/AgCl for 30 min. Error bars represent ± one standard deviation of six measurements using one electrode.

Table 3. Analytical characteristic of GOD-PPD sensor response to glucose solutions in 0.1 M phosphate buffer pH 7.0. Platinization was carried out at –100 mV vs. Ag/AgCl from 2 mM H_2PtCl_6, 1 mM $Pb(C_2H_3O_2)$, 0.1 M KCl oxygen-free solution. Electropolymerization was carried out for 30 min in 5 mM o-phenylenediamine, 10 g·l^{-1} GOD, 0.2 M acetate buffer pH 5.

Platinization charge density (mC.cm^{-2})	Sensitivity (μA.cm^{-2}. mM^{-1})	Repeatability (%)	Limit of detection (mM)	Linearity (mM)	Sensor-to-sensor reproducibility (%)
Polished	3.09 ± 0.09	7.04 ± 1.23	0.15 ± 0.06	15	8 (4 electrodes)
0.5	23.3 ± 6.61	1.02 ± 0.05	0.2 ± 0.13	15	30+ (4 electrodes) 25 (3 electrodes)
2	192 ± 48	2.32 ± 1.22	0.3 ± 0.37	25	24 (7 electrodes)

+ Includes defective electrodes with low sensitivity and low repeatability.

Mathematical model of GOD-PPD electrodes on polished electrodes

The kinetics of GOD has been reported to follow a "ping-pong" mechanism. In the absence of products, the rate equation reduces to the expression used in the model proposed by (Leypoldt and Gough, 1984), used by Gros and Bergel (1995) and in this study (see Table 1). In the case of an immobilized enzyme product inhibition could occur and in that case, the equilibrium constants would change. A study on glucose oxidase kinetics using a rotating disk electrode showed that 10 mM glucolactone produced little inhibition (van Stroe-Biezen et al., 1994). Inhibition by H_2O_2 was observed when concentration was changed from 0 to 0.75 mM. However, maximum calculated H_2O_2 and glucolactone concentrations in the immobilization matrix are in the order of 0.045 mM and less than 5 mM respectively in the immobilization matrix (see Figure 10). Therefore, product inhibition was assumed negligible. Kinetic parameters for GOD in solution were used and kept constant for all simulations.

Effect of diffusion coefficients and film thickness

Because diffusion coefficients of PPD films are not available, values of GOD-polypyrrole films were used as a starting point and values 10 times larger and 10 times smaller were used to assess their effect on electrode response. The output of the model is shown in Figure 8. These results are similar to those reported by Gros and Bergel (1995) using the same parameters, in particular, the maximum response at 250 nm that divides the kinetic-controlled regime from the diffusion-controlled one. Because the model used here does not account for glucose adsorbed at the platinum surface and at the polymer

solution interface, the estimated electrode response was slightly lower. With diffusion coefficients 10 times larger, the response of the electrode increases and the maximum shifts to around 750 nm. The opposite effect occurs for diffusion coefficients 10 times smaller where the maximum shifts to around 70 nm. As film thickness decreases, kinetic effects become increasingly dominant and diffusive effects become almost negligible for film thickness of 30 nm and below. Because the thickness of PPD films has been reported to be of the order of 10 nm (Malitesta et al., 1990) we assumed diffusion effects negligible and used the same diffusion coefficients as for GOD-PPY films.

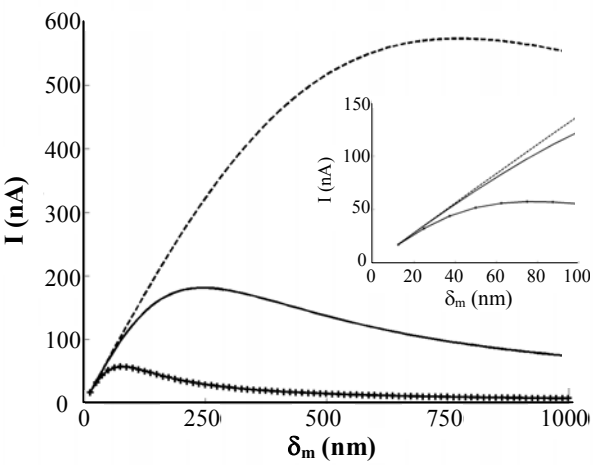

Figure 8. Modeled effect of film thickness on current response assuming diffusion coefficients (—) reported by Gros and Bergel (1995) (---) 10 times larger and (++) 10 times smaller. A = 0.03 cm^2.

Effect of glucose concentration, data fitting

The model was run using the same kinetic and diffusion parameters as for GOD-PPY electrodes. However, this time, to compare to experimental results, the geometric surface area (7.9 x 10^{-7} m) of the electrode and a film thickness of 10 nm was used. As shown in Figure 9, this approach (continuous line) largely underestimates experimental

results (dots). The use of the electrochemical surface area (1.1 x 10^{-5} m) brings the modeled response closer to the experimental values. However, film thickness has to be adjusted to 30 nm to closely fit the experimental values. The adjustments to fit our experimental data are most likely inaccurate because our model does not account for adsorbed enzyme, partial blockage of the platinum sites by the polymer film and we do not have accurate values of film thickness. However, it is reasonable to conclude that for PPD films, a wide range of diffusion coefficients (2 orders of magnitude) do not affect the model of the electrode's response because films are very thin, that is, below 30 nm (Malitesta et al., 1990). The large response observed for polished electrodes, is most likely due to the effective use not of the geometric surface area but a much larger (about 14 times) surface area closer to the electrochemical surface area. This supports our hypothesis that multidirectional diffusion of H_2O_2 takes place, even with polished electrodes and this would explain the large sensitivity obtained with these electrodes.

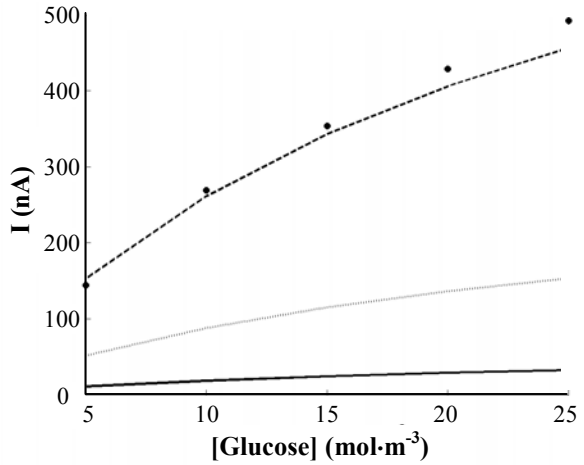

Figure 9. Effect of glucose concentration assuming (—) geometric surface area (7.9 x 10^{-7} m and film thickness = 10 nm; (….) electrochemical surface area (1.1 x 10^{-5} m) and film thickness = 10 nm; (---) electrochemical surface area (1.1 x 10^{-5} m) and film thickness = 30 nm and (•) experimental data using polished electrodes.

The model also indicates that that H_2O_2 concentration does not exceed 4.5 μmol.l^{-1} in 30 nm films or 45 μmol.l^{-1} in 100 nm films grown using 10 g.l^{-1} GOD in the presence of 50 mM glucose as shown in Figure 10. This confirms that H_2O_2 oxidation is not the rate-limiting step in glucose detection using GOD-PPD covered electrodes.

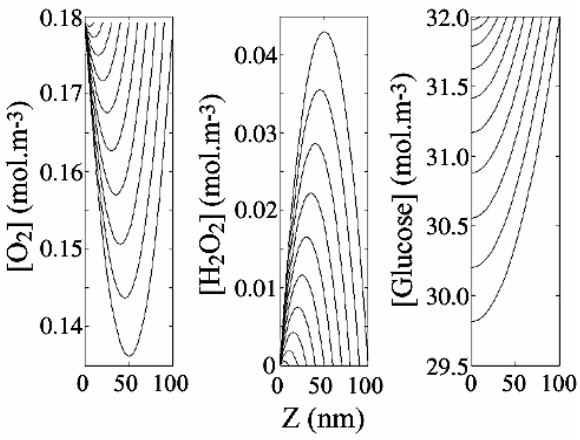

Figure 10. Concentration profiles for films with thickness 10 to 100 nm in the presence of 50 mM glucose.

Finally, for platinized electrodes, the large increase in the response of the electrode is due to the increase in surface area and in enzyme load. However, because the amount of immobilized enzyme does not increase linearly with roughness and resistance to diffusion throughout the porous matrix is larger than for polished electrodes, the mathematical model presented here does not apply to platinized electrodes.

Schematic interpretation of the results

Simplified schematic representations of polished and platinized GOD-electropolymer biosensors (Figures 11A and 11B) have been reported (Vidal et al., 2000). However, in that arrangement, H_2O_2 is produced in a layer that does not overlap with the platinum

deposit. Therefore all the H_2O_2 that is produced in the enzyme layer has to diffuse to the platinized surface and as we discussed above, an approximately three-fold increase in response would be the maximum to expect. Our experimental results suggest that the arrangement in Figure 11(C) would be a better representation. From scanning electron micrographs, we estimate that the size of the pores in the platinized matrix is approximately 100 to 500 nm and the thickness of PPD is 10 nm to 30 nm. Also, diffusion in the macropores would explain why the response of platinized electrodes is smaller than what would be expected from the increase in surface area as compared to polished electrodes. Conversely, for other electrochemically generated polymers like polypyrrole, where much thicker films can be grown, Figure 11(D) would be a reasonable representation of the system. Furthermore, if the thickness of the film is much larger than the thickness of the platinum deposit, then Figure 11(B) becomes a good representation. In those cases, it is not surprising to obtain much lower responses.

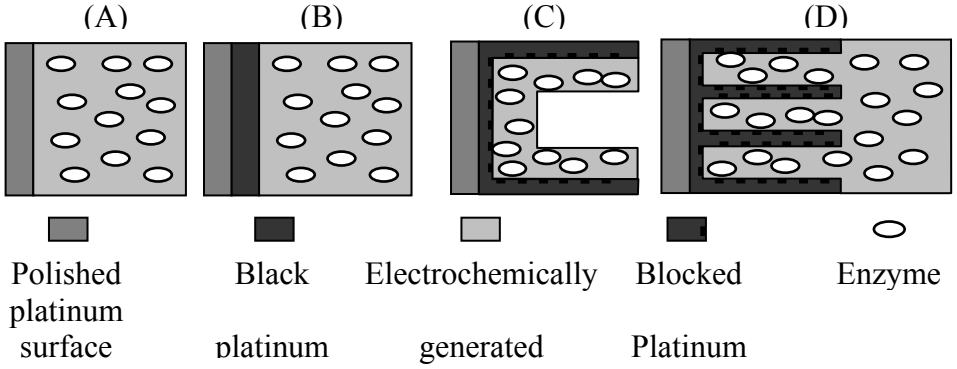

Figure 11. Schematic representations of electrodes with an enzyme immobilized in electrochemically generated polymers for (A) films grown on a polished electrode, (B) films grown on platinized electrodes assuming the platinum black layer is not porous, (C) thin films grown on the surface of the pores of platinized electrodes assuming the platinum black layer is porous and some catalytic sites are blocked by the polymer and (D) thick films grown on porous platinized electrodes where the film thickness extends well beyond the platinized surface.

Conclusions

Very sensitive glucose electrodes were fabricated by first platinizing at –100 mV vs. Ag/AgCl and immobilizing 10 $g.l^{-1}$ GOD in electrochemically generated PPD. Electrode platinization increased sensitivity by providing a porous matrix allowing large amounts of enzyme-polymer to be immobilized with an increased active surface area. Large concentrations of glucose oxidase did not inhibit the electropolymerization of o-phenylenediamine. Repeatability and limit of detection were very good. However, sensor-to-sensor reproducibility was rather poor and needs to be addressed. The reported increase in sensitivity should enable the fabrication of ultramicroelectrodes with increased current responses. Also, by covering the enzyme membrane with a non-catalytic film, one should be able to produce electrodes operating under diffusion control with larger linear range and operational life with reasonable sensitivity. While by using less negative potentials more robust platinum deposits were formed, the stability of the enzyme and the polymer need to be studied to ensure acceptable sensor operational life.

Acknowledgments

The authors are grateful for the financial support of Mr. Reyes-De-Corcuera by Fulbrght-CONACyT (National Council for Science and Technology Mexico) and for the assistance of Dr. Lynch-Holm and Dr. Dewitt at the WSU Electron Microscopy Center. This project was also supported by a grant from the WSU IMPACT Center and by the WSU Agricultural Research Center.

References

[1] M. Umana and J. Waller, Anal. Chem. 58 (1986) 2979.

[2] N. C. Foulds and C. R. Lowe, J. Chem. Soc., Faraday Trans. 82 (1986) 1259.

[3] H. Liu, H. Li, T. Ying, K. Sun, Y. Qin, D. Qi, Anal. Chim. Acta 358 (1998) 137.

[4] S. Cosnier, Biosens. Bioelectron. 14 (1999) 443.

[5] M. Trojanowicz, O. Geschke, T. C. K. Krawczynsky vel Krawczyk, Sens. Actuators, B 28 (1995) 191.

[6] P. N. Bartlett and J. M. Cooper, J. Electroanal. Chem. 362 (1993) 1.

[7] L. Coche-Guerente, S. Cosnier, C. Innocent, P. Mailley, Anal. Chim. Acta 311 (1995) 23.

[8] F. Palmisano , A. Guerrieri, M. Quinto, P. G. Zambonin, Anal. Chem. 67 (1995) 1005.

[9] S. B. Adeljou and A. N. Moline, Biosens. Bioelectron. 16 (2001) 133.

[10] R. Yang, C. Ruan, J. Deng, J. Appl. Electrochem. 28 (1998) 1269.

[11] M. C. Shin and H. S. Kim, Anal. Lett. 28 (1995) 1017.

[12] M. C. Shin and H. S. Kim, Biosens. Bioelectron. 11 (1996) 161.

[13] S. Mu and K. Jinquing, Electrochim. Acta 40 (1995) 241.

[14] Q. Pei and R. Qian, J. Electroanal. Chem. 322 (1992) 153.

[15] D. Bélanger, J. Nadreau, G. Fortier, J. Electroanal. Chem. 274 (1989) 143.

[16] G. Fortier, E. Brassard, D. Bélanger, Biosens. Bioelectron. 5 (1990) 473.

[17] B. F. Y. Yon Hin and C. R. Lowe, J. Electroanal. Chem. 374 (1994) 167.

[18] X. Chen, N. Matsumoto, Y. Hu, G. S. Wilson, Anal. Chem. 74 (2002) 368.

[19] L. Coche-Guerente, A. Deronzier, P. Mailley, J.-C. Moutet, Anal. Chim. Acta 289 (1994) 143.

[20] J. Kulys and H. E. Hansen, Biosens. Bioelectron. 9 (1994) 491.

[21] S. Bharathi and M. Nogami, The Analyst 126 (2001) 1919.

[22] C. Malitesta, F. Palmisano, L. Torsi, P. G. Zambonin, Anal. Chem. 62 (1990) 2735.

[23] M. Quinto, I. Losito, F. Palmisano, C. G. Zambonin, Anal. Chim. Acta 420 (2000) 9.

[24] A. Guerrieri, G. E. De Benedetto, F. Palmisano, P. G. Zambonin, Biosens. Bioelectron. 13 (1998) 103.

[25] M. E. Baumgärtner and Ch. J. Raub, Plat. Met. Rev. 32 (1988) 188.

[26] D. B. Kell and C. L. Davey. in Cass, A. E. G. Biosensors. A practical approach. 137. IRL Press, Oxford. 1990.

[27] C. S. Kim and S. M. Oh, Electrochim. Acta 41 (1996) 2433.

[28] W. Schuhmann, in Mulchandani, A. and Rogers, K. Enzyme and microbial biosensors: Techniques and protocols. Humana Press, Totwa NJ, 1998, pp 143-156

[29] Y. Ikariyama, S. Yamauchi, T. Yukiashi, H. Ushioda, J. Electroanal. Chem. 251 (1988) 267.

[30] Y. Ikariyama, S. Yamauchi, T. Yukiashi, H. Ushioda, J. Electrochem. Soc. (1989) 702.

[31] C. Hsueh and A. Brjter-Toth, Anal. Chem. 66 (1994) 2458.

[32] J. K. Leypoldt and D. A. Gough, Anal. Chem. 56 (1984) 2896.

[33] P. Gros and A. Bergel, J. Electroanal. Chem. 386 (1995) 65.

[34] Angerstein-Kozolowska H. in Yaeger, Ernest , Bockris J.O'M, Conway, Brian E., and Sarangapani, S. Eds. Comprehensive treatise of electrochemistry vol. 9 Electrodics: experimetal techniques. Plenum Press, New York, 1984.

[35] W. Schuhmann, Sens. Actuators, B 4 (1991) 41.

[36] M. C. Shin and H. S. Kim, Biosens. Bioelectron. 11 (1996) 171.

[37] J. I. Reyes-De-Corcuera, R. P. Cavalieri, J. R. Powers, Synth. Met. (2003) in press.

[38] S. B. Hall, E. A. Khudaish, A. L. Hart, Electrochim. Acta 43 (1998) 2015.

[39] S. A. M. van Stroe-Biezen, A. P. M. Janssen, L. J. J. Janssen, Bioelectrochemistry and Bioenergetics 33 (1994) 55.

[40] J. C. Vidal , E. Garcia-Ruiz, J. R. Castillo, J. Pharm. Biomed. Anal. 24 (2000) 51.

CHAPTER FIVE

AN ENZYME-BASED AMPEROMETRIC BIOSENSORS FOR USE AS TIME-TEMPERATURE INTEGRATOR

(To be submitted for publication in the Journal of Agricultural and Food Chemistry)

CHAPTER FIVE

AN ENZYME-BASED AMPEROMETRIC BIOSENSORS FOR USE AS TIME-TEMPERATURE INTEGRATOR

Abstract

A novel exogenous time-temperature integrator (TTI) based on an amperometric glucose oxidase biosensor is presented. The TTI consists of the enzyme entrapped within an electrochemically generated poly-o-phenylenediamine (PoPD) thin film deposited on the interior wall of a platinized stainless steel capsule. After thermal treatment, the TTI is mounted in a continuous flow system and connected to a potentiostat for amperometric detection of residual enzyme activity. A measurement is completed within five min of extracting the device from the thermal process. In addition to the rapid response of the TTI, instrumentation is inexpensive and each TTI can be fabricated for less than $3.00 US. Isothermal treatments were carried out between 70 and 79.7 ºC. Thermal inactivation of the immobilized enzyme followed first order kinetics with z-value of 6.9 ºC which makes it suitable for assessing pasteurization processes at 70 to 80 ºC.

Introduction

In view of the need for assessing the efficacy of thermal food processing operations where traditional instrumentation like thermocouples or resistance temperature detectors cannot be implemented because of mechanical or cost impediments, several research groups have been developing time-temperature integrators (TTI). Exogenous

and endogenous TTIs from different origins (microbiological, enzymatic, chemical and physical) have been compared (*1*). Enzymatic TTIs offer the advantage of being relatively easy to assay, they can be inexpensive and the thermal resistance of some enzymes to denaturation or loss of activity is similar to the thermal resistance of several pathogens of interest to the food industry. Endogenous TTIs have the disadvantage of the intrinsic variability in the concentration of the TTI component and its thermal stability. For example, triose phosphate isomerase has been proposed to verify roast beef processing (*2*) but the its activity and thermal stability varied with muscle type. Other components present in the food in variable concentrations can also affect the thermal stability of the TTI. In contrast, exogenous TTIs can operate under controlled composition. The stability of some enzymes used as TTIs has been adjusted by changing their pH (*3,4*) or by adding of stabilizing agents (*5*). Amylase (*6-10*), horseradish peroxidase (*11-14*) and r-phycoerytrhin (*15*) have been used as exogenous TTI for food pasteurization. Some exogenous TTIs have some drawbacks. If the TTI volume is relatively large (i.e. gel cubes), temperature gradients may develop throughout its volume and their application may be limited to processes where the heating transient is negligible with respect to processing time. When the substance used as indicator needs to be extracted from a capsule that substance might adhere to the surface of the capsule, making its recovery difficult for rapid assay. Finally, once the substance used as indicator is retrieved, analysis often requires long preparation which sometimes include grinding, centrifugation, incubation and finally the assay time itself (*9*).

Amperometric enzyme-based biosensors have been studied since the early 1960s (*16*). In the early 1990s, amperometric enzyme-based biosensors using enzymes immobilized in

electrochemically generated conducting and non-conducting polymers were developed (*17,18*). The main advantage of this type of sensors is that such polymers can grow to a controlled thickness from aqueous buffered solutions where most enzymes are soluble and stable, resulting in reproducible sensors and some of these films provided selective permeability to the substrate of interest (mainly glucose) (*19*). Most of these amperometric sensors have been grown on noble metals or glassy carbon electrodes. Inert substrates need to be used because electrochemical polymerization takes place at potentials (typically 700 mV vs. Ag/AgCl) where other metals oxidize.

The objective of this research was to design, fabricate and characterize an inexpensive rapid-response TTI based on an amperometric enzyme-based biosensor. GOD immobilized in an electrochemically-generated PoPD film deposited on the interior wall of a platinized stainless steel capsule is presented as a potential TTI for food pasteurization.

Materials and Methods

Glucose oxidase (EC 1.1.3.4 type X-S from *Aspergillus niger*), o-phenylenediamine free base, chloroplatinic acid hexahydrate, hydrogen peroxide, and potassium chloride were purchased from Sigma Chemical Co. (St Louis, MO). Lead acetate trihydrate was purchased from Aldrich Chemical Co. (Milwaukee, WI). Platinum wire (0.4 mm diameter) was purchased from Fisher Scientific (Fair Lawn, NJ). Stainless steel type 316 tubing 3.25 mm OD, 1.75 mm ID was purchased from the Microgroup Inc. (Medway, MA). All other reagents and solvents were purchased from Sigma-Aldrich or

Baker Analyzed and were reagent grade. Solutions were prepared in deionized ultrafiltered ($\Omega > 18$ MΩ.cm).

Platinization, electropolymerization and cyclic voltammetry experiments were performed with a potentiostat/galvanostat, EG&G 263A, (Perkin Elmer Instruments, Oak Ridge, TN), interfaced to a personal computer, through a GPIB (National Instruments, Austin, TX). Amperometric measurement of residual enzyme activity of the TTI was carried out with a low cost 'in house-built' potentiostat interfaced to a personal computer using an analog to digital board PCI 6032E (National Instruments, Austin, TX). A schematic of the potentiostat with a list of its components is shown in Figure 1. All potentials are reported with respect to Ag/AgCl, 3.0 M KCl reference electrode model EE008 from Cypress Systems Inc. (Lawrence, KS). A platinum wire was used as counter electrode. A syringe pump model 210 from Kd Scientific (New Hope, PA) was used for the injection of buffer and glucose solutions. The syringe pump was interfaced to the PC through a serial RS-232 port. The cost of all the potentiostat components was under $350 USD. The estimated total cost of the equipment required for the measurement of the residual enzyme activity of the TTI's including a personal computer and the data acquisition board was under $5000.00. Data acquisition and control of the potentiostats was done using computer programs written using LabVIEW 6.0 (National Instruments, Austin, TX).

Electrode cleaning

Stainless steel capsules were made by cutting 15 mm long tubes. The interior wall of the tubes was washed with soap and thoroughly rinsed with deionized water, polished with a

5 µm alumina slurry (Buehler Lake Bluff IL, USA), rinsed again with deionized water and immersed immediately in 5 M H_2SO_4solution at 60 ºC. Then the capsules were thoroughly rinsed with deionized water and immediately platinized.

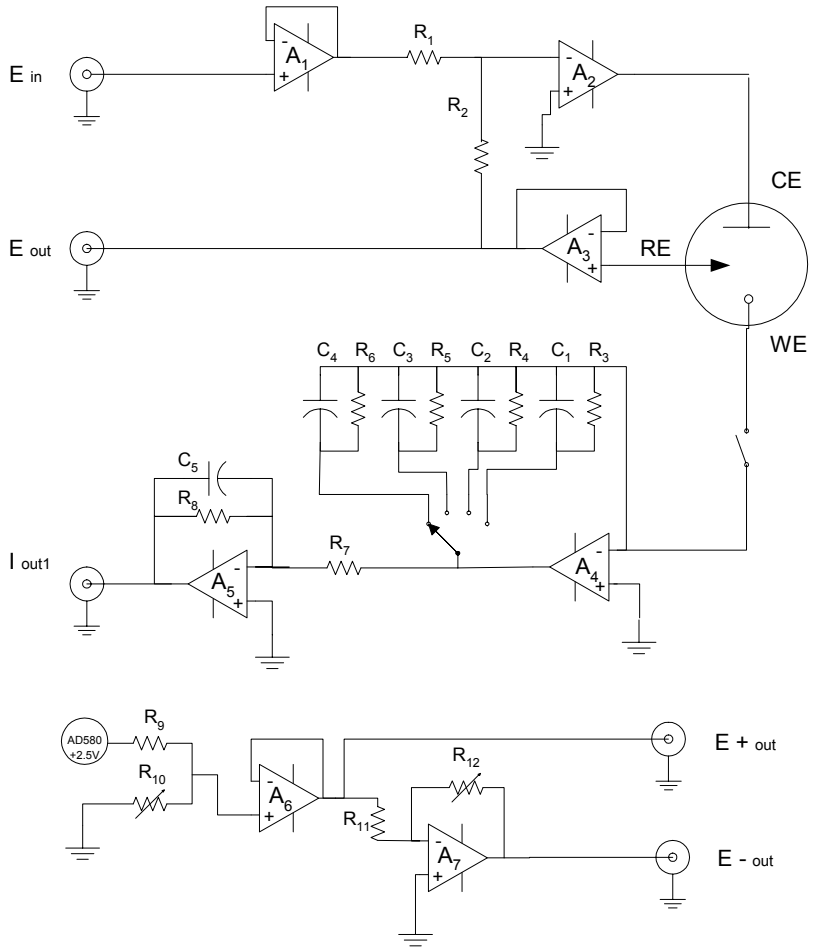

Operational Amplifiers
$A_1 – A_5$: ¼ LF444
$A_6 – A_7$: ¼ LF347
National semiconductors
Resistors
R_1, R_2, R_4, R_7, R_8 and R_9: 10 kΩ
R_3: 1 kΩ
R_5: 100 kΩ
R_6: 1 MΩ
R_{10}: 10 kΩ 10 turn trim pot 5%
R_{11}: 5 kΩ
R_{12}: 5 kΩ trim pot 5%
Capacitors
C_1: 0.1 µF
C_2: 0.01µF
C_3: 0.001µF
C_4: 100 pF
C_5: 0.01µF
Main Power Supply
HTAA-16W-A (+/- 15 VDC)
Power-one
Precision constant voltage power supply
AD580 (+2.5 VDC)
Analog Devices

Figure 1. Schematic of the potentiostat used for the research.

Electrode platinization

Potentiostatic platinization of the electrodes was carried out at -100 mV vs. Ag/AgCl in 4 mM H_2PtCl_6, 1 mM $Pb(C_2H_3O_2)$ (used as crystal growth promoter), 0.1 M KCl oxygen-free solution for 60 min at room temperature. A platinum wire inserted in the platinized tube was used as counter electrode. To prevent the counter electrode from touching the working electrode, thin glass beads were fused on the wire. Platinized tubes were rinsed with deionized ultrafiltered water. The presence of the platinum layer was verified by cyclic voltammetry in 0.5 M H_2SO_4 between –0.2 and 1.18 V vs. Ag/AgCl.

Enzyme immobilization

Potentiostatic electropolymerization was carried out in 5 mM o-phenylenediamine, 2 M acetate buffer pH 5.2, and 2.5 to 10 $g{\cdot}L^{-1}$ GOD oxygen-free solutions at 600 mV vs. Ag/AgCl for 30 min. Prior to applying the polymerization potential, electrodes were immersed for 5 min in the monomer-enzyme solution to allow monomer and enzyme to diffuse into the porous platinum deposit. Three electrodes were prepared for each level of GOD concentration. The effect of glucose oxidase concentration was the studied to determine the range of glucose oxidase concentration that would allow the TTI to operate under a kinetically controlled regime. Because at enzyme concentrations higher than 5 $g{\cdot}L^{-1}$ the increase in TTIs response was small and presumably diffusion regime started to affect the response, 5 $g{\cdot}L^{-1}$ was chosen for the remaining experiments.

Adjustment of operating conditions

Freshly prepared TTIs were tested in a continuous flow system depicted in Figure 2.

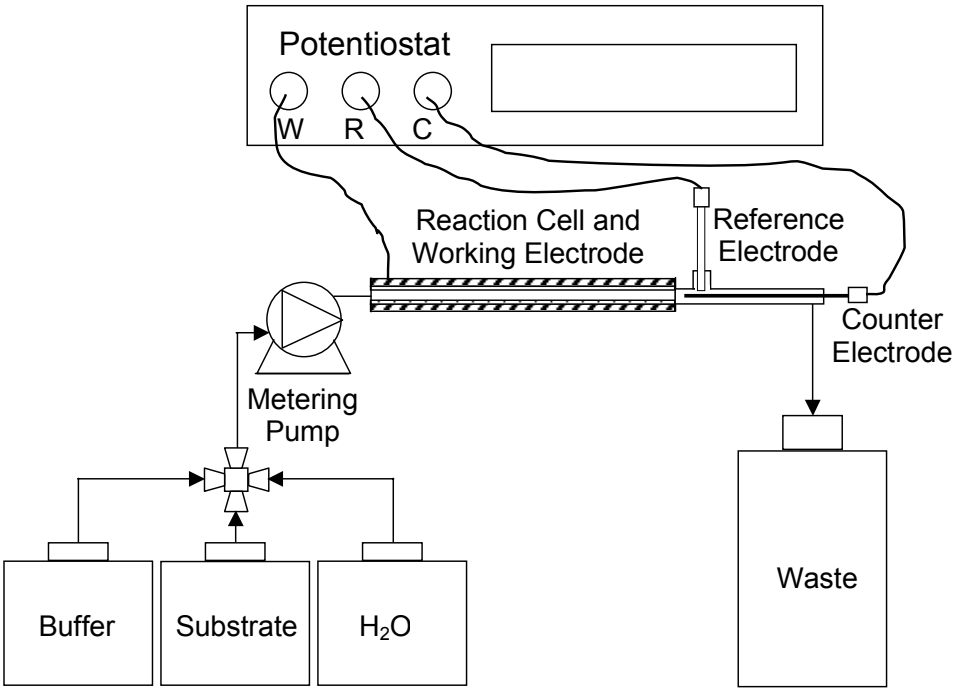

Figure 2. Schematic representation of the TTI flow system

Electrodes prepared using a solution containing 2 $g{\cdot}L^{-1}$ glucose oxidase were used to determine the apparent kinetics of the immobilized electrode and determine the glucose concentration necessary to reach V_{max}. Operation at V_{max} ensures a high and reproducible amperometric response. Finally, substrate flow rate was adjusted to further increase the amperometric response.

Thermal inactivation studies

A thermocouple type T was tightly inserted into the TTI at one end, caped at the other and immersed into a temperature controlled water bath at 84.8 ºC for 20 seconds followed by immersion in iced water to assess the heating transient phase of the TTI. After fabrication, each TTI was calibrated. The background subtracted current response was defined as 100% activity. TTIs were capped and immersed in a water bath at 70, 72.4, 77.2, or 79.7 ºC for five different periods of time predicted to be sufficient for 50% inactivation at the longest incubation time. TTIs were immersed in iced water immediately after incubation and left there until tested for activity. To verify whether a first order kinetic model describes well GOD rate of inactivation, a single tube was heated at 74.2º C for 2.5, 5, 7.5 and 10 min. To determine the thermal inactivation parameters of the immobilized GOD, each temperature and each incubation time was carried out in triplicate using a different capsule for each treatment. The experiment was blocked by incubation temperature treatment and each TTI was randomly assigned to an incubation time. Pseudo-first order inactivation kinetics was assumed and linear regression was used for the calculation of the kinetic constant of inactivation. Arrhenius-type behavior was assumed and linear regression was used for the calculation of the apparent activation energy.

Results and Discussion

Electrode platinization

Stainless steel 316 was selected for construction of the TTI because this material is approved by the FDA for use in contact with foods. Electrochemical polymerization on

stainless steel for corrosion protection has been carried out from aniline (*20-24*) , pyrrole (*25,26*), and using multilayers of polyaniline and polypyrrole (*27*). However, in most cases, polymers are generated in organic solvents unsuitable for enzyme immobilization. We attempted to polymerize 5 mM o-phenylenediamine in 0.2 M acetate buffer pH 5.2. However, because of the small concentration and the high potential (500 to 700 mV vs. Ag/AgCl), stainless steel oxidation occurred at a faster rate than the polymerization and no polymer deposit was obtained. Attempts using 50 mM o-phenylenediamine also failed. As an alternative, we coated the interior wall of the TTI by electrodepositing a black platinum layer. Platinization of platinum electrodes is a common practice to increase the surface area of amperometric biosensors (*28-30*) and it has been recently improved. Platinization of stainless steel has been reported to result in fragile platinum black layers with poor adhesion (*31*) due to the presence of the metal oxide passive layer that forms on stainless steel in contact with air or oxygen-containing solutions. However, polishing and activation with sulfuric acid of stainless steel for electroplating has been recommended (*32*) . Using that activation procedure we obtained platinum black deposits that adhered well. Platinum black deposits on the interior wall of the TTI were characterized by cyclic voltammetry in 0.5 M H_2SO_4. While a pristine platinum surface profile (Figure 3C) could not be obtained probably because the porous matrix did not completely cover the stainless steel surface area and some of the stainless steel components might have dissolved and incorporated into the black platinum layer, still the presence of the platinum can be observed when comparing the profiles of the platinized stainless steel (Figure 3B) with those of platinized platinum Figure 3C, and of stainless steel (Figure 3A).

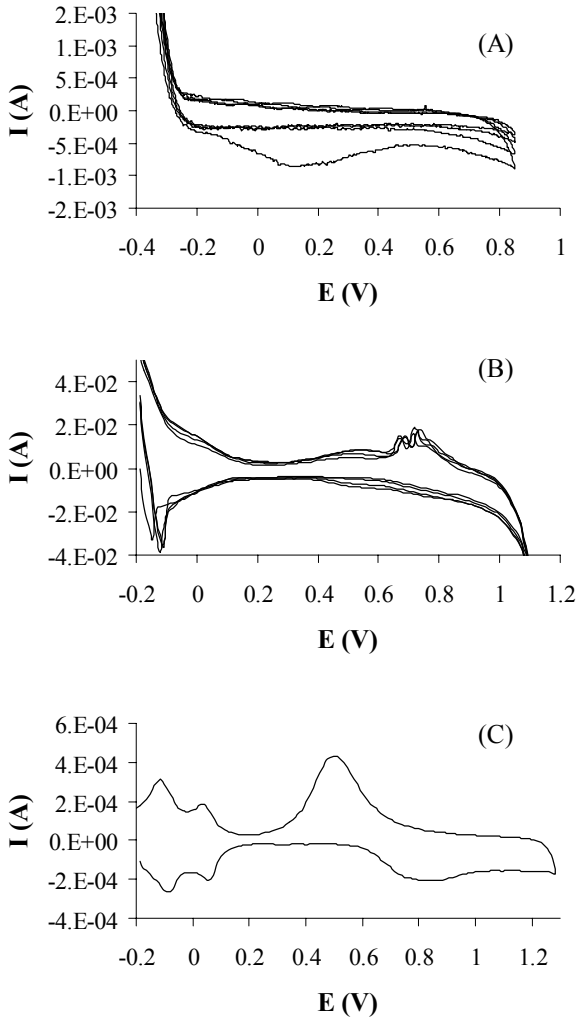

Figure 3. Cyclic voltammograms in 0.5 M H_2SO_4 at 100 $mV \cdot s^{-1}$ of (A) stainless steel 316, (B) platinized stainless steel and (C) platinized platinum.

Enzyme immobilization.

Electrochemical polymerization of o-phenylenediamine on the platinized TTI was carried out successfully as evidenced by the shape of the voltammograms and the decrease in current response upon potential cycling depicted in Figure 4. As the non-conducting polymer grows, less monomer can reach the metal surface where it oxidizes;

therefore, the current signal decreases. Similar results have been reported for PoPD films grown on polished platinum electrodes (*33*) .

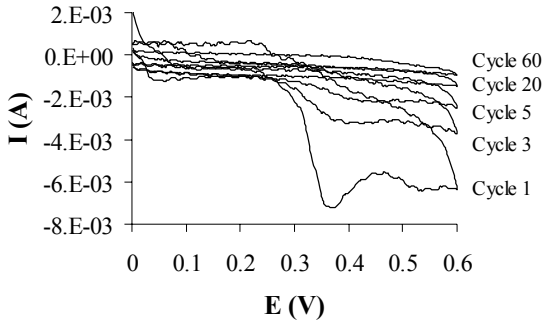

Figure 4. Cyclic voltammograms of platinized stainless steel tube in 5 mM o-phenylenediamine, 5 $g \cdot L^{-1}$ GOD in 0.2 M acetate buffer pH 5.2

Adjustment of operating conditions

Glucose oxidase catalyzes the oxidation of glucose according to Scheme 1

$$Glucose + O_2 \overset{GOD}{\rightarrow} Gluconic\ Acid + H_2O_2$$

Scheme 1. GOD catalyzed oxidation of glucose

While the mechanism of this reaction has been proven to follow a two substrate ping-pong mechanism, and that it is product inhibited (*34*) , if the O_2 supply is sufficient, glucose, glucolactone and H_2O_2 concentrations are below inhibition levels, the kinetics of the reaction can still be described using a simple one-substrate Michaelis-Menten with apparent parameters. After simplification, the immobilized reaction diffusion system under steady state conditions can be described by equations (1) and (2)

$$D_{Gluc}^{film} \frac{d^2 C_{gluc}}{dx^2} - \frac{V_{\max} C_{gluc}}{K_M + C_{gluc}} = 0 \qquad (1)$$

$$D_{H_2O_2}^{film}\frac{d^2C_{H_2O_2}}{dx^2}+\frac{V_{\max}C_{gluc}}{K_M+C_{gluc}}=0 \quad (2)$$

In the reaction diffusion system, H_2O_2 diffuses and is then electrochemically oxidized at the platinized electrode at 700 mV vs. Ag/AgCl. The current produced in the circuit is given by equation (3).

$$i=nAFD_{H_2O_2}^{polym}\left(\frac{dC_{H_2O_2}}{dx}\right)_{x=0} \quad (3)$$

Where n is the number of electrons exchanged per oxidized molecule, F is Faraday's number, A is the effective surface area of the electrode $D_{H_2O_2}^{polym}$ is the diffusion coefficient of H_2O_2 in the PoPD film, $C_{H_2O_2}$ is the concentration of H_2O_2 and x is the radial diffusion coordinate. A modified Michaelis-Menten equation can be written as:

$$i=\frac{i_{\max}C_{Glu}}{K_M+C_{Gluc}} \quad (4)$$

and

$$i_{\max}=k_3C_{E_0} \quad (5)$$

where k_3 is the rate constant of the release of the product and the free enzyme from Michaelis-Menten mechanism and C_{E_0} is the initial concentration of active enzyme. Therefore the current is a measure of the rate of production of H_2O_2 by the enzymatic reaction, in other words, at a given glucose oxidase concentration, the current is a measure of active GOD concentration. This is the principle of operation of amperometric GOD biosensors. Because we are interested in measuring the concentration of active enzyme, experiments are run at constant glucose concentration. The effect of glucose oxidase concentration in the polymerization solution on the current response of the TTI is

shown in Figure 5. The current response approximately doubled as the GOD concentration doubled from 2.5 to 5 $g{\cdot}L^{-1}$ like it would be expected for the enzyme in solution. However, at higher GOD concentrations the current response remained unchanged and finally decreased slightly at 10 $g{\cdot}L^{-1}$. This behavior is in agreement with previous reports (*35,36*) . At low GOD concentrations diffusion of glucose, O_2 and H_2O_2 throughout the immobilization matrix is rapid and enzyme kinetics limit the overall rate of reaction. Therefore, the higher GOD concentration, the more glucose is oxidized and the more H_2O_2 is produced and oxidized at the metal surface of the electrode resulting in a higher current. When GOD reaches a high enough level, glucose is consumed at a faster rate than it diffuses from the bulk of the solution through the polymer film. At this point, diffusion starts controlling the overall rate of reaction. At even higher GOD concentrations, glucose is rapidly oxidized at an outer layer of the polymer film; more H_2O_2 diffuses back to the bulk of the solution than to the surface of the electrode resulting in a decrease of current response. It has also been reported (*37*) that at high GOD concentrations electrochemically generated films have lower permeability resulting in a decrease in the rate of diffusion of substrates and products and therefore, of the current response. To obtain the largest current response, glucose concentration is increased to operate at $i = i_{max}$. The apparent kinetic parameters of the immobilized GOD-catalyzed oxidation of glucose were determined from equation 2 using Lineweaver-Burk approach. K_M was 34 mM and i_{max} was 4.1×10^{-5} A very similar to the reported K_M for the enzyme in solution (*38*). Theoretically, i_{max} is reached at infinite substrate concentration and its value is equal to two times the rate of reaction at substrate concentration equal to K_M.

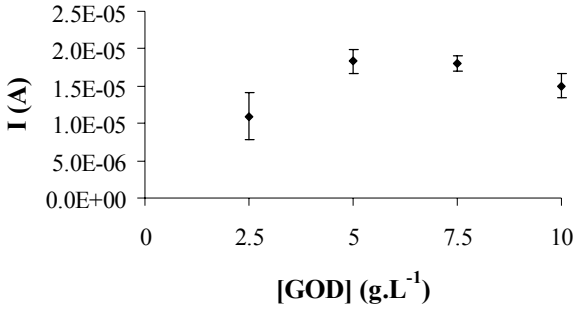

Figure 5. Effect of GOD concentration on TTI's current response to 120 mM glucose solution in 0.1 M phosphate buffer pH 7.0. Error bars represent +/- one standard deviation of three TTI.

From a practical approach, i_{max} is reached when glucose concentration is large enough so that the K_M value becomes negligible with respect to it. Figure 6 shows that at glucose concentrations of 60 mM or higher the current is fairly constant with a slight decrease at 120 mM, which is in agreement with reported substrate inhibition occurring at concentrations above 100 mM. Therefore, a glucose concentration of 100 mM was chosen for operation of the system. Because of the inhibition effect, the double reciprocal plot deviates from linearity at low values of the reciprocal of glucose concentration. For that reason, apparent kinetic parameters were determined using only high values of the reciprocal of glucose concentrations in the linear regression as shown in the insert of Figure 6.

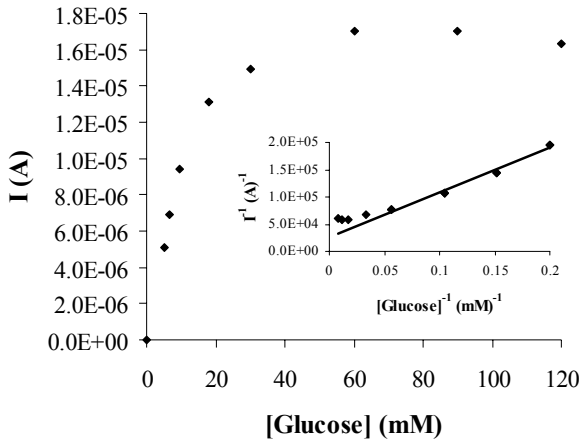

Figure 6. Effect of glucose concentration on TTI's current response. Polymer film was grown from a 5 mM o-phenylenediamine, 2.5 g·L^{-1} GOD in 0.2 M acetate buffer pH 5.2. Insert, double reciprocal plot of the same data used to determine kinetic parameters.

Thermal inactivation studies

Although compared to pure metals and other steel alloys stainless steel has a low thermal conductivity, it is about 10 times that of glass and about 30 times that of water; which reduces thermal transient response allowing the TTI to more accurately experience the temperature history of the product that surrounds it. In addition electrochemically generated PoPD forms very thin films, in the order of 10 nm thick (*39*); which means that the immobilized enzyme reaches the temperature of the interior wall of the TTI practically instantaneously and no temperature gradients exist throughout the enzyme immobilization matrix. Therefore, the enzyme is uniformly inactivated and the only transient of concern is caused by the thickness of the stainless steel tube. The transient heating phase of the TTI is illustrated in Figure 7. It took about 10 s for the interior wall to reach the final temperature after immersion in the water bath. Therefore, to ensure isothermal treatment of the TTI, all experiments were carried using incubation times of at least 100 s. The thickness of the proposed TTI capsule was 0.79 mm, therefore, this

transient time could be considerably reduced with commercially available tubing with wall thickness as small as 0.15 mm that.

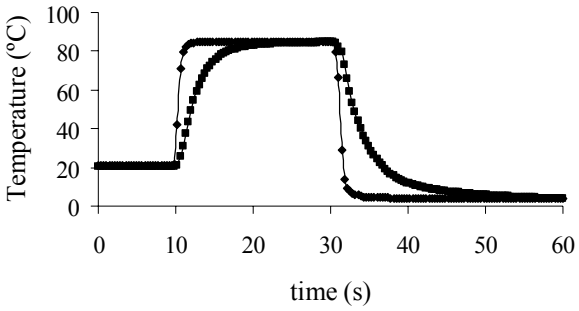

Figure 7. Heating transient of (♦) a thermocouple type T and (+) the interior wall of the TTI using the same thermocouple tightly inserted in the TTI

The thermal inactivation 60 ºC of GOD in solution and immobilized in polypyrrole has been reported to follow pseudo-first order kinetics with k-values of 18.3 x 10^{-4} and 6.7 x 10^{-5} s^{-1} respectively *(40).* We compared orders 0, 0.5, 1 and 2 for the inactivation of one GOD-based TTI immersed in a water bath 74.8 ºC for 2.5 min and then cooled with iced water residual activity was measured after each heating-cooling cycle. Correlation coefficients (R^2) of 0.89, 0.97, 0.99 and 0.94 were obtained. These results suggest that the kinetics of inactivation follow 2nd order. However, first order gave also a very high correlation coefficient allowing us to assume first order inactivation, which is usually assumed for microbial inactivation. Rate constants (k) were calculated from the slope of the linear regression of ln(% residual activity) vs. time. The activation energy for the thermal inactivation of the immobilized GOD was calculated from the slope of the linear regression of ln(k) vs. the reciprocal of the absolute temperature assuming that the effect of temperature on the rate constant can be described using

Arrhenius-type equation. Figure 8 shows the inactivation curves for the GOD-PPD TTIs and Table 1 summarizes the rate constants at different temperatures and the activation energy. Thermal inactivation parameters are also calculated in terms of D and z values. The z value for the proposed GOD TTI was 6.9 ºC making it a suitable candidate for the assessment of microbial inactivation during pasteurization and very similar to α-amylase from *Bacillus lichenformis* at reduced water content (*41*) This result can be compared to recently published TTI summarized in Table 2.

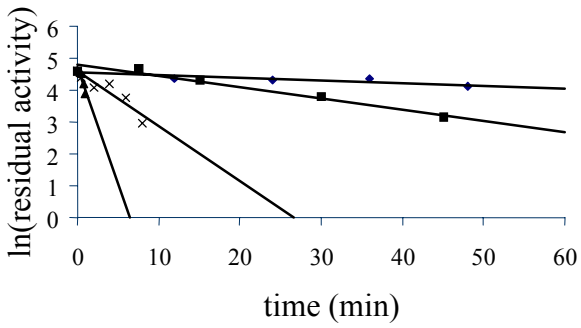

Figure 8 Thermal inactivation of GOD-PPD TTIs at (♦)70 ºC, (■)72.4 ºC, (▲)77.2 ºC and (x)79.8 ºC.

The small and uniform thickness of this film minimizes temperature gradients while maximizing heat transfer to the capsule and minimizing variability. For assessing the degree of inactivation, the capsule becomes a tube reaction cell and at the same time works as an electrode for electrochemical detection. Variability within TTIs was unexpectedly high due to the difficulty of fabricating reproducible TTIs. Most probably the activation and platinization step were the main source of variability. Activation of

Table 1. Thermal inactivation kinetic parameters for GOD immobilized in an electrochemically generated PoPD film deposited on platinized stainless steel.

T (ºC)	*k* (s^{-1})	$r^{2\,a}$	D (min)	*Ea* ($kJ.mol^{-1}$)	$r^{2\,b}$	*z* value (ºC)	$r^{2\,c}$
70.0	$4.31 \times 10^{-4} \pm 1.12 \times 10^{-4}$	0.55	89.0	335.5 ± 45.7	0.97	6.6	0.97
72.4	$7.04 \times 10^{-4} \pm 6.79 \times 10^{-5}$	0.87	54.5				
77.2	$2.97 \times 10^{-3} \pm 3.69 \times 10^{-4}$	0.80	12.9				
79.7	$1.22 \times 10^{-2} \pm 1.82 \times 10^{-3}$	0.79	3.2				

[a] Correlation coefficients of $\ln(A/A_0)$ vs. time that apply to *k* and D. All replicates were considered.
[b] Correlation coefficient of $\ln(k)$ vs. T^{-1} using the values of *k* obtained from linear regression of $\ln(A/A_0)$ vs. time.
[c] Correlation coefficient of Log (D) vs. T

stainless steel surface in sulfuric acid was variable as observed by the different time require for hydrogen evolution to be observed. Also, platinization curves were not always reproducible, indicating the growth of platinum deposits with different properties. This explains the low correlation coefficients obtained for the regression of $\ln(A/A_0)$ vs. time. While this did not prevent obtaining reasonable estimates of kinetic constants, it requires improvement for practical use.

Supporting Information

Because D and z values are more commonly used than k and Ea in the food processing industry, the equations to calculate them are included here

A first order kinetic equation in the integrated form is:

Table 2. Characteristics of some TTIs recently reported.

TTI	z value (ºC)	Method of determination of residual activity	Time required for determination (min)	Reference
α-amylase from Bacillus lichenformis at different reduced water content	6.81 - 11.81 6.41 - 8.98	Differential scanning calorimetry Spectrophotometric assay (Sigma)	≈ 5 [a] ≈ 10 [a]	(*10,40*)
α-amylase from *Aspergillus oryzae* immobilized in different polyacrylamide gels	7.78 - 10.9	Spectrophotometric assay	> 30	(*9*)
Pectinmethylesterases from tomato and cucumbers	4.55 – 6.63	Potentiometric titration	≈ 10 [a]	(*5*)
R-phicoerythrin from *Porphyra yezoensis*	5.99	Fluorescence assay		(*4,15*)

[a] estimated

$$\ln\left(\frac{A}{A_0}\right) = -kt \qquad \text{(A-1)}$$

where A_0 is the initial activity A is the activity after incubation, t is the incubation time and k the rate constant

D value is defined as the time required for a decimal decrease in a given property at a given temperature.

$$\log\left(\frac{A}{A_0}\right) = -\frac{kt}{\ln(10)} = -\frac{t}{D} \qquad \text{(A-2)}$$

$$\Rightarrow D = \frac{\ln(10)}{k} \qquad \text{(A-3)}$$

The dependence of a rate constant with temperature can be expressed by the equation proposed by Arrhenius:

$$k = Be^{\frac{-E_a}{RT}} \quad \text{(A-4)}$$

Where B is the Arrhenius constant, E_a is the activation energy, R is the ideas gas constant and T is the absolute temperature

The z value is defined as the change in temperature that is required to modify the reaction rate by a factor of ten:

$$z = \frac{\ln(10)}{E_a / R} T_1 T_2 \quad \text{(A-5)}$$

Where $|T_1\text{-}T_2| = 10$

Acknowledgement

The authors are grateful for the financial support of Mr. Reyes-De-Corcuera by Fulbrght-CONACyT (National Council for Science and Technology Mexico). This project was also supported by a grant from the Washington State University IMPACT Center and by the Washington State University Agricultural Research Center.

Literature Cited

1. Haentjens, T. H., Van Loey, A. M., Hendrickx, M. E., Tobback P.P. The use of α-amylase at reduced water content to develop time temperature integrators for sterilization processes. *Lebensm.-Wiss. Technol.* **1998**, *31*, 467-472.

2. Hsu, Y. C., Sair, A. I., Booren, A. M., Smith, D. M. Triose phosphate isomerase, as an endogenous time-temperature integrator to verify adequacy of roast beef processing. *J. Food Sci.* **2000**, *65*, 236-240.

3. Lemos, M. A., Oliveira, J. C., Saraiva, J. A. Influence of pH on the Thermal Inactivation Kinetics of Horseradish Peroxidase in Aqueous Solution. *Lebensm.-Wiss. Technol.* **2000**, *33*, 362-368.

4. Orta-Ramirez, A., Merrill, J. E., Smith, D. M. pH affects the thermal inactivation parameters of R-phycoerythrin from *Porphyra yezoensis*. *J. Food Sci.* **2000**, *65*, 1046-1050.

5. Guiavarc'h, Y., Sila, D., Duvetter, T., Van Loey, A., Hendrickx, M. Influence of sugars and polyols on the thermal stability of purified tomato and cucumber pectinmethylesterases: a basis for TTI development. *Enzyme Microb. Technol.* **2003**, *33*, 544-555.

6. Van Loey, A. M., Arthawan, A., Hendrickx, M. E., Haentjens, T. H., Tobback P.P. The development and use of an α-amylase-based time-temperature integrator to evaluate in-pack pasteurization processes. *Lebensm.-Wiss. Technol.* **1997**, *30*, 94-100.

7. De Cordt, S., Hendrickx, M. E., Maesmans, G., Tobback P.P. Immobilized α-amylase from *Bacillus lichenformis*: a potential enzymic time-temperature integrator for thermal processing. *Int. J. Food Sci. Technol.* **1992**, *27*, 661-673.

8. Tucker, G. S. , Lambourne, T., Adams, J. B., Lach, A. Application of a biochemical time-temperature integrator to estimate pasteurisation values in continuous food processes. *Innov. Food Sci. Emerg. Technol.* **2002**, *3*, 165-174.

9. Raviyan, P., Tang, J., Rasco B.A. Thermal stability of α-amylase from aspergillus

oryzae entrapped in polyacrylamide gel. *J. Agric. Food Chem.* **2003**, *51*, 5462-5466.

10. Guiavarc'h, Y.; Dintwa, E.; Van Loey, A. M.; Zuber, F.; Hendrickx, M. E. Validation and use of an enzymic time-temperature integrator to monitor thermal impacts inside a solid/liquid model food. *Biotechnol. Prog.* **2002**, *18*, 1087-1094.

11. Weng, Z. M., Hendrickx, M. E., Maesmans, G., Tobback P.P. Immobilized peroxidase: A potential bioindicator for evaluation of thermal processes. *J. Food Sci.* **1991**, *56*, 567-570.

12. Weng, Z. M., Hendrickx, M. E., Maesmans, G., Gebruers, K., Tobback P.P. Thermostability of soluble and immobilized horseradish peroxidase. *J. Food Sci.* **1991**, *56*, 574-578.

13. Hendrickx, M. E.; Weng, Z. M.; Maesmans, G.; Tobback P.P. Validation of a time-temperature integrator for thermal processing of foods under pasteurization conditions. *Int. J. Food Sci. Technol.* **1992**, *27*, 21-31.

14. Hendrickx, M. E.; Saraiva, J.; Lyssens, J.; Oliveria, J.; Tobback P.P. The influence of water activity on thermal stability of horseradish peroxidase. *Int. J. Food Sci. Technol.* **1992**, *27*, 33-40.

15. Smith, S. E. , Orta-Ramirez, A., Ofolo, R. Y., Ryser, E. T. , Smith, D. M. R-

phycoerithrin as a time-temperature integrator to verify the thermal processing adequacy of beef patties. *J. Food Prot.* **2002**, *65*, 814-819.

16. Clark, L. C. and Lyons, C. Electrode systems for continuous monitoring of cardiovascular surgery. *Ann. N. Y. Acad. Sci.* **1962**, *102*, 29-45.

17. Trojanowicz, M.; Geschke, O.; Krawczynsky vel Krawczyk, T.C.K. Biosensors based on oxidases immobilized in various conducting Polymers. *Sens. Actuators, B* **1995**, *28*, 191-199.

18. Palmisano, F., Zambonin, P. G., Centonze, D. Amperometric biosensors based on electrosynthesised polymeric films. *Fresenius. J. Anal. Chem.* **2000**, *366*, 586-601.

19. Palmisano, F., Centonze, D., Guerrieri, A., Zambonin, P. G. An interference-free biosensor based on glucose oxidase electrochemically immobilized in a non-conducting poly(pyrrole) film for continuous subcutaneous monitoring of glucose through microdialysis sampling. *Biosens. Bioelectron.* **1993**, *8*, 393-399.

20. Kraljic, M., Mandic, Z., Duic, Lj. Inhibition of steel corrosion by polyaniline coatings. *Corros. Sci.* **2003**, *45*, 181-198.

21. Kilmartin, P. A., Trier, L., Wright, G. A. Corrosion inhibition of polyaniline and poly(o-methoxyaniline) on stainless steels. *Synth. Met.* **2002**, *131*, 99-109.

22. Rajendra Prasad, K. and Munichandraiah, N. Potentiodynamic deposition of polyaniline on non-platinum metals and characterization. *Synth. Met.* **2001**, *123*, 459-468.

23. Malik, M. A., Galkowski, M. T., Bala, H., Grzybowska, B., Kulesza, P. J. Evaluation of polyaniline films containing traces of dispersed platinum for protection of stainless steel against corrosion. *Electrochim. Acta* **1999**, *44*, 2157-2163.

24. Santos, J. J. R., Mattoso, L. H. C., Motheo, A. J. Investigation of corrosion protection of steel by polyaniline films. *Electrochim. Acta* **1998**, *43*, 309-313.

25. Herrasti, P. and Ocon, P. Polypyrrole layers for steel protection. *Appl. Surf. Sci.* **2001**, *172*, 276-284.

26. Su, W. and Iroh, J. O. Formation of polypyrrole coatings on stainless steel in aqueous benzene sulfonate solution. *Electrochim. Acta* **1997**, *42*, 2685-2694.

27. Tan, C. K. and Blackwood, D. J. Corrosion protection by multilayered conducting polymer coatings. *Corros. Sci.* **2003**, *45*, 545-557.

28. Kim, C.S.; Oh, S.M. Enzyme sensors prepared by electrodeposition on platinized platinum electrodes. *Electrochim. Acta* **1996**, *41*, 2433-2439.

29. Ikariyama, Y.; Yamauchi, S.; Yukiashi, T.; Ushioda, H. Surface control of platinized platinum as a transducer matrix for micro-enzyme electrodes. *J. Electroanal. Chem.* **1988**, *251*, 267-274.

30. Vidal, J.C.; Garcia-Ruiz, E.; Castillo, J.R. Strategies for the improvement of an amperometric cholesterol biosensor based on electropolymerization in flow systems: use of charge-transfer mediators and platinization of the electrode. *J.*

Pharm. Biomed. Anal. **2000**, *24*, 51-63.

31. Stoychev, D., Papoutsis, A., Kelaidopoulou, A., Kokkinidis, G., Milchev, A. Electrodeposition of platinum on metallic and nonmetallic substrates -- selection of experimental conditions. *Mater. Chem. Phys.* **2001**, *72*, 360-365.

32. ASTM B 252-92 Standard practice for preparation of and electroplating on stainless steel. **1998**

33. Centonze, D. ; Malitesta, C.; Palmisano, F.; Zambonin, P.G. Permeation of solutes through an electropolymerized ultrathin poly-o-phenylenediamine film used as an enzyme-entrapping membrane. *Electroanalysis* **1994**, *6*, 423-429.

34. van Stroe-Biezen, S. A. M., Janssen, A. P. M., Janssen, L. J. J. A kinetic study of soluble glucose oxidase using a rotating-disc electrode. *Bioelectrochem. Bioenerg.* **1994**, *33*, 55-60.

35. Shin, M.-C.; Kim, H.-S. Effects of enzyme concentration and film thickness on the analytical performance of a polypyrrole/ glucose oxidase biosensor. *Anal. Lett.* **1995**, *28*, 1017-1031.

36. Fortier, G.; Brassard, E.; Bélanger, D. Optimization of a polypyrrole glucose oxidase biosensor. *Biosens. Bioelectron.* **1990**, *5*, 473-490.

37. Reyes-De-Corcuera, J. I., Cavalieri, R. P., Powers, R. P. Simultaneous determination of film permeability to H_2O_2 and substrate surface area coverage of overoxidized polypyrrole. *Synth. Met.* **2004**, *in press (Available on-line)*.

38. Gros, P. and Bergel, A. Improved model of a polypyrrole glucose oxidase modified electrode. *J. Electroanal. Chem.* **1995**, *386*, 65-73.

39. Malitesta, C.; Palmisano, F.; Torsi, L.; Zambonin, P.G. Glucose fast-response amperometric sensor based on glucose oxidase immobilized in an electropolymerized poly(o-phenylenediamine) film. *Anal. Chem.* **1990**, *62*, 2735-2740.

40. Wolowacz, S.E.; Yon Hin, B.F.Y.; Lowe, C.R. Covalent electropolymerization of glucose oxidase in polypyrrole. *Anal. Chem.* **1992**, *64*, 1541-1545.

41. Guiavarc'h, Y., Deli, V., Van Loey, A. M., Hendrickx, M. E. Development of an ezymic time temperature integrator for sterilization processes based on Bacillus lichenformis α–amylase at reduced water content. *J. Food Sci.* **2002**, *67*, 285-291.

CHAPTER SIX

CONCLUSIONS AND RECOMMENDATIONS FOR FURTHER RESEARCH

CHAPTER SIX

CONCLUSIONS AND RECOMMENDATIONS FOR FURTHER RESEARCH

We developed an improved method for simultaneously determine permeability to H_2O_2 and substrate surface area coverage of overoxidized PPY that compensates for non-idealities.

Electropolymerization of PPY films on polished platinum electrodes from aqueous solutions using KCl as supporting electrolyte result in very irreproducible substrate surface area coverage due to variability in PPY nucleation and film detachment upon overoxidation.

Permeability of PPY films was of the same order of magnitude for all treatments studied i.e. 0.5×10^{-4} to 5.0×10^{-4} $m.s^{-1}$.

PPY films grown under the conditions described in Chapter Three are not suitable for the fabrication of reproducible enzyme biosensors. However, the use of rougher surfaces and thinner films needs to be researched.

Glucose biosensors with sensitivity of 192 ± 48 $\mu A.cm^{-2}.mM^{-1}$ were fabricated by increasing electrode roughness by a factor of 120 with respect to polished electrodes using improved platinization conditions in combination with electrochemically-generated PPD thin films. These electrodes had a precision of 2.3% but sensor-to-sensor reproducibility was only 24%.

GOD concentration could be increased to at least 50 $g.L^{-1}$ without decreasing the rate of polymerization of PPD.

Diffusion experiments on polished and platinized electrodes suggest that when glucose oxidase is immobilized in a thin poly-o-phenylenediamine film, substrate rapidly diffuses through the porous matrix and H_2O_2 is produced throughout the enzyme-polymer film. Under these conditions, diffusion is multidirectional and platinization causes an effectively large increase in surface area that results in high amperometric response. A mathematical model of the reaction-diffusion matrix of polished electrodes supports this interpretation of the increased response.

GOD biosensors in a tubular configuration can be used as TTIs for food pasteurization at 70 ºC to 80 ºC as suggested by the z-value of 6.6 ºC and the D-value of 3.2 min at 79.7 ºC.

Platinization of the interior wall of acid-activated stainless steel small tubes using 4 mM H_2PtCl_6, 1 mM $Pb(C_2H_3O_2)$ results in TTIs with low reproducibility.

In relation to enzyme biosensors, the following research topics are suggested:

1) The effects of chemical modification of GOD on its thermal stability
2) The effects of enzyme stabilization and multipoint covalent attachment on the operational life of electrodes.
3) Use different platinization baths and platinization temperatures to ensure robust and adherent deposits
4) The effect of platinum deposit morphology on polypyrrole thin films growth from electrolyte-free solutions
5) Mathematical modeling of biosensors for optimization in terms of sensitivity, linearity and stability

To advance the development of novel food processing technologies, research for the implementation of TTIs needs to be carried out as follows:

1) Fabrication of TTIs on platinum tubing to verify that the lack of reproducibility is due to the platinum deposit and not to the enzyme-polymer matrix.
2) Optimization of stainless steel platinization to produce reproducible disposable TTIs
3) Determine the kinetics of thermal inactivation of GOD under high hydrostatic pressure.
4) Development of a TTI for pasteurization using microwave and radio frequency treatments.
5) Development of a TTI for food sterilization using enzymes produced by hyperthermophilic microorganisms

APPENDICES

APPENDIX A

ELECTRIC DIAGRAMS OF EQUIPMENT AND CIRCUITS BUILT DURING THIS RESEARCH

A) Multielectrode Potentiostat

1) Diagram

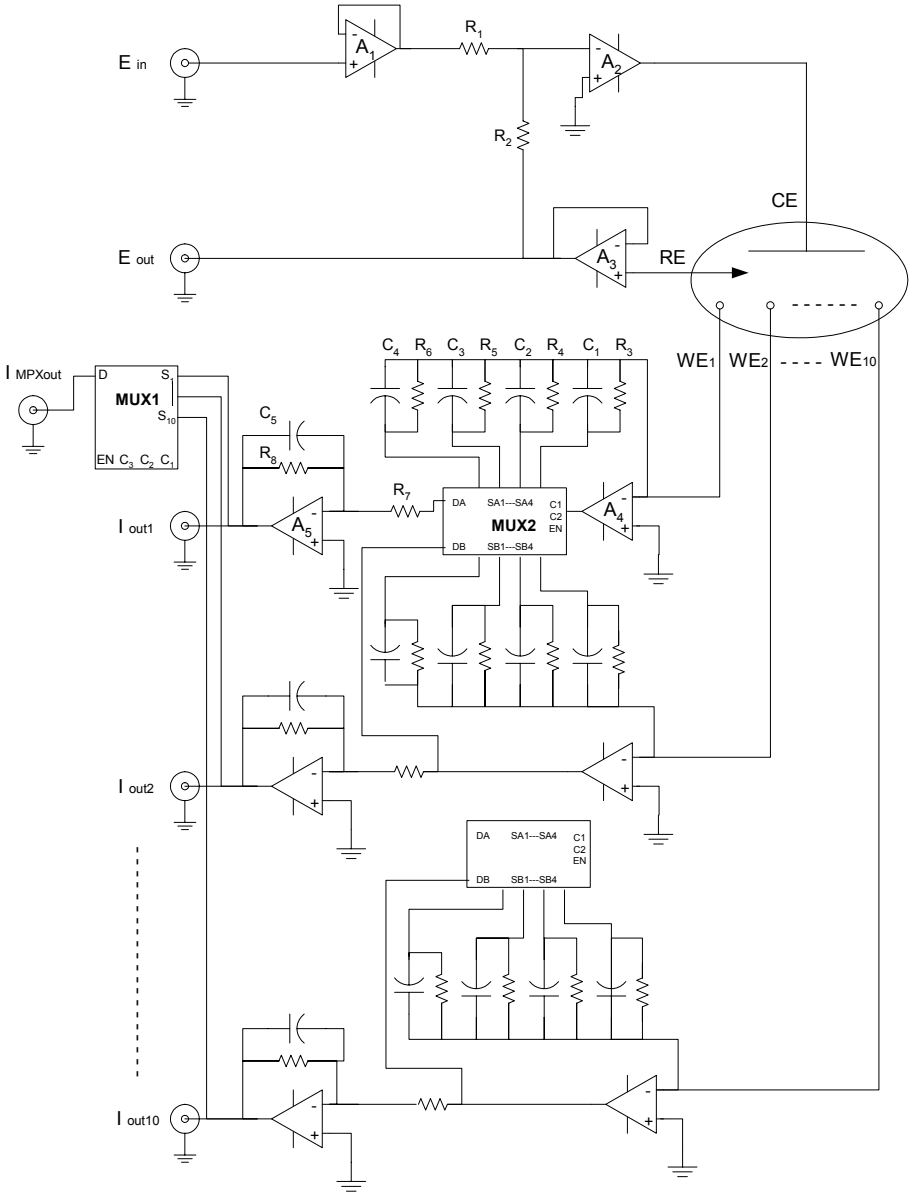

2) List of components

Operational Amplifiers
$A_1 – A_5$: ¼ LF444, National semiconductors

Multiplexers
MUX1 ADG507AKN, Analog Devices
MUX2 CD4052BE, Texas Instruments

Switches
CD74HC4066E, Texas Instruments.

Resistors
$R_,$ R_2, R_4, R_7 and R_8:
10 kΩ
R_3: 1 kΩ
R_5: 100 kΩ
R_6: 1 MΩ

Capacitors
C_1: 0.1 μF
C_2: 0.01μF
C_3: 0.001μF
C_4: 100 pF
C_5: 0.01μF

Main Power Supply
HTAA-16W-A (+/- 15 VDC), Power-one

B) MOSFET switch

1) Diagram

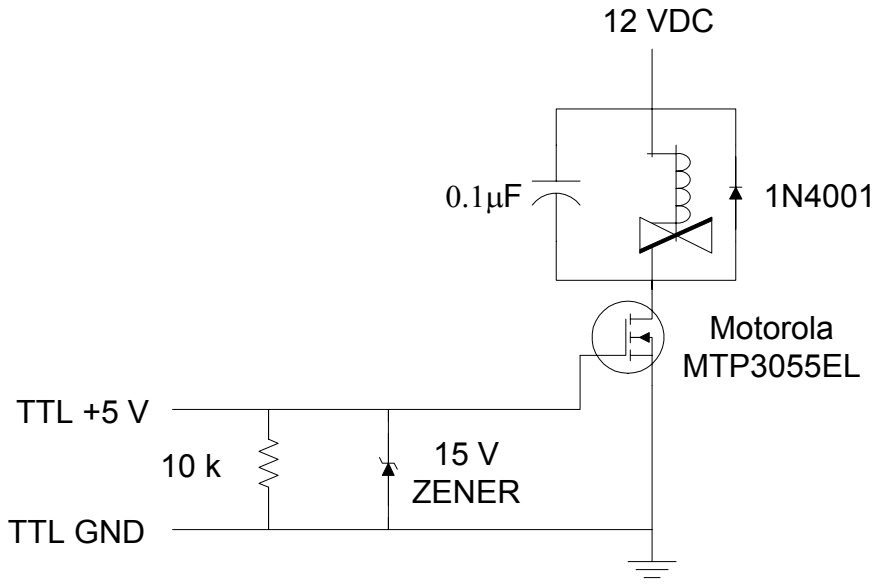

APPENDIX B
COMPUTER PROGRAM USED FOR DETERMINATION OF ROTATING DISK ELECTRODE SURFACE AREA OR DIFFUSION COEFFICIENT

This program controls the electrode rotator (Model AFMSRX, Pine Instrument Co., Grove City PA, U.S.A.), collect data and calculate electrode surface area is based on the Levich approach (See Chapter three for details on the theory). Rotational speed was adjusted through an analog output from an A/D data acquisition board (Product No. PCI 1200, National Instruments, Austin TX, U.S.A.). Potential at the potentiostat (Model 263-A EG&G Princeton Applied Research, Oak Ridge TN, U.S.A.) is controlled (ramped) with the second analog output of the A/D board. Potential, current and rotational speed are recorded with analog inputs of the A/D board. To calculate the surface area, the diffusion coefficient of the salt being used needs to be written in the front panel before starting the program. The default value is 7.62E-6 $cm^2.s^{-1}$ (corresponding to 4 mM ferricyanide in 0.1M KCl). A slight very similar program was used for calculation of diffusion coefficients of ascorbic acid and hydrogen peroxide. In that case instead, the surface area was input in the information subroutine and the diffusion coefficient is calculated from Levich equation. Because of its similarity to the first program the program for calculating diffusion coefficients is not included here. This program was also used to collect the data with polypyrrole-covered electrodes for calculation of permeability and surface area coverage. The information subroutine is also used for the electrode calibration program (see Appendix C).

A) Main Program

1) Icon

2) Control panel

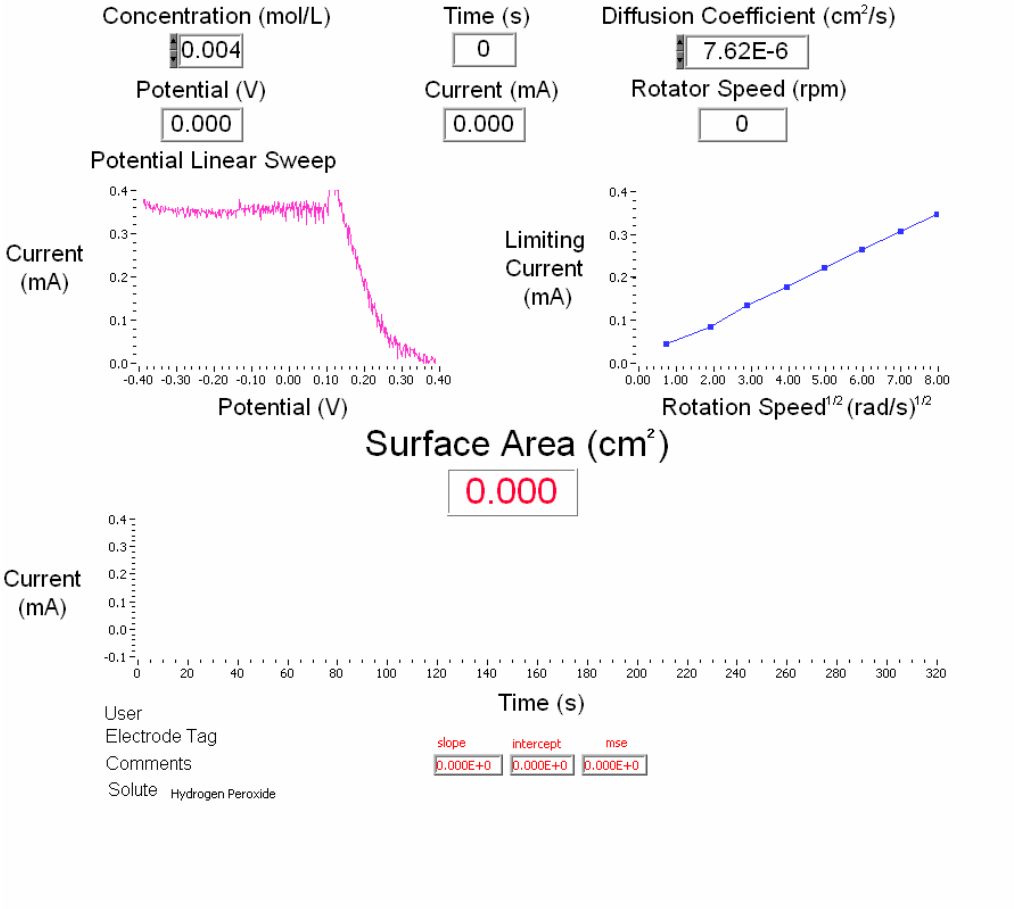

3) Diagram

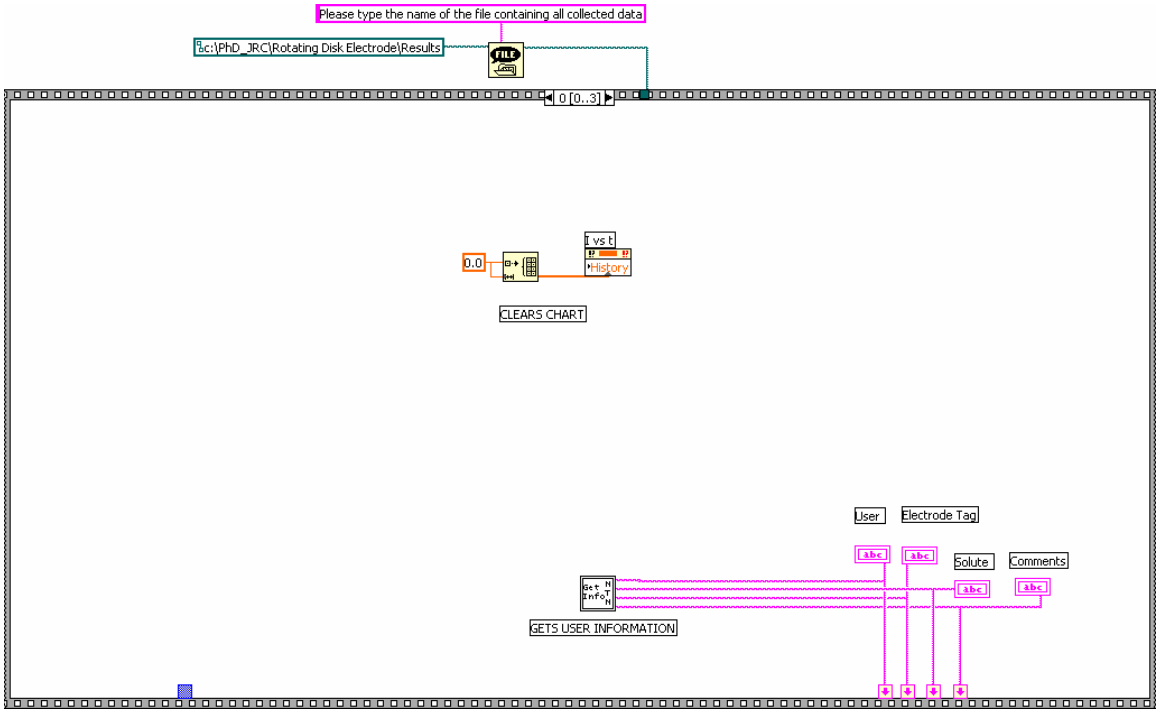
Please type the name of the file containing all collected data
c:\PhD_JRC\Rotating Disk Electrode\Results
0 [0..3]
0.0
I vs t
History
CLEARS CHART
User
Electrode Tag
Solute
Comments
GETS USER INFORMATION

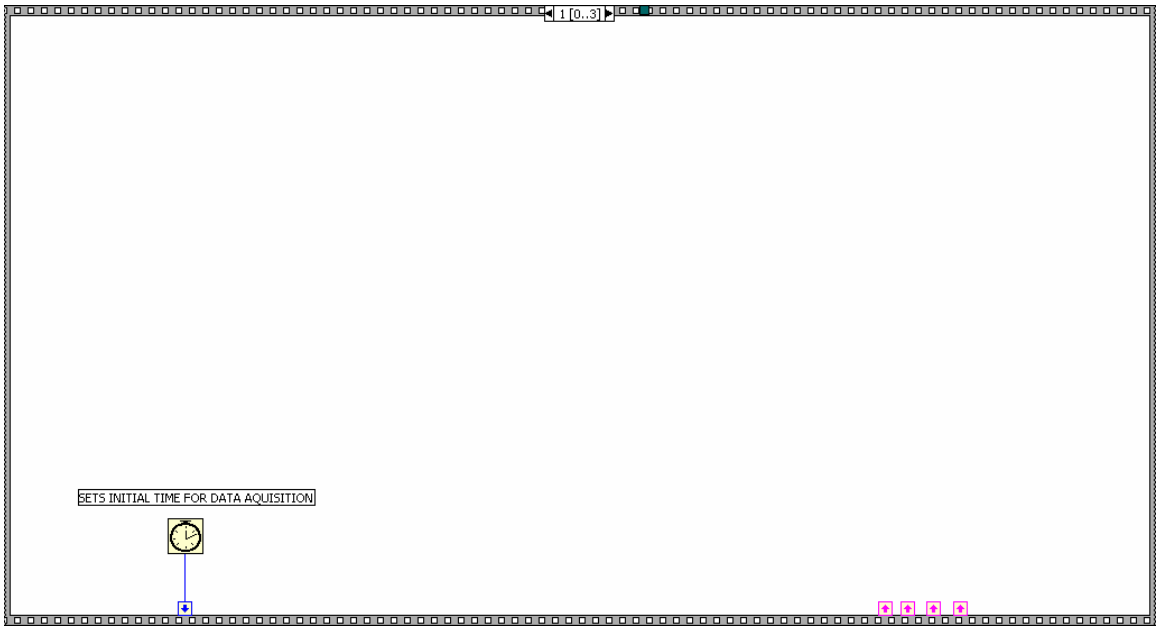
1 [0..3]
SETS INITIAL TIME FOR DATA AQUISITION

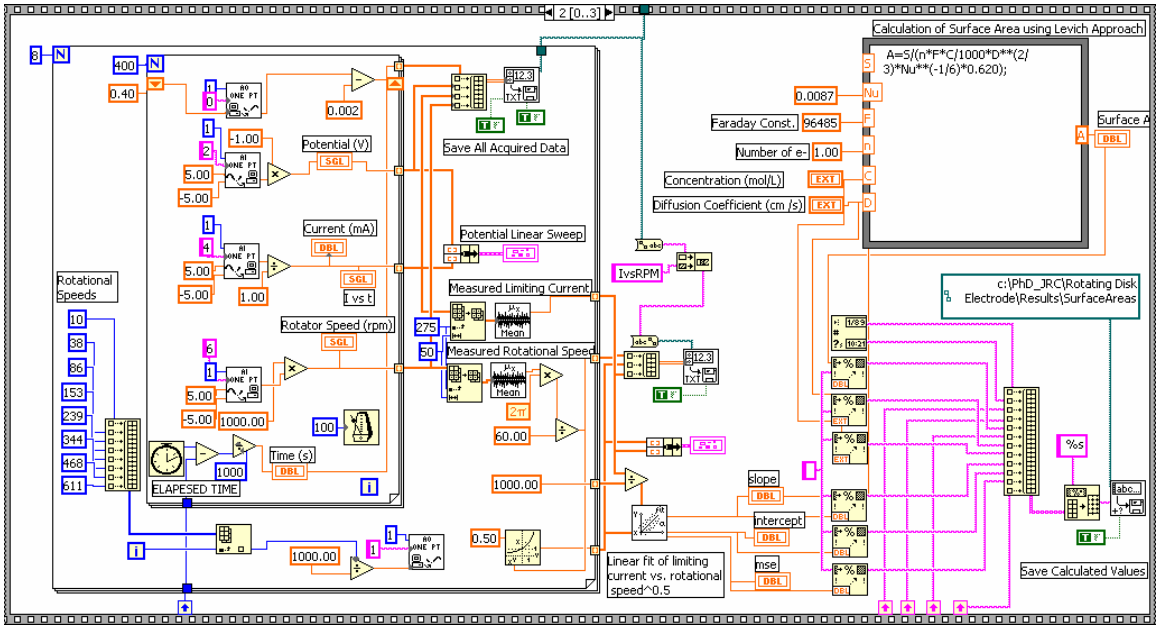
2 [0..3]
Calculation of Surface Area using Levich Approach
A=S/(n*F*C/1000*D**(2/3)*Nu**(-1/6)*0.620);
Save All Acquired Data
Potential (V)
Current (mA)
Potential Linear Sweep
Measured Limiting Current
Rotator Speed (rpm)
Measured Rotational Speed
Rotational Speeds
Time (s)
ELAPSED TIME
IvsRPM
Linear fit of limiting current vs. rotational speed^0.5
Faraday Const.
Number of e-
Concentration (mol/L)
Diffusion Coefficient (cm /s)
Surface A
slope
intercept
mse
c:\PhD_JRC\Rotating Disk Electrode\Results\SurfaceAreas
Save Calculated Values

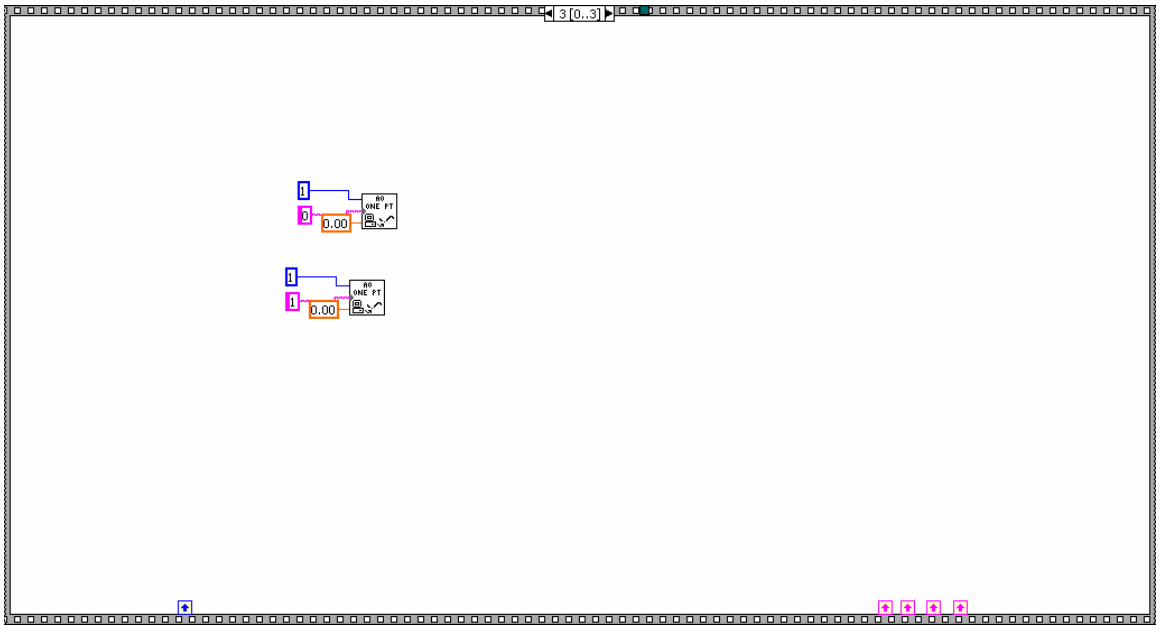
3 [0..3]

B) Information Subroutine

1) Icon

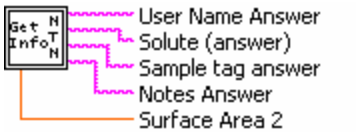

2) Front panel

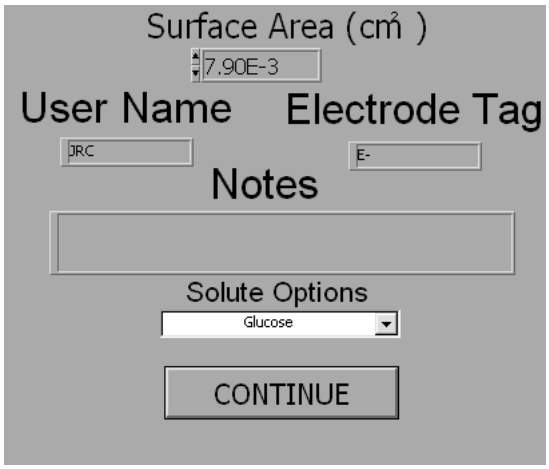

3) Diagram

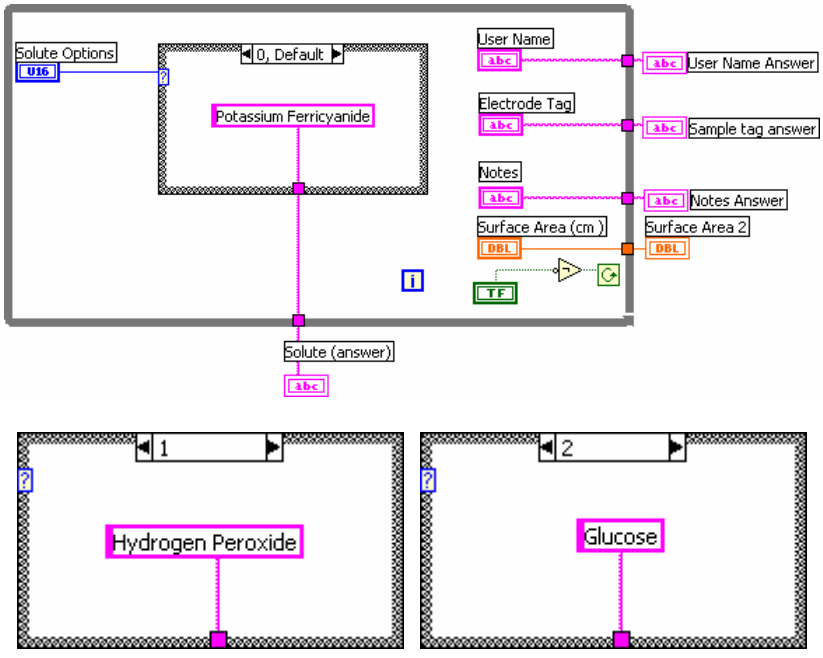

APPENDIX C

COMPUTER PROGRAM FOR ELECTROCHEMICAL POLYMERIZATION AND PLATINIZATION OF ELECTRODES

This program was written to control the electrochemical polymerization of polypyrrole films. The program communicates with the potentiostat (Model 263-A EG&G Princeton Applied Research, Oak Ridge TN, U.S.A.) through a GPIB board (Product No. PCI GPIB, National Instruments, Austin TX, U.S.A.) to set the polymerization potential and total charge calculated from the surface area of the bare electrode and the desired film thickness assuming 0.1μm requires 45 $mC.cm^{-2}$ (see Chapter three). Later experiments on polymerization of poly-o-phenylenediamine and on platinization required time instead of charge control. Therefore, the program was modified to set the potential at a given value and record potential, current and charge for a given amount of time. Because both programs are very similar, only the first is presented here.

A) Main Program

1) Icon

2) Front panel

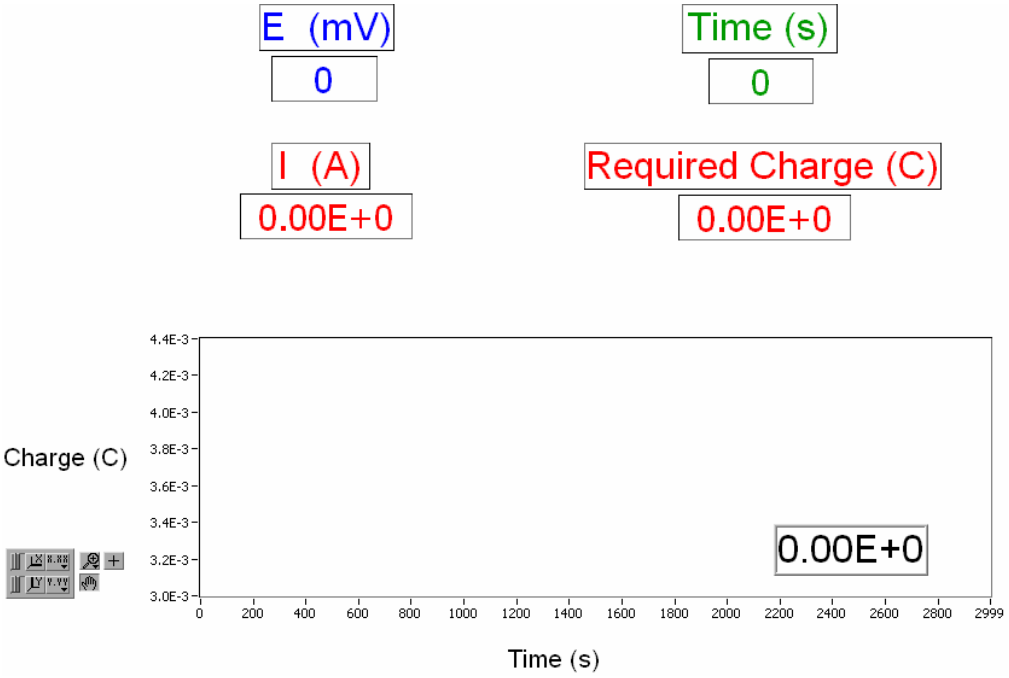

3) Diagram

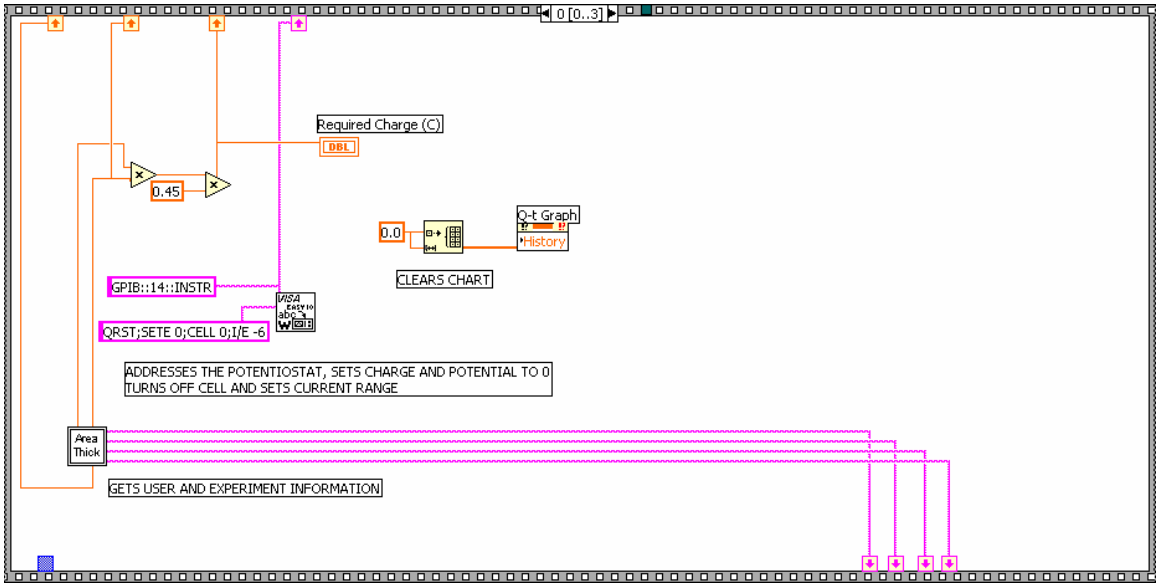

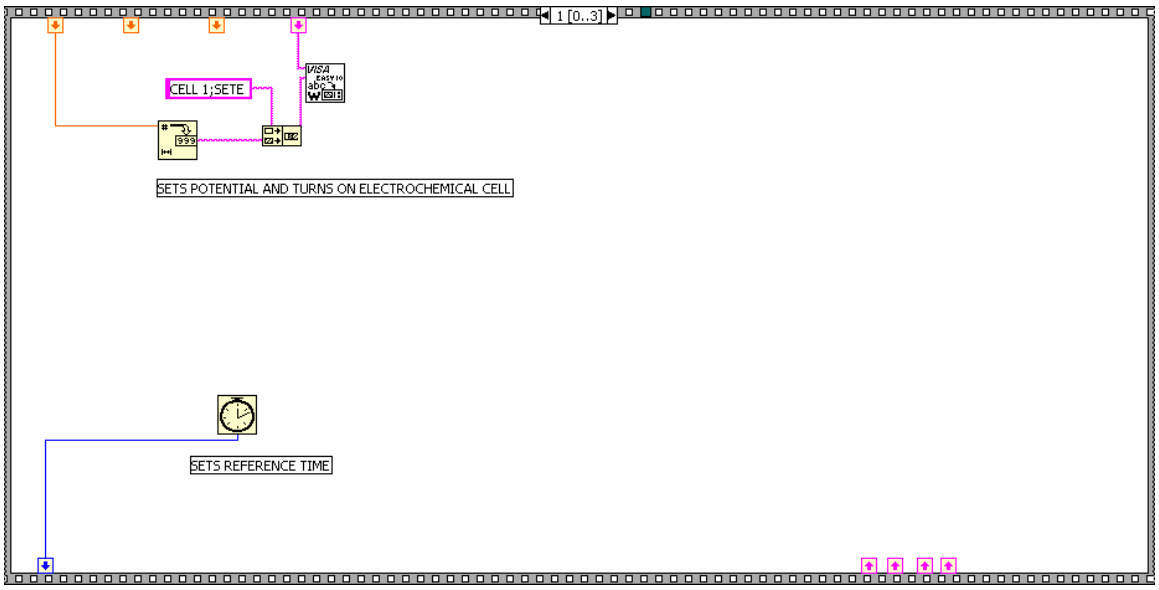
1 [0..3]
CELL 1;SETE
SETS POTENTIAL AND TURNS ON ELECTROCHEMICAL CELL
SETS REFERENCE TIME

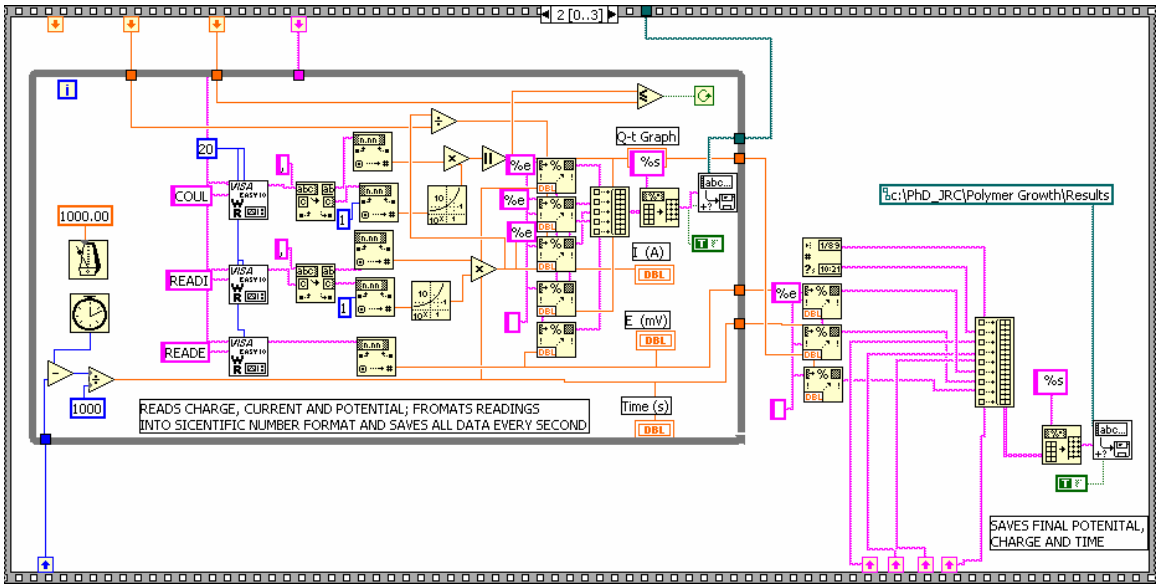
2 [0..3]
20
COUL
READI
READE
1000.00
1000
Q-t Graph
%e
%s
I (A)
E (mV)
Time (s)
READS CHARGE, CURRENT AND POTENTIAL; FROMATS READINGS
INTO SICENTIFIC NUMBER FORMAT AND SAVES ALL DATA EVERY SECOND
c:\PhD_JRC\Polymer Growth\Results
SAVES FINAL POTENITAL,
CHARGE AND TIME

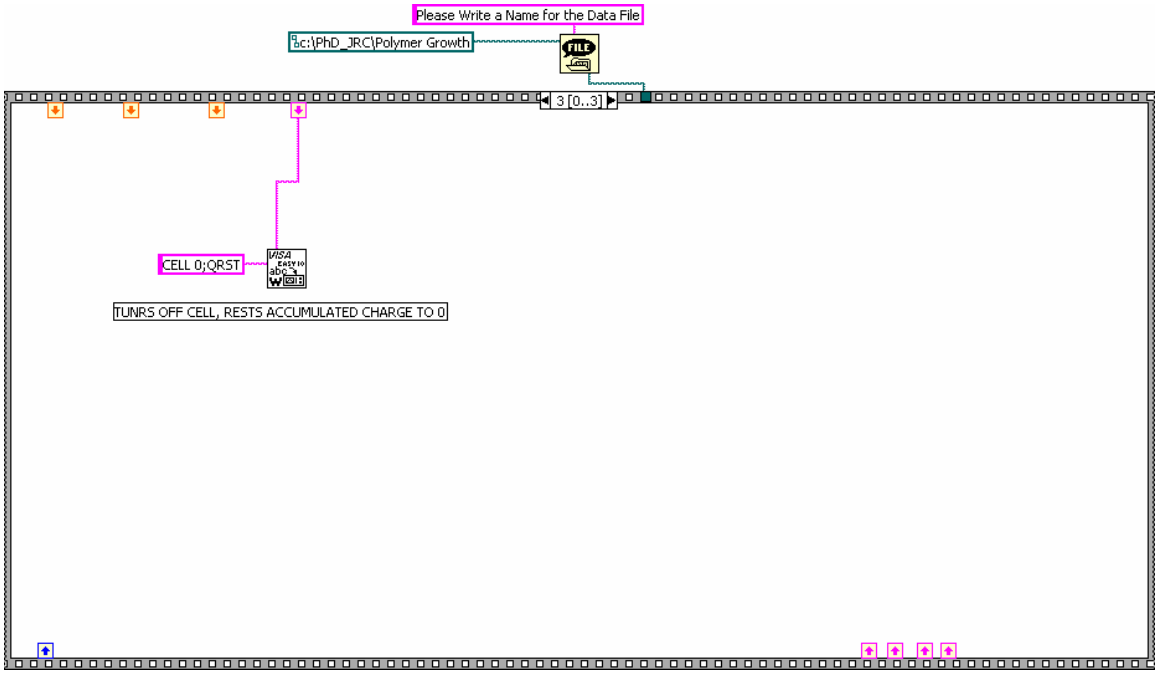

B) Information Input Subroutine

1) Icon

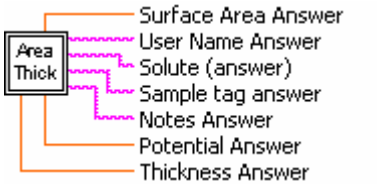

2) Front panel

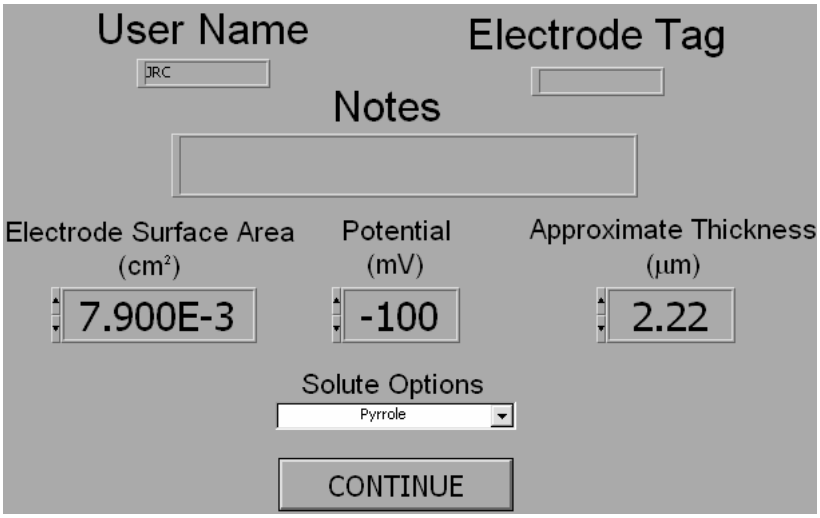

3) Diagram

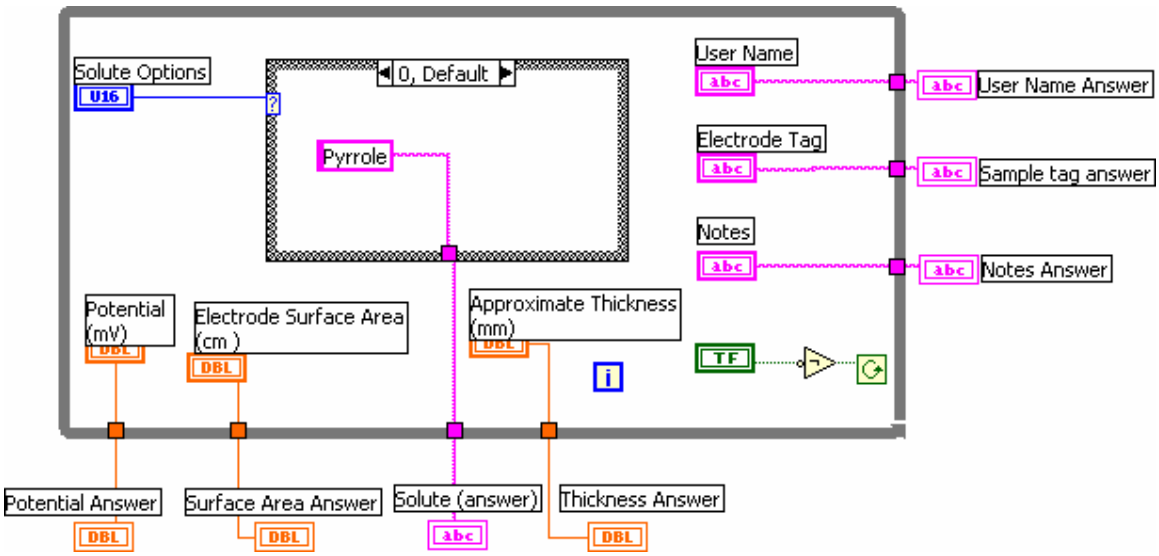
Solute Options
U16
0, Default
Pyrrole
User Name
abc
User Name Answer
Electrode Tag
Sample tag answer
Notes
Notes Answer
Potential (mV)
DBL
Electrode Surface Area (cm)
Approximate Thickness (mm)
TF
Potential Answer
Surface Area Answer
Solute (answer)
Thickness Answer

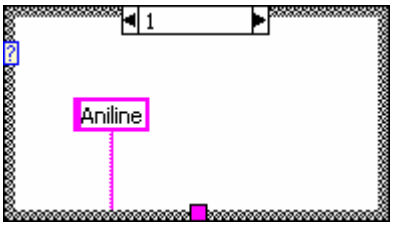
1
Aniline

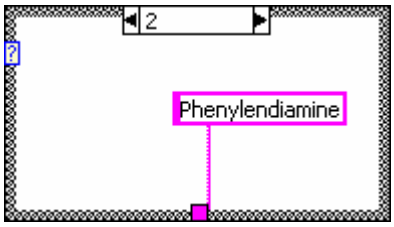
2
Phenylendiamine

APPENDIX D

COMPUTER PROGRAM FOR ELECTRODE CALIBRATION AND CHARACTERIZATION

This computer program controls the automatic positioning of an enzyme biosensor, a reference electrode and a counter electrode, in six solutions with different substrate concentration. A rotating table and a vertical displacement arm are controlled with stepping motors (Model 86MM-2, Velmex, Inc. East Bloomfield NY, U.S.A.). Commands from the LabVIEW program are sent to the stepping motor controller through RS-232 serial communication. This program also controls the potentiostat (Model 263-A EG&G Princeton Applied Research, Oak Ridge TN, U.S.A.) using a GPIB board (Product No. PCI GPIB, National Instruments, Austin TX, U.S.A.). Amperometric response of the glucose biosensors at 700 mV vs. Ag/AgCl for each concentration is recorded using also the GPIB. Steady state amperometric response to each concentration is recorded three times. With the complete set of data, the program calculates Michael-Menten kinetic parameters K_M and v_{max} from the double reciprocal plot of the amperometric response and glucose concentration. The computer program also calculates the sensitivity of the sensor from the linear portion of the curve of amperometric response vs. glucose concentration and the limit of detection as three times the standard deviation of the steady state current in buffer (i.e. glucose concentration equal to zero). Precision is also calculated at each glucose concentration as the standard deviation of three consecutive measurements of the steady state amperometric response.

A) Main Program

1) Icon

2) Front panel

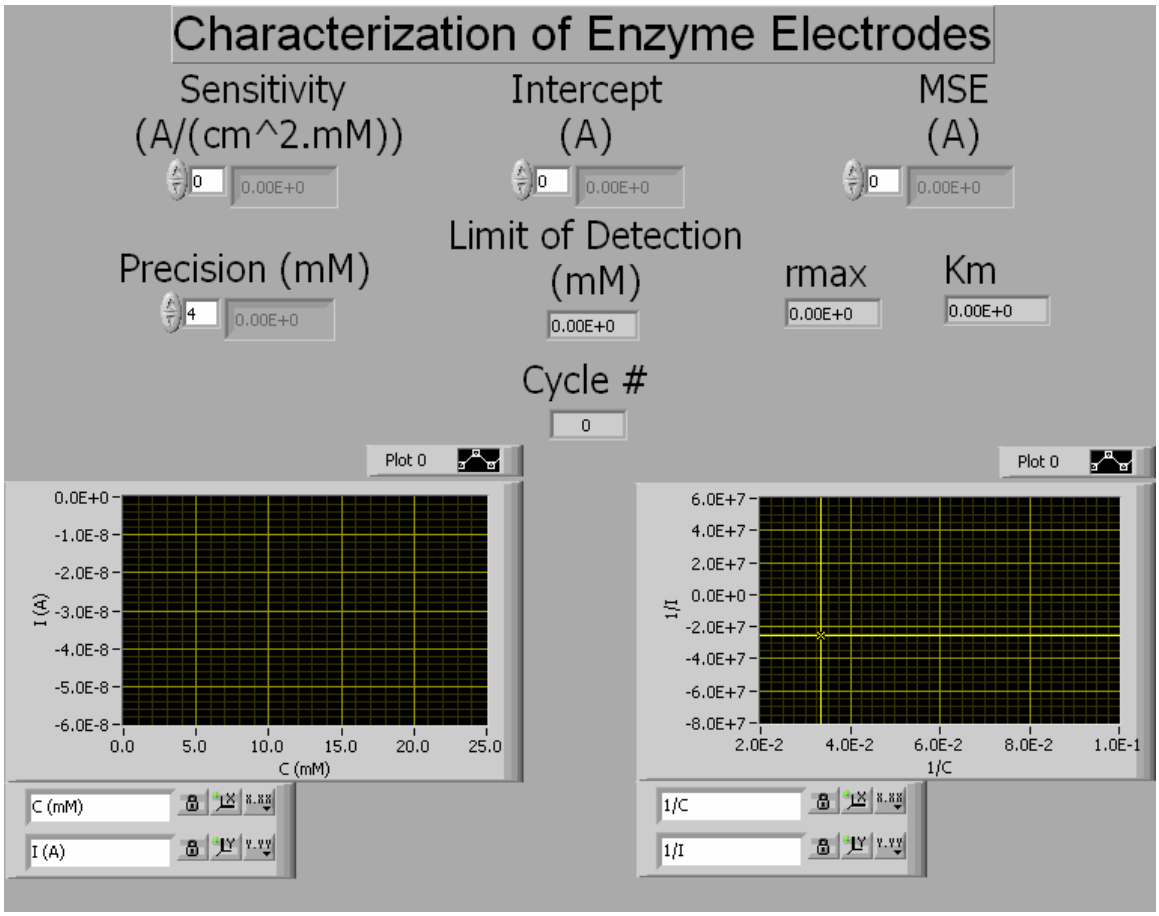

3) Diagram

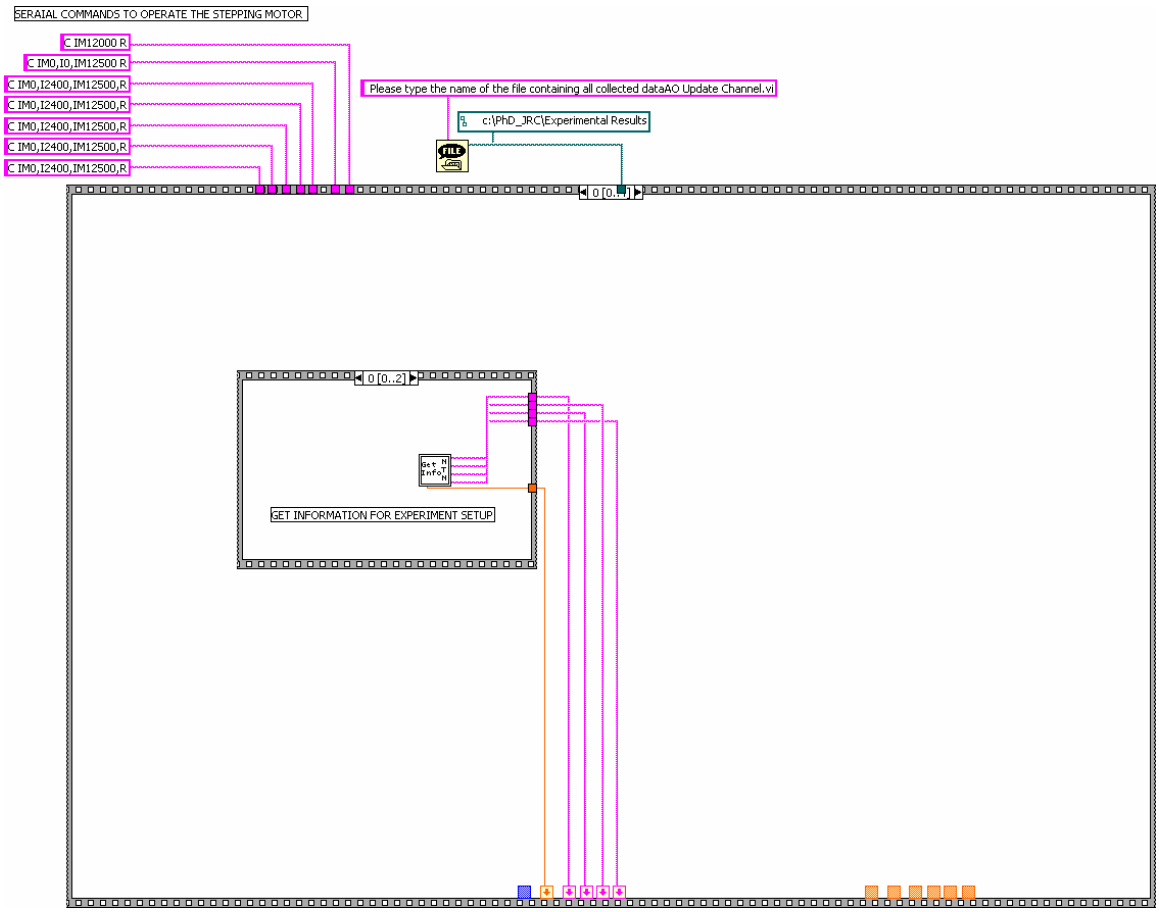
SERAIAL COMMANDS TO OPERATE THE STEPPING MOTOR
C IM12000 R
C IM0,I0,IM12500 R
C IM0,I2400,IM12500,R
C IM0,I2400,IM12500,R
C IM0,I2400,IM12500,R
C IM0,I2400,IM12500,R
C IM0,I2400,IM12500,R
Please type the name of the file containing all collected dataAO Update Channel.vi
c:\PhD_JRC\Experimental Results
0 [0..2]
GET INFORMATION FOR EXPERIMENT SETUP
1 [0..2]
INITIALIZE VELMEX STEPPING MOTORS CONTROLLER
0
E C IM-20000 R
10
N
2000
i
2 [0..2]
ZERO STEPPING MOTOR LOCATION
0
C Z R
10
N
1000
i

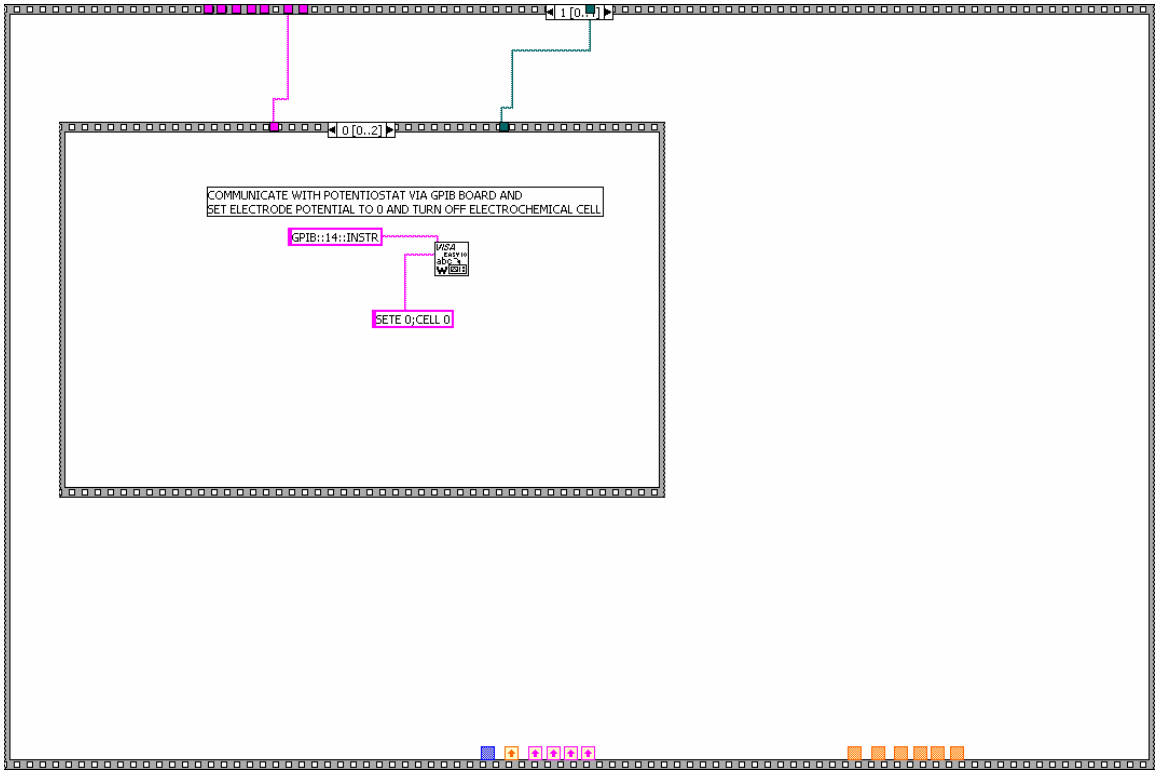
1 [0..4]
0 [0..2]
COMMUNICATE WITH POTENTIOSTAT VIA GPIB BOARD AND
SET ELECTRODE POTENTIAL TO 0 AND TURN OFF ELECTROCHEMICAL CELL
GPIB::14::INSTR
SETE 0;CELL 0

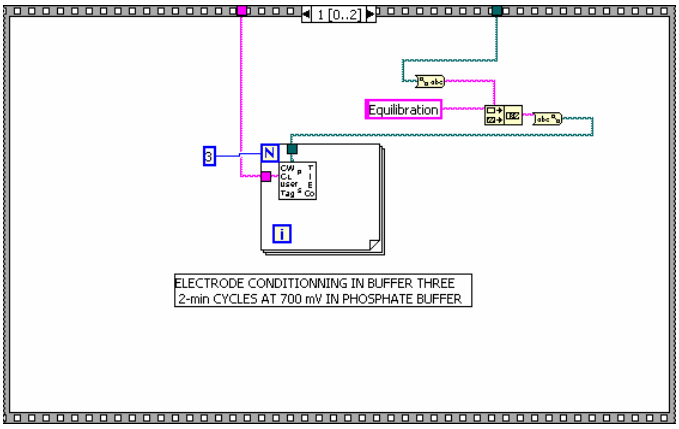
1 [0..2]
Equilibration
5
ELECTRODE CONDITIONNING IN BUFFER THREE
2-min CYCLES AT 700 mV IN PHOSPHATE BUFFER

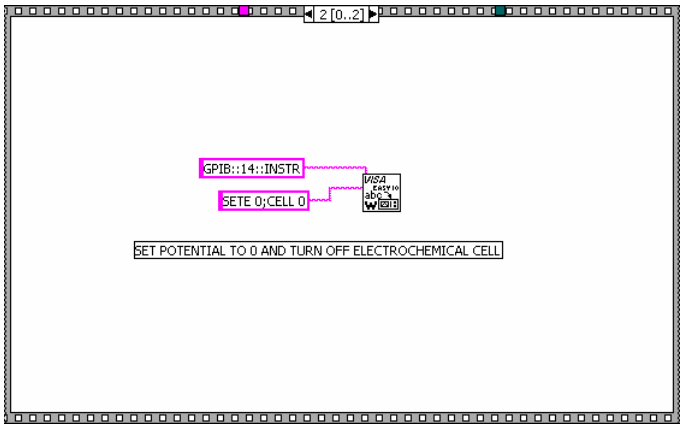
2 [0..2]
GPIB::14::INSTR
SETE 0;CELL 0
SET POTENTIAL TO 0 AND TURN OFF ELECTROCHEMICAL CELL

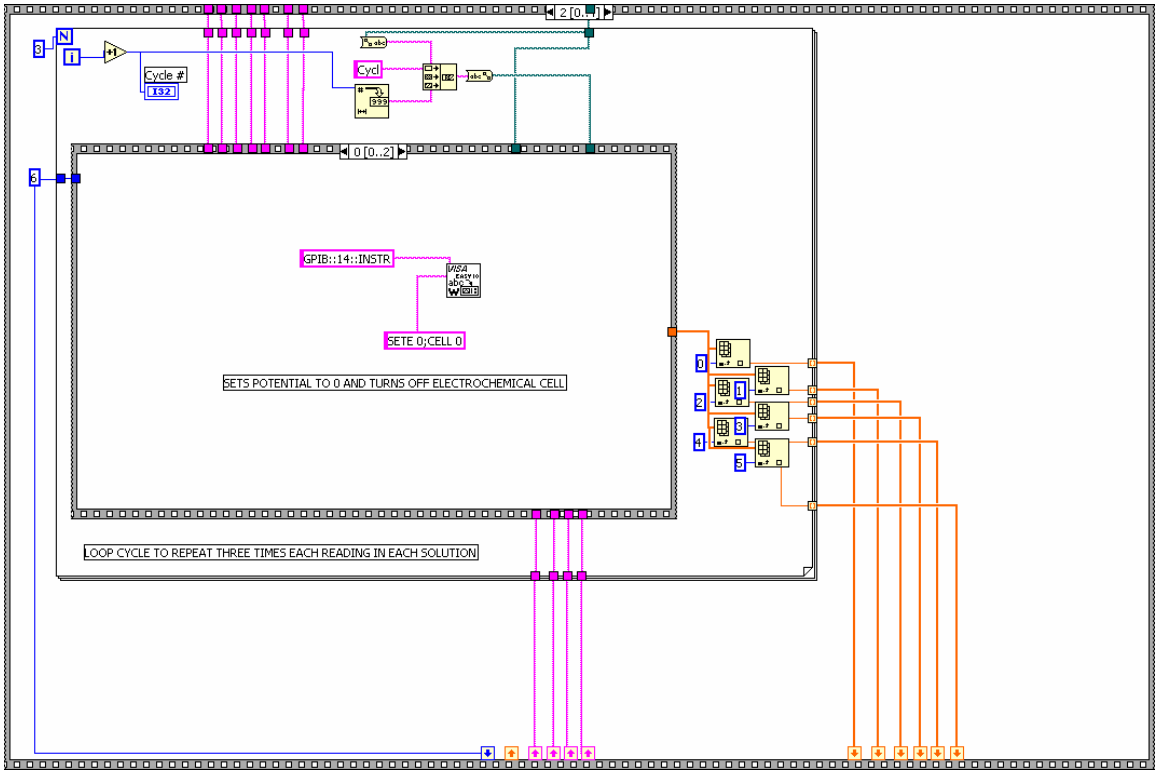
2 [0..]
Cycle #
192
Cycl
0 [0..2]
GPIB::14::INSTR
SETE 0;CELL 0
SETS POTENTIAL TO 0 AND TURNS OFF ELECTROCHEMICAL CELL
LOOP CYCLE TO REPEAT THREE TIMES EACH READING IN EACH SOLUTION

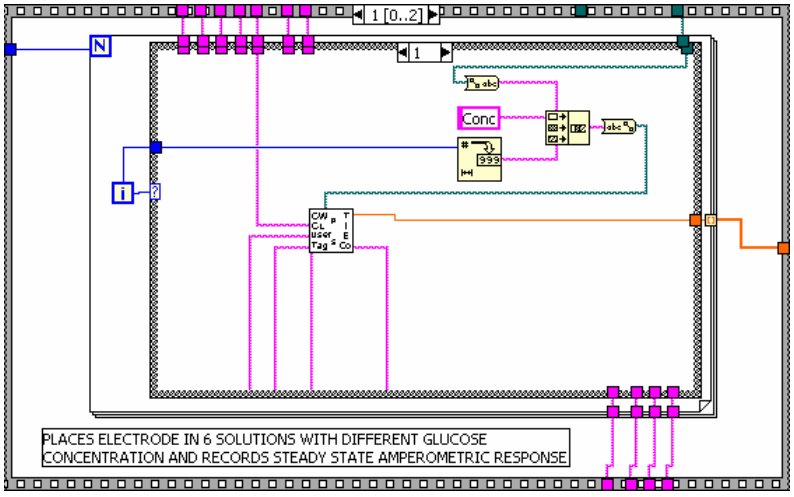
1 [0..2]
Conc
PLACES ELECTRODE IN 6 SOLUTIONS WITH DIFFERENT GLUCOSE
CONCENTRATION AND RECORDS STEADY STATE AMPEROMETRIC RESPONSE

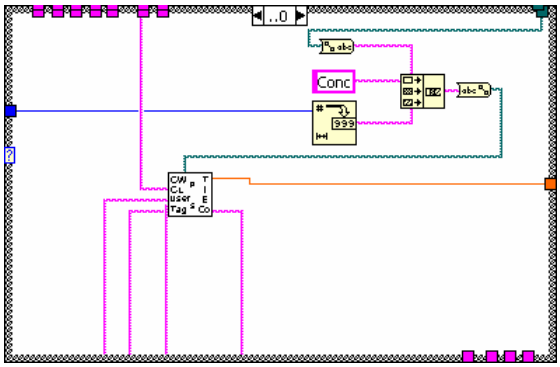
..0
Conc

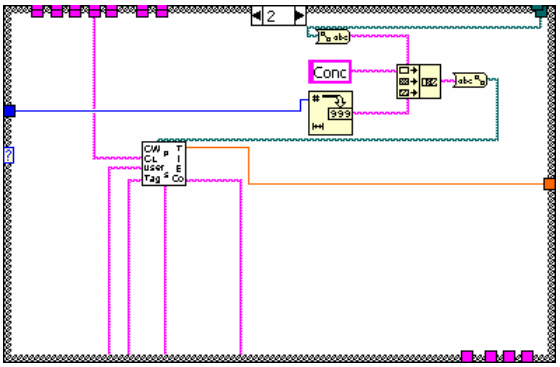
2
Conc

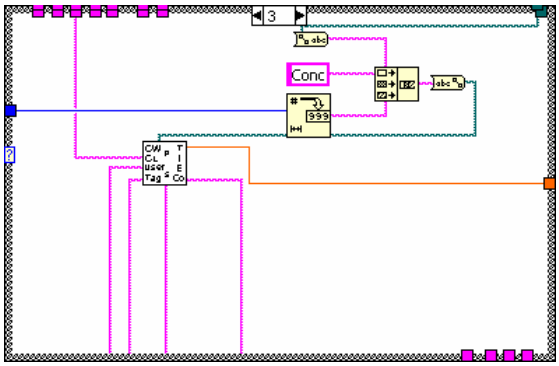
3
Conc
999

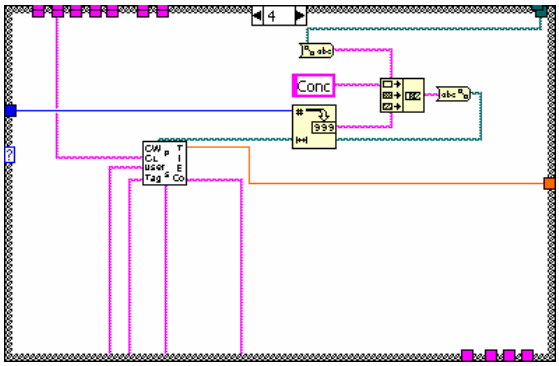
4
Conc
999

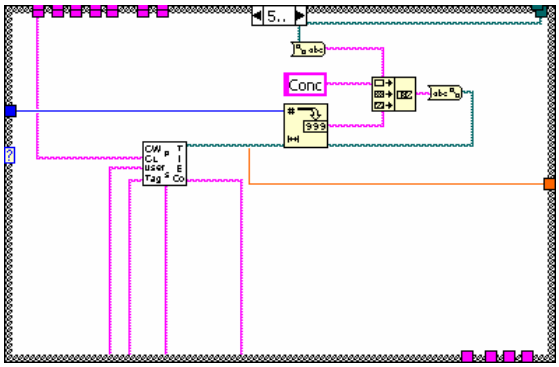
5..
Conc
999

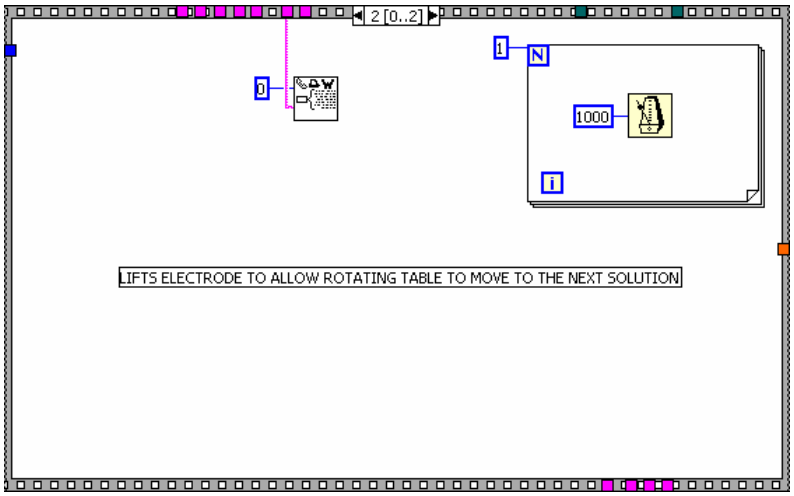
2 [0..2]
0
1
N
1000
i
LIFTS ELECTRODE TO ALLOW ROTATING TABLE TO MOVE TO THE NEXT SOLUTION

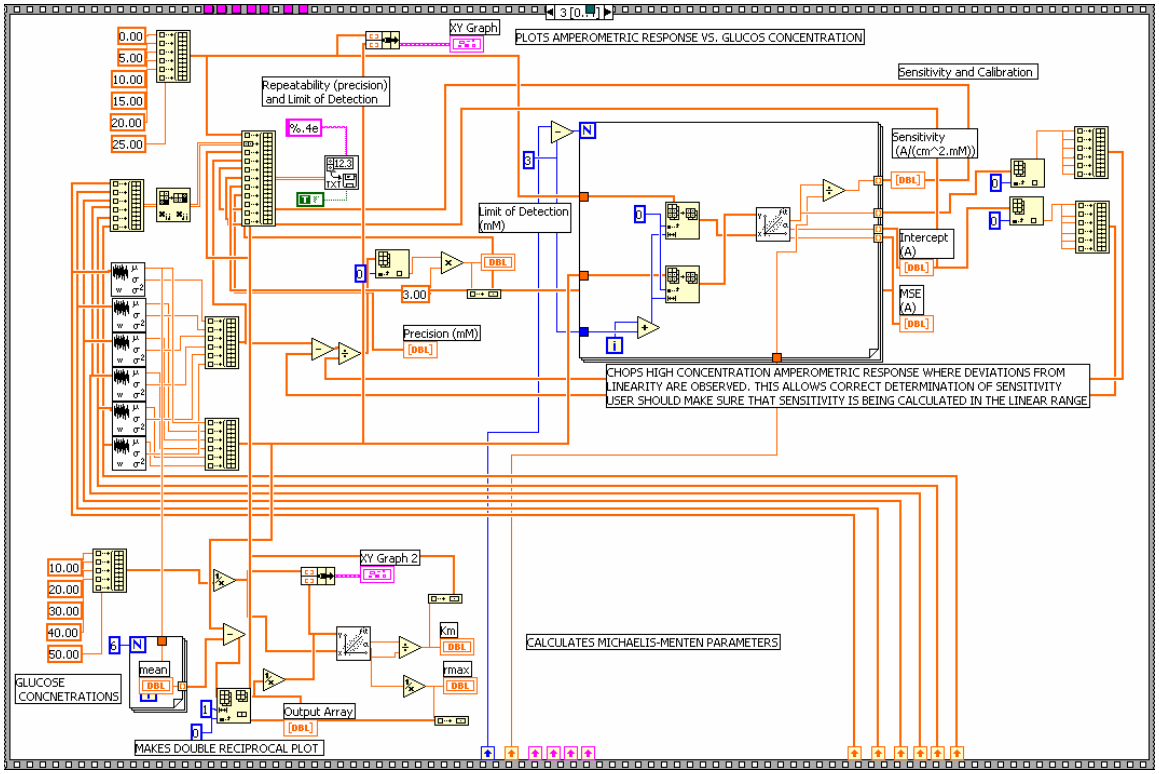
3 [0..]
XY Graph
PLOTS AMPEROMETRIC RESPONSE VS. GLUCOS CONCENTRATION
Sensitivity and Calibration
0.00
5.00
10.00
15.00
20.00
25.00
Repeatability (precision) and Limit of Detection
%.4e
Limit of Detection (mM)
3.00
Precision (mM)
Sensitivity (A/(cm^2.mM))
Intercept (A)
MSE (A)
CHOPS HIGH CONCENTRATION AMPEROMETRIC RESPONSE WHERE DEVIATIONS FROM LINEARITY ARE OBSERVED. THIS ALLOWS CORRECT DETERMINATION OF SENSITIVITY
USER SHOULD MAKE SURE THAT SENSITIVITY IS BEING CALCULATED IN THE LINEAR RANGE
XY Graph 2
10.00
20.00
30.00
40.00
50.00
GLUCOSE CONCNETRATIONS
mean
Output Array
Km
Vmax
CALCULATES MICHAELIS-MENTEN PARAMETERS
MAKES DOUBLE RECIPROCAL PLOT

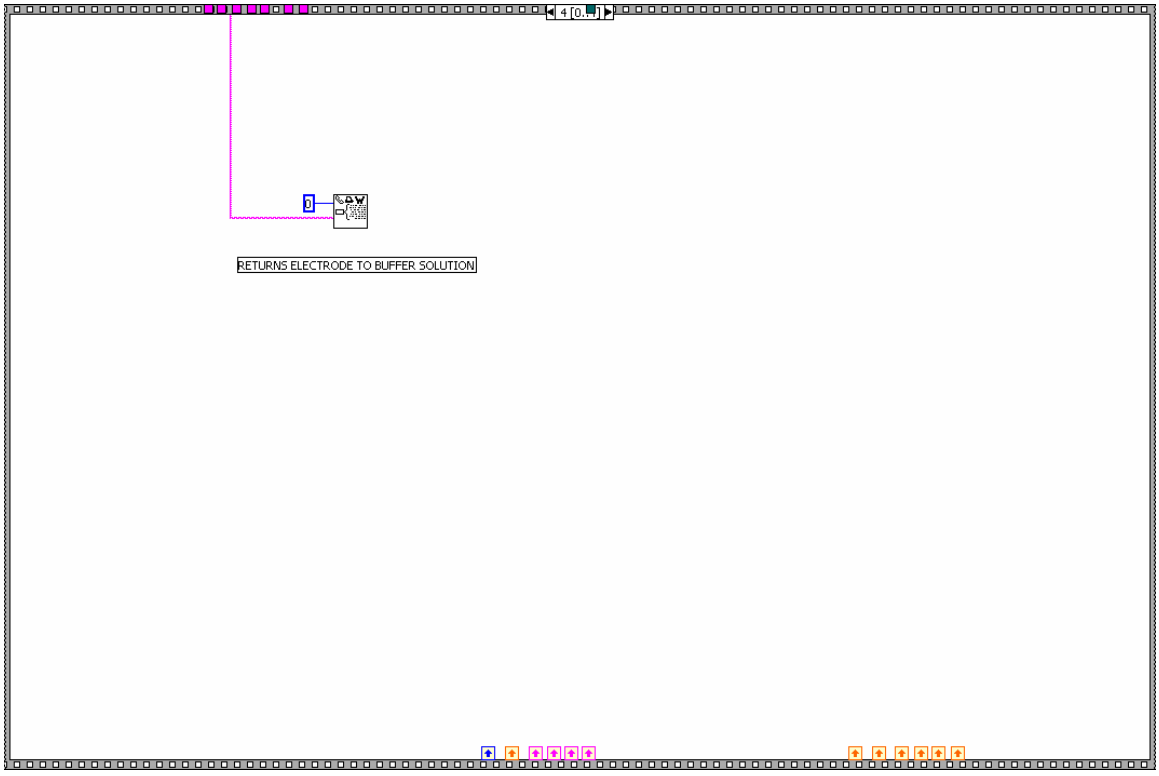
4 [0..]
RETURNS ELECTRODE TO BUFFER SOLUTION

B) Data Acquisition Subroutine

1) Icon

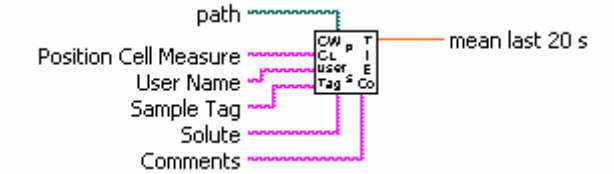

2) Front panel

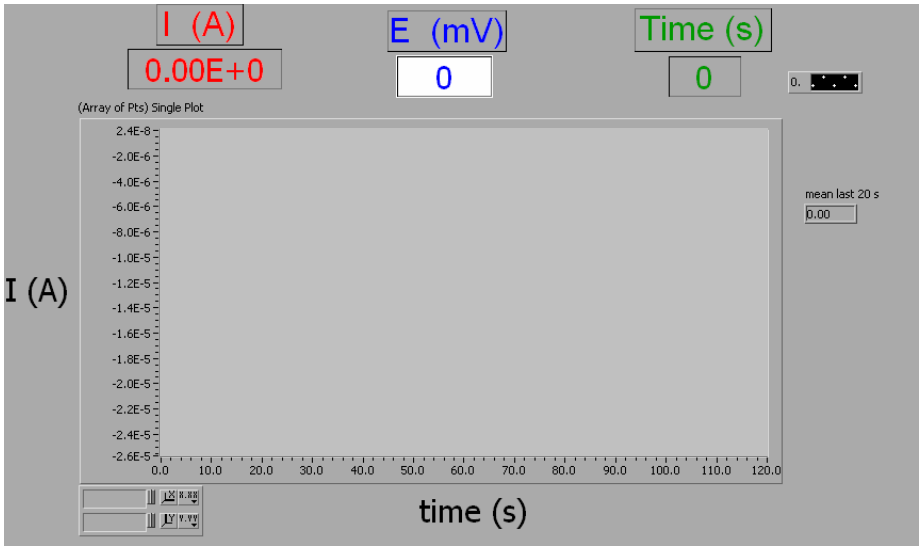

3) Diagram

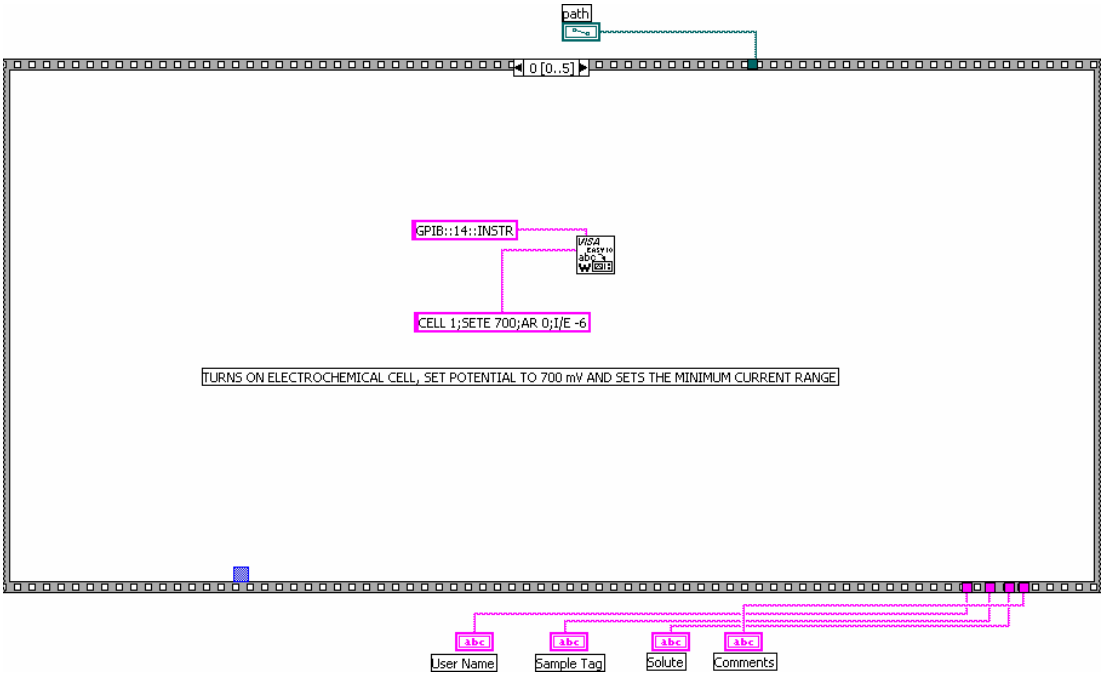
path
0 [0..5]
GPIB::14::INSTR
CELL 1;SETE 700;AR 0;I/E -6
TURNS ON ELECTROCHEMICAL CELL, SET POTENTIAL TO 700 mV AND SETS THE MINIMUM CURRENT RANGE
User Name
Sample Tag
Solute
Comments

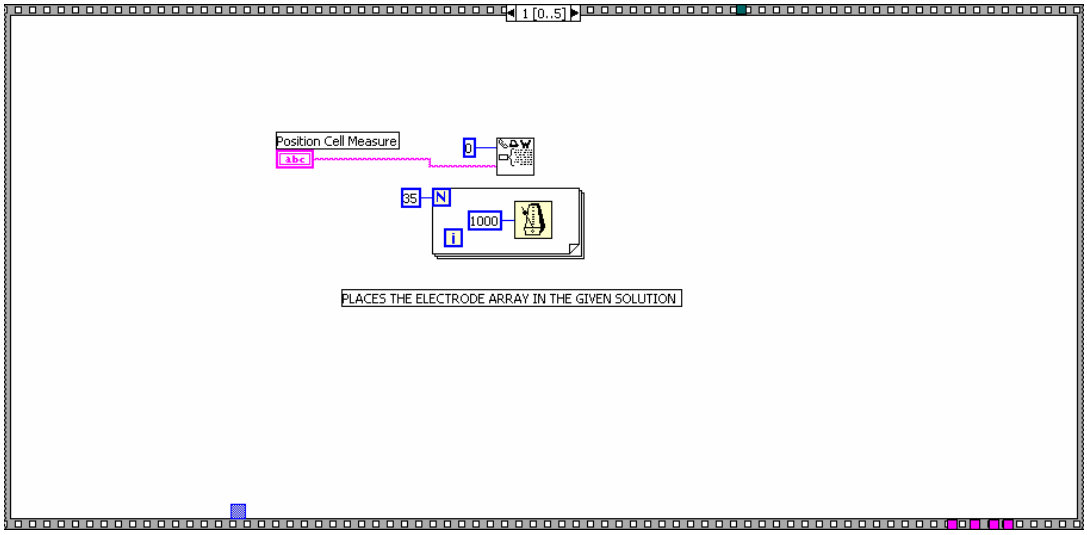
1 [0..5]
Position Cell Measure
0
35
N
1000
i
PLACES THE ELECTRODE ARRAY IN THE GIVEN SOLUTION

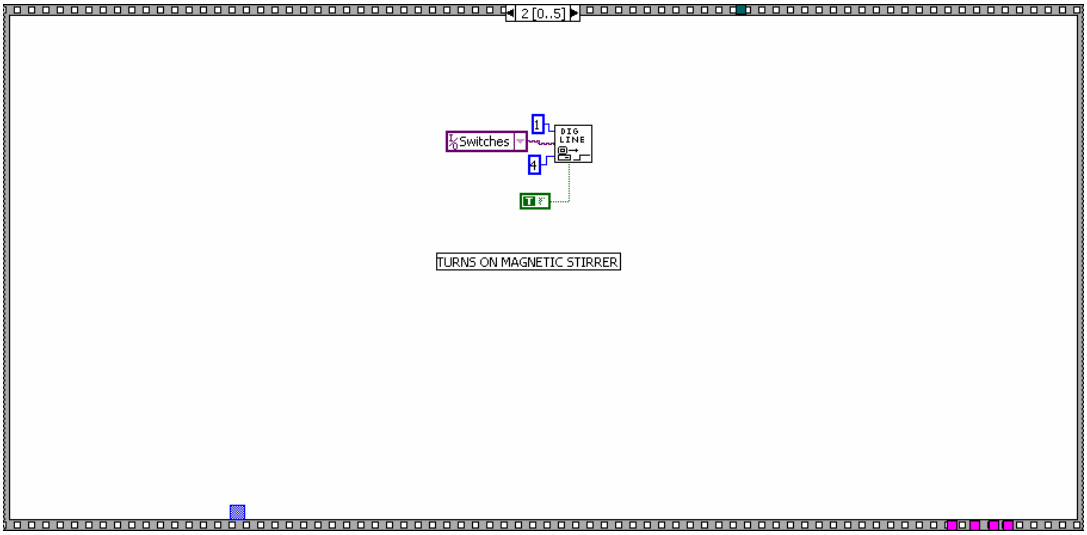
2 [0..5]
Switches
DIG LINE
TURNS ON MAGNETIC STIRRER


3 [0..5]
SETS REFERENCE TIME

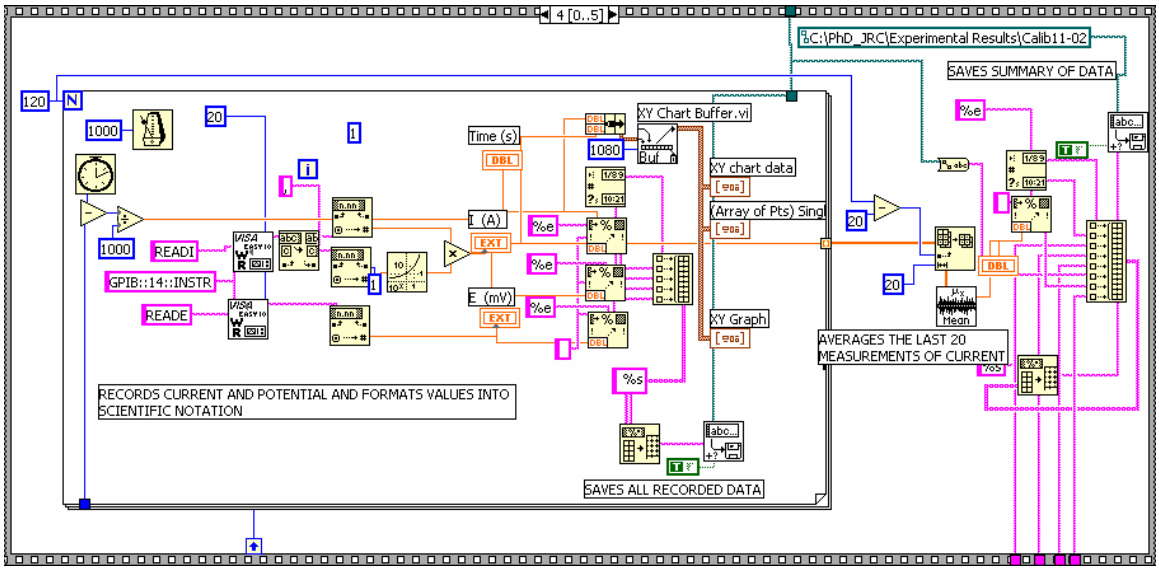
4 [0..5]
C:\PhD_JRC\Experimental Results\Calib11-02
SAVES SUMMARY OF DATA
120
N
1000
20
1
Time (s)
1080
XY Chart Buffer.vi
XY chart data
(Array of Pts) Sing
I (A)
E (mV)
READI
GPIB::14::INSTR
READE
XY Graph
AVERAGES THE LAST 20 MEASUREMENTS OF CURRENT
RECORDS CURRENT AND POTENTIAL AND FORMATS VALUES INTO SCIENTIFIC NOTATION
SAVES ALL RECORDED DATA

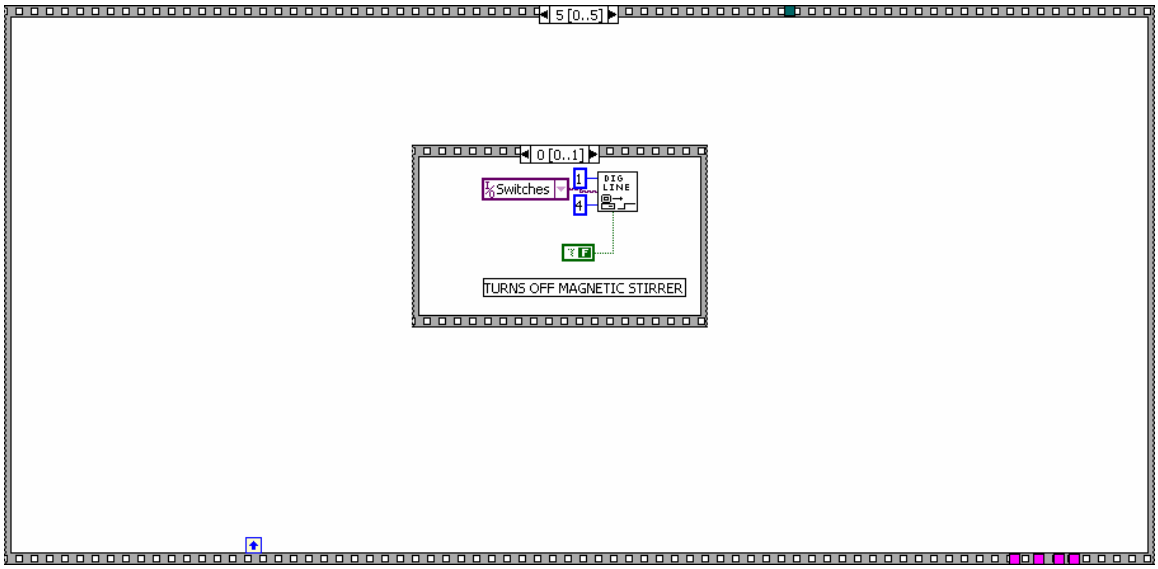
5 [0..5]
0 [0..1]
Switches
DIG LINE
TURNS OFF MAGNETIC STIRRER

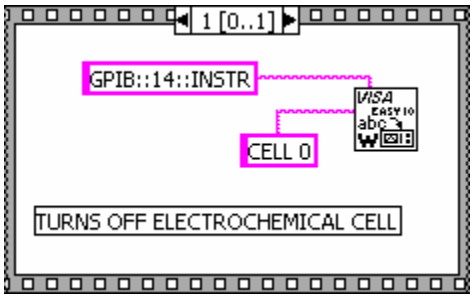
1 [0..1]
GPIB::14::INSTR
VISA
CELL 0
TURNS OFF ELECTROCHEMICAL CELL

APPENDIX E

COMPUTER PROGRAM USED FOR THE AUTOMATIC CONTROL OF THE TTI FLOW SYSTEM AND DATA ACQUISITION

This computer program controls the operation of the syringe pump (Model 200i, kdScientific New Hope PA, U.S.A.), the operation a manifold with three 12-V solenoid valves (Cole Parmer Cat. No. A-01367-81) and data collection. Syringe control was done through RS-232 serial communication. Valve operation was done via 5V TTL digital outputs form an A/D data acquisition board (Product No. PCI 6032E, National Instruments, Austin TX, U.S.A.) connected to MOSFET switches (see Appendix A). Data collection of current and potential from the homemade analog potentiostat (see Figures 3-6, Appendix F) and temperature recording was also carried out using the analog inputs of the A/D board. Because the A/D board does not come with thermocouple inputs, an additional thermocouple module (5B47 Isolated, Linearized Thermocouple Input mounted on a Backplane 5B04, Analog Devices, Norwood, MA, U.S.A.). A picture of the temperature module is shown in Figure 5, Appendix F.

A) Main Program

1) Icon

2) Front panel

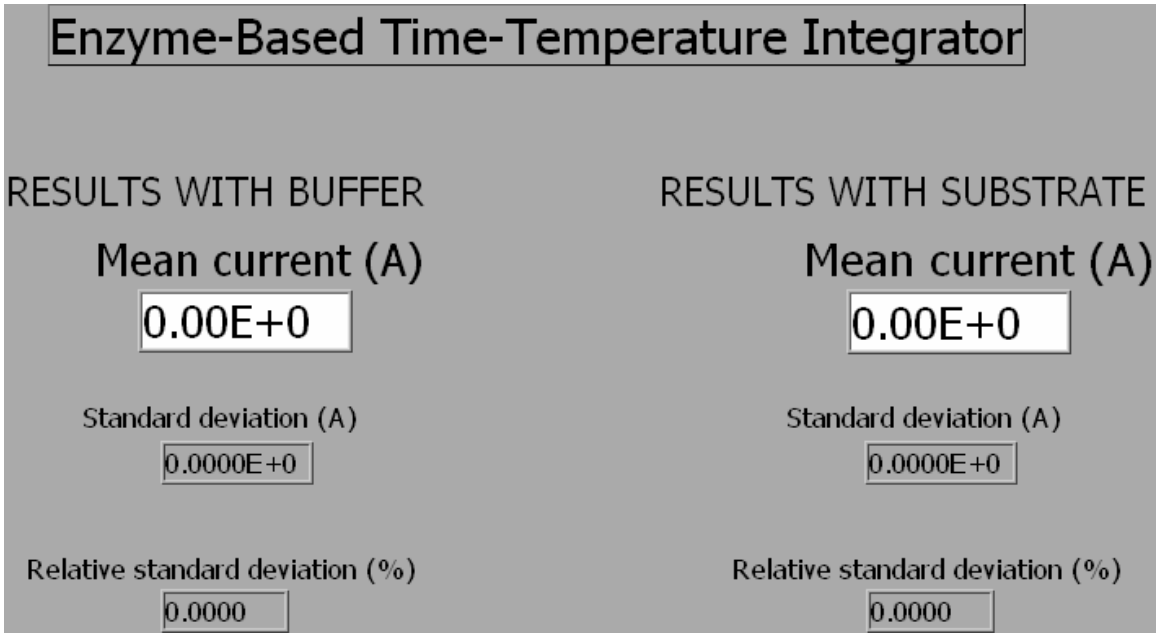

3) Diagram

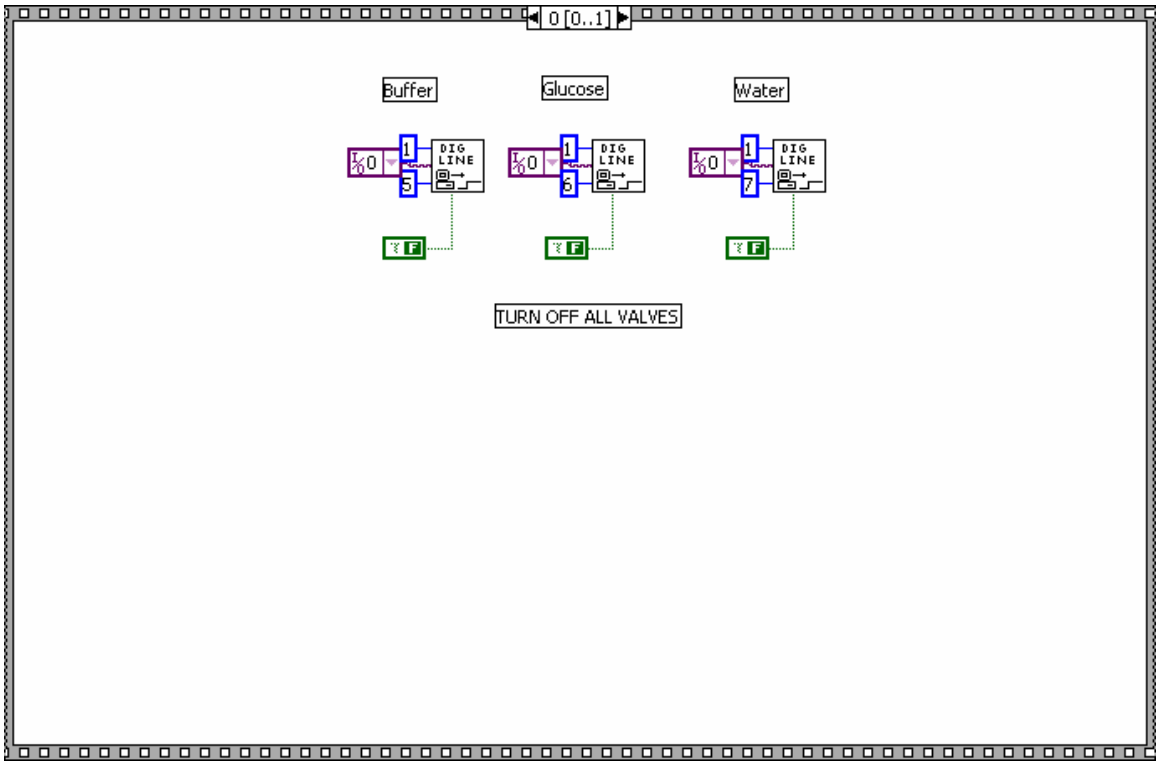

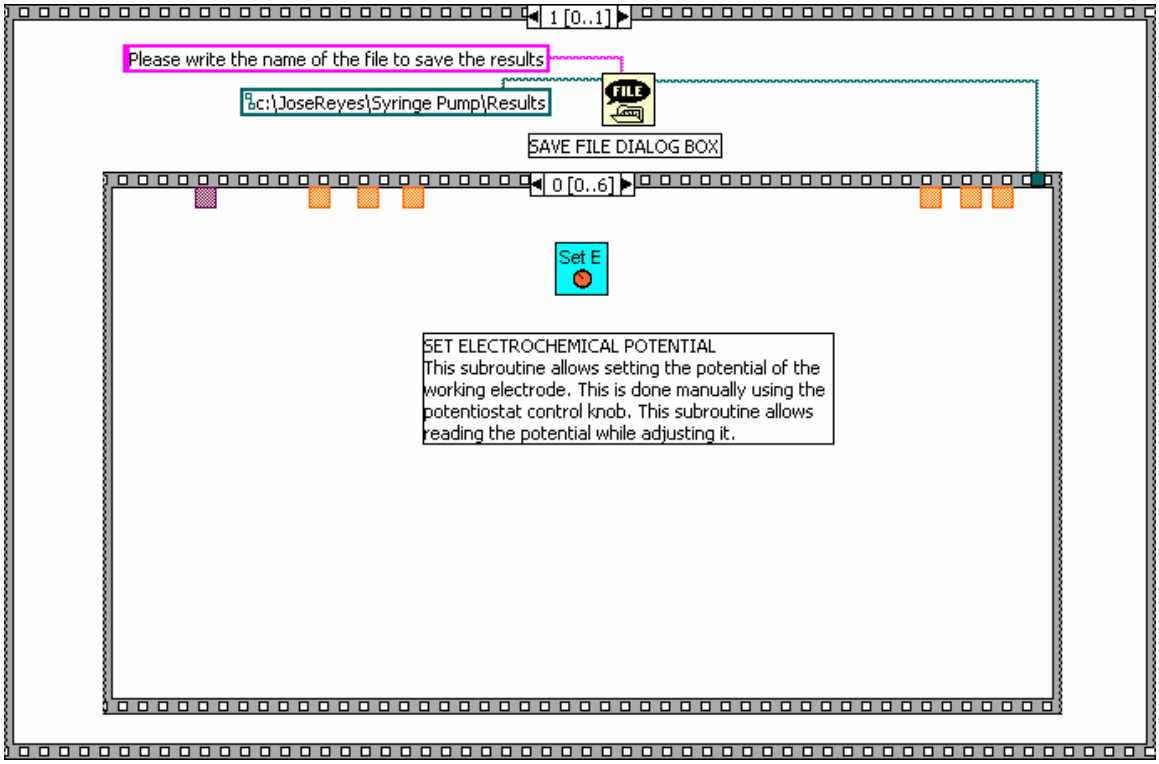
1 [0..1]
Please write the name of the file to save the results
c:\JoseReyes\Syringe Pump\Results
FILE
SAVE FILE DIALOG BOX
0 [0..6]
Set E
SET ELECTROCHEMICAL POTENTIAL
This subroutine allows setting the potential of the working electrode. This is done manually using the potentiostat control knob. This subroutine allows reading the potential while adjusting it.

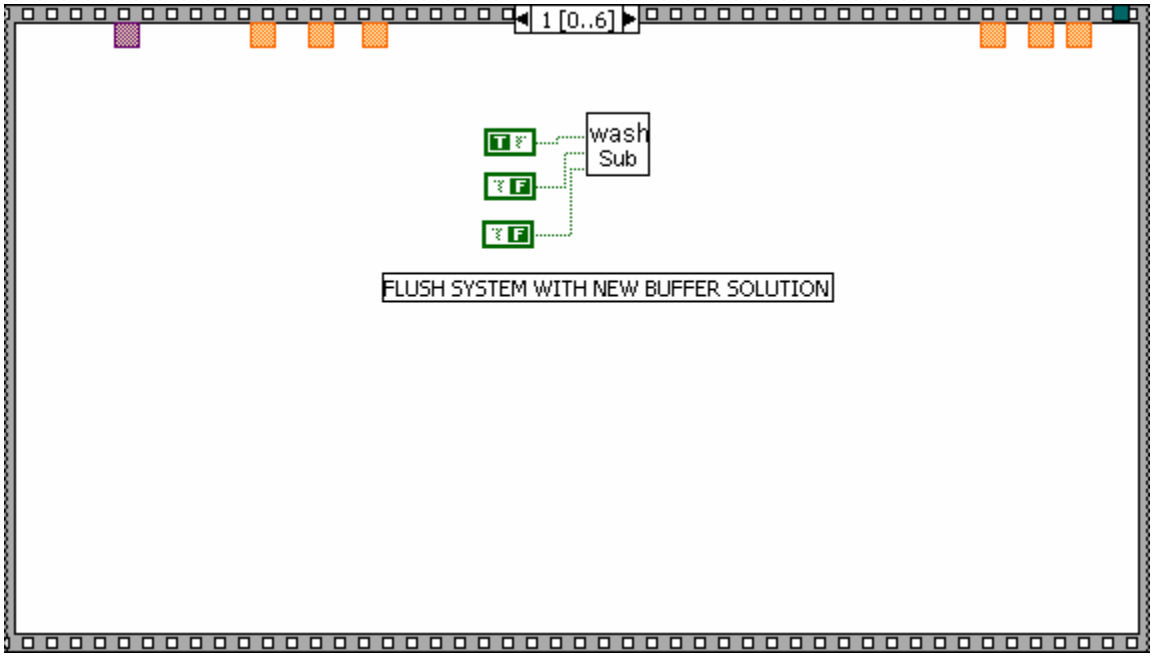
1 [0..6]
T
F
F
wash
Sub
FLUSH SYSTEM WITH NEW BUFFER SOLUTION

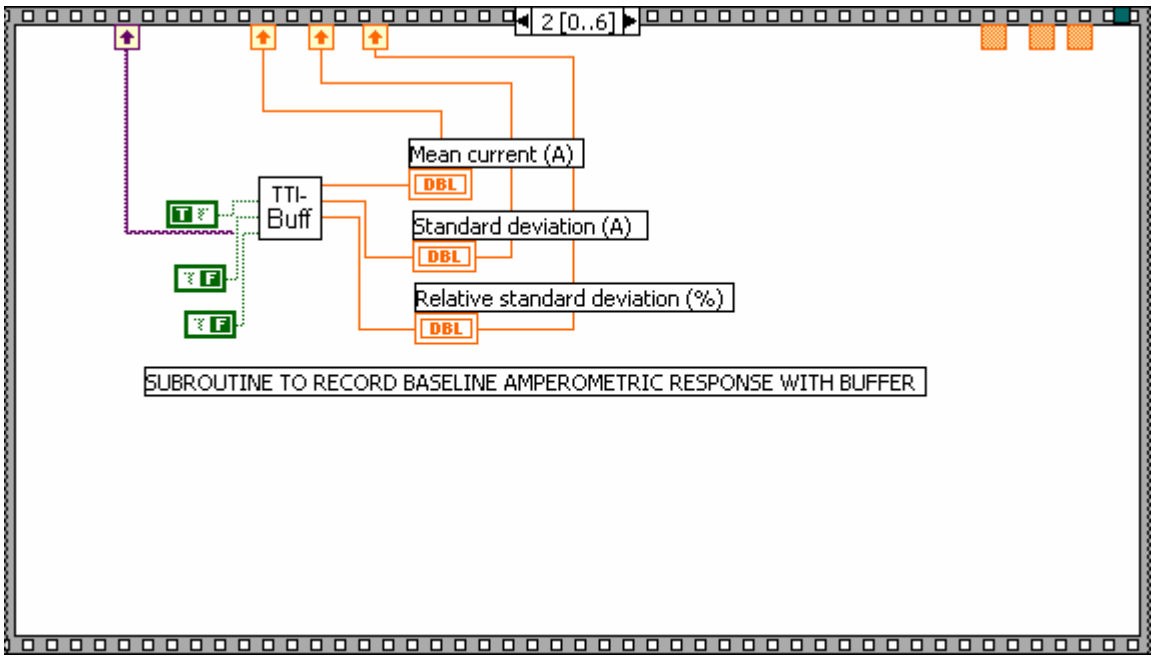
2 [0..6]
Mean current (A)
DBL
TTI-
Buff
Standard deviation (A)
DBL
Relative standard deviation (%)
DBL
SUBROUTINE TO RECORD BASELINE AMPEROMETRIC RESPONSE WITH BUFFER

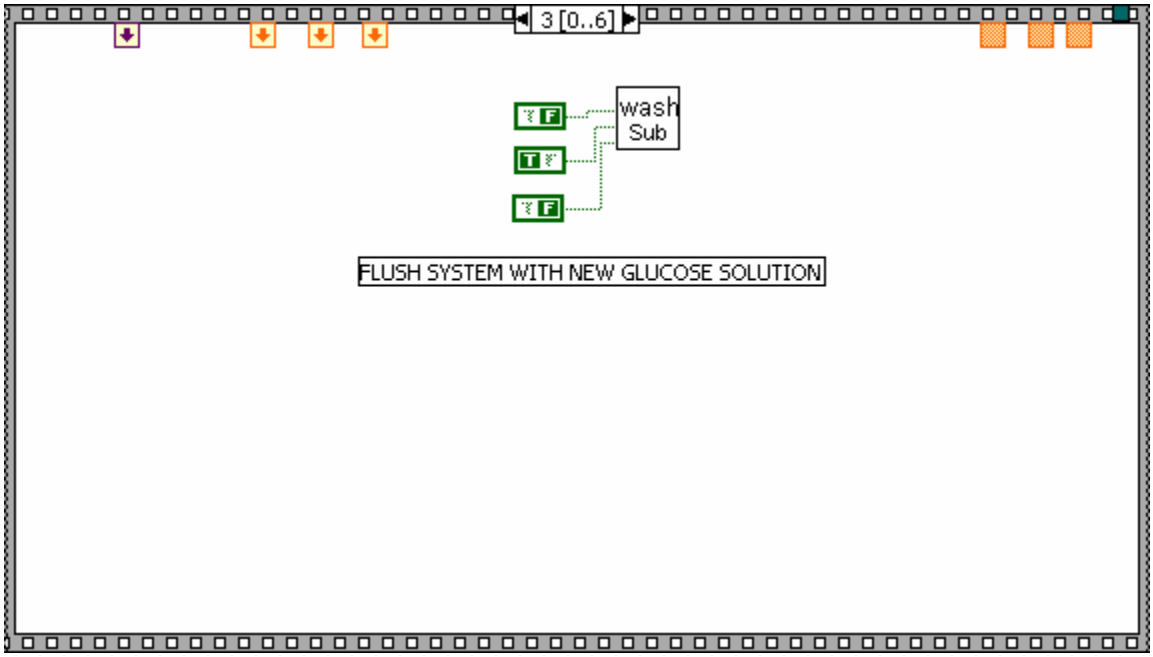
3 [0..6]
wash
Sub
FLUSH SYSTEM WITH NEW GLUCOSE SOLUTION

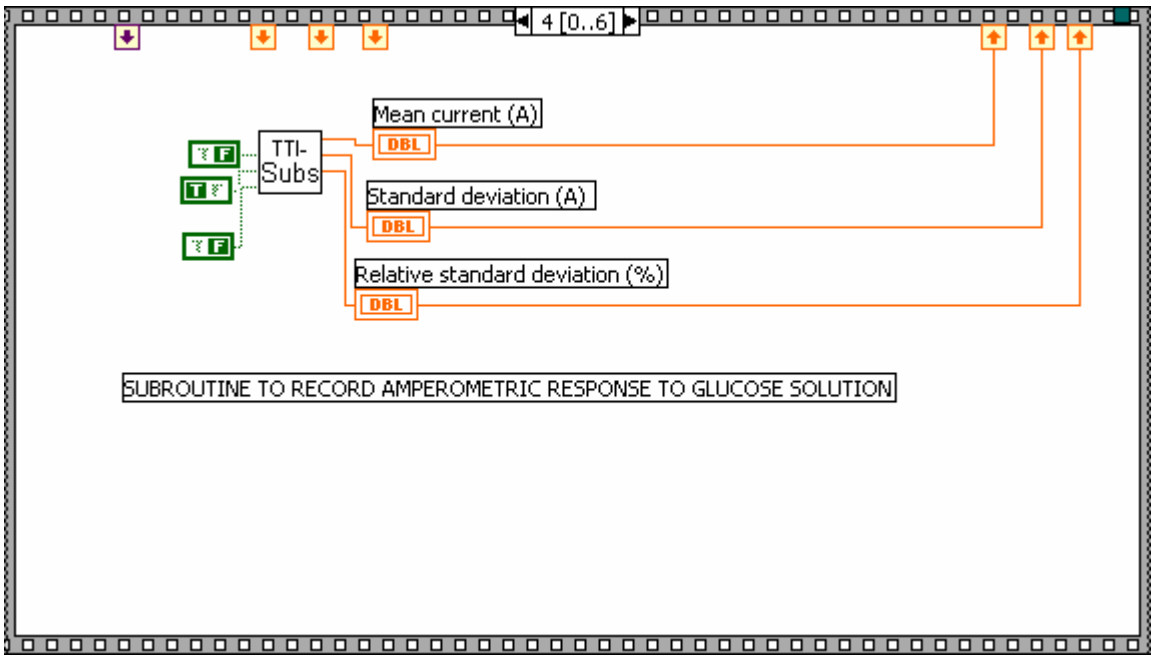
4 [0..6]
Mean current (A)
DBL
TTI-Subs
Standard deviation (A)
DBL
Relative standard deviation (%)
DBL
SUBROUTINE TO RECORD AMPEROMETRIC RESPONSE TO GLUCOSE SOLUTION

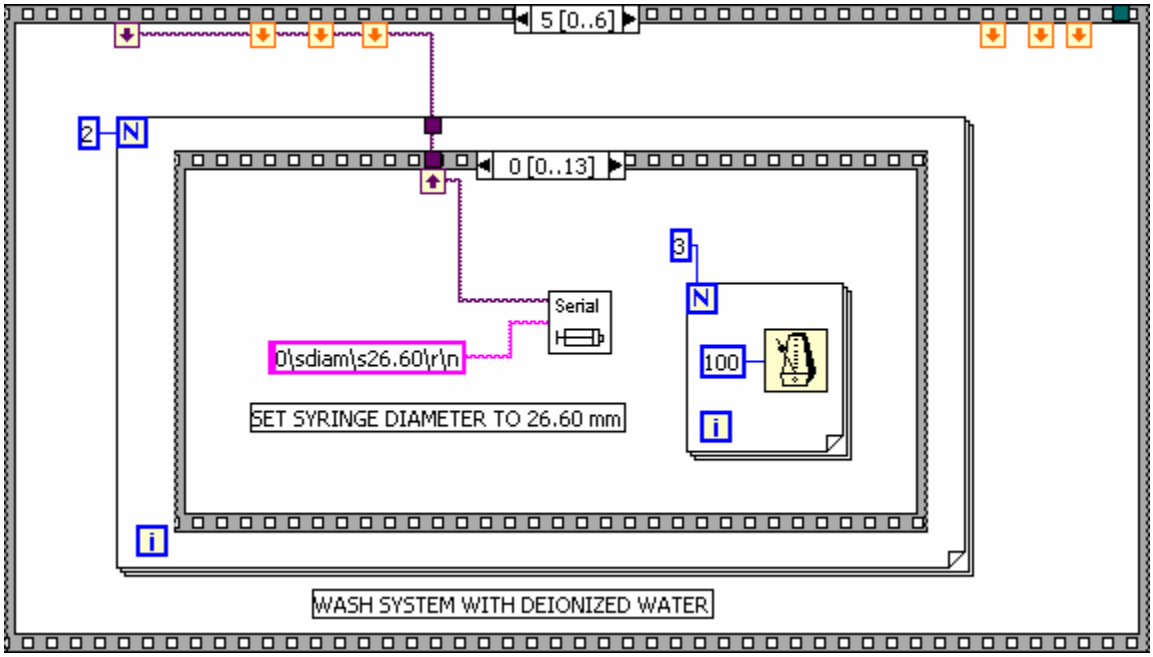
5 [0..6]
2
N
0 [0..13]
3
N
Serial
0\sdiam\s26.60\r\n
100
i
SET SYRINGE DIAMETER TO 26.60 mm
i
WASH SYSTEM WITH DEIONIZED WATER

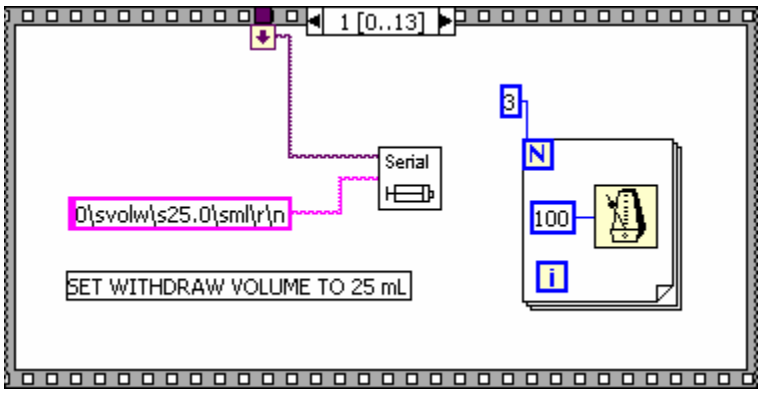
1 [0..13]
3
N
Serial
0\svolw\s25.0\sml\r\n
100
i
SET WITHDRAW VOLUME TO 25 mL

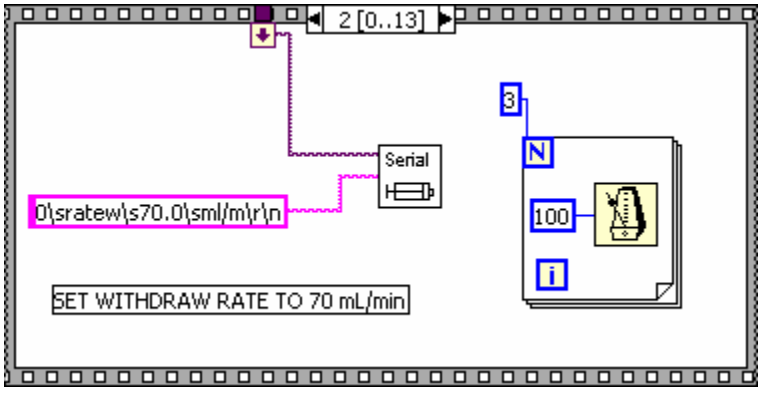
2 [0..13]
3
N
Serial
0\sratew\s70.0\sml/m\r\n
100
i
SET WITHDRAW RATE TO 70 mL/min

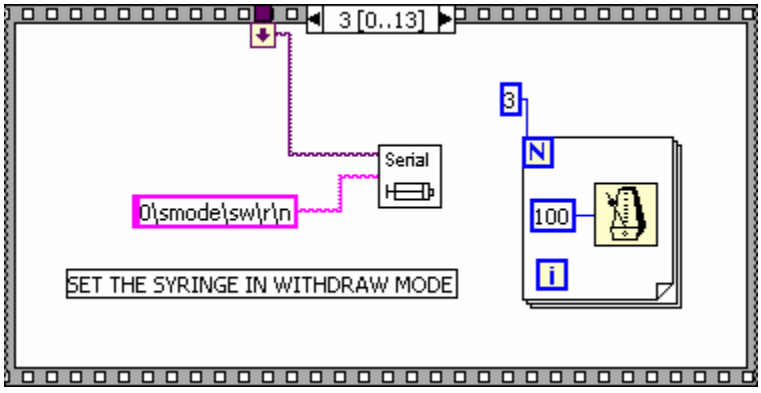
3 [0..13]
3
N
Serial
0\smode\sw\r\n
100
i
SET THE SYRINGE IN WITHDRAW MODE

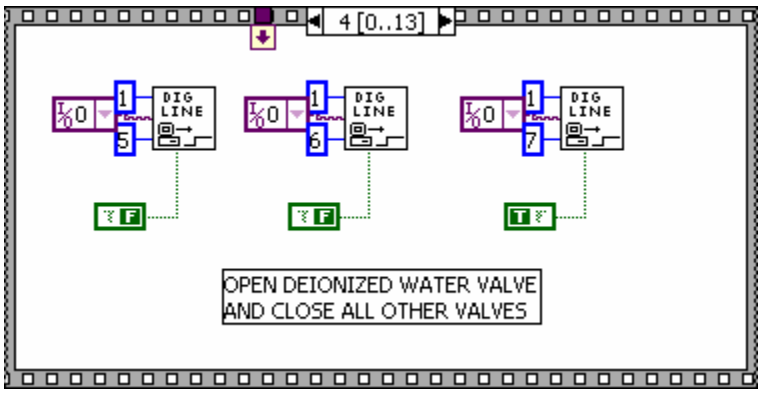
4 [0..13]
DIG LINE
1
5
6
7
F
F
T
OPEN DEIONIZED WATER VALVE
AND CLOSE ALL OTHER VALVES

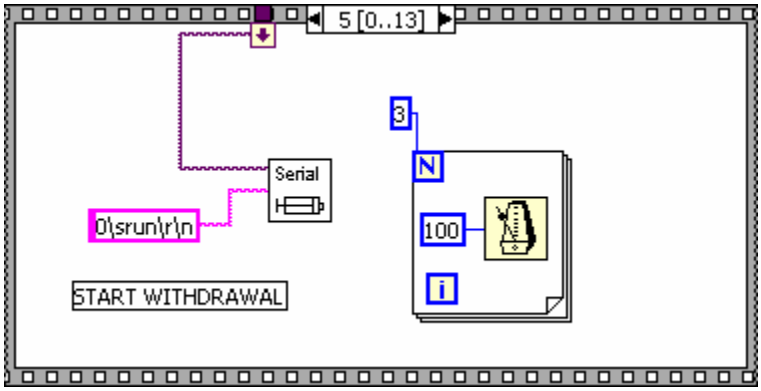
5 [0..13]
3
N
Serial
0\srun\r\n
100
i
START WITHDRAWAL

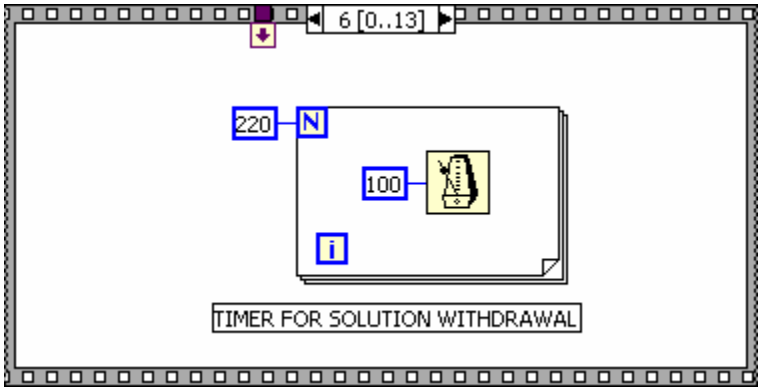
6 [0..13]
220
N
100
i
TIMER FOR SOLUTION WITHDRAWAL

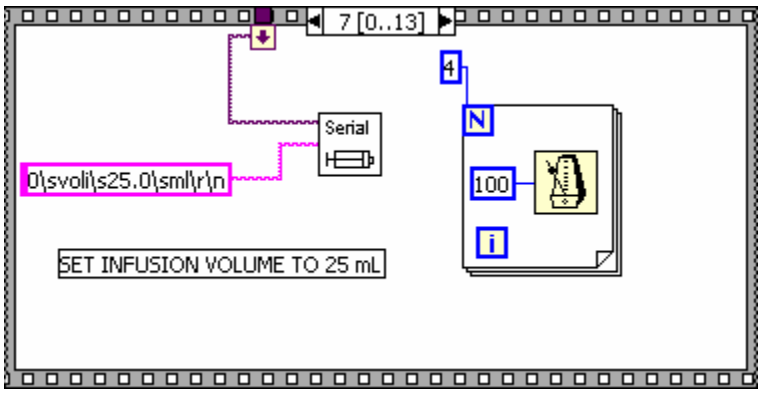
7 [0..13]
4
N
Serial
0\svoli\s25.0\sml\r\n
100
i
SET INFUSION VOLUME TO 25 mL

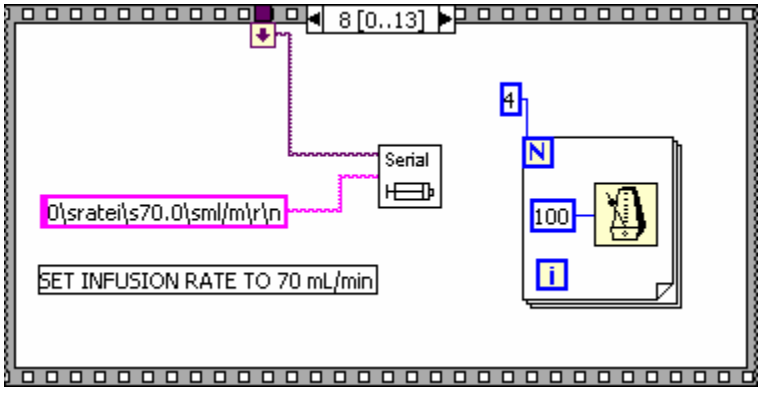
8 [0..13]
4
N
Serial
0\sratei\s70.0\sml/m\r\n
100
i
SET INFUSION RATE TO 70 mL/min

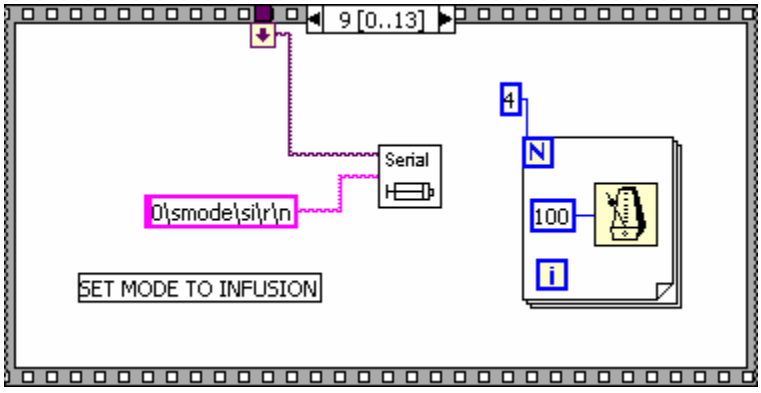
9 [0..13]
4
N
Serial
0\smode\si\r\n
100
i
SET MODE TO INFUSION

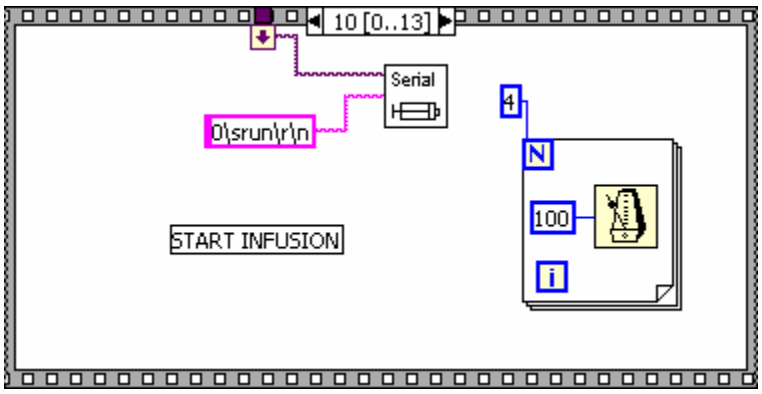
10 [0..13]
Serial
0\srun\r\n
4
N
100
i
START INFUSION

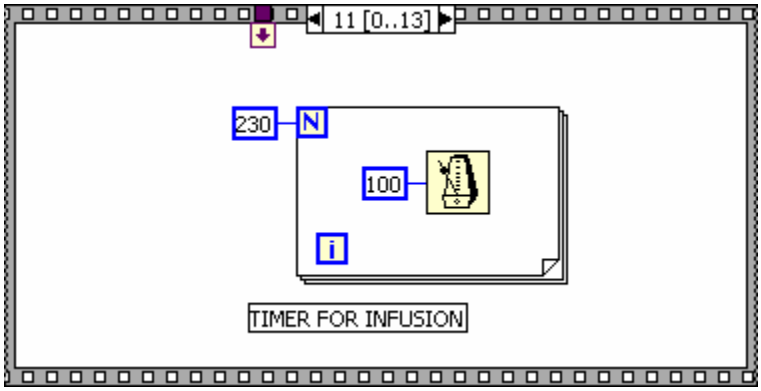
11 [0..13]
230
N
100
i
TIMER FOR INFUSION

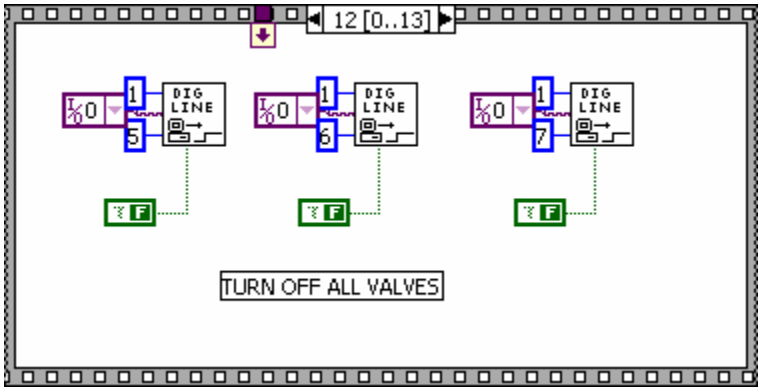
12 [0..13]
1
5
DIG LINE
1
6
DIG LINE
1
7
DIG LINE
F
F
F
TURN OFF ALL VALVES

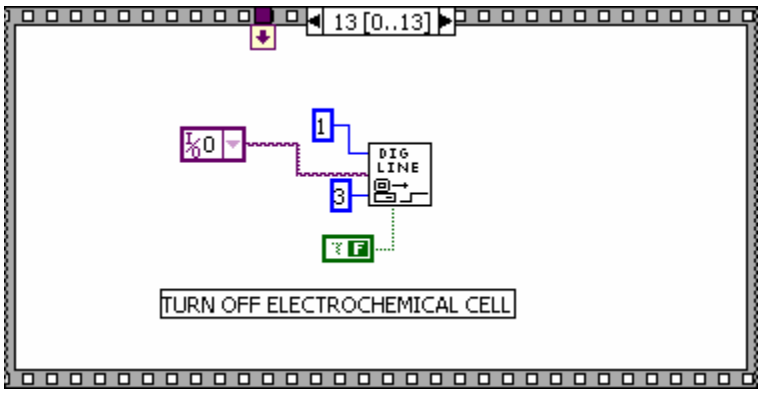

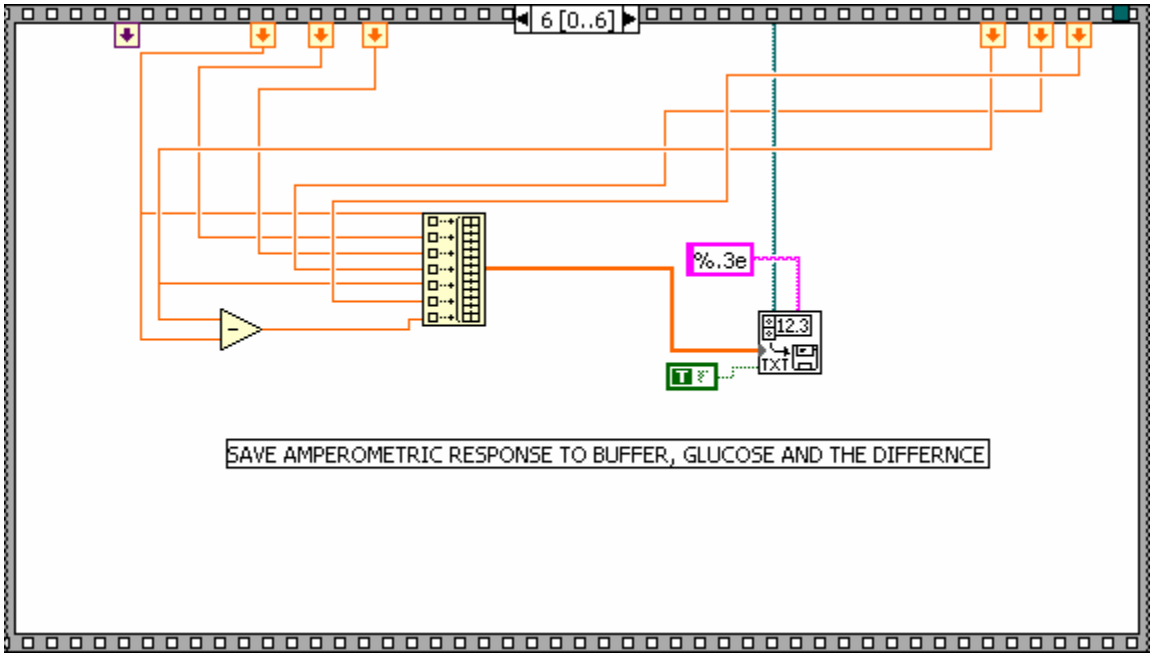

B) Subroutine to Adjust Potential

1) Icon

2) Front panel

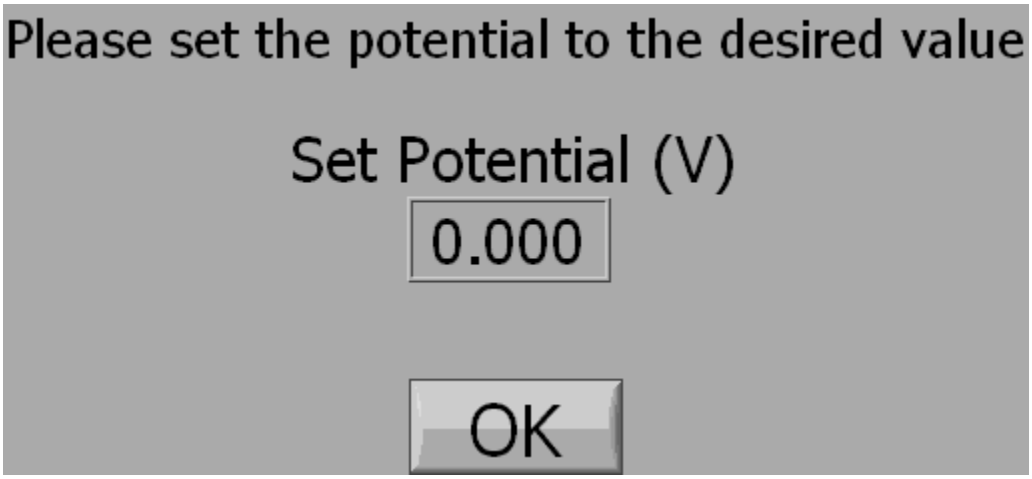

3) Diagram

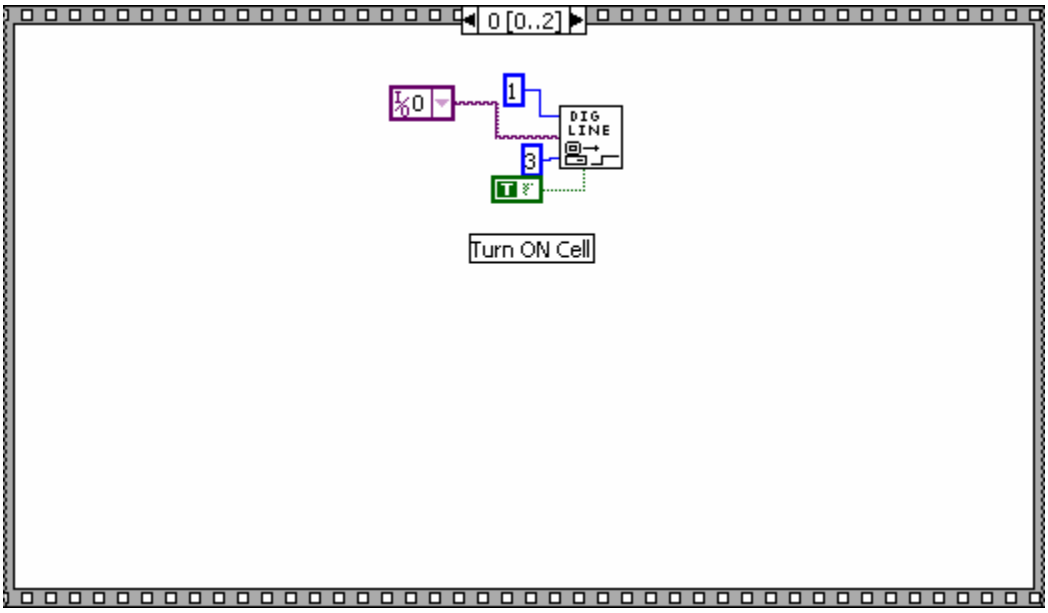

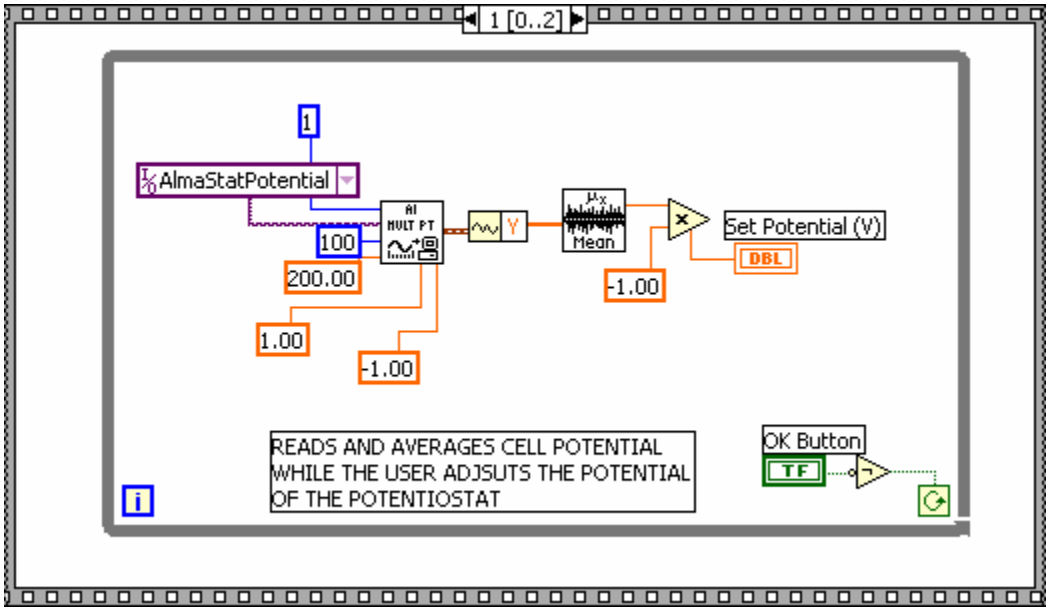

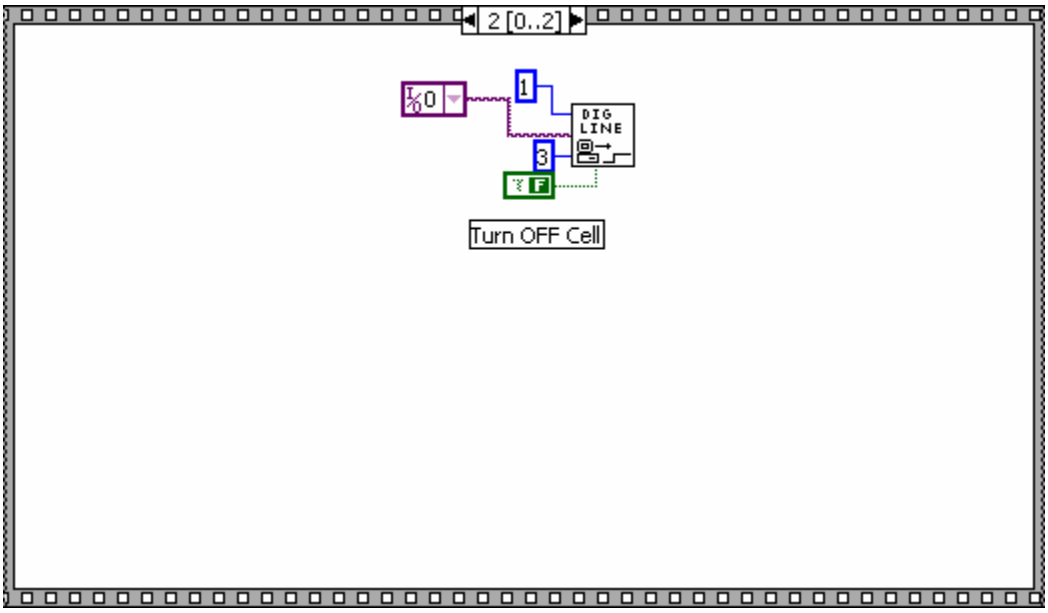

C) System Flush Subroutine

1) Icon

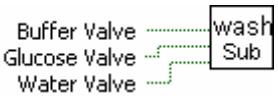

2) Front panel

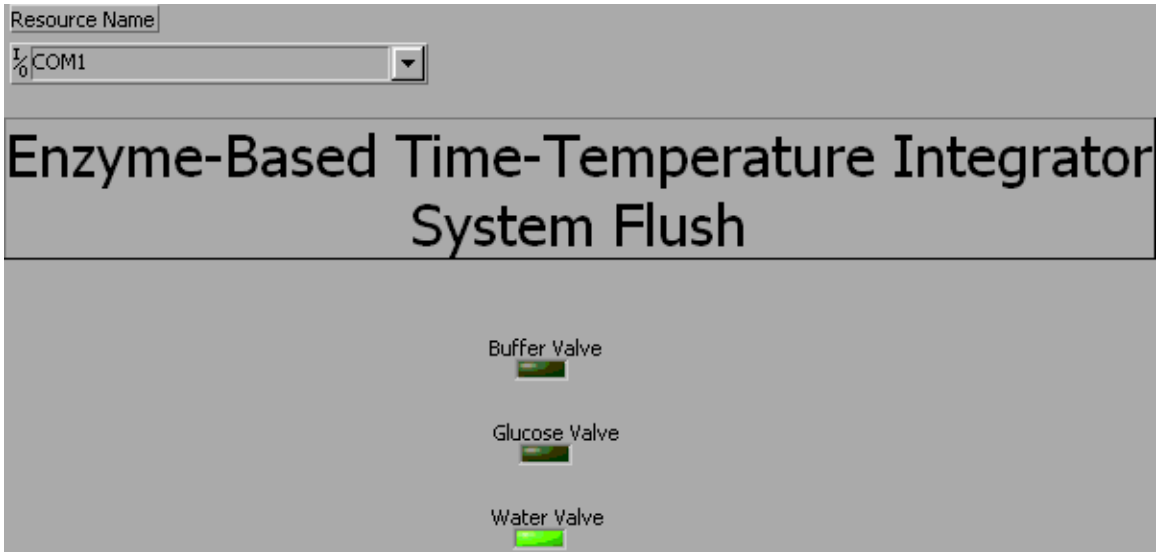

3) Diagram

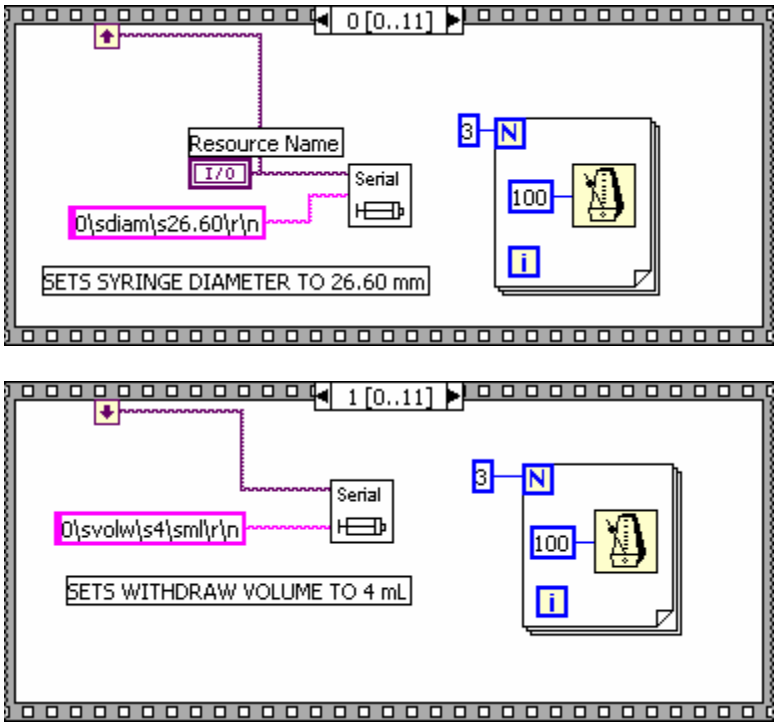

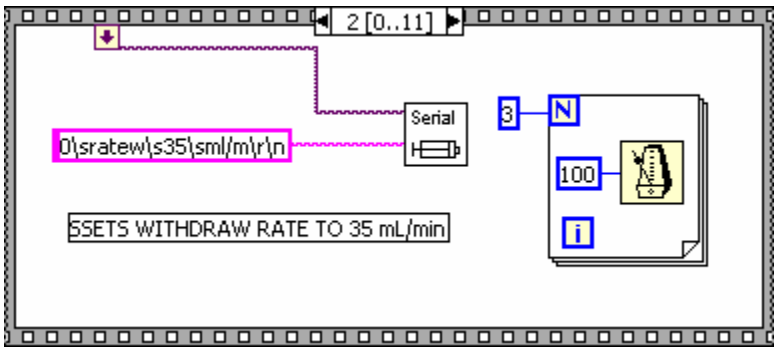
2 [0..11]
Serial
0\sratew\s35\sml/m\r\n
3
N
100
i
SSETS WITHDRAW RATE TO 35 mL/min

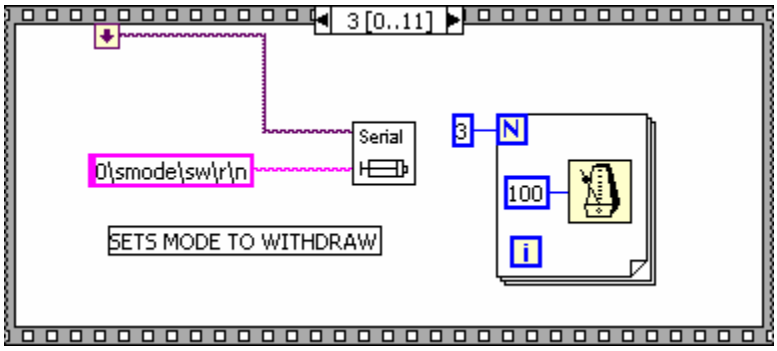
3 [0..11]
Serial
0\smode\sw\r\n
3
N
100
i
SETS MODE TO WITHDRAW

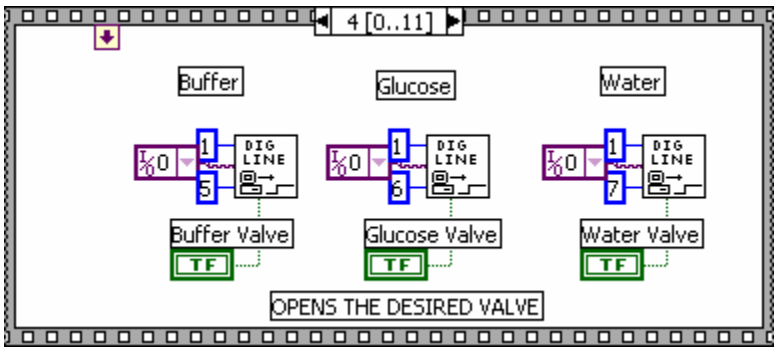
4 [0..11]
Buffer
Glucose
Water
DIG LINE
1
5
6
7
Buffer Valve
Glucose Valve
Water Valve
TF
OPENS THE DESIRED VALVE

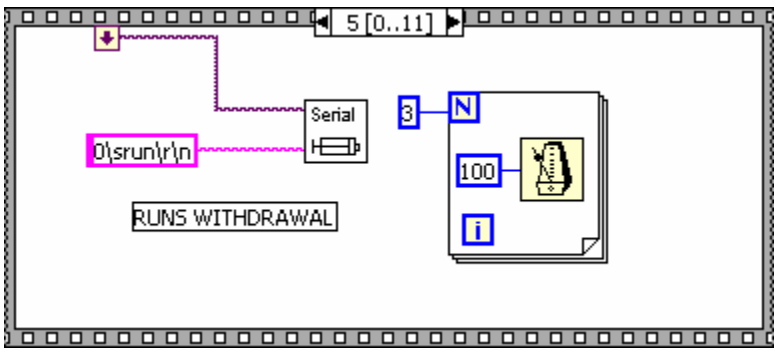
5 [0..11]
Serial
0\srun\r\n
3
N
100
i
RUNS WITHDRAWAL

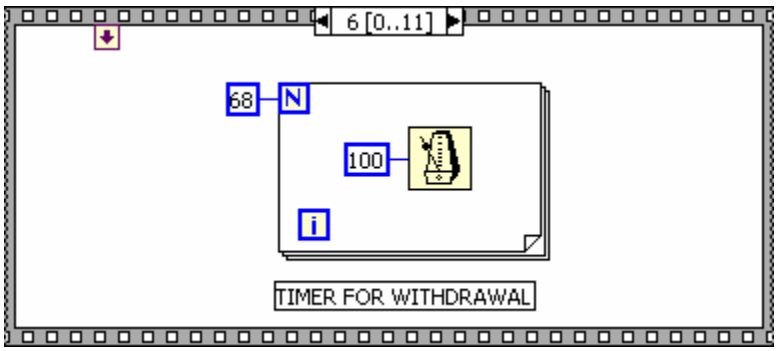
6 [0..11]
68
N
100
i
TIMER FOR WITHDRAWAL

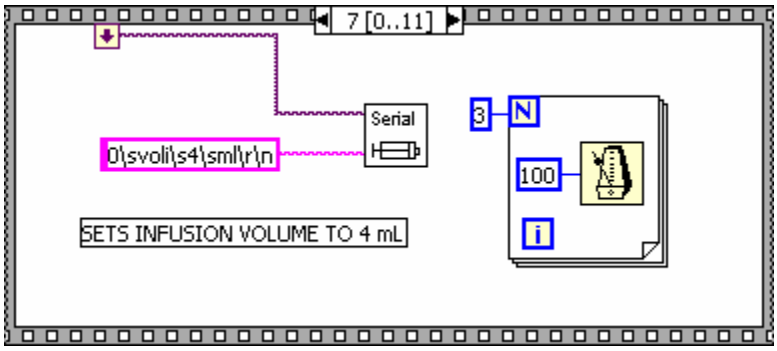
7 [0..11]
Serial
0\svoli\s4\sml\r\n
3
N
100
i
SETS INFUSION VOLUME TO 4 mL

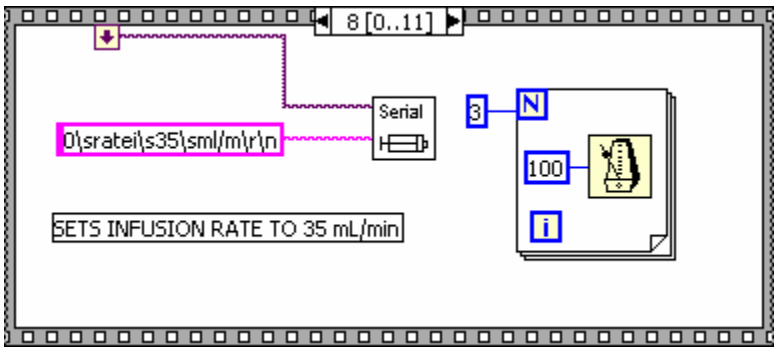
8 [0..11]
Serial
0\sratei\s35\sml/m\r\n
3
N
100
i
SETS INFUSION RATE TO 35 mL/min

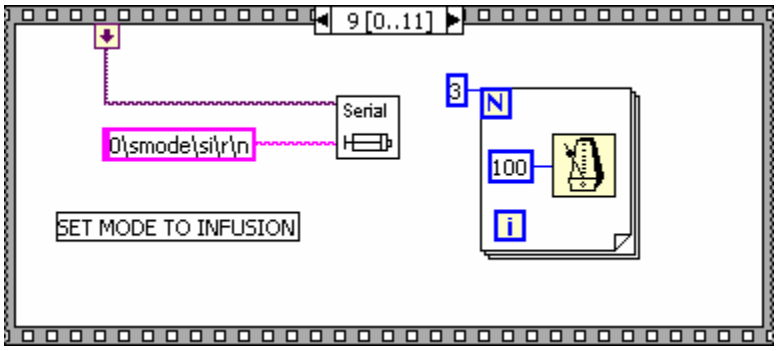
9 [0..11]
Serial
0\smode\si\r\n
3
N
100
i
SET MODE TO INFUSION

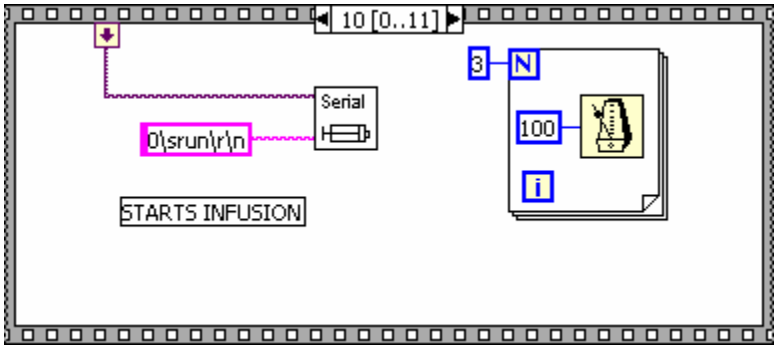
10 [0..11]
3
N
Serial
0\srun\r\n
100
i
STARTS INFUSION

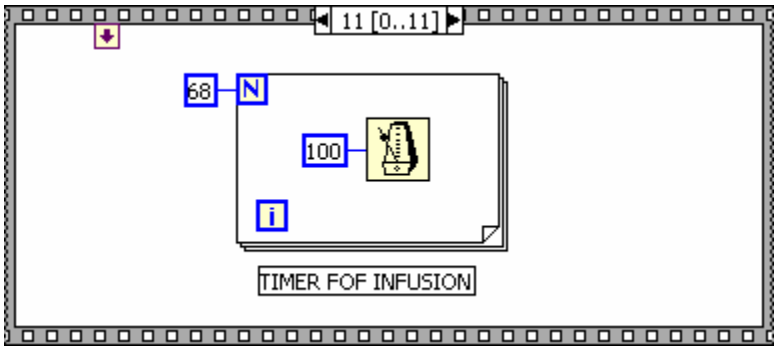
11 [0..11]
68
N
100
i
TIMER FOF INFUSION

D) TTI Amperometric Response to Buffer and Substrate.

While saved as separate subroutines, they could be combined as a single subroutine for the withdrawal and injection of buffer or substrate. They differ only in the injection volume, data collection time and the valve that is opened. This difference is due to the fact that it takes longer for the buffer to reach steady state amperometric response. Also, diagram frame sequence 1 to 10 is identical to the sequence in the system flush subroutine except for the injection volume and the flow rate. Therefore, these frames are not printed here. Instead, Table 1 shows the values of the variables for each subroutine.

Subroutine	Opened valve	Withdraw/ Injection Volume (mL)	Withdraw flow rate (mL/min)	Injection flow rate (mL/min)	Injection time (s)
System flush	Buffer or glucose	4	35	35	6.8
Buffer	Buffer	10	35	4	150
Substrate	Glucose	4	35	4	60

1) Icons

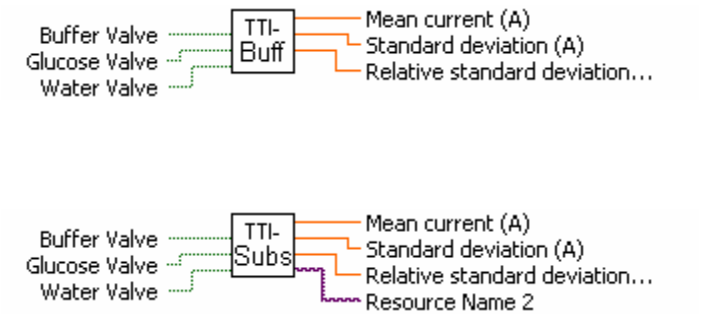

2) Front panel

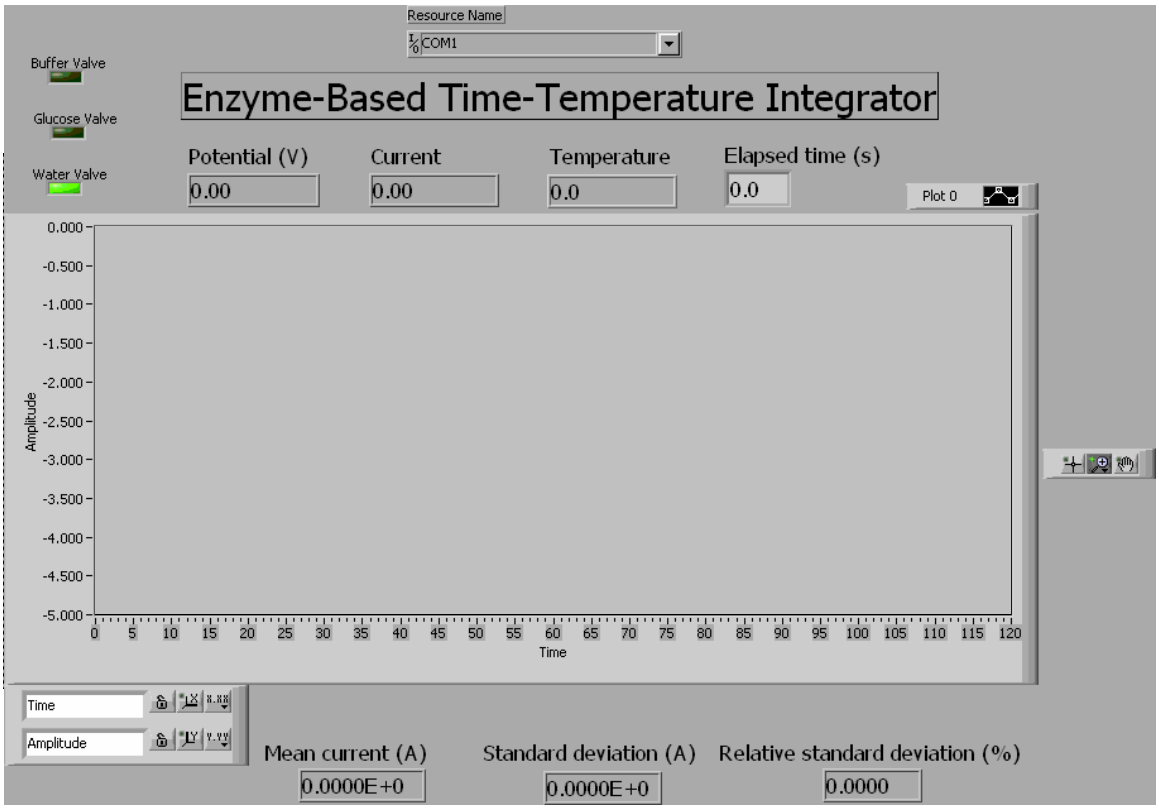

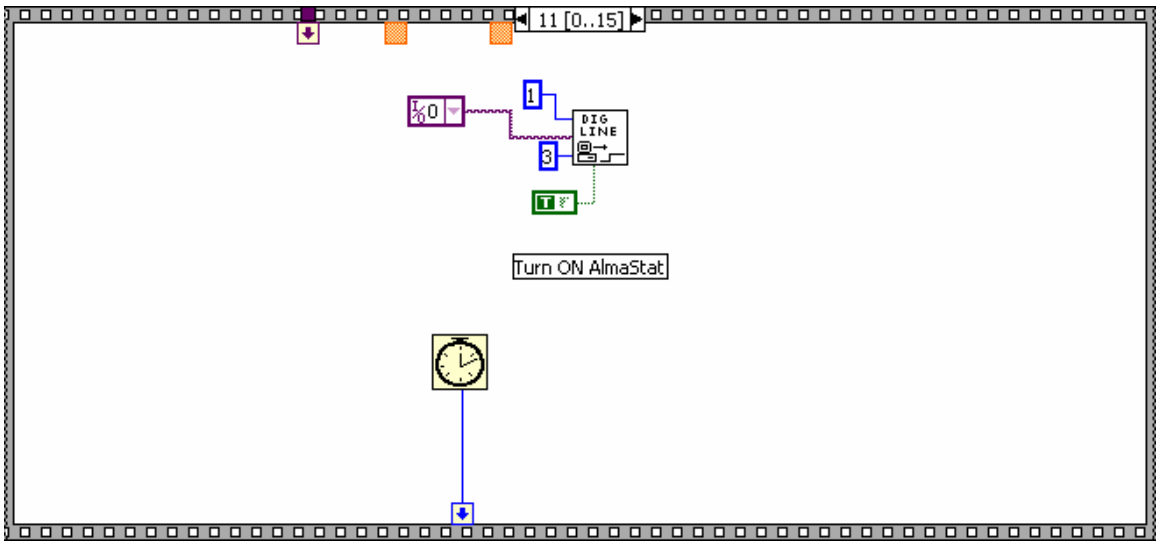

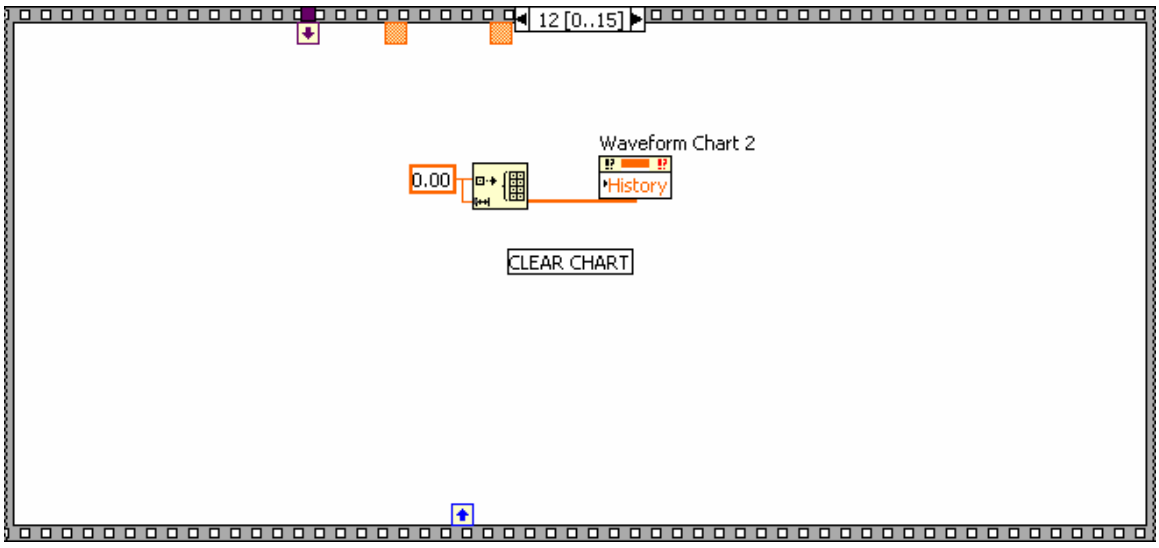
12 [0..15]
Waveform Chart 2
0.00
History
CLEAR CHART

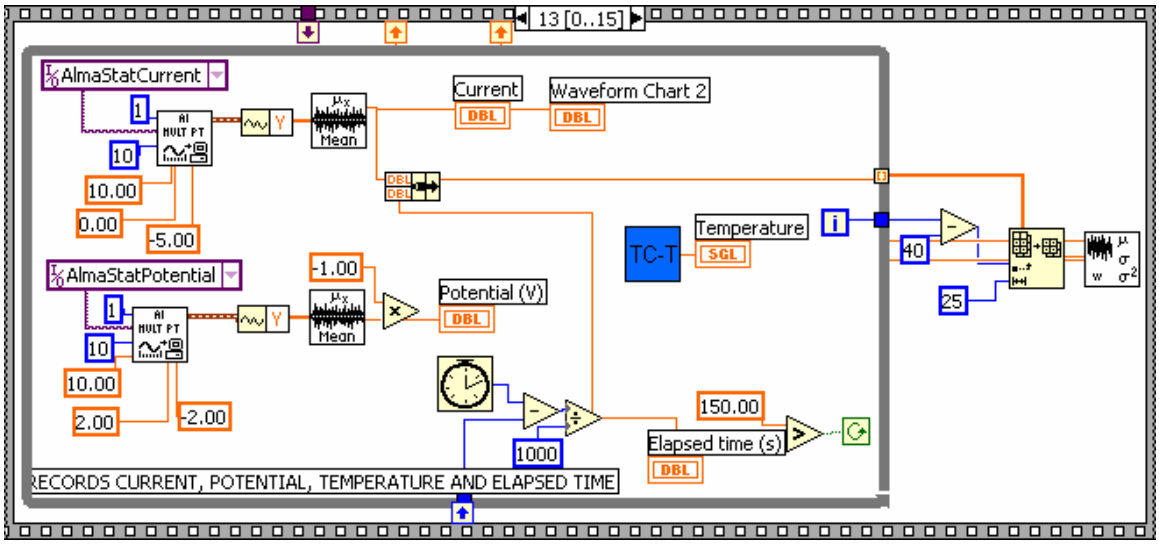
13 [0..15]
AlmaStatCurrent
1
10
10.00
0.00
-5.00
AI MULT PT
Y
Mean
Current
DBL
Waveform Chart 2
DBL
AlmaStatPotential
-1.00
Potential (V)
2.00
-2.00
TC-T
Temperature
SGL
i
40
25
150.00
Elapsed time (s)
1000
RECORDS CURRENT, POTENTIAL, TEMPERATURE AND ELAPSED TIME

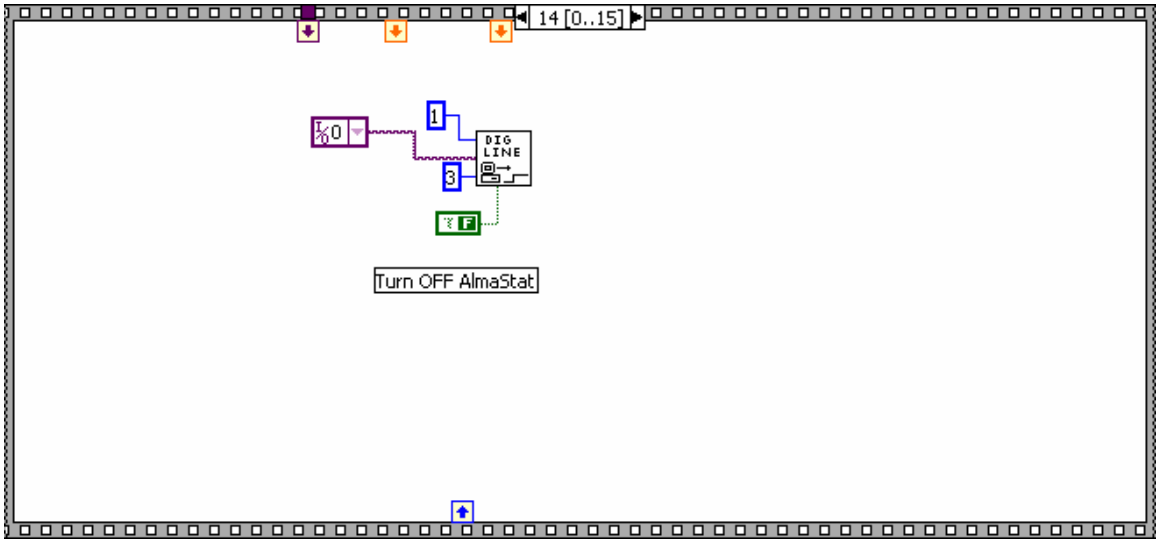
14 [0..15]
0
1
3
DIG LINE
F
Turn OFF AlmaStat

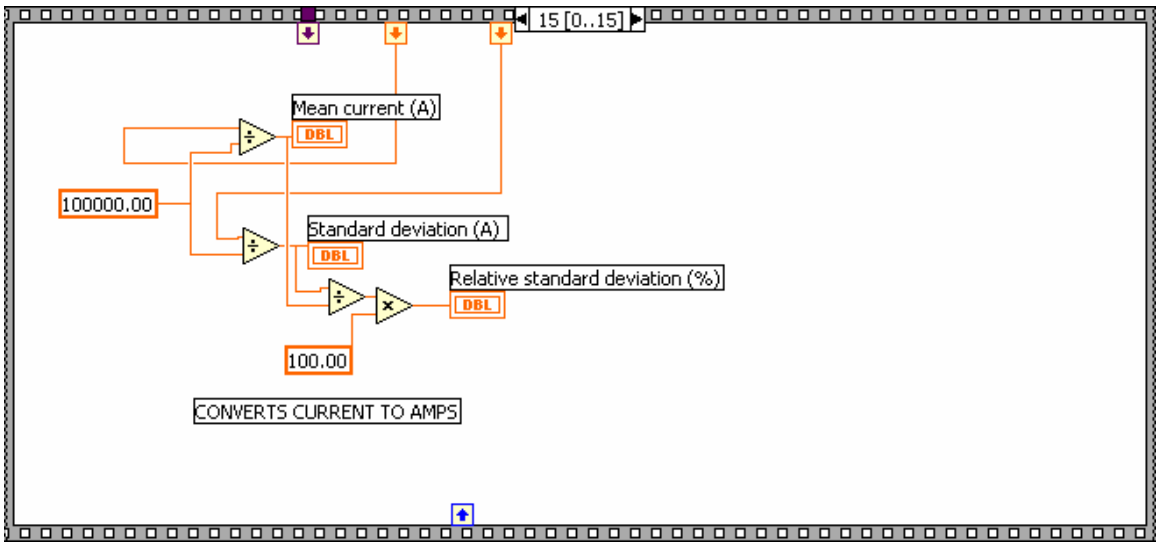

E) Temperature Subroutine

1) Icon

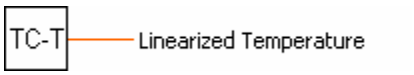

2) Front panel

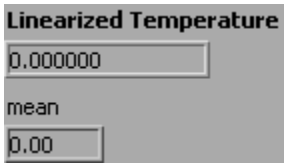

3) Diagram

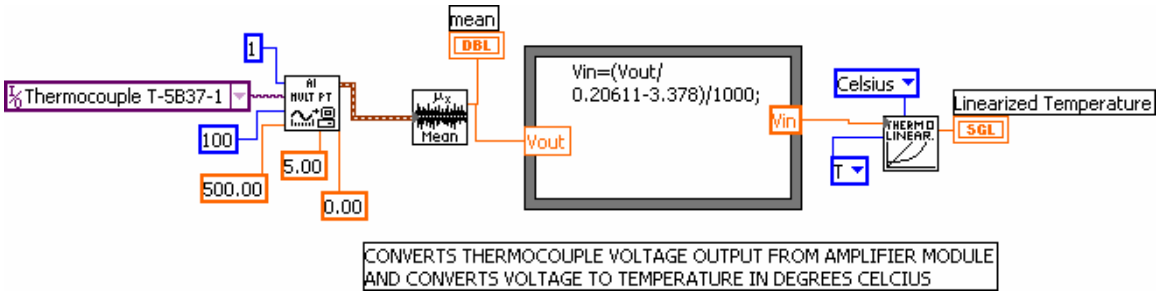

APPENDIX F

PICTURES OF EQUIPMENT FABRICATED FOR THIS RESEARCH AND EQUIPMENT SETUP

This appendix is included to illustrate some of the equipment fabricated and equipment setup used in this research. It also aims to help those who take over this research identify some of the items in the 'black boxes' of the laboratory. More detail on the electrical circuits can be found in Appendix A.

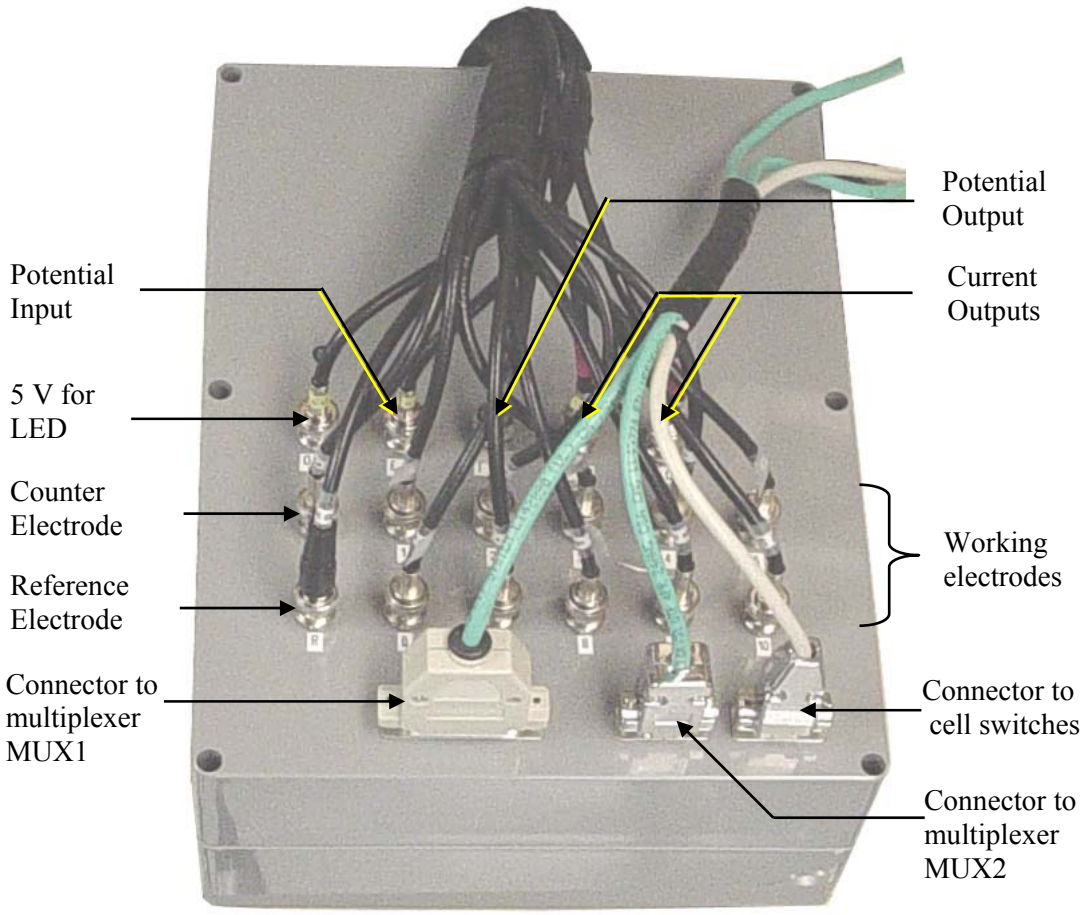

Figure 1. Multielectrode Potentiostat 'CougarStat'

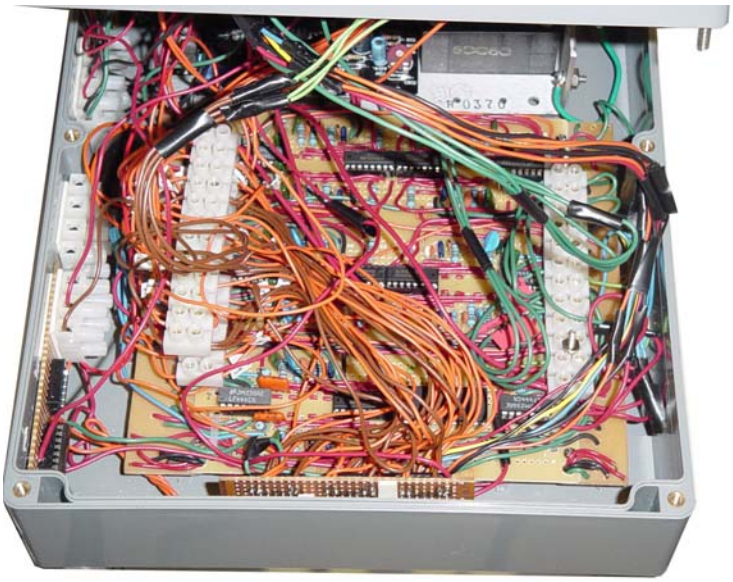

Figure 2. Bread board of the multichannel potentiostat.

Figure 3. Potentiostat (AlmaStat 2003) data acquisition connector box

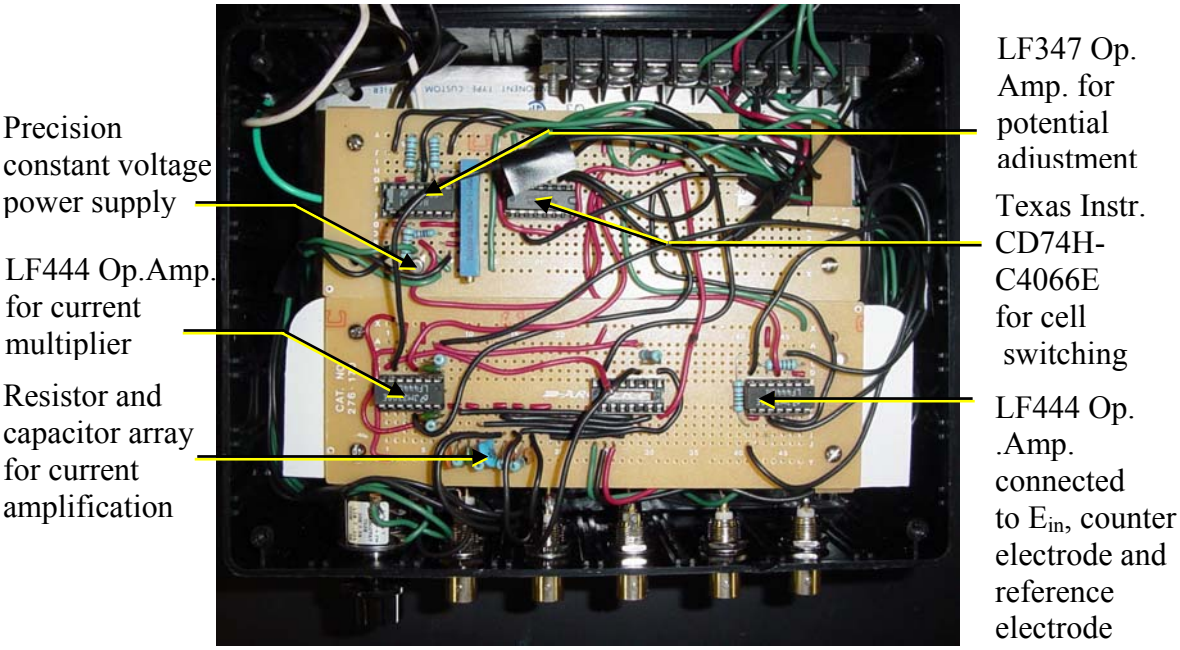

Figure 4. Breadboard of the AlmaStat 2003

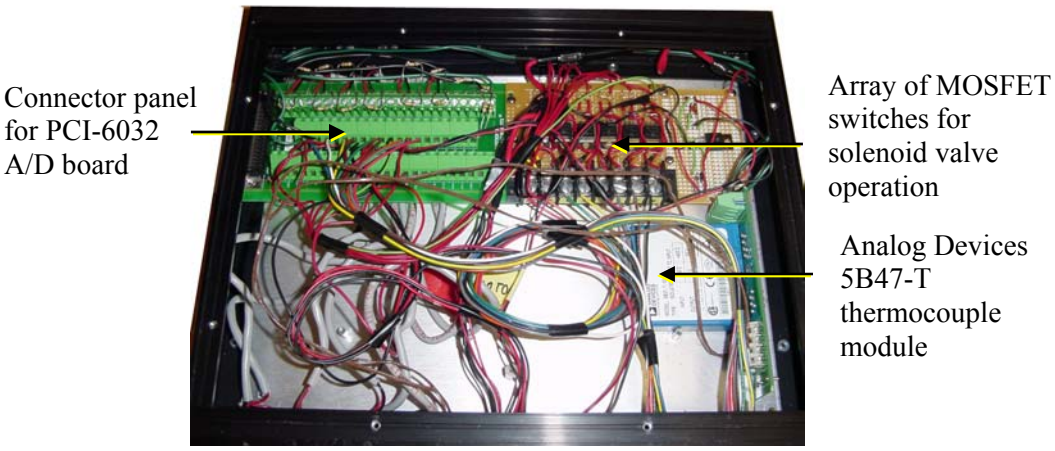

Figure 5. Connector enclosure.

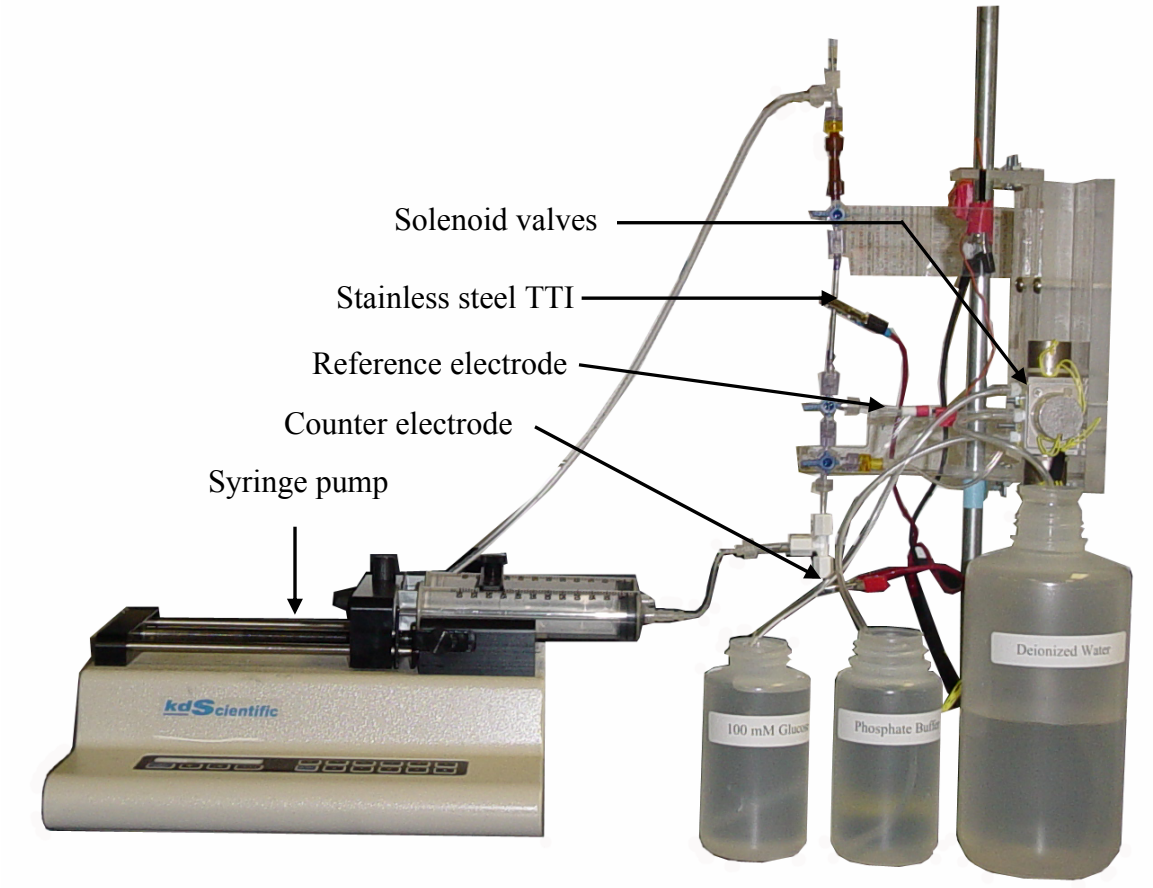

Figure 6. TTI mounted in the continuous flow system

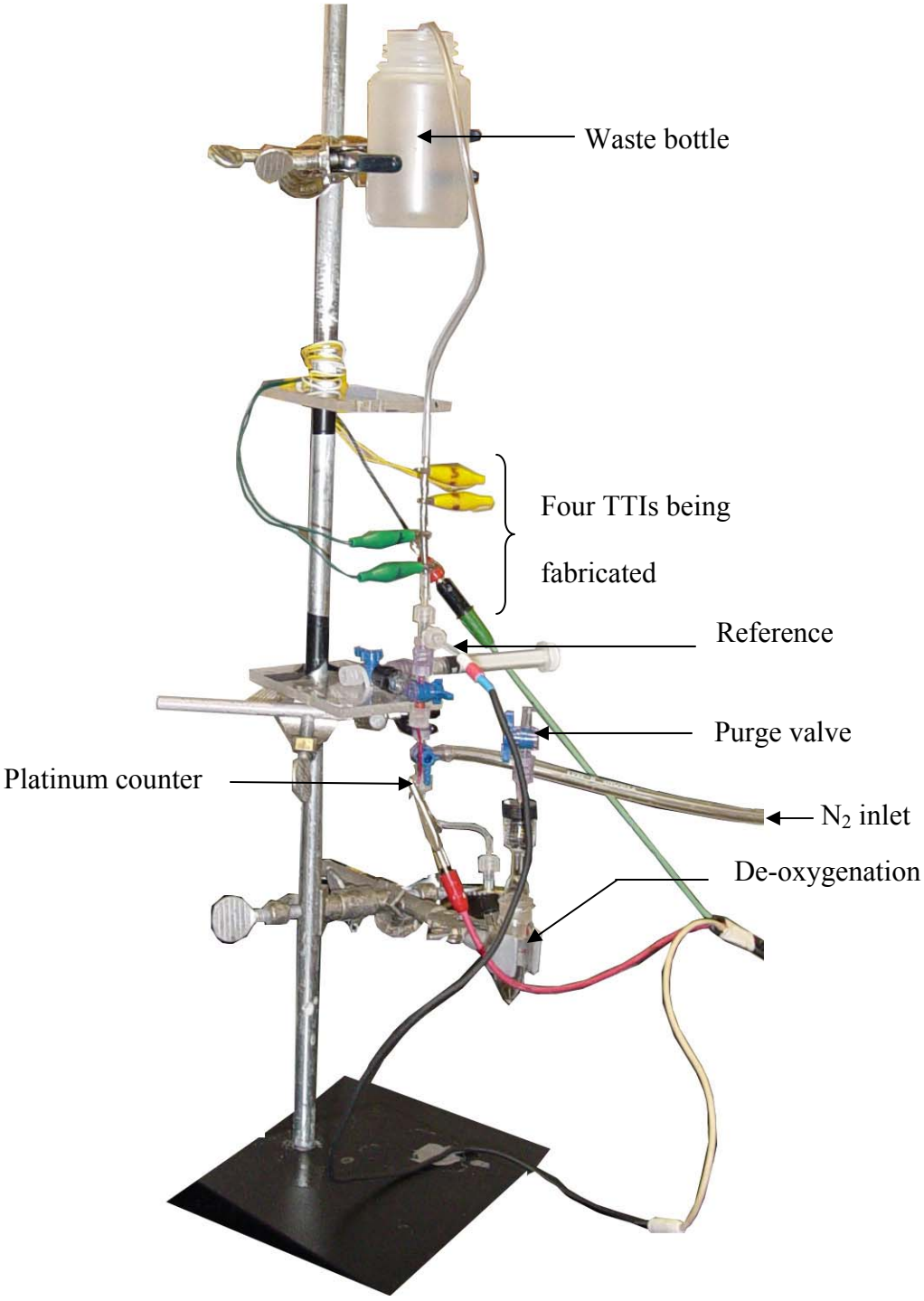

Figure 7. Setup for TTI Fabrication